Spatial patterns of genetic diversity of the genus *Eumerus* (Diptera: Syrphidae) in the Balkans

Antonia Chroni

Biochemist – Biotechnologist, MSc

Doctoral Dissertation
Department of Geography of the University of the Aegean
Defended in public on
Friday 22 December 2017

page intentionally left blank

Χωρικά πρότυπα γενετικής ποικιλότητας του γένους *Eumerus* (Δίπτερα: Συρφίδες) στα Βαλκάνια

Αντωνία Χρόνη

Βιοχημικός – Βιοτεχνολόγος, MSc

Διδακτορική Διατριβή
Τμήμα Γεωγραφίας του Πανεπιστημίου Αιγαίου
Ημερομηνία δημόσιας υποστήριξης
Παρασκευή 22 Δεκεμβρίου 2017

Chroni, A. 2018. Spatial patterns of genetic diversity of the genus *Eumerus* (Diptera: Syrphidae) in the Balkans. Doctoral Dissertation, University of the Aegean, Mytilene. (pp. 269).

Χρόνη, Α. 2018. Χωρικά πρότυπα γενετικής ποικιλότητας του γένους *Eumerus* (Δίπτερα: Συρφίδες) στα Βαλκάνια. Διδακτορική Διατριβή, Πανεπιστήμιο Αιγαίου, Μυτιλήνη (σελ. 269).

Η έγκριση της διδακτορικής διατριβής από το Τμήμα Γεωγραφίας του Πανεπιστημίου Αιγαίου δεν υποδηλώνει την αποδοχή των γνωμών της συγγραφέως (Ν. 5343/1932, Άρθρο 202, Παράγραφος 2).

Funding

The current PhD dissertation was conducted at the Laboratory of Ecology and Biogeography at the Department of Geography of the University of the Aegean (Mytilene, Greece). DNA and phylogenetic analyses were carried out at the Laboratory of Genetics at the Department of Biology and Ecology of the University of Novi Sad (Faculty of Sciences, Serbia).

This PhD research was funded mainly by the project POL-AEGIS (The pollinators of the Aegean: biodiversity and threats), which was co-funded by the European Union (European Social Fund – ESF) and Greek national funds through the Operational Program 'Education and Lifelong Learning' of the National Strategic Reference Framework (NSRF) – Research Funding Program: THALES – Investing in knowledge society through the European Social Fund (PhD fund received: April 2013 – November 2015).

Additional funding was provided by the following projects/programs: (i) the project «ExpeER» (Experimentation in Ecosystem Research, 7th Framework Programme of the EC, FP2007-2013) (funded period: June – July 2013); (ii) the Mobility Program «Grants IKY» (Short Terms, Greek State Scholarships Foundation) (in the frame of the «Education and Lifelong Learning» of the European Social Fund (ESF) – NSRF, 2007–2013) (funded period: June – November 2014); and (iii) the Erasmus+ Programme/ International Credit Mobility (funded period: February – May 2017).

Χρηματοδότηση

Η παρούσα διδακτορική διατριβή εκπονήθηκε στο Εργαστήριο Βιογεωγραφίας και Οικολογίας του Τμήματος Γεωγραφίας του Πανεπιστημίου Αιγαίου (Μυτιλήνη, Ελλάδα). Οι εργαστηριακές και φυλογενετικές αναλύσεις διεξήχθησαν στο Εργαστήριο Γενετικής του Τμήματος Βιολογίας και Οικολογίας του Πανεπιστημίου του Νόβι Σαντ (Σχολή Θετικών Επιστημών, Σερβία).

Η διδακτορική έρευνα χρηματοδοτήθηκε κυρίως από το έργο POL-AEGIS (Οι επικονιαστές του Αιγαίου: βιοποικιλότητα και απειλές), το οποίο συγχρηματοδοτήθηκε από την Ευρωπαϊκή Ένωση (Ευρωπαϊκό Κοινωνικό Ταμείο – ΕΚΤ) και από εθνικούς πόρους μέσω του Επιχειρησιακού Προγράμματος «Εκπαίδευση και Δια Βίου Μάθηση» του Εθνικού Στρατηγικού Πλαισίου Αναφοράς (ΕΣΠΑ) – Ερευνητικό Χρηματοδοτούμενο Έργο: ΘΑΛΗΣ – Επένδυση στην κοινωνία της γνώσης μέσω του Ευρωπαϊκού Κοινωνικού Ταμείου (χρήματοδότηση PhD: Απρίλιος 2013 – Νοέμβριος 2015).

Επιπρόσθετη χρηματοδότηση προήλθε από τα παρακάτω έργα/προγράμματα: (i) Ερευνητικό έργο «ExpeER» (Experimentation in Ecosystem Research, χρηματοδοτούμενο από το 7ο Πρόγραμμα Πλαίσιο της Ευρωπαϊκής Επιτροπής, FP2007-2013) (χρήματοδότηση PhD: Ιούνιος – Ιούλιος 2013), (ii) Πρόγραμμα Χορήγησης Υποτροφιών Κινητικότητας ΙΚΥ για Βραχεία Μετεκπαίδευση (Short Terms) στο πλαίσιο του «Εκπαίδευση και Δια Βίου Μάθηση», χρηματοδοτούμενο από το Ευρωπαϊκό Ταμείο (ΕΚΤ) του ΕΣΠΑ, 2007 – 2013) (χρήματοδότηση PhD: Ιούνιος – Νοέμβριος 2014), και (iii) Πρόγραμμα Erasmus+ Διεθνούς κινητικότητας (χρήματοδότηση PhD: Φεβρουάριος – Μάιος 2017).

Author contributions

Chapter 1: A. Chroni wrote Chapter 1.

Chapter 2: A. Chroni, D. Obreht Vidaković, T. Petanidou and A. Vujić designed the study; A. Vujić collected and identified part of the specimens analyzed; A. Chroni carried out the DNA analyses; A. Chroni and M. Djan carried out the phylogenetic analyses and the results' interpretation; A. Chroni wrote the paper; D. Obreht Vidaković, T. Petanidou, A. Vujić and M. Djan critically reviewed the paper.

Chapter 3: A. Grković, A. Vujić and S. Radenković identified the specimens and conducted the morphology descriptions; A. Chroni carried out the DNA analyses; A. Grković and A. Chroni wrote the paper; A. Vujić, S. Radenković and T. Petanidou critically reviewed the paper.

Chapter 4: A. Grković, A. Vujić, J. van Steenis and S. Radenković identified the specimens and conducted the morphology descriptions; A. Chroni carried out the DNA and phylogenetic analyses, and M. Djan participitated to the results' interpretation; A. Grković and A. Chroni wrote the paper; A. Vujić, J. van Steenis and S. Radenković reviewed the paper.

Chapter 5: A. Chroni, A. Vujić and M. Djan designed the study; A. Chroni and N. Veličković carried out the DNA analyses; A. Chroni (phylogenetic and phylogeographic), A. Grković (morphology descriptions), J. Ačanski (wing morphometry) conducted the analyses and wrote the paper; A. Vujić, M. Djan and T. Petanidou reviewed the paper.

Chapter 6: A. Chroni, A. Vujić and T. Petanidou designed the study; A. Chroni, L. Šašić Zorić and N. Kočiš Tubić conducted the DNA analyses; A. Chroni, M. Stefanović and M. Djan analysed the data; A. Chroni wrote the paper. A. Vujić, M. Djan and T. Petanidou reviewed the paper.

In Chapters (2) – (6), A. Vujić and T. Petanidou collected and directed data collection; T. Petanidou, A. Vujić, M. Djan, D. Obreht Vidaković and A. Chroni obtained funding for the projects.

Figures/photos credits

Photo used in the cover is reproduced with permission by Jelle Devalez, and photo editing was conducted by Christos Kardampikis. Figures (1a) and (3) of the Chapter (1) are reproduced with permission by Dr Dana Krempels and Dr Andrew Young, respectively. Photos used in the Chapters (3) and (4) are reproduced with the kind permission by Ana Grković.

Σχήματα/φωτογραφίες credits

Η φωτογραφία του εξωφύλλου είναι του Jelle Devalez, και η επεξεργασία της φωτογραφίας του Χρήστου Καρδαμπίκη. Τα σχήματα (1a) και (3) του Κεφαλαίου (1) είναι ελεύθερα δικαιωμάτων αναπαραγωγής σύμφωνα με τους Δρ Dana Krempels και Δρ Andrew Young, αντίστοιχα. Οι φωτογραφίες των Κεφαλαίων (3) και (4) είναι της Ana Grković.

Thesis committee/ Εξεταστική Επιτροπή

Advisory Committee/ Συμβουλευτική Επιτροπή

1. Theodora Petanidou, Professor, Department of Geography, University of the Aegean (Mytilene, Greece) (Dissertation Advisor).
2. Ante Vujić, Professor, Department of Biology and Ecology, University of Novi Sad, Faculty of Sciences (Novi Sad, Serbia).
3. Mihajla Djan, Associate Professor, Department of Biology and Ecology, University of Novi Sad, Faculty of Sciences (Novi Sad, Serbia).

Examiners/ Επταμελής Εξεταστική Επιτροπή

1. Theodora Petanidou, Professor, Department of Geography, University of the Aegean (Mytilene, Greece).
2. Ante Vujić, Professor, Department of Biology and Ecology, University of Novi Sad, Faculty of Sciences (Novi Sad, Serbia).
3. Mihajla Djan, Associate Professor, Department of Biology and Ecology, University of Novi Sad, Faculty of Sciences (Novi Sad, Serbia).
4. Snežana Radenković, Associate Professor, Department of Biology and Ecology, University of Novi Sad, Faculty of Sciences (Novi Sad, Serbia).
5. Nevena Velićković, Assistant Professor, Department of Biology and Ecology, University of Novi Sad, Faculty of Sciences (Novi Sad, Serbia).
6. Dimitrios Avtzis, Senior Researcher, Forest Research Institute, Hellenic Agricultural Organization ‘Demeter’ (Thessaloníki, Greece).
7. Thomas Tscheulin, Assistant Professor, Department of Geography, University of the Aegean (Mytilene, Greece).

Publications

Chroni, A., Stefanović, M., Djan, M., Vujić, A., Šašić Zorić, L., Kočiš Tubić, N., Petanidou, T. Connecting the dots: Bridging genetic to spatial differentiation of the genus *Eumerus* (Diptera: Syrphidae) in the Mediterranean Basin and the Balkans. Paper in prep.

Chroni, A., Grković, A., Ačanski, J., Vujić, A., Radenković, S., Veličković, N., Djan, M., Petanidou, T. Is there more out there? Disentangling cryptic species complex and new species within *Eumerus minotaurus* group (Diptera: Syrphidae) based on integrative taxonomy and Aegean palaeogeography. Paper under revision in Contributions to Zoology.

Grković, A., Vujić, A., **Chroni, A.**, van Steenis, J., Đan, M., Radenković, S. (2017) Taxonomy and systematics of three species of the genus *Eumerus* Meigen, 1822 (Diptera: Syrphidae) new in southeastern Europe. Zoologischer Anzeiger, 270, 176–192, https://doi.org/10.1016/j.jcz.2017.10.007.

Chroni, A., Djan, M., Vidaković, D.O., Petanidou, T., Vujić, A. (2017) Molecular species delimitation in the genus *Eumerus* (Diptera: Syrphidae). Bulletin of Entomological Research, 107(1), 126–138, http://dx.doi.org/10.1017/S0007485316000729.

Grković A., Vujić, A., Radenković, S., **Chroni, A.**, Petanidou, T. (2015) Diversity of the genus *Eumerus* Meigen (Diptera, Syrphidae) on the eastern Mediterranean islands with description of three new species. Annales de la Société Entomologique de France (N.S.), 51(4), 361–373, http://dx.doi.org/10.1080/00379271.2016.1144483.

Conference Contributions

Chroni, A., Djan, M., Obreht Vidaković, D., Vujić, A., Petanidou, T., Šašić Zorić, L., Velićković, N., Kočiš Tubić, N., Tataris, G., Radenković, S. (2017) A DNA barcode library of the Mediterranean species of *Eumerus* (Diptera: Syrphidae) (poster) Proceedings of the 9th International Symposium on Syrphidae, 28 August-01 September, Curitiba, Paraná, Brazil, p. 26–27.

Chroni, A., Djan, M., Obreht, D., Tscheulin, T., Petanidou, T., Vujic, A. (2014) Molecular Systematics of the genus *Eumerus* (Diptera: Syrphidae) in the Aegean Archipelagos (poster). Proceedings of the 7th Congress of the Hellenic Ecological Society, 9-12 October, Mytilene, p. 276.

Chroni, A., Djan, M., Obreht, D., Petanidou, T., Vujic, A. (2014) The validity of COI gene in species identification: The case of the genus *Eumerus* (Diptera: Syrphidae) in Southeastern Europe (poster). Proceedings of the Seventh International Symposium on Molecular Insect Science, 13-16 July, Amsterdam, P3.08.

Acknowledgments

«…I've been in my mind, it's such a fine line. That keeps me searching…»
Neil Young - Heart of Gold

Writing the acknowledgments might have been one of the most difficult things I ever wrote. The last five years involved two countries, many new friends, life changes. And here, it comes to an end this long journey, and all these memories are bringing tears to my eyes. I was granted with luck to meet so many people that trusted me from the first moment, helped me, loved me, shared their time and life with me, and are still standing next to me. How it is possible to thank all and enough?!

At first, I would like to thank my supervisor, Professor Theodora Petanidou, for the immensely trust, advices and scientific guidance that she provided me with since we met in 2011. She was the first person to introduce me to the amazing world of pollinators. Her teaching ability, scientific mind and reason convinced me to choose the so interesting path of research. She taught me that patience, persistence and hard work are the fundamental stones of science. I thank her for the so many late nights she has spent on me, and for her fruitful thoughts.

I genuinely thank from my heart, Professor Ante Vujić, Dr Dragana Obreht-Vidaković and Associate Professor Mihajla Djan (University of Novi Sad, Serbia) for their collaboration, their guidance, their advices, their company and their warm welcome to their laboratory, homes and to their country. All of them, they were always there to patiently listen to whatever question I had, to consult me and share their knowledge with me: Prof. Ante Vujić introduced me to (molecular) taxonomy; Dr Dragana Obreht-Vidaković taught me the laboratory techniques; and Assoc. Prof. Mihajla Djan guided me in the fields of phylogeny and phylogeography. Хвала вам много на свему!

Fieldwork and collection of entomological specimens were conducted from Dr Michael de Courcy, Jelle Devalez, Stavroula Dimitriou, Sofia Margaroni, Kostas Minachilis, Vangelis Mizerakis, Giorgos Nakas, Larry Neokosmidis, Prof. Theodora Petanidou, Dr Antonio Ricarte, Prof. Santos Rojos, Dr Gunilla Ståhls, Panagiotis Tsalkatis, Giannis Vavitsas and Prof. Ante Vujić.

Prof. Ante Vujić, Ana Stefanović Grković, Dr Zorica Nedeljković, Laura Likov (University of Novi Sad, Serbia) and Jelle Devalez (University of the Aegean) were involved in the sorting and identification processes of the entomological specimens.

Assoc. Prof. Mihajla Djan, Dr Nataša Kočiš Tubić, Llilja Šašić Zorić, Dr Dragana Obreht-Vidaković and Assistant Professor Nevena Velicković assisted with DNA analyses.

Ana Stefanović Grković (University of Novi Sad, Serbia) conducted all species morphology descriptions in the Chapters (3) – (5), and she has been a valuable collaborator and my '*Eumerus*' partner the last couple of years. Хвала ти Ana! :)

Dr Jelena Ačanski (BioSens Institute, Serbia) conducted the wing morphometry analyses in the Chapter 5.

Milomir Stefanović (University of Novi Sad, Serbia) shared his knowledge about spatial genetic patterns, and contributed to the Chapter 6. I also thank him for all the scientific and 'supporting' talks we had.

I want to thank all the people from the University of Novi Sad and BioSens Institute (Serbia): Dr Jelena Ačanski, Dr Nataša Kočiš Tubić, Dr Snezana Radenković, Lliljana Šašić Zorić, Ana Stefanović Grković, Milomir Stefanović, Assist. Prof. Nevena Velicković, and many more; it was a pleasure to work and have coffee breaks with you guys! :)

I thank Dr Giorgos Tataris (University of the Aegean) for sharing his knowledge and love about cartography.

My special thanks go also to Dr Dimitrios Avtzis (Hellenic Agricultural Organization 'Demeter') who happily accepted to participate in the Examination Committee of my thesis.

Dr Apostolos Trichas (Natural History Museum of Crete) assisted me to translate the morphological terminology in Greek; thank you.

I thank all people from the Laboratory of Biogeography and Ecology (University of the Aegean), who accompanied me all these years; your friendship and help have been invaluable: Dr Aphrodite Kantsa, Giorgos Nakas, Panagiotis Tsalkatis, Jelle Devalez, Larry Neokosmidis, Vangelis Mizerakis and Stavroula Sotiropoulou.

I own a special thank you to Assistant Professor Thomas Tscheulin (University of the Aegean) for his friendship, talks, camping and gatherings all these years; he has managed many times to supply me with courage.

I thank my friends for being here for quite some time now, for loving me and being patient: Giorgos M., Niki, Aphrodite, Giorgos N., Panalekos, Dusanka, Zdravko, Snežana, Andrijana, Yoka. I also appreciate the great companionship of 'Bobiras'; Vasilis, Manolis, Aristea, and many more. :) My sister Myrsini has supported me all these years, and has been a friend to me. I will never thank enough my friend Christina for the support she has provided me all these years, and for how much she has believed on me; I would never have made it without you. Christos is such a big part of my life, rendering the little things of life, so important. *Još malo*, thank you for your devotion, understanding, encouragement and love you bestowed upon me during my PhD..

My family is supporting me no matter what, since I remember myself; I thank them for being there. I hope that, at the very end, I made them proud of me. Μαμά, Μπαμπά, σας ευχαριστώ πολύ! :)

A.C.
Mytilene, 29 November 2017

Στους γονείς μου και στην Χριστίνα

[...] Σαν έτοιμος από καιρό, σα θαρραλέος,
σαν που ταιριάζει σε που αξιώθηκες μια τέτοια πόλι,
πλησίασε σταθερά προς το παράθυρο,
κι άκουσε με συγκίνησιν, αλλ' όχι
με των δειλών τα παρακάλια και παράπονα,
ως τελευταία απόλαυσι τους ήχους,
τα εξαίσια όργανα του μυστικού θιάσου,
κι αποχαιρέτα την, την Αλεξάνδρεια που χάνεις.

Κ.Π. Καβάφη, Απολείπειν ο θεός Αντώνιον, από τα Ποιήματα 1897-1933

Contents

ABSTRACT

ABSTRACT

The Balkans is considered a hotspot of hoverfly diversity and endemism, and *Eumerus* Meigen, 1822 one of its most species-rich hoverfly genera. Here, the account of a limited number of species within the genus and their geographic distribution in the Balkans (and adjacent regions) were addressed by implementing an integrative taxonomical approach employing morphological characters (viz. wing geometric morphometry), molecular markers (mitochondrial and nuclear DNA), and phylogeographic and biogeographic approaches. MtDNA was adequate to (a) diagnose and delimit species; (b) reveal monophyletic lineages and taxon groups; (c) infer high number of mitochondrial haplotypes; and (d) detect star-like patterns. Integrative taxonomic approach methods lead to identification and description of five new species, revealed one cryptic species complex, resolved one synonymy, revised the geographical range of one species, and suggested that the formation of the mid-Aegean Trench and the Messinian Salinity Crisis were related to speciation processes within a taxon group. Finally, spatial genetic structure analyses inferred the presence of (a) two genetic clusters ascribed to allopatric and peripatric processes, as well as to landscape discontinuities formed due to palaeogeological and palaeoclimatic events; (b) one genetic cluster, pointing to the hypothesis of relict taxa; and (c) high- and low-genetic divergent regions.

Η Βαλκανική Χερσόνησος έχει χαρακτηρισθεί ως θερμό σημείο βιοποικιλότητας και ενδημισμού για την οικογένεια των Συρφίδων, με το γένος *Eumerus* Meigen, 1822 να είναι από τα πλέον πλούσια σε είδη στην περιοχή. Με σκοπό την διερεύνηση ειδών του *Eumerus*, και την γεωγραφική κατανομή τους στην ευρύτερη Βαλκανική, εφαρμόστηκε η μέθοδος της ενοποιητικής ταξινομικής με την χρήση μορφολογικών (π.χ. γεωμετρική μορφομετρία πτερύγων) και μοριακών (μιτοχονδριακό και πυρηνικό DNA) εργαλείων, σε συνδυασμό με μεθόδους φυλογένεσης και φυλογεωγραφίας. Το mtDNA δείχθηκε κατάλληλο για την (α) διάγνωση και οριοθέτηση ειδών, (β) ανάδειξη μονοφυλετικών κλάδων και ομάδων ειδών, (γ) ανίχνευση υψηλού αριθμού μιτοχονδριακών απλοτύπων, και (δ) διάκριση αστεροειδών δομών. Βάσει της ενοποιητικής ταξινομικής, ταυτοποιήθηκαν και περιγράφηκαν πέντε νέα είδη για την επιστήμη, αποκαλύφθηκε ένας κρυπτικός εξελικτικός κλάδος, επιλύθηκε μια συνωνυμία, αναθεωρήθηκε η γεωγραφική εξάπλωση ενός είδους, και αποδείχθηκε

ότι ο σχηματισμός της μεσο-Αιγαιακής Τάφρου και η Κρίσης Αλατότητας Μεσσηνίου σχετίζονται με διεργασίες ειδογένεσης ομάδας ειδών εντός του γένους. Τέλος, οι αναλύσεις χωρικών γενετικών δομών σε εννέα είδη, έδειξαν την ύπαρξη (α) δύο γενετικών ομάδων, πιθανόν λόγω αλλοπατρικών και περιπατρικών διεργασιών ή παλαιογεωλογικών και παλαιοκλιματικών γεγονότων, (β) μιας γενετικής ομάδας, υποδηλώνοντας ότι τα είδη αυτά είναι υπολειμματικά είδη, και γ) περιοχών υψηλής και χαμηλής γενετικής ποικιλότητας.

page intentionally left blank

CHAPTER 1

General Introduction, Scientific objectives & Thesis outline

Molecular systematics and phylogenetics towards species delimitation

The science of taxonomy reflects our way of perception of the diverse units of life as it encompasses identification, description, and nomenclature of species. Taxonomy is often associated with molecular systematics, i.e. the employment of molecular genetics tools to infer phylogenetic relationships among individuals and species, and the use of such information to classify species and to provide insight into an organism's natural history and evolutionary processes. The latter is related to cladistics or phylogenetic systematics, through which a phylogenetic tree is reconstructed based on the affinity and dissimilarity of the share-derived characters of the organisms under study. Phylogenetic trees show the evolutionary, ancestor–descendant relationships among OTUs, and unveil the patterns of relationships among them. Based on the type of data (character states or distance matrix), a variety of phylogenetic trees can be applied with Maximum parsimony, Maximum likelihood and Bayesian inference to pilot (for a thorough review see Yang & Rannala, 2012).

The role of molecular tools in molecular and phylogenetic systematics is invaluable; they have assisted and accelerated species identification, diagnosis of new species, and species delimitation; revealed cryptic species complexes; and shed light into species evolution and biology (Rubinoff, 2006). The most popular molecular tool is the 'DNA barcode', i.e. the retrieval of a short DNA sequence from a standard part of the genome (gene-specific region) of the study specimen (Folmer *et al*., 1994; Hebert *et al*., 2003; Hajibabaei *et al*., 2007). Mitochondrial DNA (mtDNA) has taken precedence over other molecular markers because it is maternally inherited (haploid) lacking recombination, less prone to degradation, easy to isolate and assay (high number of copies with limited sample required), and it is quite variable among individuals (evolution rate is 5-10 times faster than in nuclear DNA) (Avise *et al.*, 1987). MtDNA deficiencies (reduced effective population size and introgression, maternal inheritance, lacking of recombination, inconsistent mutation rate, heteroplasmy and compounding evolutionary processes; Moritz & Cicero, 2004; Rubinoff, 2006) should also be considered when inferring species diagnosis and delimitation, as mtDNA may result to false positive or negative signals when used alone.

In addition to the above, species inference from molecular data transcends over morphological/ physiological traits for several reasons (see Table 1; Graur & Li, 2000). In order to conclude on species delimitation and infer evolutionary

relationships or driving forces of speciation, it is fundamental to use more than one molecular marker or other complementary disciplines. Nowadays, there is a trend to employ an integrative taxonomical approach by employing morphological (e.g. structure of genitalia, wing morphometry), molecular (DNA, RNA and proteins) and biochemical data (e.g. alloenzymes), sometimes vis-à-vis environmental (e.g. temperature) and/or ecological (e.g. habitat use) factors (Dayrat, 2005).

Table 1. Comparative table of molecular vs. morphological/ physiological traits (based on data from Graur & Li, 2000).

Πίνακας 1. Συγκριτικός πίνακας των μοριακών έναντι των μορφολογικών/ φυσιολογικών χαρακτηριστικών (βάσει δεδομένων από τους Graur & Li, 2000).

Molecules	Morphological/ physiological traits
Strictly inherited	May also result due to environmental factors
No	Relies on subjective criteria and scientists may disagree
Evolution is characterized by regularity	No
Quantitative (statistical) analyses	Qualitative (more often) analyses
Easier to deduct apomorphic traits	No
Easier to study evolutionary relationships even between remote organisms	Few morphological characters can offer that
Abundant characters	Not many available characters

Species, speciation and mtDNA phylogeography

What is a species? It is extremely difficult to define the concept of the species so that it applies to all living organisms, as there are numerous species 'concepts', probably even more than 24, major ones referred and explained in Table 2 (Mayr, 1996; Mayden, 1997; De Queiroz, 2007). The phenomenon of confrontation about species delimitation is known as species problem (Mayr, 1957). Scientists accept that 'species' is the basic unit of biological classification and taxonomic rank. The species classification criteria anticipate that individuals of the same species: (a) originate from a common ancestral population (common origin); (b) share similar/ common (molecular and morphological) features; and (c) interbreed and produce fertile offspring (Mayr, 1996).

Speciation events occur often in nature, i.e. the formation of new species from species that become reproductively isolated and eventually, diverge. Based on the type and degree of geographic and reproductive isolation, four types of speciation are

distinguished (Fig. 1a, Lemey *et al.*, 2009): (1) Allopatric speciation occurs when populations are geographically isolated due to a physical barrier, e.g. a mountain or a river. Populations start to adapt to the new environment, and progressively become so different that cannot breed with each other. (2) Peripatric speciation occurs when the populations adjacent, but still geographically isolated; although it resembles allopatric, it differs from this because, here, one population consists of few individuals. (3) Sympatric speciation occurs when within a population there is an instant or progressive reproductive isolation (gene polymorphism) without geographic isolation, e.g. feed in different habitats, interact with different host or mate in different seasons. (4) Parapatric speciation is a sub-type of sympatric, relatively rare to happen, and is due to extreme change in the habitat, e.g. soil contamination in mines due to heavy metals. In this case, the natural selection favors different, rare alleles in two adjacent or parapatric populations, reduces the fitness of the heterozygotes, and eventually leads to selection of reproductive behaviors or mechanisms that prevent the interbreeding of the populations. The founder effect, i.e. the loss of genetic variation within a new population established by a very small number of individuals from a larger population, appears also to play a role in speciation (Fig. 1b; Lemey *et al.*, 2009). The founder effect can cause genotypic and/or phenotypic variations and in extreme cases, to lead to speciation.

In a phylogenetic tree, we can detect monophyletic groups (a clade of an ancestral species and all its descendants), paraphyletic (all the descendants of a common ancestor minus one or more monophyletic groups), and polyphyletic (all the descendants sharing convergent, not inherited from a common ancestor, features or habits) (Fig. 2; Baldauf, 2003). The formation of monophyletic group may indicate either the presence of speciation or events such as population expansion, population bottlenecks, vicariance and migration. The inferred conclusions from phylogenetics and population genetics can be interpreted and integrated in light of the science of mtDNA phylogeography, where micro- and macro-evolutionary phenomena, liable for species geographic distribution, are considered (Avise *et al.*, 1987). Phylogeography encounters great admirers as, by choosing the appropriate molecular marker, the genetic information can be associated to historical processes of a geographic area (palaeoclimatic and palaeogeological events), and interpret and predict the species occurrence and distribution (Hickerson *et al.*, 2010; Chan *et al.*, 2011).

From the biogeography perspective, vicariance and dispersal are the two main processes tightly involved to phylogenetic and phylogeographic inferences. Through the dispersal process, species move spontaneously from their ancestral habitat for a matter e.g. of breeding, while in vicariance, a habitat discontinuity occurs due to a physical barrier e.g. a river, leading to forced species relocations (Crisp & Cook, 2005).

Table 2. Pros and cons of the major concepts of species definition (based on data from De Queiroz, 2007).

Πίνακας 2. Εννοιολογικά πλεονεκτήματα και μειονεκτήματα των βασικών εννοιών σχετικά με τον ορισμό των ειδών (βάσει δεδομένων από τον De Queiroz, 2007).

Species concept	Application	Pros and cons
Biological	Difficult	Works well for most members of the Animalia Kingdom in which strong barriers to interbreeding exist (common gene pool, reproductive isolation); fails to describe hybrids, fossils and species that reproduce asexually.
Phenetic	Common	Identified most species to date; defines species by structural (morphological) features, which reflect, but not always, the real clustering and relationships of the individuals; can be applied to asexual organisms and fossils; problematic with the cryptic species.
Ecological	Difficult	Views a species in terms of its ecological niche.
Phylogenetic	Increasing	Species delimitation can be successfully achieved; no specific statistical threshold

Molecular clock

Molecular divergence time estimations are based on a molecular clock that ticks on a constant rate over time or across phylogenetic lineages (Yang & Rannala, 2012), and can be fast or slow depending on the employed genes. The molecular clock was assumed after the Neutral Theory (Kimura, 1968; 1983) stating the intra- and interspecific variation is due to genetic drift of mutant alleles (neutral mutations) and not to natural selection. According to this hypothesis, each gene or protein with a conservative function to organism can serve to calibrate the molecular clock, with cytochrome c to be the first protein ever used to estimate divergence times (Fitch & Margoliash, 1970).

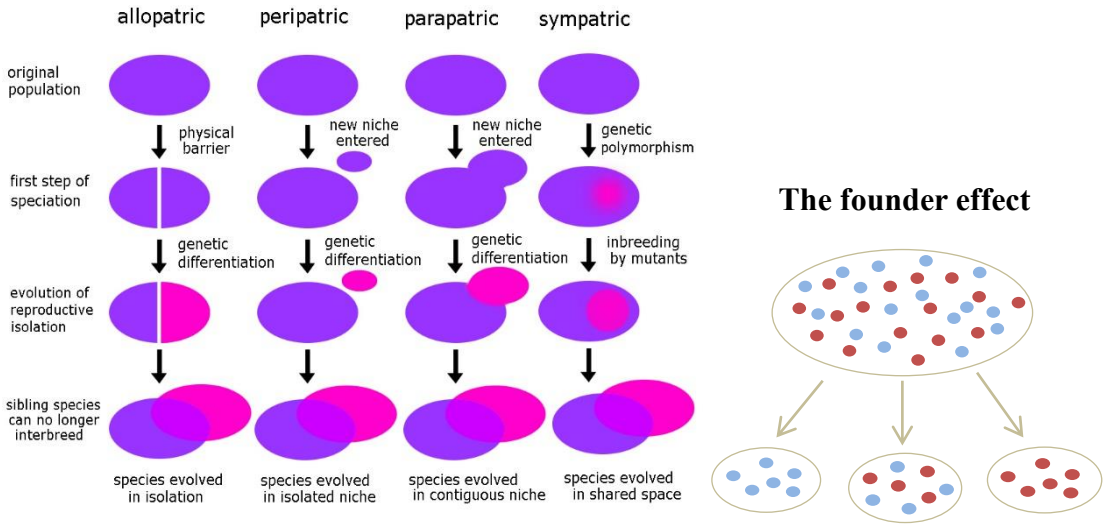

(a) (b)

Fig 1. (a) The different modes of speciation: allopatric, peripatric, parapatric and sympatric; and (b) the founder effect. Figure (a) reproduced from Dr Dana Krempels (included in Lecture notes for Evolution and Biodiversity-BIL 160 Section HJ at University of Miami, Spring 2006) with permission by herself.

Σχήμα 1. (α) Πρότυπα ειδογένεσης: αλλοπάτρια, περιπάτρια, παραπάτρια, συμπάτρια, και (β) η αρχή του ιδρυτή. Το σχήμα (α) προέρχεται από τις σημειώσεις της Δρ Dana Krempels για το μάθημα Εξέλιξη και Βιοποικιλότητα (BIL 160) του Πανεπιστημίου του Μαϊάμι (Άνοιξη 2006), και είναι ελεύθερο δικαιωμάτων σύμφωνα με την ίδια.

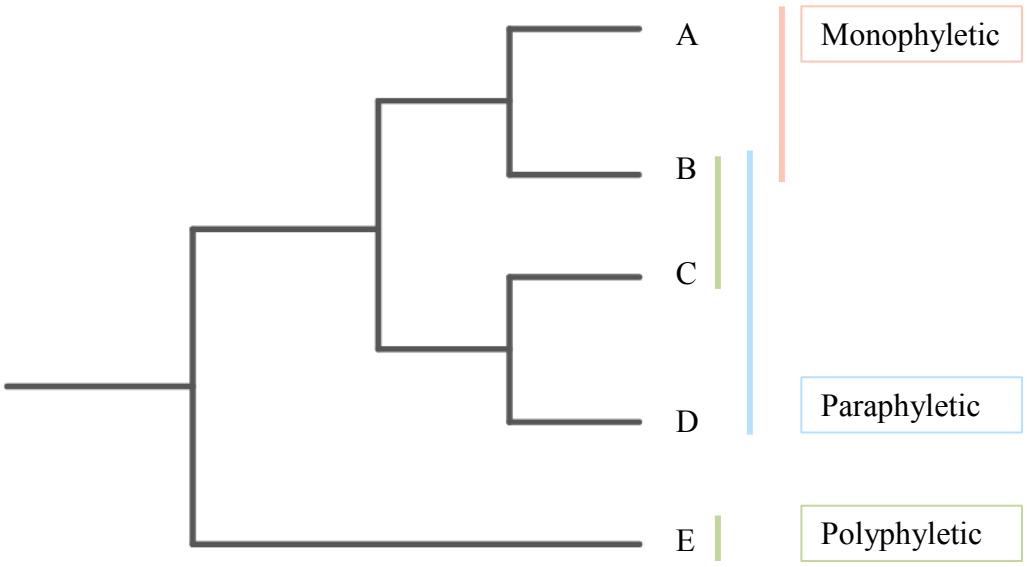

Fig 2. Possible groups encountering in a phylogenetic tree: monophyletic, paraphyletic and polyphyletic.

Σχήμα 2. Σχηματική απόδοση των φυλογενετικών προτύπων της μονοφυλετικότητας, παραφυλετικότητας και πολυφυλετικότητας των taxa.

A mutation rate is required for the calibration, which can be extracted from either a fossil record or a palaeogeographic event. The existence of such a clock has assisted to better comprehend the evolutionary relationships and to correlate them to historic processes, though it has provoked much debate regarding its application as the hypothesis of a mutation rate consistency comes in contrast to e.g. the inconstant evolutionary rate on morphological and physiological aspects (Kimura, 1969; Goodman, 1981), or inconsistencies in divergence time rates on human mtDNA (Howell *et al*., 2007, and references therein) or the relative constant rate observed on proteins' sequences to support the neutrality theory (Kimura, 1969).

Even though the molecular clock is the only approach (when fossils are not available) to track down and see over time an organism's evolutionary history, much attention is required. The choice of the appropriate gene(s), the way the gene(s) are subjected to mutations, and their adequacy as to visualize the molecular clock (whether the chosen gene display or not temporal signal, and therefore, the data are suitable to perform the molecular clock models; Rambaut *et al*., 2016) while considering the wright way of measuring the substitution rate will reassure the validation of as much as possible accurate molecular clock. One should not forget the issues arising from the employment of a universal substitution rate between distant lineages (there are cases of genes evolving with a different mutation rate between lineages e.g. the case of the insulin; King & Jukes, 1969), but rather dispute, and further explore the acquired divergence times in relation to e.g. the palaeogeology of an area (Papadopoulou *et al*., 2010). All these imply that a 'global' molecular clock (where substitution rate is constant over time and all lineages share the same rate) does not exist, but rather a 'local' one, where rate shifts infrequently over the tree (closely related lineages have equivalent rates).

The genus *Eumerus* (Diptera: Syrphidae) as study model

Hoverflies or flower flies (Diptera: Syrphidae) is an insect group notable for its species diversity, encompassing four subfamilies (Microdontinae, Eristalinae, Pipizinae and Syrphinae; Fig. 3 from Young *et al.*, 2016), 200 genera and more than 6100 species recorded worldwide (Thompson *et al*., 2010). The family is common throughout the world, and can be found in all continents except Antarctica. Hoverflies provide substantial ecosystem services as pollinators in a wide range of flowering

plants, predators of plant pests, herbivores and effective nutrient recyclers from dead matter (Rotheray & Gilbert, 2011).

Study group in the present dissertation is the genus *Eumerus* Meigen, 1822 (Diptera: Syrphidae: Eristalinae: Merodontini). The genus is widely distributed in Palaearctic, Afrotropical, Oriental and Australian regions (Stackelberg, 1961), recently imported also to Nearctic and Neotropical regions through commercialized import of plant bulbs (Marinoni & Morales, 2007). There are 256 *Eumerus* species worldwide (Pape & Thompson, 2015) of which 140 occur in the Palaearctic; among the latter 75 species are encountered in Europe, the majority of them occurring in the southern regions (Doczkal, 1996; Chroni *et al.*, unpubl.; Grković *et al.*, 2015, 2017; Markov *et al.*, 2016; Speight *et al.*, 2016; Grković, in prep.). It is worth mentioning that many of these species were described only recently or will be described soon, which explains the rapid increase of their species number known for Europe (i.e. 50 species according to Speight *et al.*, 2016).

One of the main difficulties in studying the genus is the successful diagnosis and delimitation of the included species, caused by the lack of updated identification keys for European species, and to existing obscurities regarding nomenclature including synonymies (Peck, 1988). The only existing comprehensive key for *Eumerus* is that of Stackelberg (1961), which is based on a fraction only of the Palaearctic taxa. From the morphological viewpoint, species of *Eumerus* vary a lot: small to medium-sized, blackish or reddish, often with white or black markings on tergites, and with a distinctive habitus showing strong metalegs and a narrow or broadly oval abdomen (for more details see Grković *et al*., 2015; Doczkal *et al*., 2016).

Up to the present dissertation, there was a limited study focus on *Eumerus*, mainly oriented to taxonomic and ecological viewpoints (Ricarte *et al*., 2008, 2012, 2013; Doczkal & Pape, 2009; Speight *et al*., 2013). For example, studies were focused on life cycle and habitat preferences of *Eumerus* species, revealing e.g. restriction to larval dependence on plant underground storage organs (Ricarte *et al.*, 2008 and references therein) or adults usual preference for warm and sunny places for resting, while visiting flowers (Apiaceae, Asteraceae, Euphorbiaceae and Ranunculaceae; Speight, 2016). On the contrary, other hoverfly genera, such as *Merodon* Meigen, 1803 (Milankov *et al.*, 2008a, b; Ståhls *et al*., 2009; Šašić *et al*., 2016), *Cheilosia* Meigen, 1838 (Ståhls *et al*., 2004; Milankov *et al*., 2010a, b), *Chrysotoxum* Meigen, 1803 (Nedeljković *et al*., 2013) and tribe Pipizini (Vujić *et al*., 2013), are more

thorough studied from molecular, morphological and phylogeographic aspects by using multiple disciplines, e.g. mtDNA and/or nuclear gene fragments, alloenzymes, wing morphometry. Therefore, recent studies on *Eumerus* (Doczkal & Pape, 2009; Speight *et al.*, 2013; Chroni *et al.*, 2017; unpubl.) have also implemented multiple disciplines under the service of *Eumerus*, e.g. DNA barcoding, wing morphometry,

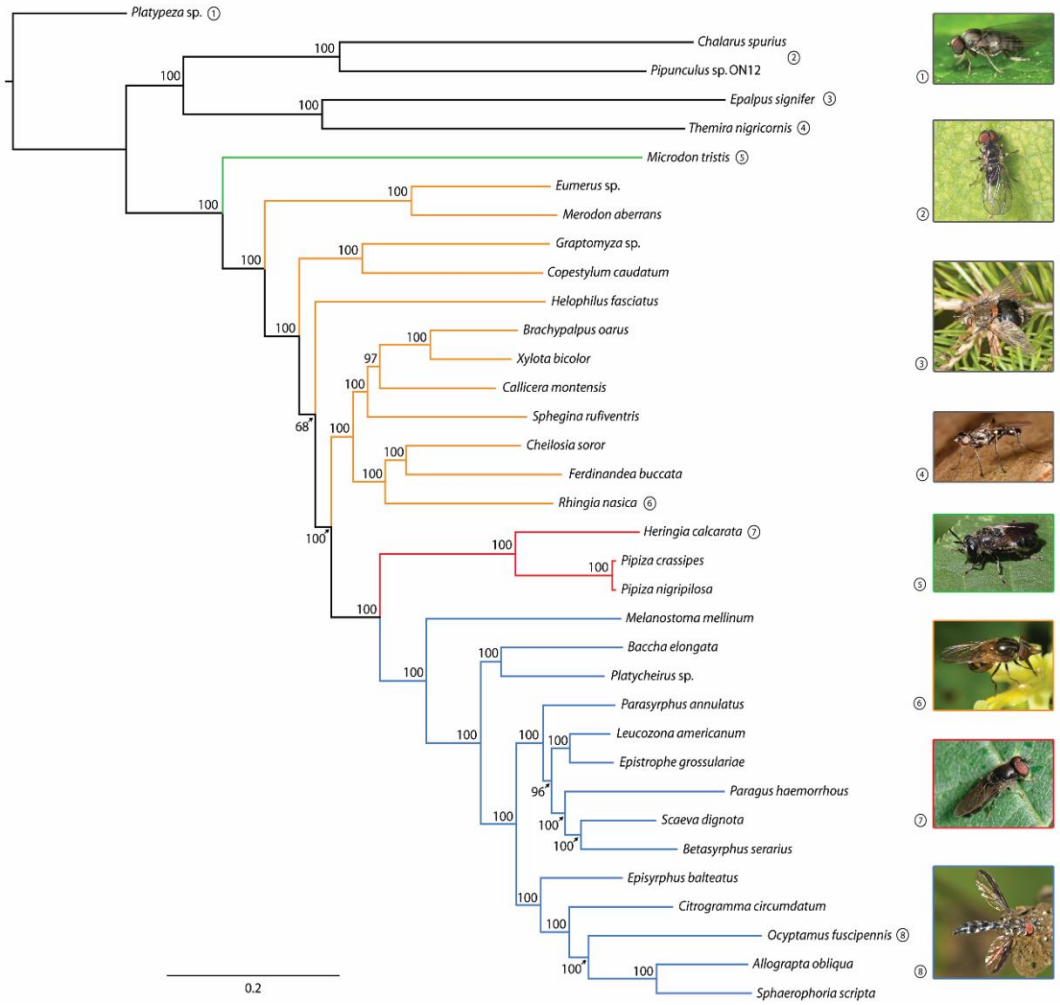

Fig. 3. A Maximum likelihood tree that shows the phylogenetic position of the subfamilies within the hoverflies; outgroups (black), Microdontinae (green), Eristalinae (orange), Pipizinae (red) and Syrphinae (blue). Bootstrap support values are depicted above the nodes. The phylogenetic method employed was RAxML under the model GTR+G. Figure reproduced from Young *et al.* (2016) with permission by the corresponding author.

Σχήμα 3. Δέντρο μέγιστης πιθανοφάνειας (ML), το οποίο δείχνει την φυλογενετική θέση των υπο-οικογενειών των συρφίδων: εξωομάδα (μαύρο), Microdontinae (πράσινο), Eristalinae (πορτοκαλί), Pipizinae (κόκκινο) και Syrphinae (μπλέ). Δίνεται η στατιστική υποστήριξη των κλάδων (με την μέθοδο Bootstrap, πάνω από τους κλάδους). Χρησιμοποιήθηκε η φυλογενετική μέθοδος RAxML υπό το νουκλεοτιδικό μοντέλο GTR+G. Το σχήμα προέρχεται από τους Young *et al.* (2016), και είναι ελεύθερο δικαιωμάτων σύμφωνα με τον αντεπιστέλλων συγγραφέα.

phylogeography, which have indicated the existence of monophyly and of several taxon groups (groups of species morphologically and genetically similar) as well as several new species and one cryptic species complex within the genus. All aforementioned findings on *Eumerus* indicate for an urge investigation and genus revision, where species identification, nomenclature clarifications, and insights about speciation processes will be granted.

Balkans, the study area

Study area of this dissertation is the Balkan Peninsula (hereinafter the Balkans) including the Aegean Archipelago, and adjacent countries within the Mediterranean Basin (hereinafter Mediterranean). To discuss the Balkans species-richness and its drivers, one must first consider the geographical context the Balkans are placed, i.e. the Mediterranean. The contemporary species distribution of the Mediterranean is often referred as the outcome of the special palaeogeography, and unique location in the crossroad of three continents (Africa, Asia and Europe). Two major palaeogeological events shaped the Basin: (1) continuous collision of the African and the European tectonic plates, with (2) simultaneous eastward displacement of the Anatolian plate, driven from the northward displacement of the Arabian plate, with the latter causing in turn a fan-like expansion of the Aegean southward (Fassoulas, 2000; Lymberakis & Poulakakis, 2010).

The Balkans were connected to Anatolia through the Hellenic Peninsula, a united region called Ägäis at mid-Miocene (~ 16-12 Mya; Philippson, 1898). At the onset of the mid-Miocene, Ägäis was connected to Asia and Central Europe, and through land bridges, species relocations were facilitated (Steininger & Rögl, 1984). Four geological events that occurred between Miocene (23 Mya) and Holocene (0.0117 Mya) are responsible for the fragmentation of Ägäis and the consolidation of the region in its present form, including the islands of the Aegean Archipelago: (1) the formation of the mid-Aegean Trench (MAT) in the middle Miocene (12–9 Mya), (2) the Messinian Salinity Crisis (MSC) in the late Miocene (5.96–5.33 Mya), (3) an extensive segregation and widening of the Aegean Sea and the separation of Karpathos–Kassos island group from Rhodos in the Pliocene (5–2 Mya), and (4) orogenetic and eustatic sea-level changes during the Pleistocene (2-0 Mya) (Dermitzakis, 1990; Perissoratis and Conispoliatis, 2003; Lymberakis & Poulakakis, 2010; Kougioumoutzis et al., 2017; Sfenthourakis & Triantis, 2017).

Anatolia, in the east, is also a significant neighbor of the Balkans and the Aegean. It is located among three acknowledged global biodiversity hotspots (viz. Caucasus, the Irano-Anatolian hotspot and the Mediterranean; Myers *et al*., 2000), encompassing significant mountain ranges: the Western Anatolian, the Taurus ranges in the south, the Northern Anatolian, and the Anatolian Diagonal running from the northeast to the Mediterranean (Şekercioğlu *et al*., 2011). These mountains have sheltered Mediterranean species during glaciations, with Western Anatolia, Taurus and Amanus being the main ones (Médail & Diadema, 2009), while the Anatolian Diagonal constituted a dispersal corridor for many plant and animal species (Davis, 1971; Ansell *et al*., 2011). Indeed, Anatolia has been regarded as the potential biodiversity center for several biota including bats (Furman *et al*., 2010), insects (Çiplak *et al*., 1993; Rokas *et al*., 2003; Dapporto, 2010; Çoruh *et al*., 2014; Mutun, 2016), reptiles (Veith *et al*., 2003; Joger *et al*., 2007; Akin *et al*., 2010), fungi (Sesli & Denchev, 2008), shrews (Dubey *et al*., 2006, 2007) and plants (Biltekin *et al*., 2015).

The palaeoclimatic events from the Cenozoic until the Holocene Period have also played a major role in speciation and species distribution within the study area (Blondel *et al*., 2010; Feliner, 2014; Vogiatzakis *et al*., 2016). There were continuous climate alternations (coolings and warmings), stabilized and shaped to their present form after the Last Glacial Maxima (for a thorough review see Hewitt, 2011). Many phylogeographic studies have pointed out the Balkans as the major source of postglacial colonization of Central and Northern Europe, which engendered and contributed to the species diversity of the Peninsula (including cryptic and endemics; Poulakakis *et al*., 2015 and references therein). As regards the genus *Eumerus*, the Balkans is very species-rich, with new species being described and cryptic species complexes recorded (e.g. Chroni *et al.*, unpubl.; Grković *et al.*, 2015).

Another factor that enhanced the biodiversity of the study area is the alterations of the topographic relief. An example is the impact of the continuous collision of the African northwards, which resulted to great orogenesis and generated the Dinaric Alps, Mts Pindus, Mts Taurus etc. In addition, the occurred erosions of the climatic oscillations during the Late Cenozoic caused uplifts of the relief, and eventually shaped it (Westaway *et al*., 2009).

Finally, the great impact of human's presence and life on the Mediterranean must be considered when accounting for studies related to e.g. biodiversity, ecosystems etc. The location of the region as well as the Mediterranean Sea facilitated the interaction

between diverse civilizations, the formation of new settlements, and the trade development. As a consequence, the Mediterranean endured landscape and ecosystems' alterations in a great scale from human, and in many ways; hunting, agriculture, livestock, deforestation (and soil degradation), active or passive transport of plant or animal species to name a few (Blondel, 2006).

All the aforementioned factors have led to the formation of the Mediterranean peninsulas of Iberia, Italy and the Balkans, and isolation of Anatolia, each region with its own different, diverse and complex geological history, landscape and species distribution. These landscape discontinuities are granted for species divergence, speciation and ultimately, for today's high species diversity and endemism. All in all they have rendered the Mediterranean as one of the 36 global hotspots (Myers *et al.*, 2000; CEPF.net-The Biodiversity Hotspots, www.cepf.net).

Scientific objectives and emerging questions of the thesis

In the current dissertation, the genus *Eumerus* is studied for the first time from the perspective of molecular taxonomy, phylogenetics and phylogeography. More specifically, the main aim is to address the account of a limited number of species within the genus and their geographic distribution in the Balkans by implementing an integrative approach of morphological characters (male genitalia, antenna segments etc), molecular markers (viz. two fragments of the mitochondrial cytochrome-c oxidase subunit I gene, COI; one fragment of the nuclear 28S D2 ribosomal DNA gene, 28S), wing geometric morphometry as well as in combination with phylogeographic and biogeographic approaches. Directed by the above framework, the dissertation seeks to answer questions related to the genus phylogeny and phylogeography, as well as to the historic processes accounted for the inferred evolutionary and biogeographic relationships in the Balkans. In pursuit of the above goal, the emerging questions and objectives of the dissertation are:

1. Are the mitochondrial COI sequences sufficient to achieve species diagnosis and delimitation within the genus *Eumerus*? Is the inclusion of morphological features meaningful regarding the species identification?
2. Can the molecular markers (COI, 28S) detect cryptic species complexes and indicate evolutionary forces that have led to the observed biogeographic patterns and speciation processes?

3. Are there spatial patterns of genetic diversity within *Eumerus*? What is the role of the landscape discontinuities (e.g. mountain), isolation by distance, palaeogeological events or palaeoclimatic alterations on the observed spatial genetic patterns?

All results and conclusions stemming from the above questions will (a) assist to the taxonomic revision of the genus *Eumerus*, (b) encourage the study on *Eumerus* in the Mediterranean Basin and worldwide, (c) enhance and contribute general hoverfly research (e.g. ecology and biogeography), and (d) determine the status within the genus *Eumerus*, as to the level of endemism, and conservation priorities in area.

Thesis outline

The following chapters sought to answer the abovementioned questions. As the species diagnosis and delimitation within the genus *Eumerus* has been proven a challenge, Chapter (2) explores the effectiveness of a molecular identification system employed to assist with species diagnosis and delimitation of the genus. Chapters (3) – (4) display the practical potential of such a molecular identification system to delimit (new) species, resolve synonymies and revise the range of one species of *Eumerus*, and account for a more integrative approach. Chapter (5) discourses the use of integrative taxonomy on the detection of cryptic species complexes within *Eumerus*, and the correlation of phylogeographic inferences to the speciation processes. Finally, Chapter (6) is a broad- and large-scale data analysis on the hoverfly genus *Eumerus* and considers for the intraspecific genetic differentiation in relevance of phylogeography and historical biogeography.

References

Akin, Ç., Can Bilgin, C., Beerli, P., Westaway, R., Ohst, T., Litvinchuk, S.N., Uzzell, T., Bilgin, M., Hotz, H., Guex, G.D. & Plötner, J. (2010) Phylogeographic patterns of genetic diversity in eastern Mediterranean water frogs were determined by geological processes and climate change in the Late Cenozoic. *Journal of Biogeography*, 37 (11), 2111–2124.

Ansell, S.W., Stenøien, H.K., Grundmann, M., Russell, S.J., Koch, M.A., Schneider, H. & Vogel, J.C. (2011) The importance of Anatolian mountains as the cradle of global diversity in *Arabis alpina*, a key arctic-alpine species. *Annals of Botany*, 108, 241–252.

Avise, J.C., Arnold, J., Ball, R.M., Bermingham, E., Lamb, T., Neigel, J.E., Reeb, C.A. & Saunders, N.C. (1987) Intraspecific phylogeography: the mitochondrial DNA bridge between population genetics and systematics. *Annual Review of Ecology, Evolution, and Systematics*, 18, 489–522.

Baldauf, S.L. (2003) Phylogeny for the faint of heart: a tutorial. *TRENDS in Genetics*, 19 (6), 345–351.
Biltekin, D., Popescu, S.M., Suc, J.P., Quézel, P., Jiménez-Moreno, G., Yavuz, N. & Çağatay, M.N. (2015) Anatolia: a long-time plant refuge area documented by pollen records over the last 23million years. *Review of Palaeobotany and Palynology*, 215, 1–22.
Blondel, J. (2006) The 'design'of Mediterranean landscapes: a millennial story of humans and ecological systems during the historic period. *Human Ecology*, 34(5), 713–729.
Blondel, J., Aronson, J., Bodiou, J.-Y. & Boeuf, G. (2010) The Mediterranean Region Biological Diversity in Space and Time. USA: Oxford University Press. p. 392.
Chan, L.M., Brown, J.L. & Yoder, A.D. (2011) Integrating statistical genetic and geospatial methods brings new power to phylogeography. *Molecular phylogenetics and evolution*, 59 (2), 523–537.
Chroni, A., Djan, M., Vidaković, D.O., Petanidou, T. & Vujić, A. (2017) Molecular species delimitation in the genus *Eumerus* (Diptera: Syrphidae). *Bulletin of the Entomological Research*, 107(1), 126–138.
Çiplak, B., Demirsoy, A. & Bozcuk, A.N. (1993) Distribution of Orthoptera in relation to the Anatolian Diagonal in Turkey. *Articulata*, 8(1), 1–20.
Crisp, M.D. & Cook, L.G. (2005) Do early branching lineages signify ancestral traits?. *Trends in Ecology & Evolution*, 20 (3), 122–128.
Çoruh, S., Kolarov, J. & Özbek, H. (2014) The fauna of *Ichneumonidae* (Hymenoptera) of eastern Turkey with zoogeographical remarks and host data. *Journal of Insect Biodiversity*, 2(16), 1–21.
Dapporto, L. (2010) Speciation in Mediterranean refugia and post-glacial expansion of *Zerynthia polyxena* (Lepidoptera, Papilionidae). *Journal of Zoological Systematics and Evolutionary Research*, 48(3), 229–237.
Dayrat B. (2005) Towards integrative taxonomy. *Biological Journal of the Linnean Society*, 85, 407–415.
Davis, P.H. (1971) Distribution patterns in Anatolia with particular references to endemism in Plant life of south-west Asia (eds. Davis, P. H., Harper, P. C. & Hedge, I. C.) 15–27 (Botany Society of Edinburgh).
Dermitzakis, D.M. (1990) Paleogeography, geodynamic processes and event stratigraphy during the late Cenozoic of the Aegean area. *Academia Nazionale Lincei*, 85, 263–288.
De Queiroz, K. (2007) Species concepts and species delimitation. *Systematic Biology*, 56, 879–886.
Doczkal, D. (1996) Description of two new species of the genus *Eumerus* Meigen (Dipt., Syrph.) from Corsica. *Volucella*, 2, 3–19.
Doczkal, D. & Pape, T. (2009) *Lyneborgimyia magnifica* gen. et sp. n. (Diptera: Syrphidae) from Tanzania, with a phylogenetic analysis of the Eumerini using new morphological characters. *Systematic Entomology*, 34 (3), 559–573, http://dx.doi.org/10.1111/j.1365-3113.2009.00478.x.
Doczkal, D., Radenković, S., Lyneborg, L. & Pape, T. (2016) Taxonomic revision of the Afrotropical genus *Megatrigon* Johnson, 1898 (Diptera: Syrphidae). *European Journal of Taxonomy*, 238, 1–36, http://dx.doi.org/10.5852/ejt.2016.238.
Dubey, S., Cosson, J.F., Vohralik, V., Krystufek, B., Diker, E. & Vogel, P. (2007) Molecular evidence of Pleistocene bidirectional faunal exchange between Europe and the Near East: the case of the bicoloured shrew (*Crocidura leucodon*, Soricidae). *Journal of evolutionary biology*, 20 (5), 1799–1808.
Dubey, S., Zaitsev, M., Cosson, J.F., Abdukadier, A. & Vogel, P. (2006) Pliocene and Pleistocene diversification and multiple refugia in a Eurasian shrew (*Crocidura suaveolens* group). *Molecular phylogenetics and evolution*, 38(3), 635–647.
Fassoulas, C. (2000) Field guide to the geology of Crete (in Greek). Heraklion: Natural History Museum of Crete, University of Crete.
Feliner, G.N. (2014) Patterns and processes in plant phylogeography in the Mediterranean Basin. A review. *Perspectives in Plant Ecology, Evolution and Systematics*, 16 (5), 265–278.

Fitch, W.M. & Margoliash, E. (1970) The usefulness of amino acid and nucleotide sequences in evolutionary studies. *Journal of Evolutionary Biology*, 4, 67–109.

Folmer, O., Black, M., Hoeh, W., Lutz, R. & Vrijenhoek, R. (1994) DNA primers for amplification of mitochondrial cytochrome c oxidase subunit I from diverse metazoan invertebrates. *Molecular Marine Biology and Biotechnology*, 3, 294–299.

Furman, A., Postawa, T., Öztunç, T. & Çoraman, E. (2010) Cryptic diversity of the bent-wing bat, *Miniopterus schreibersii* (Chiroptera: Vespertilionidae), in Asia Minor. *BMC evolutionary biology*, 10 (1), 121.

Goodman, M. (1981) Globin evolution was apparently very rapid in early vertebrates. A reasonable case against the rate-constancy hypothesis. *Journal of Molecular Evolution*, 17, 114–120.

Graur, D. & Li, W.H. (2000) Fundamentals of Molecular Evolution. Sinauer Associates, Sunderland, Massachusetts.

Grković, A., Vujić, A., Radenković, S., Chroni, A. & Petanidou, T. (2015) Diversity of the genus *Eumerus* Meigen (Diptera, Syrphidae) on the eastern Mediterranean islands with description of three new species.*Annales de la Société Entomologique de France*, 51, 361–373.

Grković, A., Vujić, A., Chroni, A., van Steenis, J., Đan, M. & Radenković, S. (2017) Taxonomy and systematics of three species of the genus *Eumerus* Meigen, 1822 (Diptera: Syrphidae) new in southeastern Europe. *Zoologischer Anzeiger*, 270, 176–192, https://doi.org/10.1016/j.jcz.2017.10.007.

Hajibabaei, M., Singer, G.A., Hebert, P.D. & Hickey, D.A. (2007) DNA barcoding: how it complements taxonomy, molecular phylogenetics and population genetics. *TRENDS in Genetics*, 23 (4), 167–172.

Hebert, P.D.N., Cywinska, A., Ball, S.L. & DeWaard, J.R. (2003) Biological identifications through DNA barcodes. *Proceedings of the Royal Society B – Biological Sciences*, 270, 313–321.

Hewitt, G.M. (2011) Mediterranean Peninsulas: The Evolution of Hotspots. In: Zachos F., Habel J. (eds) Biodiversity Hotspots. Springer, Berlin, Heidelberg.

Hickerson, M.J., Carstens, B.C., Cavender-Bares, J., Crandall, K.A., Graham, C.H., Johnson, J.B., Rissler, L., Victoriano, P.F. & Yoder, A.D. (2010) Phylogeography's past, present, and future: 10 years after. *Molecular Phylogenetics and Evolution*, 54 (1), 291–301.

Howell, N., Elson, J.L., Howell, C. &Turnbull, D.M. (2007) Relative rates of evolution in the coding and control regions of African mtDNAs. *Molecular Biology and Evolution*, 24, 2213–2221.

Joger, U., Fritz, U., Guicking, D., Kalyabina-Hauf, S., Nagy, Z.T. & Wink, M. (2007) Phylogeography of western Palaearctic reptiles–Spatial and temporal speciation patterns. *Zoologischer Anzeiger-A Journal of Comparative Zoology*, 246 (4), 293–313.

Kimura, M. (1968). Evolutionary rate at the molecular level. *Nature*, 217, 624–626.

Kimura, M. (1969) The rate of evolution considered from the standpoint of population genetics. *Proceedings of the National Academy of Sciences*, 78, 454–458.

Kimura, M. (1983) The Neutral Theory of Molecular Evolution. Cambridge, UK: Cambridge University Press.

King, J.L. & Jukes, T.H. (1969) Non-darwinian evolution. *Science*, 164 (3881),788–798.

Kougioumoutzis, K., Valli, A.T., Georgopoulou, E., Simaiakis, S., Triantis, K.A. & Trigas, P. (2017) Network biogeography of a complex island system: the Aegean archipelago revisited. *Journal of Biogeography*, 44(3), 651–660.

Lemey, P., Salemi, M. & Vandamme, A.M. (2009) The Phylogenetic Handbook: a Practical Approach to Phylogenetic Analysis and Hypothesis Testing,(eds.). Published by Cambridge University Press. pp. 751.

Lymberakis, P. & Poulakakis, N. (2010) Three continents claiming an archipelago: the evolution of Aegean's herpetofaunal diversity. *Diversity*, 2(2), 233–255.

Marinoni, L. & Morales, M. (2007) The second record of the Genus *Eumerus* Meigen, 1822 (Diptera: Syrphidae) for the neotropical region and the first for Brazil. *Proceedings of the Entomological Society of Washington*, 109, 493–495.

Markov, Z., Nedeljković, Z., Ricarte, A., Vujić, A., Jovičić, S., Józan, Z., Mudri-Stojnić, S., Radenković, S. & Ćetković, A. (2016) Bee (Hymenoptera: Apoidea) and hoverfly (Diptera: Syrphidae) pollinators in Pannonian habitats of Serbia, with a description of a new *Eumerus* Meigen species (Syrphidae). *Zootaxa*, 4154 (1), 027–050.

Mayden, R.L. (1997) A hierarchy of species concepts: The denouement in the saga of the species problem. Pages 381–424 in Species: The units of biodiversity (M. F. Claridge, H. A. Dawah, and M. R. Wilson, eds.). Chapman and Hall, London.

Mayr, E. (1957) Species concepts and definitions, in E. Mayr (ed.), The Species Problem. Amer. Assoc. Adv. Sci., Publ. No. 50.

Mayr, E. (1996). What is a species, and what is not?. *Philosophy of science*, 63 (2), 262–277.

Médail, F. & Diadema, K. (2009) Glacial refugia influence plant diversity patterns in the Mediterranean Basin. *Journal of Biogeography*, 36, 1333–1345.

Milankov, V., Francuski, L., Ludoški, J., Ståhls, G. & Vujić, A. (2010a) Estimating genetic and phenotypic diversity in a northern hoverfly reveals lack of heterozygosity correlated with significant fluctuating asymmetry of wing traits. *Journal of Insect Conservation*, 14, 77–88.

Milankov, V., Francuski, L., Ludoški, J., Ståhls, G. & Vujić, A. (2010b) Genetic structure and phenotypic diversity of two northern populations of *Cheilosia* aff. *longula* (Diptera: Syrphidae) has implications for evolution and conservation. *European Journal of Entomology*, 107, 305–315.

Milankov, V., Ståhls, G., Stamenković, J. & Vujić, A. (2008a) Genetic diversity of populations of *Merodon aureus* and *M. cinereus* species complexes (Diptera, Syrphidae): integrative taxonomy and implications for conservation priorities on the Balkan Peninsula. *Conservation Genetics*, 9, 1125–1137.

Milankov, V., Ståhls, G. & Vujić, A. (2008b) Molecular diversity of populations of the *Merodon ruficornis* group (Diptera, Syrphidae) on the Balkan Peninsula. *Journal of Zoological Systematics and Evolutionary Research*, 46, 143–152.

Moritz, C. & Cicero, C. (2004) DNA barcoding: promise and pitfalls. *PLoS Biology* 2, 1529–1531.

Mutun, S. (2016) Review of oak gall wasps phylogeographic patterns in Turkey suggests a main role of the Anatolian diagonal. *Turkish Journal of Fore*stry, 17, 1–6.

Myers, N., Mittermeier, R., Fonseca, G. & Kent, J. (2000) Biodiversity hotspots for conservation priorities. *Nature*, 403, 853–858.

Nedeljković, Z., Ačanski, J., Vujić, A., Obreht, D., Dan, M., Ståhls, G. & Radenković, S. (2013) Taxonomy of *Chrysotoxum festivum* Linnaeus, 1758 (Diptera: Syrphidae) – an integrative approach. *Zoological Journal of the Linnean Society*, 169, 84–102.

Papadopoulou, A., Anastasiou, I. & Vogler, A.P. (2010) Revisiting the insect mitochondrial molecular clock: the mid-Aegean trench calibration. *Molecular Biology and Evolution*, 27, 1659–1672

Pape, T. & Thompson, F.C. (Eds) (2015) Systema Dipterorum. Version 1.5. Available online at http://www.diptera.org/.

Peck, L.V. (1988) Syrphidae. In: Soos A, Papp L, editors. Catalogue of Palaearctic Diptera. Akadémiai Kiadó: Budapest; p. 11–230.

Perissoratis, C. & Conispoliatis, N. (2003) The impacts of sea-level changes during latest Pleistocene and Holocene times on the morphology of the Ionian and Aegean seas (SE Alpine Europe). *Marine Geology*, 196, 145–156.

Philippson, A. (1898) La tectonique de l'Egéide. *Annales de Géographie*, 112–141.

Poulakakis, N., Kapli, P., Lymberakis, P., Trichas, A., Vardinoyiannis, K., Sfenthourakis, S. & Mylonas, M. (2015) A review of phylogeographic analyses of animal taxa from the Aegean and surrounding regions. *Journal of Zoological Systematics and Evolutionary Research*, 53, 18–32.

Rambaut, A., Lam, T.T., Carvalho, L.M. & Pybus, O.G. (2016) Exploring the temporal structure of heterochronous sequences using TempEst (formerly Path-O-Gen). *Virus Evolution*, 2 (1), vew007.

Ricarte, A., Marcos-García, M.Á. & Rotheray, G.E. (2008) The early stages and life histories of three *Eumerus* and two *Merodon* species (Diptera: Syrphidae) from the Mediterranean region. *Entomologica Fennica*, 19, 129–141.

Ricarte, A., Nedeljković, Z., Rotheray, G.E., Lyszkowski, R.M., Hancock, E.G., Watt, K., Hewitt, S.M., Horsfield, D. & Wilkinson, G. (2012) Syrphidae (Diptera) from the Greek island of Lesvos, with description of two new species. *Zootaxa*, 3175, 1–23.

Ricarte, A., Quinto, J., Speight, M.C. & Marcos-García, M.A. (2013) A contribution to knowledge of the biodiversity of Syrphidae (Diptera) in Spain. *Archives of Biological Sciences*, 65 (4), 1533–1537.

Rokas, A., Atkinson, R.J., Webster, L., Csóka, G. & Stone, G.N. (2003) Out of Anatolia: longitudinal gradients in genetic diversity support an eastern origin for a circum-Mediterranean oak gallwasp *Andricus quercustozae*. *Molecular Ecology*, 12 (8), 2153–2174.

Rotheray, G.E. & Gilbert, F. (2011) The Natural History of Hoverflies. UK, Ceredigion.

Rubinoff, D. (2006) Utility of mitochondrial DNA barcodes in species conservation. *Conservation Biology*, 20, 1026–1033.

Šašić, L., Ačanski, J., Vujić, A., Ståhls, G., Radenković, S., Milić, D., Vidaković, D.O. & Đan, M. (2016) Molecular and Morphological Inference of Three Cryptic Species within the *Merodon aureus* Species Group (Diptera: Syrphidae). *PLoS ONE* 11 (8): e0160001.

Şekercioğlu, Ç.H., Anderson, S., Akçay, E., Bilgin, R., Can, Ö.E., Semiz, G., Tavşanoğlu, Ç., Yokeş, M.B., Soyumert, A., Ipekdal, K. & Sağlam, İ.K. (2011) Turkey's globally important biodiversity in crisis. *Biological Conservation*, 144 (12), 2752–2769.

Sesli, E. & Denchev, C.M. (2008) Checklists of the myxomycetes, larger ascomycetes, and larger basidiomycetes in Turkey. *Mycotaxon*, 106, 65.

Sfenthourakis, S. & Triantis, K.A. (2017) The Aegean archipelago: a natural laboratory of evolution, ecology and civilisations. *Journal of Biological Research-Thessaloniki*, 24, 4.

Speight, M.C.D. (2016) Species accounts of European Syrphidae (Diptera). Syrph the Net, the database of European Syrphidae. Dublin. 93: Syrph the Net publications p. 288.

Speight, M.C.D., Hauser, M. & Withers, P. (2013) *Eumerus narcissi* Smith (Diptera, Syrphidae), presence in Europe confirmed, with a redescription of the species. *Dipterists Digest*, 20, 17–23.

Stackelberg, A.A. (1961) Palaearctic species of the genus *Eumerus* Mg. (Diptera, Syrphidae). *Trudy Vsesojuznogo Entomologiceskogo Obscestva*, 48, 181–229.

Ståhls, G., Stuke, J.H., Vujić, A., Doczkal, D. & Muona, J. (2004) Phylogenetic relationships of the genus *Cheilosia* and the tribe Rhingiini (Diptera, Syrphidae) based on morphological and molecular characters. *Cladistics – the International Journal of the Willi Hennig Society*, 20, 105–122.

Ståhls, G., Vujić, A., Pérez-Bañón, C., Radenković, S., Rojo, S. & Petanidou, T. (2009) COI barcodes for identification of *Merodon* hoverflies (Diptera, Syrphidae) of Lesvos Island, Greece. *Molecular Ecology Resources*, 9, 1431–1438.

Steininger, F.F. & Rögl, F. (1984) Paleogeography and palinspastic reconstruction of the Neogene of the Mediterranean and Paratethys. Geological Society, London, Special Publications, 17 (1), 659–668.

Thompson, F.C., Rotheray, G.E. & Zimbado, M.A. (2010) Syrphidae (flower flies), in: Brown, B.V., Borkent, A., Cumming, J.M., Wood, D.M., Woodley, Norman, E. & Zumbado, M.A. (Eds.), Manual of Central American Diptera. Ottawa, NRC Research Press. pp. 763–792.

Veith, M., Schmidtler, J.F., Kosuch, J., Baran, I. & Seitz, A. (2003) Palaeoclimatic changes explain Anatolian mountain frog evolution: a test for alternating vicariance and dispersal events. *Molecular Ecology*, 12 (1), 185–199.

Vogiatzakis, I.N., Mannion, A.M. & Sarris, D. (2016) Mediterranean island biodiversity and climate change: the last 10,000 years and the future. *Biodiversity and conservation*, 25 (13), 2597–2627.

Vujić, A., Ståhls, G., Ačanski, J., Bartsch, H., Bygebjerg, R. & Stefanović, A. (2013) Systematics of Pipizini and taxonomy of European *Pipiza* Fallen: molecular and morphological evidence (Diptera, Syrphidae). *Zoologica Scripta*, 42, 288–305.

Yang, Z. & Rannala, B. (2012) Molecular phylogenetics: principles and practice. Nature reviews. *Genetics*, 13 (5), 303.

Young, A.D., Lemmon, A.R., Skevington, J.H., Mengual, X., Ståhls, G., Reemer, M., Jordaens, K., Kelso, S., Lemmon, E.M., Hauser, M. & De Meyer, M. (2016) Anchored enrichment dataset for true flies (order Diptera) reveals insights into the phylogeny of flower flies (family Syrphidae). *BMC evolutionary biology*, 16 (1), 143.

Westaway, R., Bridgland, D. R., Sinha, R. & Demir, T. (2009) Fluvial sequences as evidence for landscape and climatic evolution in the Late Cenozoic: a synthesis of data from IGCP 518. *Global and Planetary Change*, 68(4), 237–253.

CHAPTER 2

Molecular species delimitation in the genus *Eumerus* (Diptera: Syrphidae)

Molecular species delimitation in the genus *Eumerus* (Diptera: Syrphidae)

Antonia Chroni, Mihajla Djan, Dragana Obreht Vidaković, Theodora Petanidou and Ante Vujić

Published in Bulletin of Entomological Research (2017) 107, 126–138.

Abstract

Eumerus is one of the most diverse genera of hoverfly worldwide. Species delimitation within genus is considered to be difficult due to: (a) lack of an efficient key; (b) non-defined taxonomical status of a large number of species; and (c) blurred nomenclature. Here, we present the first molecular study to delimit species of the genus by using a fragment of the mitochondrial cytochrome-c oxidase subunit I gene (COI) gene. We assessed 75 specimens assigned to 28 taxa originating from two biogeographic zones: 22 from the western Palaearctic and six from the Afrotropical region. Two datasets were generated based on different sequence lengths to explore the significance of availability of more polymorphic sites for species delimitation; dataset A with a total length of 647 bp and dataset B with 746 bp. Various tree inference approaches and Poisson tree processes models were applied to evaluate the putative 'taxonomical' vs. 'molecular' taxa clusters. All analyses resulted in high taxonomic resolution and clear species delimitation for both the dataset lengths. Furthermore, we revealed a high number of mitochondrial haplotypes and high intraspecific variability. We report two major monophyletic clades, and seven 'molecular' groups of taxa formed, which are congruent with morphology-based taxonomy. Our results support the use of the mitochondrial COI gene in species diagnosis of *Eumerus*.

Keywords: DNA barcoding, COI, species Key Delimitation, hoverflies, *Eumerus*

Introduction

Hoverflies (Diptera: Syrphidae), also known as flower flies, constitute a cosmopolitan and highly diverse insect group with more than 6100 taxa described globally (Thompson et al., 2010). Hoverflies influence ecosystems in many ways, such as: (a) pollinating a wide range of flowering plants; (b) controlling plant pests of which they

are effective predators; (c) having phytophagous larvae feeding on bulbs; and (d) effectively recycling nutrients from dead matter (Rotheray & Gilbert, 2011). Because of their heterogeneous character and their wide distribution, hoverflies constitute an important and diverse group for ecological and biogeographical studies.

One of the most species-rich of the hoverfly genera is *Eumerus* Meigen, 1822, with 256 species recorded worldwide (Pape & Thompson, 2015), of which 89 occur in the western Palaearctic region (total species number of the entire Palaearctic is 140: Peck, 1988; Speight, 2014) and 72 in the Afrotropical region (Pape & Thompson, 2015). The only existing comprehensive key for Eumerus is that of Stackelberg (1961) based on only some of the Palaearctic taxa, which was used by Speight (2014) to compile a list of European *Eumerus*. Due to the lack of an up-to-date European identification key, species delimitation is often not feasible, especially for poorly studied areas, e.g., the Mediterranean. In addition, the taxonomic status of a considerable number of taxa is uncertain, with confusing nomenclature and synonymies frequently present (Peck, 1988). It is often unclear to which taxon many names refer, and a broad revision of the genus is needed, perhaps employing more sophisticated taxonomical tools, e.g., molecular systematics.

Over the last two decades, DNA barcoding has been introduced to taxonomy and has greatly expedited species identification, assisted in species delimitation and elucidated species evolution and biology (Rubinoff, 2006). DNA barcoding can be a fast and efficient way to identify species, to diagnose new species, and to provide molecular operational units for ecological and biodiversity studies (DeWalt, 2011). However, opposing opinions exist regarding the application of DNA barcoding as a primary means of species delimitation. Rubinoff (2006) claimed that mitochondrial DNA (mtDNA) is not adequate as a sole source of species-defining data because of reduced effective population size and introgression, maternal inheritance, recombination, inconsistent mutation rate, heteroplasmy and compounding evolutionary processes. As a consequence, there are cases where some sister taxa cannot be identified because they have identical or nearly identical DNA barcodes, giving a false negative signal of species differentiation (Moritz & Cicero, 2004). In contrast, taxa with a wide geographical distribution may exhibit relatively large genetic divergence and, thus, might present a false positive signal (i.e., incorrectly indicating the occurrence of differentiated taxa) (Avise, 2000). Notwithstanding the controversy about its effectiveness, DNA barcoding has been highly effective in

species identification, especially for resolving insect taxonomy (Ball et al., 2005; Smith et al., 2005). To overcome any false phylogenetic signal, it is recommended to use multiple and complementary tools to better delimit biodiversity ('integrative taxonomy': Dayrat, 2005). This implies that morphological features, and molecular (e.g., DNA sequences) and biochemical (e.g., alloenzymes) data, as well as morphometric data should be utilized for species delimitation (Mengual et al., 2006).

The mitochondrial cytochrome-c oxidase subunit I gene (COI, cox1) is widely used in species identification due to its phylogenetic signal, which can discriminate species (Hebert et al., 2003a, 2010; Hebert & Gregory, 2005). A fragment of approximately 650 bp of the 5′ end of the COI, i.e., the 'Folmer' fragment (Folmer et al., 1994), is the most frequently used gene fragment in DNA barcoding of animals, and this approach has been successfully applied to hoverflies (Pérez-Bañón et al., 2003; Ståhls et al., 2009; Gibson et al., 2011; Marcos-García et al., 2011; Radenković et al., 2011). Furthermore, primers amplifying a fragment of the 3′ end of the COI have been effectively applied to obtain longer sequences, i.e., >800 bp. According to Hebert et al. (2003b) COI-3′ regions present similar sequence divergence profiles as COI-5′ fragments, which imply that COI-3′ can be used as an alternative DNA barcode. Indeed, the COI-3′ region has proven valuable for solving taxonomical uncertainties in various hoverfly genera (Milankov et al., 2005, 2008a, 2009, 2010a, b, 2013; Mengual et al., 2006; Vujić et al., 2012; Francuski et al., 2013).

Molecular and morphological studies have been carried out on many hoverfly genera such as *Merodon* (Milankov et al., 2008a, b; Ståhls et al., 2009), *Cheilosia* (Ståhls et al., 2004; Milankov et al., 2010a, b), *Chrysotoxum* (Nedeljković et al., 2013) and tribe Pipizini (Vujić et al., 2013). In these studies, an integrative taxonomic approach was applied, i.e., complementary use of molecular markers (mtDNA and/or nuclear gene fragments) and morphological characters, which often provided rather good taxonomic resolution (Milankov et al., 2008a, b). However, in certain cases, different taxa shared the same haplotypes (Milankov et al., 2008b, 2010a, b; Ståhls et al., 2009) or possessed character differences of solely one nucleotide (Ståhls et al., 2009; Milankov et al., 2010b). In the latter cases, this outcome indicated the insufficiency of a COI-based identification system alone, to delimit species or species complexes within the genus *Merodon* (Milankov et al., 2008b; Ståhls et al., 2009), and underlined the importance of integrative taxonomic inference.

Here, our aim is to validate usage of COI-3′ region for species delimitation of the genus *Eumerus* using different sequence lengths in order to identify species and explore intra- and interspecific variability. We address two specific questions: (1) Can COI-3′ barcoding reveal intra- and interspecific genetic variation in *Eumerus*? (2) Is a short sequence of COI-3′ (647 bp) sufficient to accurately resolve species taxonomy compared to a more elongated one (746 bp)?

Materials and Methods

Taxon sampling

We used dry pinned specimens deposited in two entomological collections: the Melissotheque of the Aegean located at the University of the Aegean, Greece (M-UAegean; Petanidou et al., 2013); and the collection of the Faculty of Sciences at the Department of Biology and Ecology of the University of Novi Sad, Serbia (FSUNS). The specimens used in this study were collected from 2009 to 2014. In total, 75 specimens were used from two geographical areas: 69 derived from the western Palaearctic and six from Afrotropical region (RSA) (table S1). Initial species identification was based on morphology. Specimens were assigned to 28 taxa (table S1) of which three had been previously undescribed (*Eumerus* aff. *barbarous* Coquebert, 1804; *E.* aff. *rubiginosus* Lyneborg, in litt. and *E.* aff. *tarsatus* Lyneborg, in litt.). The selected taxa are mainly of Palaearctic origin (22 taxa), while six taxa originated from the RSA. Identifications were carried out by Dieter Doczkal (Afrotropical taxa) and Ante Vujić (Palaearctic taxa). Taxa identification for specimens derived from the RSA was based on Lyneborg's revision (Lyneborg, in litt.). A list of the specimens used in the analysis, together with their GenBank accession numbers and collection data, is given in table S1.

To detect intraspecific variation, *Eumerus amoenus* Loew, 1848 was analyzed, since its broad distribution in the Mediterranean appears to be the widest within the genus. Two populations from the Aegean islands of Lesvos (three specimens) and Samos (seven specimens) were assayed. Measurements of interspecific variation were determined through the taxa, *E. pulchellus* Loew, 1848 and *E. pusillus* Loew, 1848 by comparing the genetic distances between adjacent and distant populations. For *E. pulchellus*, molecular diversity indices were calculated by using one specimen for each geographical area (i.e., Chios, Dadia, Lesvos, Limnos, Rhodes, Samos and Sardinia). Molecular diversity indices were also calculated for *E. pusillus*, but in this

case, two or more samples per geographical area (Chios, Crete, Karpathos and Naxos) were selected.

DNA extraction and PCR amplification

Total genomic DNA was extracted using the head and/or two to three legs from each specimen. We used the protocol by Chen et al. (2010) for Sodium Dodecyl Sulfate (SDS) extraction with the following modifications: (a) RNase A solution was not added; (b) the concentration of proteinase K solution was 40 mg ml−1; and (c) an additional step of chloroform/isoamyl alcohol (24:1) was applied. Samples were re-suspended in 30 μl of TAE buffer.

PCR amplifications of the COI-3′ were performed in a total volume of 25 μl, containing 25 ng μl−1 template DNA, 5 pmol μl−1 of each primer, 0.08 mM of dNTPs, 1× Reaction Buffer (Thermo Scientific, USA) and 1.25 units of Polymerase (Taq poly or Dream Taq poly, Thermo Scientific, USA). Amplifications were performed in an Authorized PCR Thermal Cycler (Mastercycler® personal, Eppendorf, Germany). Thermocycling conditions consisted of initial denaturation at 95°C for 2 min, 29 cycles of 30 s denaturing at 94°C, 30 s annealing at 49°C, 2 min extension at 72°C, followed by a final extension of 8 min at 72°C (Vujić et al., 2013). We employed universally conserved primers toamplify and sequence the COI-3′: forward primer C1-J-2183 (5′-CAACATTTATTTTGATTTTTTGG-3′) (alias JERRY) and reverse primer TL2-N-3014 (5′-TCCAATGCACTAATCTGCCATATTA-3′) (alias PAT) (Simon et al., 1994). Amplified products were run on 1.5% agarose gels for visual inspection. Purification of the PCR products was done with the ExoSap-IT kit (USB, Cleveland, OH, USA) and clean products were thereafter Sanger sequenced in both directions on an ABI 3730 DNA analyzer (Applied Biosystems, USA) at the Sequencing Service laboratory of the Finnish Institute for Molecular Medicine (http://www.fimm.fi).

Sequence alignment

Two datasets of different sequence length were produced. Dataset A comprised sequences of 647 nucleotides in total length, obtained by forward sequencing of the COI-3′ region, from 75 *Eumerus* specimens and four outgroups. We chose *Platynochaetus setosus* Fabricius, 1794 (Accession No. KM224512), *Merodon erivanicus* Paramonov, 1925 (Accession No. KT157919) and two species of the genus

Megatrigon Johnson, 1898 (Accession No. KT157920 and KT157921) as outgroups. Dataset B consisted of full length of the COI-3′ (746 nucleotides), acquired through bidirectional sequencing, for the aforementioned 75 *Eumerus* taxa and outgroups. All trees were rooted based on *P. setosus* sequence.

As required, sequences were edited by eye using BioEdit 7.2.5 (Hall, 1999). For multiple sequence alignment we employed the L-INS-i algorithm, which is considered to be more accurate as an iterative refinement method incorporating local pairwise alignment information (Katoh et al., 2005). Alignments were implemented using MAFFT version 7 (http://mafft.cbrc.jp/alignment/server/index.html). Both datasets were trimmed to their final lengths using BioEdit 7.2.5 (Hall, 1999). Polymorphic sites, DNA polymorphism and basic molecular diversity indices were calculated using DnaSP 5.10.01 (Librado & Rozas, 2009), which also generated nexus files. Sequences were checked for possible presence of stop codons (Buhay, 2009) using the Mesquite 2.75 system for phylogenetic computing (Maddison & Maddison, 2011). All sequences were translated using the invertebrate mitochondrial code. The evolutionary models used for maximum-likelihood (ML) and Bayesian inference (BI) analyses were implemented in the HIV sequence database (http://www.hiv.lanl.gov/content/sequence/findmodel/findmodel.html) (Posada & Crandall, 2001).

Molecular data analysis

PTP models

Several studies have highlighted the ability of Poisson tree processes (PTP) models to reveal and resolve taxonomic issues (Leasi & Norenburg, 2014; Soldati et al., 2014; Tang et al., 2014). Because this approach does not require ultrametrization of trees (and its associated biases), it constitutes a reasonable alternative to other species delineation models such as the General mixed Yule coalescent model (Pons et al., 2006). In PTP models, the numbers of substitutions (branch lengths) represent speciations or branching events and, therefore they only require a phylogenetic input tree. PTP models have previously been implemented to reveal putative molecular species clusters (Zhang et al., 2013). PTP analyses were conducted on the web server for PTP (available at http://species.h-its.org/ptp/) using the best ML tree resulting from the RA ×ML analysis (see below).

Maximum parsimony (MP)

MP analyses were performed in the program NONA (Goloboff, 1999), spawned in WINCLADA version 1.00.08 (Nixon, 2002). A heuristic search algorithm with 1000 random addition replicates (mult × 1000) was performed, holding 100 trees per round (hold/100), max trees set to 100,000, and applying TBR branch swapping.

Table 1. Results generated for dataset A (i.e. forward sequencing of the COI-3' region) and dataset B (i.e. bidirectional sequencing) in DNaSP 5.10.01, after excluding the outgroups.

Πίνακας 1. Τα αποτελέσματα του προγράμματος DNaSP 5.10.01 για τις ομάδες δεδομένων A (αλληλούχιση με εμπρόσθιο εκκινητή της κωδικής περιοχής COI-3'), και B (αμφίδρομη αλληλούχιση), έχοντας αποκλείσει τις εξωομάδες.

	Dataset A	**Dataset B**
1. Polymorphic sites		
Number of sites	647	746
Total number of sites (excluding sites with gaps / missing data)	629	717
Invariable (monomorphic) sites	421	474
Variable (polymorphic) sites	208	243
Total number of mutations	268	325
Singleton variable sites	*30*	*37*
Parsimony informative sites	*178*	*206*
2. DNA polymorphism		
2.1 without gaps		
Number of Haplotypes, h	53	56
Haplotype (gene) diversity, Hd	0.976	0.983
Variance of Haplotype diversity	0.00008	0.00005
Standard Deviation of Haplotype diversity	0.009	0.007
Nucleotide diversity, Pi	0.07111	0.07350
Theta (per site) from Eta	0.08717	0.09273
Average number of nucleotide differences, k	44.731	52.699
2.2 with gaps		
Number of pairwise comparisons	2775	2775
Average number of sites analyzed	646.31	745.07
Average number of differences	48.586	57.865
Nucleotide diversity, Pi	0.07517	0.07766
Analysis at Individual Sites (column by column)		
Number of sites analyzed	647.00	746.00
Number of polymorphic sites, S	221	261
Average number of differences	48.720	58.055
Nucleotide diversity, Pi	0.07530	0.07782
Theta-W, per sequence	45.22285	53.40954
Theta-W, per site	0.06990	0.07159

Maximum likelihood

ML trees were generated using RAxML 8.0.9 (Stamatakis, 2006; Stamatakis et al., 2008) in the Cipres Science Gateway (Miller et al., 2010) under the general time-reversible (GTR) evolutionary model with a gamma distribution (GTR + G) (Rodriguez et al., 1990) and 1000 bootstrap replicates.

Bayesian inference

BI topologies were assessed using MrBayes 3.2.6 (Huelsenbeck & Ronquist, 2001) in the Cipres Science Gateway (Miller et al., 2010) with the GTR + G nucleotide substitution model (Rodriguez et al., 1990) proposed by the Akaike information criterion (AIC). For BI, two analyses were run based on codon partition models: (1) partitioned (MBP), i.e., each codon position was treated separately, as they are subject to different evolutionary rates, and (2) nonpartitioned (MBUP). The settings for the Bayesian Markov chain Monte Carlo (MCMC) process for the non-partitioned dataset A and partitioned datasets A and B included two runs of 10 × 106 MCMC generations (×4 chains) with a sampling frequency of 1000 generations. For the non-partitioned dataset B, the same settings were applied except that the number ofMCMCgenerations, i.e., 15 × 106, was increased in order to diminish the autocorrelation. The relative burn-in was 10%. MCMC results were checked with the program Tracer 1.6.0 and all trees were displayed using FigTree 1.4.0 (both available at http://tree.bio.ed.ac.uk/software/).

Median-joining (MJ) network

The software NETWORK 4.6.1.2 (Bandelt et al., 1999) (http://www.fluxus-engineering.com/sharenet.htm) was applied to construct the MJ networks aiming to multistate the characters. For MJ reconstructions the mitochondrial haplotypes of outgroups were excluded.

Results

The proportion of gaps and completely undetermined characters in the alignment as generated in RA ×ML was 0.09 and 0.06% for datasets A and B, respectively; the relevant distinct alignment patterns were 250 and 274. The genetic polymorphism of datasets A and B is shown in table 1.

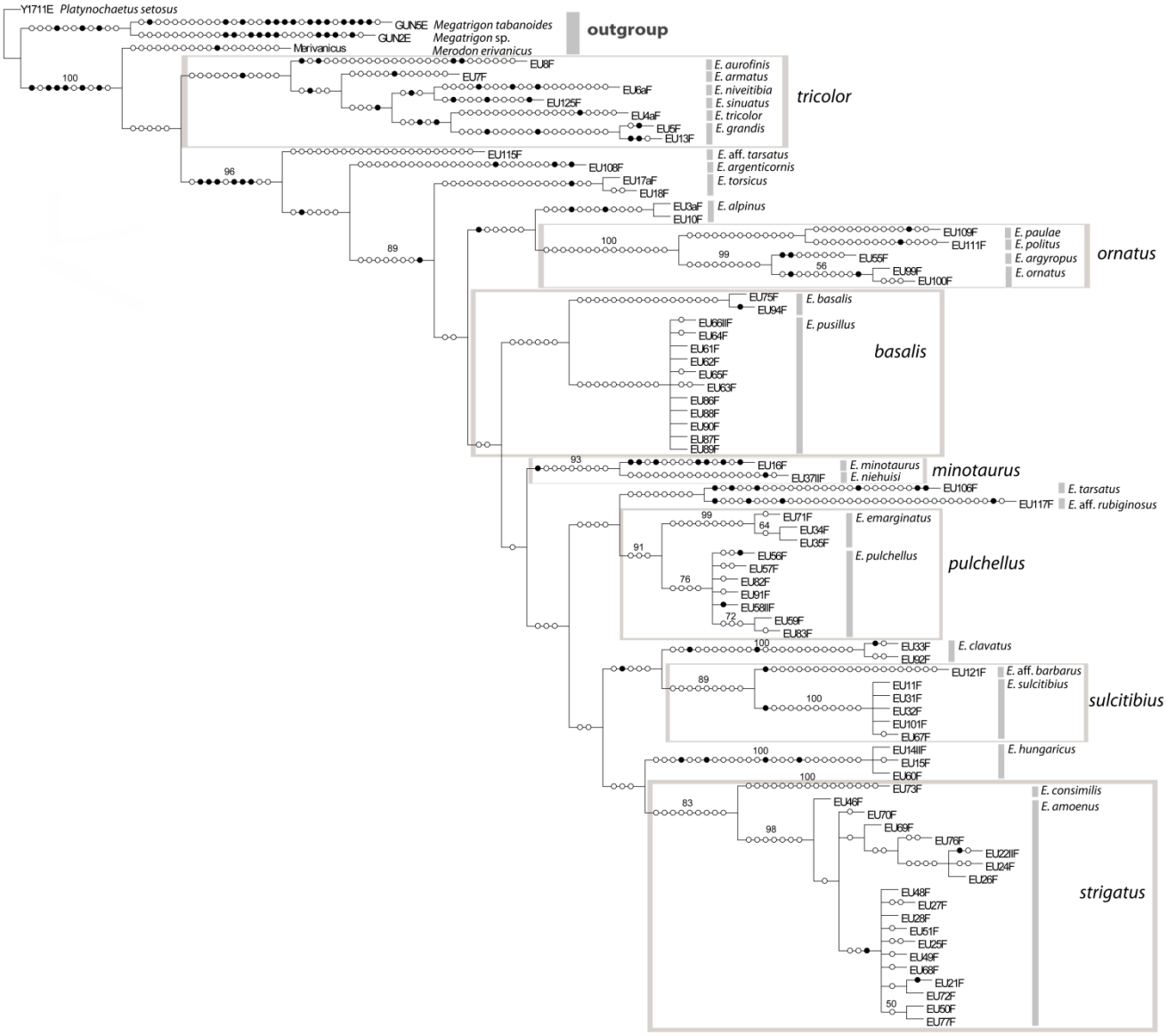

Fig. 1. Maximum parsimony analysis for dataset A produced 72 equally parsimonious trees; the strict consensus tree is illustrated here. Length 989 steps, Consistency index (CI) = 33, Retention index (RI) = 71; filled circles denote unique changes, open circles non-unique. Bootstrap support values (>50) are illustrated above the branches.

Σχήμα 1. Αποτελέσματα ανάλυσης με την μέθοδο της μέγιστης φειδωλότητας (MP) για την ομάδα δεδομένων Α, η οποία παρήγαγε 72 εξίσου φειδωλά δέντρα· εδώ δίνεται το συναινετικό δένδρο. Μήκος 989 εξελικτικά βήματα, Δείκτης Ομοπλασίας (CI) = 33, Δείκτης Retention (εκφράζει το ποσοστό των taxa τα οποία δεν εμφανίζουν ομοπλασία, RI) = 71. Οι μοναδικές νουκλεοτιδικές υποκαταστάσεις σημειώνονται με μαύρο κύκλο, και οι μη-μοναδικές με απλή περιφέρεια κύκλου. Για να ελεγχθεί η στατιστική στήριξη των κλάδων, πραγματοποιήθηκαν 1000 επαναλήψεις bootstrap, των οποίων οι τιμές παρουσιάζονται πάνω από τους κλάδους του MP δέντρου (μόνον τιμές μεγαλύτερες του 50).

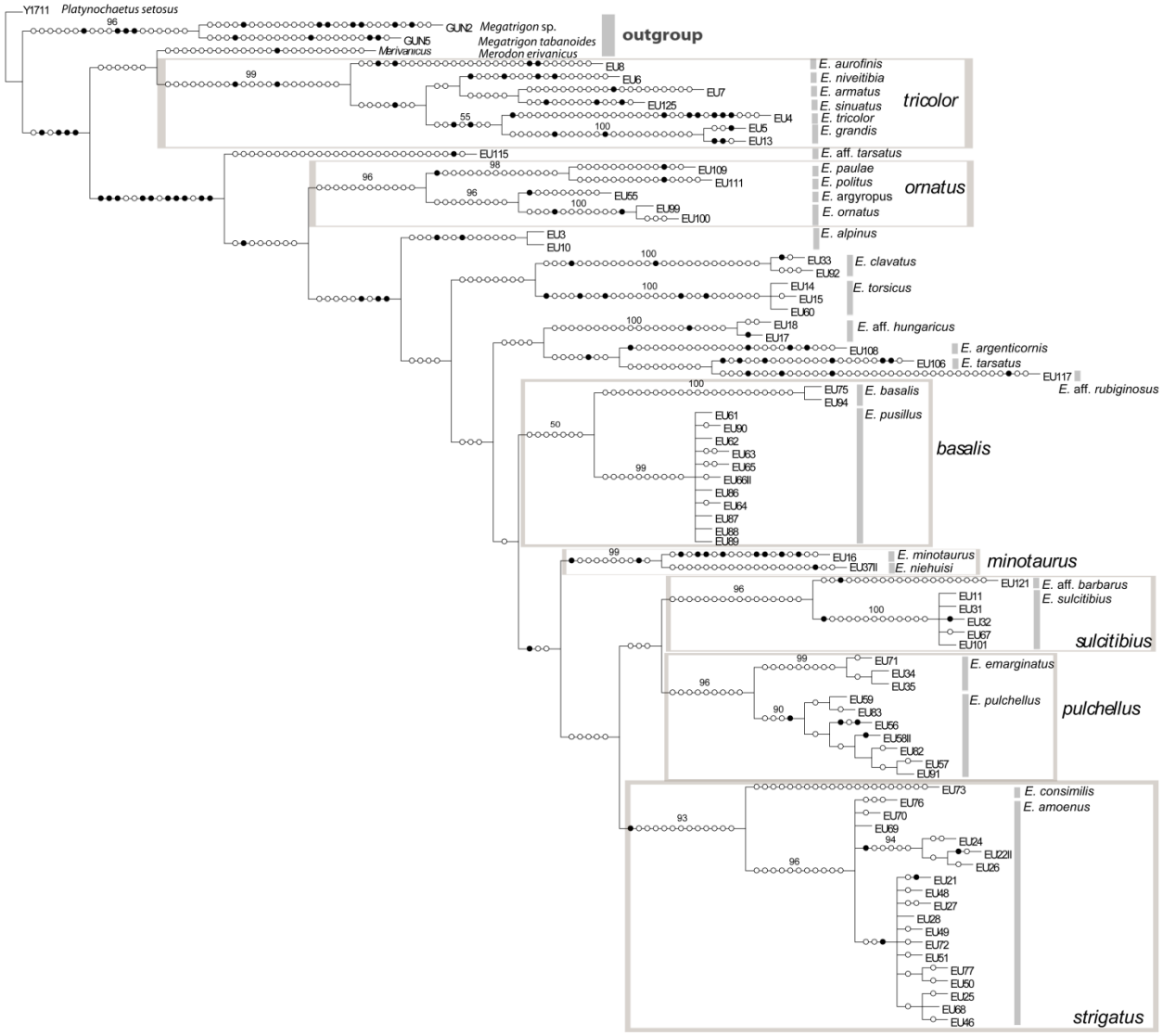

Fig. 2. Maximum parsimony analysis for dataset B produced 30 equally parsimonious trees; the strict consensus tree is illustrated here. Length 1153 steps, Consistency index (CI) = 32, Retention index (RI) = 71; filled circles denote unique changes, open circles non-unique. Bootstrap support values (>50) are illustrated above the branches.

Σχήμα 2. Αποτελέσματα ανάλυσης με την μέθοδο της μέγιστης φειδωλότητας (MP) για την ομάδα δεδομένων B, η οποία η οποία παρήγαγε 30 εξίσου φειδωλά δέντρα· εδώ δίνεται το συναινετικό δένδρο. Μήκος 1153 εξελικτικά βήματα, Δείκτης Ομοπλασίας (CI) = 32, Δείκτης Retention (εκφράζει το ποσοστό των taxa τα οποία δεν εμφανίζουν ομοπλασία, RI) = 71. Οι μοναδικές νουκλεοτιδικές υποκαταστάσεις σημειώνονται με μαύρο κύκλο, και οι μη-μοναδικές με απλή περιφέρεια κύκλου. Για να ελεγχθεί η στατιστική στήριξη των κλάδων, πραγματοποιήθηκαν 1000 επαναλήψεις bootstrap, των οποίων οι τιμές παρουσιάζονται πάνω από τους κλάδους του MP δέντρου (μόνον τιμές μεγαλύτερες του 50).

Molecular analyses vs. morphological delimitation

Initial assignment to species level was based on morphology, with the 75 study specimens classified into 28 taxa. PTP models included the *Eumerus* taxa plus the

four outgroups and predicted 32–49 taxa for dataset A and 31–46 taxa for dataset B. MP (figs 1 and 2), ML (figs S1 and S2) and BI analyses (figs 3, 4, S3 and S4) yielded similar tree topologies for both A and B datasets, with two main clusters and the nodes of the putative taxa strongly supported. Bootstrap values in MP and ML trees were generally low for both datasets, whereas posterior probability values were much higher for BI trees.

In all trees, i.e., those generated by MP, ML and BI, the two major clades comprised the same groups of taxa in each dataset (table 2; figs 1–4 and S1–S4). One clade consisted of taxa belonging to the *tricolor* group (six taxa) with the second comprising the remaining 22 taxa. Our molecular-derived topologies revealed seven different groups of taxa, with all but eight of the 28 taxa assignable to one of these groups. We named these seven groups *basalis*, *minotaurus*, *ornatus*, *pulchellus*, *strigatus*, *sulcitibius* and *tricolor* (for more details see table 2). The eight 'ungrouped' taxa were *E. torsicus* Grković & Vujić, 2015, *E.* aff. *rubiginosus*, *E.* aff. *tarsatus*, *E. alpinus* Rondani, 1857, *E. argenticornis* Lyneborg, in litt., *E. clavatus* Becker, 1923, *E. hungaricus* Szilady, 1940, and *E. tarsatus* Lyneborg, in litt. (table 2). Slight differences were apparent in the topologies generated by datasets A and B. In dataset B, *E. argenticornis*, *E. tarsatus*, *E.* aff. *rubiginosus* and *E.* aff. *tarsatus* clustered together, close to the *ornatus* group (see figs 2, 4, S2 and S4), but in dataset A they appeared altogether, dispersed or clustered differently (see figs 1, 3, S1 and S3). Other observed discrepancies were as follows: (a) *E. clavatus* was in the sulcitibius group in all but the MP analysis of dataset B (fig. 2); (b) the position of *E. alpinus* differed in each analysis, and (c) branching topology for the tricolor group was only similar in MP, MBP and MBUP analysis of dataset A (figs 1, 3 and S3) and ML and MBUP analyses of dataset B (figs S2 and S4). Branching topology for the ornatus group was consistent across all analyses.

Among the 28 taxa, three were previously undescribed, but were closely related to known taxa and, thus, were named *E.* aff. *barbarus* (collected in Morocco), *E.* aff. *rubiginosus* and *E.* aff. *tarsatus* (both collected in South Africa). Both molecular (high nodal support) and morphological (clear diagnostic features) aspects strongly supported the species delimitation of these three taxa. The *E.* aff. *barbarus* was included in the *sulcitibius* group, whereas the other two taxa were not collapsed to any of the seven supported groups (table 2).

We noted artifacts of Long Branch Attraction (LBA) artifacts in the ML and BI analyses of both datasets, but not in MP. LBA was due to sequences EU106, EU108, EU109, EU111, EU115 and EU117 (figs 1–4 and S1–S4). MJ network reconstructions supported our other analyses with sequences from both datasets grouping similarly to the clusters present in MP, ML and BI trees. Furthermore, the number of mutational steps between haplotypes was consistent with our phylogenetic reconstructions (figs 5 and 6).

Intra- and interspecific variability

In both datasets A and B, we recorded a high number of mtDNA COI haplotypes and very rich haplotype (Hd > 0.95) and nucleotide diversity (Pi > 0.005) (table 3). No shared haplotypes between delimitated species were obtained (table 3).

The basic molecular diversity indices for *E. amoenus*, *E. pulchellus* and *E. pusillus* were calculated and are shown in table 3. For *E. amoenus*, the MJ network for dataset A showed one to nine mutational steps among haplotypes detected in the Lesvos population, and one to three mutational steps among haplotypes in the Samos population (fig. 5). The MJ network constructed using dataset B revealed one to eight mutational steps among *E. amoenus* haplotypes from Lesvos and one to four among haplotypes found in the Samos population (fig. 6). When selecting one specimen of *E. pulchellus* from each of seven geographical origins the MJ network analysis of dataset A showed one to six mutational steps, and dataset B one to seven mutational steps (figs 5 and 6). For *E. pusillus*, two or more samples from four different geographic origins were analyzed and MJ network reconstructions showed one mutational step for both datasets among different *E. pusillus* haplotypes (figs 5 and 6).

Discussion

A COI gene-based system has been successfully employed for species delimitation in various hoverfly genera such as the ruficornis group of the genus *Merodon* (Milankov et al., 2008b; Vujić et al., 2012), the *Cheilosia vernalis* complex (Ståhls et al., 2008), the genus *Chrysotoxum* (Suk & Han, 2013; Nedeljković et al., 2015), the Afrotropical hoverflies (Jordaens et al., 2015) and the genus *Platycheirus* (Young et al., 2016). Our study is the first implementation of molecular tools to infer species delimitation in the genus *Eumerus*. We assessed the feasibility of using COI-3′ fragment for *Eumerus* taxonomic inference on 75 specimens assigned to 28 putative ‘taxonomical’ taxa

clusters. Various tree inference approaches on genetic data conformed to morphological species assignment. Since species delimitation (through conventional classical taxonomy) of *Eumerus* has proven challenging in the past, generation of barcode sequences to diagnose species within this genus can prove very useful. A DNA barcode library for *Eumerus* is currently under construction, with more than 130 sequences having been generated in the last 6 months. The present study contributes to enriching accessible barcode records; an assessment of GenBank records on 11 March 2016 revealed that this study has provided more than 50% of the available *Eumerus* sequences and species to date. In addition, our study extends representation of both the number and geographic distribution of *Eumerus* species.

We generated two datasets that differed in terms of sequence length in order to test whether longer sequences improved taxonomic resolution by support values for nodes. Dataset B was 99 nucleotides longer and possessed 28 more parsimony-informative sites compared to dataset A. However, dataset A still provided high taxonomic resolution, confirming the efficacy of a COI system based on approx. 650 bp for species delimitation. Due to sample unavailability arising from fieldwork limitations (and the absence of available sequences in barcoding databases), few sequences – in some cases even only one – were obtained for some taxa. Ahrens et al. (2016) discussed the issue of the singletons' (the only representative sequence of a species) issue in DNA-based species delimitation studies and ascertained that 'a high proportion of singletons has little impact on the accuracy of inferred species limits, and thus rarity (and singletons) should not be conflated with the much more pertinent population genetics parameters'.

The outcomes of our analyses were congruent for both datasets and indicated that the genus *Eumerus* is divided into two main lineages: the *tricolor* group and a lineage consisting of all the other taxa (both grouped and the 'ungrouped'). Tree topologies differed slightly within and between dataset(s). Although longer sequences improved phylogenetic resolution, they did not fully resolve the position of some taxa, e.g., *E. argenticornis*, *E. tarsatus*, *E.* aff. *rubiginosus* and *E.* aff. *tarsatus*. As singletons were used in a few cases, employment of replicate reference specimens could be beneficial in determining the phylogenetic positions of unresolved *Eumerus* taxa. Our is only the second study to date presenting a hypothetical *Eumerus* phylogeny; Doczkal & Pape (2009) found indications of the genus being paraphyletic based on morphological characters (although this was not corroborated nor further investigated by them). Even

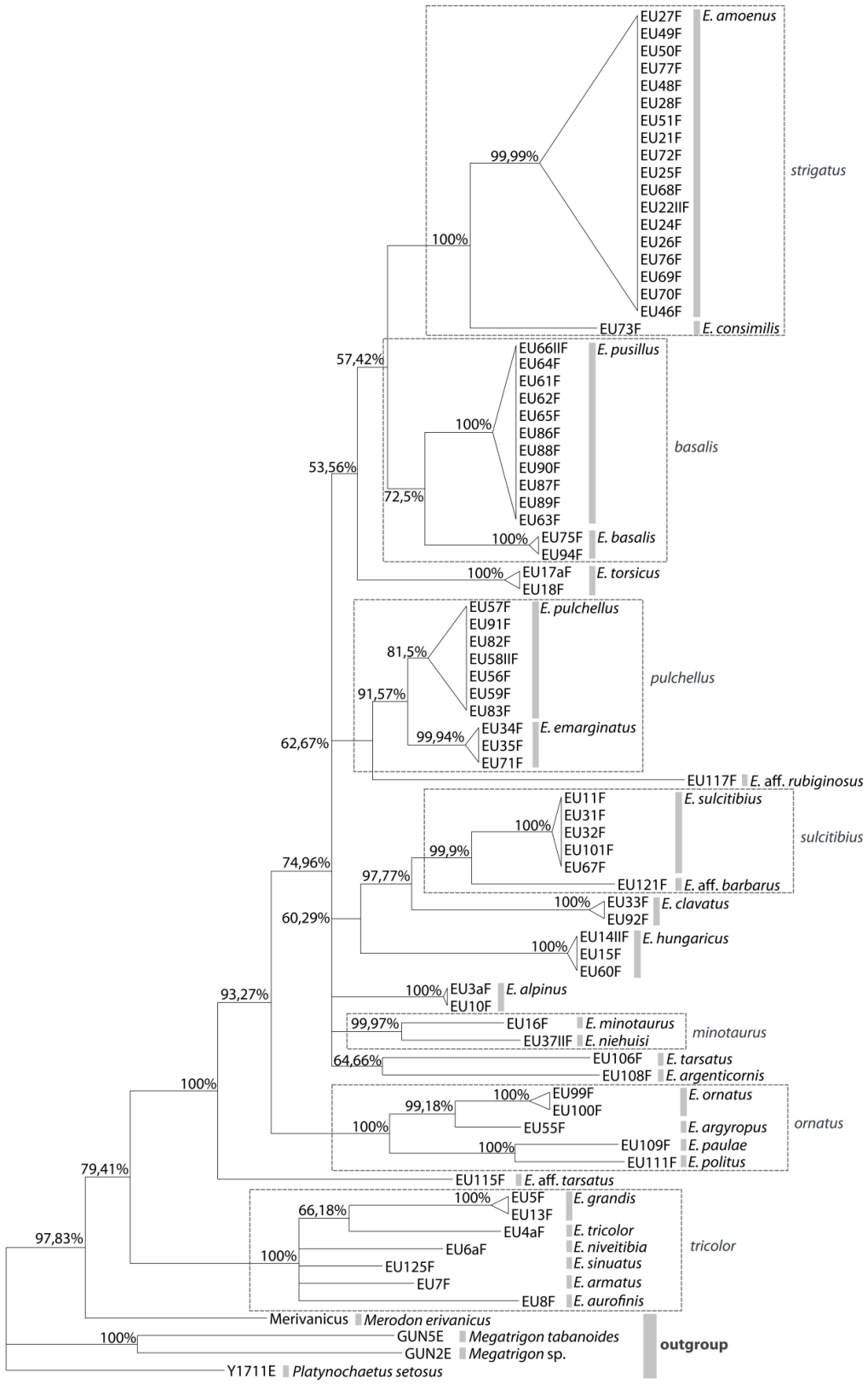

Fig. 3. Bayesian analysis of the dataset A (partitioned data). Values indicate Bayesian probability.

Σχήμα 3. Αποτελέσματα ανάλυσης με την μέθοδο της Μπεϊεσιανής Συμπερασματολογίας (BI) για την ομάδα δεδομένων Α (διαχωρισμός δεδομένων). Οι αριθμοί στους κλάδους δηλώνουν τις εκ των υστέρων πιθανότητες.

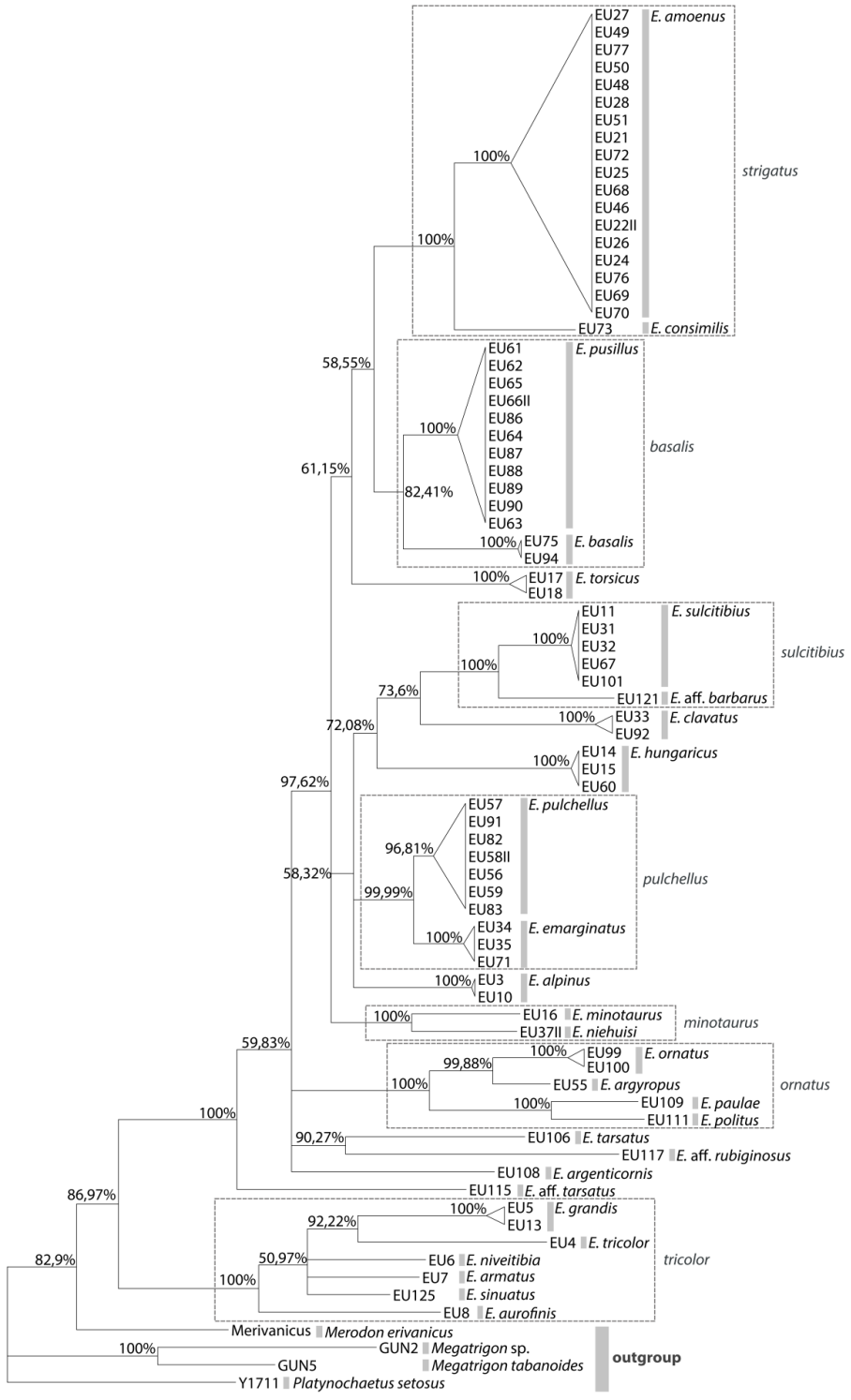

Fig. 4. Bayesian analysis of the dataset B (partitioned data). Values indicate Bayesian probability.

Σχήμα 4. Αποτελέσματα ανάλυσης με την μέθοδο της Μπεϊεσιανής Συμπερασματολογίας (BI) για την ομάδα δεδομένων Β (διαχωρισμός δεδομένων). Οι αριθμοί στους κλάδους δηλώνουν τις εκ των υστέρων πιθανότητες.

Table 2. Taxa grouping as formed after the implementation of the MP, ML and BI analyses and the MJ network reconstructions. The groups are in concordance with the taxa morphology. Taxa groups are separated with ≥19 mt steps.

Πίνακας 2. Ομαδοποίηση ειδών όπως διαμορφώθηκε μετά την εφαρμογή των φυλογενετικών αναλύσεων των MP, ML, BI και των δικτύων Σύνδεσης Γειτόνων. Οι ομάδες συμφωνούν με την μορφολογία. Οι ομάδες ειδών (taxa groups) διαχωρίζονται με ≥19 εξελικτικά βήματα.

'Molecular' taxa groups (supported by morphology)	Taxa
basalis	*E. basalis* Loew, 1848 & *E. pusillus* Loew, 1848
minotaurus	*E. minotaurus* Claussen & Lucas, 1988 & *E. niehuisi* Doczkal, 1996
ornatus	*E. argyropus* Loew, 1848, *E. ornatus* Meigen, 1822, *E. paulae* Herve-Bazin, 1913 & *E. politus* Lyneborg, in litt.
pulchellus	*E. emarginatus* Loew, 1848 & *E. pulchellus* Loew, 1848
strigatus	*E. amoenus* Loew, 1848 & *E. consimilis* Šimić & Vujić, 1996
sulcitibius	*E.* aff. *barbarus* Coquebert, 1804 & *E. sulcitibius* Rondani, 1868
tricolor	*E. aurofinis* Grković, Vujić & Radenković, 2015, *E. armatus* Ricarte & Rotheray, 2012, *E. grandis* Meigen, 1822, *E. niveitibia* Becker, 1921, *E. sinuatus* Loew, 1855 & *E. tricolor* (Fabricius), 1798
'Ungrouped' taxa	*E. torsicus* Grković & Vujić, 2015, *E.* aff. *rubiginosus* Lyneborg, in litt., *E.* aff. *tarsatus* Lyneborg, in litt., *E. alpinus* Rondani, 1857, *E. argenticornis* Lyneborg, in litt., *E. clavatus* Becker, 1923, *E. hungaricus* Szilady, 1940 & *E. tarsatus* Lyneborg, in litt.

Table 3. Results generated for dataset A (i.e. forward sequencing of the COI-3' region) and dataset B (i.e. bidirectional sequencing) in DNaSP 5.10.01 for *E. amoenus* (18 sequences), *E. pulchellus* (7 sequences) and *E. pusillus* (11 sequences).

Πίνακας 3. Τα αποτελέσματα του προγράμματος DNaSP 5.10.01 για τις ομάδες δεδομένων A (αλληλούχιση με εμπρόσθιο εκκινητή της κωδικής περιοχής COI-3'), και B (αμφίδρομη αλληλούχιση), για τα είδη *E. amoenus* (18 αλληλουχίες), *E. pulchellus* (7 αλληλουχίες) και *E. pusillus* (11 αλληλουχίες).

	Dataset A			**Dataset B**		
	E. amoenus	*E. pulchellus*	*E. pusillus*	*E. amoenus*	*E. pulchellus*	*E. pusillus*
1. Polymorphic sites						
Total number of sites (excluding sites with gaps/missing data)	636	645	646	737	746	746

Invariable (monomorphic) sites	636	636	642	716	736	740
Variable (polymorphic) sites	11	9	4	21	10	6
Total number of mutations	16	10	4	22	11	6
Singleton variable sites	*8*	*5*	*4*	*12*	*11*	*5*
Parsimony informative sites	*8*	*4*	*0*	*9*	*4*	*1*
2. DNA polymorphism						
2.1 without gaps						
Number of Haplotypes, h	13	7	5	16	7	6
Haplotype (gene) diversity, Hd	0.928	1.000	0.618	0.987	1.000	0.727
Variance of Haplotype diversity	0.00268	0.00583	0.02701	0.00053	0.00583	0.02084
Standard Deviation of Haplotype diversity	0.052	0.076	0.164	0.023	0.076	0.144
Nucleotide diversity, Pi	0.00554	0.00568	0.00113	0.00616	0.00530	0.00166
Theta (per site) from Eta	0.00731	0.00633	0.00211	0.00868	0.00602	0.00275
Average number of nucleotide differences, k	3.523	3.667	0.727	4.542	3.952	1.236
2.2 with gaps						
Number of pairwise comparisons	153	21	55	153	21	55
Average number of sites analyzed	645.27	646.43	646.82	744.59	746.00	746.00
Average number of differences	5.163	3.667	0.927	5.863	3.952	1.236
Nucleotide diversity, Pi	0.00800	0.00567	0.00143	0.00787	0.00530	0.00166
Analysis at Individual Sites (column by column)						
Number of sites analyzed	647.00	647.00	647.00	746.00	746.00	746.00
Number of polymorphic sites, S	22	9	5	26	10	6
Average number of differences	5.587	3.667	0.927	6.184	3.952	1.236
Nucleotide diversity, Pi	0.00863	0.00567	0.00143	0.00829	0.00530	0.00166
Theta-W, per sequence	6.45560	3.67347	1.71915	7.60792	4.08163	2.04850
Theta-W, per site	0.00998	0.00568	0.00266	0.01020	0.00547	0.00275

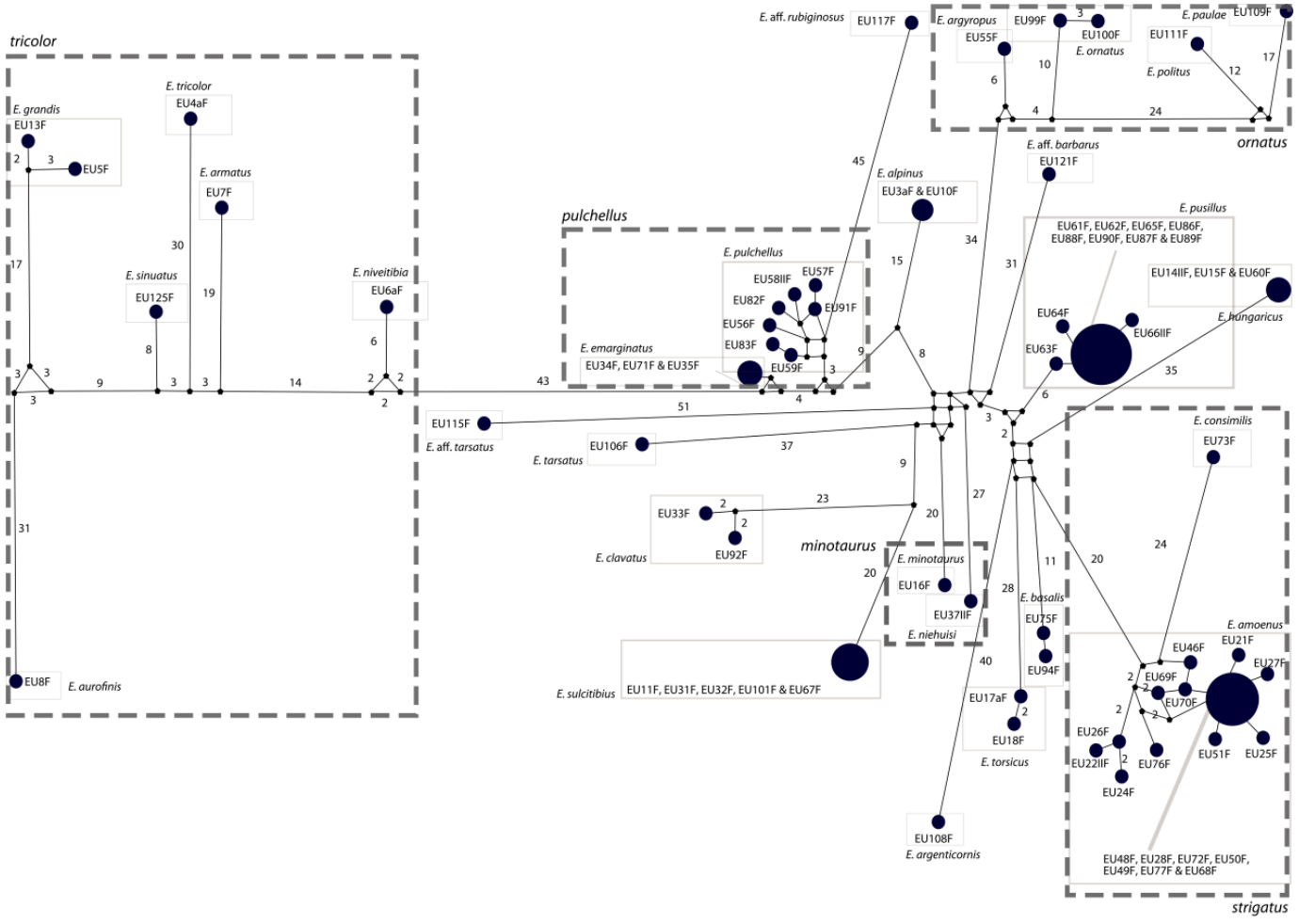

Fig. 5. The median-joining network of the haplotypes of the dataset A, as it was constructed by Network software ver. 4.6.1.2 (http://www.fluxus-engineering.com). Circle sizes are proportional to haplotype frequencies. The number of mutational steps is the one between each pair of haplotypes. When not stated, one mutational step interferes between the nodes/OTUs. Taxa and molecular taxa groups (supported by morphology) are depicted (apart of *basalis* and *sulcitibius* group).

Σχήμα 5. Το δίκτυο ανάλυσης Σύνδεσης Γειτόνων των απλοτύπων της ομάδας δεδομένων Α κατασκευάστηκε με το πρόγραμμα Network ver. 4.6.1.2 (http://www.fluxus-engineering.com). Το μέγεθος κάθε κύκλου είναι ανάλογο της συχνότητας του απλοτύπου (αριθμός ατόμων με τον ίδιο απλότυπο). Ο αριθμός των εξελικτικών βημάτων δίνεται ανά ζεύγος απλοτύπων, ενώ όταν δεν αναφέρεται, μεσολαβεί ένα εξελικτικό βήμα (μία μετάλλαξη) μεταξύ των κόμβων ή των taxa (OTUs). Παρουσιάζονται, επίσης, οι μοριακές ομάδες ειδών (taxa groups), οι οποίες υποστηρίζονται από την μορφολογία (εκτός από τις ομάδες ειδών *basalis* και *sulcitibius*).

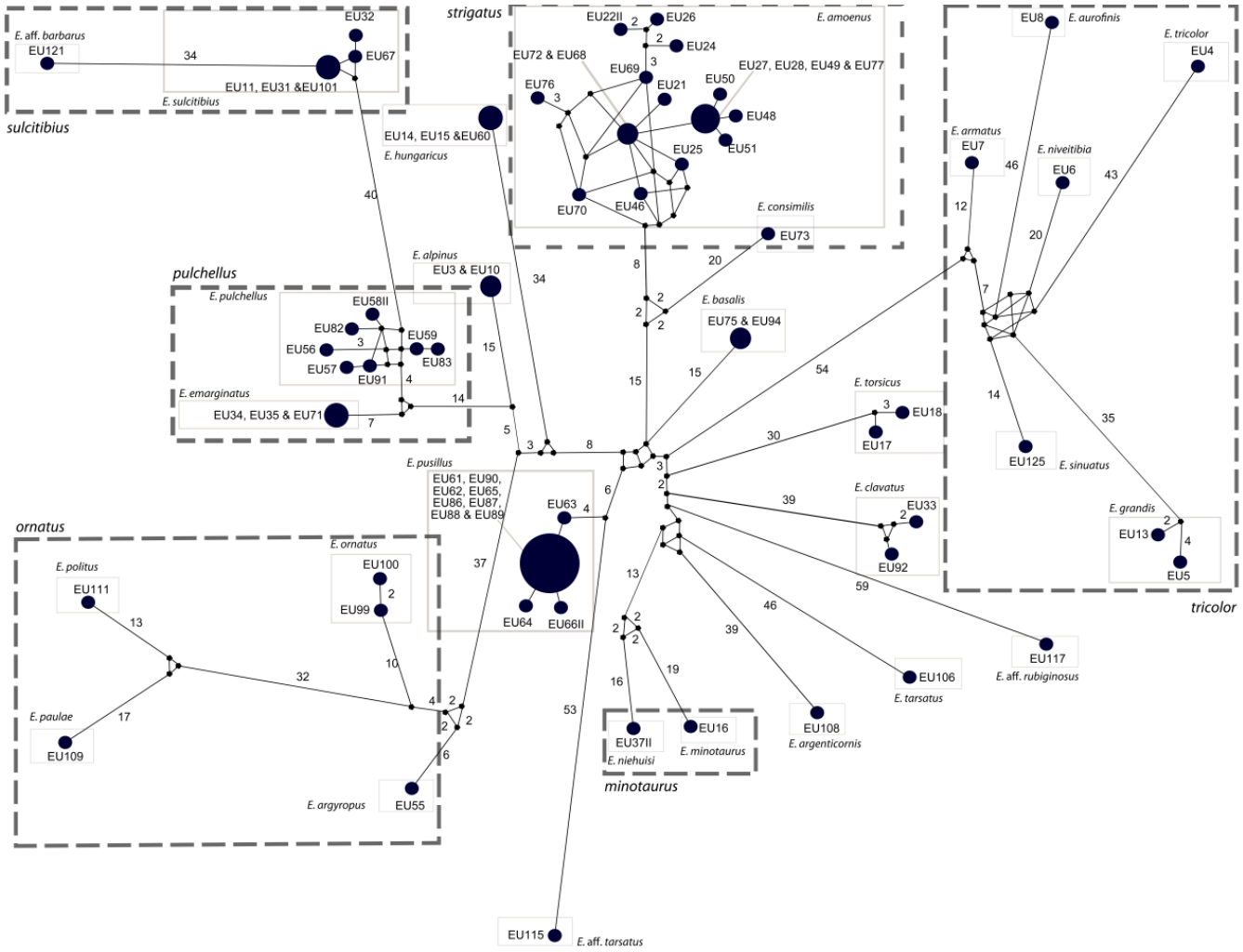

Fig. 6. The median-joining network of the haplotypes of the dataset B, as it was constructed by Network software ver. 4.6.1.2 (http://www.fluxus-engineering.com). Circle sizes are proportional to haplotype frequencies. The number of mutational steps is the one between each pair of haplotypes. When not stated, one mutational step interferes between the nodes/OTUs. Taxa and molecular taxa groups (supported by morphology) are depicted (apart of *basalis* group).

Σχήμα 6. Το δίκτυο ανάλυσης Σύνδεσης Γειτόνων των απλοτύπων της ομάδας δεδομένων Β κατασκευάστηκε με το πρόγραμμα Network ver. 4.6.1.2 (http://www.fluxus-engineering.com). Το μέγεθος κάθε κύκλου είναι ανάλογο της συχνότητας του απλοτύπου (αριθμός ατόμων με τον ίδιο απλότυπο). Ο αριθμός των εξελικτικών βημάτων δίνεται ανά ζεύγος απλοτύπων, ενώ όταν δεν αναφέρεται, μεσολαβεί ένα εξελικτικό βήμα (μία μετάλλαξη) μεταξύ των κόμβων ή των taxa (OTUs). Παρουσιάζονται, επίσης, οι μοριακές ομάδες ειδών (taxa groups), οι οποίες υποστηρίζονται από την μορφολογία (εκτός από την ομάδα είδους *basalis*).

if it was not the purpose of this study to deliberate the genus' phylogeny, based on our results *Eumerus* could be monophyletic with two main lineages. In addition, the formation of several groups within the genus reveals certain affinities among the species. Such affinities have never been discussed before, except in Speight (2014) who only commented on the *strigatus* group that included the taxa *E. consimilis* Šimić & Vujić, 1996, *E. narcissi* Smith, 1928, *E. ruficornis* Meigen, 1822, *E. sogdianus* Stackelberg, 1952, and *E. strigatus* (Fallen), 1817. Based on our data, *strigatus* group is composed of at least two taxa (*E. amoenus* and *E. consimilis*) but we did not have sequences for the other taxa considered by Speight (2014) to incorporate them into our analyses. However, our findings do suggest that *E. amoenus* has a probable (genetic) affinity with the other taxa of Speight's (2014) strigatus group, but this needs further verification.

The large number of mitochondrial haplotypes we generated underlines the high genetic diversity of *Eumerus*, despite the employment of only one genomic region. Species did not exhibit shared haplotypes and were well separated as shown by the number of mutational steps in the MJ networks. This is not always the case for hoverflies (e.g., the genus *Melanostoma* Schiner, 1860, Haarto & Stahls, 2014). Therefore, in *Eumerus*, a COI gene-based system can yield unique, distinguishing mtDNA haplotypes between species.

We also studied intraspecific variation for *E. amoenus*, *E. pusillus* and *E. pulchellus* for which we had more abundant sequences and geographic spread. These taxa are considered 'common', i.e., they are widely distributed in all the Mediterranean peninsulas (Anatolian, Apennine, Balkan and Iberian). *Eumerus amoenus*, *E. pulchellus* and *E. pusillus* were analyzed further, for intraspecific genetic diversity. *Eumerus pulchellus* exhibited the highest haplotype diversity, with each single specimen per geographic origin having a different haplotype. Genetic distances among haplotypes inferred from the number of mutational steps and geographic distances between sampling locations (Greece, Italy and Montenegro), showed no clear pattern. *Eumerus amoenus* also presented very high haplotypic diversity, which was to be expected because sampling was performed over a wider geographical area. MJ network analysis of haplotypes generated a star-like pattern for this latter taxon, suggestive of past expansion (Bandelt et al., 1995). Nucleotide diversity values were similar for *E. pulchellus* and *E. amoenus* for dataset A, whereas they appeared to be a bit higher for *E. amoenus* and *E. pusillus* based on dataset B. *Eumerus pulchellus* and

E. pusillus were represented by more than two specimens from neighboring and remote geographical areas, and in general showed the lowest values for molecular diversity indices among the three analyzed taxa. The star-like patterns observed for MJ haplotype networks for both datasets for *E. pusillus* may indicate a recent expansion of this taxon, resulting in the observed lower genetic diversity. *Eumerus pusillus* specimens originating from Crete, Karpathos and Naxos (one sequence, EU66) shared the same haplotypes in datasets A and B. Specimens from Chios and others from Naxos presented different haplotypes in both datasets. Further conclusions from these discrepancies are limited due to the low sample sizes for the population genetic analyses and, in order not to be speculative, we encourage further intraspecific analyses.

LBA is a sensitive issue in phylogenetic analyses. We used maximum parsimony and likelihood based methods (including BI), with these latter having been proven to be less sensitive to LBA-artifacts compared with maximum parsimony (Bergsten, 2005). Nevertheless, long branches appeared in both ML- and BI-derived phylogenetic trees, but not for MP, with datasets A and B sharing the same LBAs. LBA-artifacts can arise due to several factors, such as poor taxon sampling and selection of highly divergent outgroups (for more details, see the review by Bergsten, 2005). Here, our MJ network reconstructions for each dataset explain the LBAs as those taxa having the highest numbers of mutational steps. In addition, the geographic origins of samples should be taken into account. It is important to clarify that the *ornatus* clade included taxa from very geographically distant areas, i.e., Greece (Dadia) and South Africa (KwaZulu-Natal), so LBAs were to be expected. Given that long branched taxa occurred in all trees, we claim that our topologies remain robust. Adding more samples for LBA taxa could lessen the impact of the LBAs. However, taxon sampling can remain an issue for molecular and other data. We felt that inclusion of as many taxa as possible in our analyses was paramount and so we chose not to exclude any taxa.

To conclude, the present study reveals the adequacy of the COI gene fragment to delimit species in the genus *Eumerus*. Forward and bidirectional sequencing datasets led to similar results; the forward sequencing dataset appeared to be sufficient to identify taxa within *Eumerus* and the more enriched sequence dataset, i.e., bidirectional, provided slightly more information and mitigated certain (though not all) analytical problems. Moreover, we reveal high intraspecific diversity and a high

number of mitochondrial haplotypes. Our findings confirm the potential of an integrative approach – combined usage of a COI barcoding system and morphological characters – to diagnose and delimit species within the genus *Eumerus*. For a complete revision of the genus, including phylogenetic inferences, we endorse the usage of additional molecular markers and/or longer mitochondrial sequence (>800 bp). More taxa and more specimens per taxa should also be sought in order to overcome the drawbacks faced in the present study.

Acknowledgements

This research was co-financed by the European Union (European Social Fund – ESF) and Greek national funds through the Operational Program 'Education and Lifelong Learning' of the National Strategic Reference Framework (NSRF) – Research Funding Program: THALES. Investing in knowledge society through the European Social Fund. We thank John O'Brien for proof reading and making constructive suggestions to the text.

References

Ahrens, D., Fujisawa, T., Krammer, H.J., Eberle, J., Fabrizi, S. & Vogler, A.P. (2016) Rarity and incomplete sampling in DNA-based species delimitation. Systematic Biology 65(3), 478–494.

Avise, J. (2000) Phylogeography: The History and Formation of Species. Masahousette, Harvard University Press.

Ball, S.L., Hebert, P.D.N., Burian, S.K. & Webb, J.M. (2005) Biological identifications of mayflies (Ephemeroptera) using DNA barcodes. Journal of the North American Benthological Society 24, 508–524.

Bandelt, H.J., Forster, P., Sykes, B.C. & Richards, M.B. (1995) Mitochondrial portraits of human populations using median networks. Genetics 141, 743–753.

Bandelt, H.J., Forster, P. & Rohl, A. (1999) Median-joining networks for inferring intraspecific phylogenies. Molecular Biology and Evolution 16, 37–48.

Bergsten, J. (2005) A review of long-branch attraction. Cladistics 21, 163–193.

Buhay, J.E. (2009) 'Coi-Like' sequences are becoming problematic in molecular systematic and DNA barcoding studies. Journal of Crustacean Biology 29, 96–110.

Chen, H., Rangasamy, M., Tan, S.Y., Wang, H.C. & Siegfried, B. D. (2010) Evaluation of five methods for total DNA extraction from western corn rootworm beetles. PLoS ONE 5(8), 1–6.

Dayrat, B. (2005) Towards integrative taxonomy. Biological Journal of the Linnean Society 85, 407–415.

DeWalt, R.E. (2011) DNA barcoding: a taxonomic point of view. Journal of the North American Benthological Society 30, 174–181.

Doczkal, D.&Pape, T. (2009) *Lyneborgimyia magnifica* gen. et sp.n. (Diptera: Syrphidae) from Tanzania, with a phylogenetic analysis of the Eumerini using new morphological characters. Systematic Entomology 34(3), 559–573.

Folmer, O., Black, M., Hoeh, W., Lutz, R. & Vrijenhoek, R. (1994) DNA primers for amplification of mitochondrial cytochrome c oxidase subunit I from diverse metazoan invertebrates. Molecular Marine Biology and Biotechnology 3, 294–299.

Francuski, L., Djurakic, M., Ludoški, J. & Milankov, V. (2013) Landscape genetics and spatial pattern of phenotypic variation of *Eristalis tenax* across Europe. Journal of Zoological Systematics and Evolutionary Research 51, 227–238.

Gibson, J.F., Kelso, S., Jackson, M.D., Kits, J.H., Miranda, G.F.G. & Skevington, J.H. (2011) Diptera-specific polymerase chain reaction amplification primers of use in molecular phylogenetic research. Annals of the Entomological Society of America 104, 976–997.

Goloboff, P. (1999) NONA (no name). Version 2. Published by the Author, Tucuman, Argentina.

Haarto, A. & Ståhls, G. (2014) When mtDNA COI is misleading: congruent signal of ITS2 molecular marker and morphology for North European *Melanostoma* Schiner, 1860 (Diptera, Syrphidae). ZooKeys 431, 93–134.

Hall, T.A. (1999) BioEdit: a user-friendly biological sequence alignment editor and analysis program for Windows 95/98/NT. Nucleic Acids Symposium Series 41, 95–98.

Hebert, P.D.N., Cywinska, A., Ball, S.L. & DeWaard, J.R. (2003a) Biological identifications through DNA barcodes. Proceedings of the Royal Society B – Biological Sciences 270, 313–321.

Hebert, P.D.N., Ratnasingham, S. & deWaard, J.R. (2003b) Barcoding animal life: cytochrome c oxidase subunit 1 divergences among closely related species. Proceedings of the Royal Society B – Biological Sciences 270, S96–S99.

Hebert, P.D.N. & Gregory, T.R. (2005) The promise of DNA barcoding for taxonomy. Systematic Biology 54, 852–859.

Hebert, P.D.N., deWaard, J.R. & Landry, J.F. (2010) DNA barcodes for 1/1000 of the animal kingdom. Biology Letters 6, 359–362.

Huelsenbeck, J.P. & Ronquist, F. (2001) MRBAYES: bayesian inference of phylogenetic trees. Bioinformatics 17, 754–755.

Jordaens, K., Goergen, G., Virgilio, M., Backeljau, T., Vokaer, A. & De Meyer, M. (2015) DNA barcoding to improve the taxonomy of the Afrotropical Hoverflies (Insecta: Diptera: Syrphidae). PLoS ONE 10(10), e0140264.

Katoh, K., Kuma, K., Toh, H. & Miyata, T. (2005) MAFFT version 5: improvement in accuracy of multiple sequence alignment. Nucleic Acids Research 33, 511–518.

Leasi, F. & Norenburg, J.L. (2014) The necessity of DNA taxonomy to reveal cryptic diversity and spatial distribution of meiofauna, with a focus on Nemertea. PLoS ONE 9, e104385.

Librado, P. & Rozas, J. (2009) DnaSP v5: a software for comprehensive analysis of DNA polymorphism data. Bioinformatics 25, 1451–1452.

Maddison, W.P. & Maddison, D.R. (2011) Mesquite: a Modular System for Evolutionary Analysis. Version 3.03. Available online at http://mesquiteproject.org

Marcos-García, M.Á., Vujić, A., Ricarte, A. & Ståhls, G. (2011) Towards an integrated taxonomy of the *Merodon equestris* species complex (Diptera: Syrphidae) including description of a new species, with additional data on Iberian *Merodon*. Entomological Society of Canada 143, 332–348.

Mengual, X., Ståhls, G., Vujić, A. & Marcos-García, M.Á. (2006) Integrative taxonomy of Iberian *Merodon* species (Diptera, Syrphidae). Zootaxa 1377, 1–26.

Milankov, V., Stamenković, J., Ludoški, J., Ståhls, G. & Vujić, A. (2005) Diagnostic molecular markers and the genetic relationships among three species of the *Cheilosia canicularis* group (Diptera: Syrphidae). European Journal of Entomology 102, 125–131.

Milankov, V., Ståhls, G., Stamenković, J. & Vujić, A. (2008a) Genetic diversity of populations of *Merodon aureus* and *M. cinereus* species complexes (Diptera, Syrphidae): integrative taxonomy and implications for conservation priorities on the Balkan Peninsula. Conservation Genetics 9, 1125–1137.

Milankov, V., Ståhls, G. & Vujić, A. (2008b) Molecular diversity of populations of the *Merodon ruficornis* group (Diptera, Syrphidae) on the Balkan Peninsula. Journal of Zoological Systematics and Evolutionary Research 46, 143–152.

Milankov, V., Ludoški, J., Ståhls, G., Stamenković, J. & Vujić, A. (2009) High molecular and phenotypic diversity in the *Merodon avidus* complex (Diptera, Syrphidae): cryptic speciation in a diverse insect taxon. Biological Journal of the Linnean Society 155, 819–833.

Milankov, V., Francuski, L., Ludoški, J., Ståhls, G. & Vujić, A. (2010a) Estimating genetic and phenotypic diversity in a northern hoverfly reveals lack of heterozygosity correlated with significant fluctuating asymmetry of wing traits. Journal of Insect Conservation 14, 77–88.

Milankov, V., Francuski, L., Ludoški, J., Ståhls, G. & Vujić, A. (2010b) Genetic structure and phenotypic diversity of two northern populations of *Cheilosia* aff. *longula* (Diptera: Syrphidae) has implications for evolution and conservation. European Journal of Entomology 107, 305–315.

Milankov, V., Ludoški, J.L.F., Ståhls, G. & Vujić, A. (2013) Genetic and phenotypic diversity patterns in *Merodon albifrons* Meigen, 1822 (Diptera: Syrphidae): evidence of intraspecific spatial and temporal structuring. Biological Journal of the Linnean Society 110, 257–280.

Miller, M.A., Pfeiffer, W. & Schwartz, T. (2010) Creating the CIPRES Science Gateway for inference of large phylogenetic trees, pp. 1–8 in Gateway Computing Environments Workshop (GCE), New Orleans, LA.

Moritz, C. & Cicero, C. (2004) DNA barcoding: promise and pitfalls. PLoS Biology 2, 1529–1531.

Nedeljković, Z., Ačanski, J., Vujić, A., Obreht, D., Dan, M., Ståhls, G. & Radenković, S. (2013) Taxonomy of *Chrysotoxum festivum* Linnaeus, 1758 (Diptera: Syrphidae) – an integrative approach. Zoological Journal of the Linnean Society 169, 84–102.

Nedeljković, Z., Ačanski, J., Dan, M., Obreht-Vidaković, D., Ricarte, A. & Vujić, A. (2015) An integrated approach to delimiting species borders in the genus *Chrysotoxum* Meigen, 1803 (Diptera: Syrphidae), with description of two new species. Contributions to Zoology 84(4), 285–304.

Nixon, K.C. (2002) WINCLADA ver. 1.00.08. New York, University of Ithaca.

Pape, T. & Thompson, F.C. (Eds) 2015. Systema Dipterorum. Version 1.5. Available online at http://www.diptera.org/ (accessed 18 September 2015).

Peck, L.V. (1988) Syrphidae, pp. 11–230 in Soos, A. & Papp, L. (Eds) Catalogue of Palaearctic Diptera. Budapest, Akaddémiai Kiadó.

Pérez-Bañón, C., Rojo, S., Ståhls, G. & Marcos-García, M.Á. (2003) Taxonomy of European *Eristalinus* (Diptera: Syrphidae) based on larval morphology and molecular data. European Journal of Entomology 100, 417–428.

Petanidou, T., Ståhls, G., Vujić, A., Olesen, J.M., Rojo, S., Thrasyvoulou, A., Sgardelis, S., Kallimanis, A.S., Kokkini, S. & Tscheulin, T. (2013) Investigating plant pollinator relationships in the Aegean: the approaches of the project POL-AEGIS (The pollinators of the Aegean archipelago: diversity and threats). Journal of Apicultural Research 52 (2), 106–117.

Pons, J., Barraclough, T.G., Gomez-Zurita, J., Cardoso, A., Duran, D.P., Hazell, S., Kamoun, S., Sumlin, W.D. & Vogler, A.P. (2006) Sequence-based species delimitation for the DNA taxonomy of undescribed insects. Systematic Biology 55, 595–609.

Posada, D. & Crandall, K.A. (2001) Selecting the best-fit model of nucleotide substitution. Systematic Biology 50, 580–601.

Radenković, S., Vujić, A., Ståhls, G., Pérez-Bañón, C., Rojo, S., Petanidou, T. & Simić, S. (2011) Three new cryptic species of the genus *Merodon* Meigen (Diptera: Syrphidae) from the island of Lesvos (Greece). Zootaxa 2735, 35–56.

Rodriguez, F., Oliver, J.L., Marin, A. & Medina, J.R. (1990) The general stochastic-model of nucleotide substitution. Journal of Theoretical Biology 142, 485–501.

Rotheray, G.E. & Gilbert, F. (2011) The Natural History of Hoverflies. UK, Ceredigion.

Rubinoff, D. (2006) Utility of mitochondrial DNA barcodes in species conservation. Conservation Biology 20, 1026–1033.

Simon, C., Frati, F., Beckenbach, A., Crespi, B., Liu, H. & Flook, P. (1994) Evolution, weighting, and phylogenetic utility of mitochondrial gene-sequences and a compilation of conserved polymerase chain-reaction primers. Annals of the Entomological Society of America 87, 651–701.

Smith, M.A., Fisher, B.L.&Hebert, P.D.N. (2005) DNA barcoding for effective biodiversity assessment of a hyperdiverse arthropod group: the ants of Madagascar. Philosophical Transactions of the Royal Society B – Biological Sciences 360, 1825–1834.

Soldati, L., Kergoat, G.J., Clamens, A.L., Jourdan, H., Jabbour-Zahab, R. & Condamine, F.L. (2014) Integrative taxonomy of New Caledonian beetles: species delimitation and definition of the *Uloma isoceroides* species group (Coleoptera, Tenebrionidae, Ulomini), with the description of four new species. Zookeys 415, 133–167.

Speight, M.C.D. (2014) Species accounts of European Syrphidae (Diptera). Syrph the Net, the database of European Syrphidae, vol. 78, pp. 321. Syrph the Net publications, Dublin.

Suk, S.W. & Han, H.Y. (2013) Clarification of previously confused *Chrysotoxum sapporense* and *Chrysotoxum graciosum* (Insecta: Diptera: Syrphidae) in East Asia based on morphological and molecular data. Animal Cells and Systems 17(4), 277–289. doi:10.1080/19768354.2013.814588.

Stackelberg, A.A. (1961) Palaearctic species of the genus *Eumerus* Mg. (Diptera, Syrphidae). Trudy vses.ent., Obshch 48, 181–229.

Ståhls, G., Stuke, J.H., Vujić, A., Doczkal, D. & Muona, J. (2004) Phylogenetic relationships of the genus *Cheilosia* and the tribe Rhingiini (Diptera, Syrphidae) based on morphological and molecular characters. Cladistics – the International Journal of the Willi Hennig Society 20, 105–122.

Ståhls, G., Vujić, A. & Milankov, V. (2008) *Cheilosia vemalis* (Diptera, Syrphidae) complex: molecular and morphological variability. Annales Zoologici Fennici 45, 149–159.

Ståhls, G., Vujić, A., Pérez-Bañón, C., Radenković, S., Rojo, S. & Petanidou, T. (2009) COI barcodes for identification of *Merodon* hoverflies (Diptera, Syrphidae) of Lesvos Island, Greece. Molecular Ecology Resources 9, 1431–1438.

Stamatakis, A. (2006) RAxML-VI-HPC: maximum likelihood based phylogenetic analyses with thousands of taxa and mixed models. Bioinformatics 22, 2688–2690.

Stamatakis, A., Hoover, P. & Rougemont, J. (2008) A rapid bootstrap algorithm for the RAxML web servers. Systematic Biology 57, 758–771.

Tang, C.Q., Humphreys, A.M., Fontaneto, D. & Barraclough, T.G. (2014) Effects of phylogenetic reconstruction method on the robustness of species delimitation using single-locus data. Methods in Ecology and Evolution 5, 1086–1094.

Thompson, F.C., Rotheray, G.E. & Zimbado, M.A. (2010) Syrphidae (flower flies), pp. 763–792 in Brown, B.V., Borkent, A., Cumming, J.M., Wood, D.M., Woodley, Norman, E. & Zumbado, M.A. (Eds) Manual of Central American Diptera. Ottawa, NRC Research Press.

Vujić, A., Radenković, S., Ståhls, G., Ačanski, J., Stefanović, A., Veselić, S., Andrić, A. & Hayat, R. (2012) Systematics and taxonomy of the *ruficornis* group of genus *Merodon* Meigen (Diptera: Syrphidae). Systematic Entomology 37, 578–602.

Vujić, A., Ståhls, G., Ačanski, J., Bartsch, H., Bygebjerg, R. & Stefanović, A. (2013) Systematics of Pipizini and taxonomy of European *Pipiza* Fallen: molecular and morphological evidence (Diptera, Syrphidae). Zoologica Scripta 42, 288–305.

Young, A.D., Marshall, S.A. & Skevington, J.H. (2016) Revision of *Platycheirus* Lepeletier and Serville (Diptera: Syrphidae) in the Nearctic north of Mexico. Zootaxa 4082(1), 001–317.

Zhang, J.J., Kapli, P., Pavlidis, P. & Stamatakis, A. (2013) A general species delimitation method with applications to phylogenetic placements. Bioinformatics 29, 2869–2876.

page intentionally left blank

CHAPTER 3

Diversity of the genus *Eumerus* Meigen (Diptera, Syrphidae) on the eastern Mediterranean islands with description of three new species

Diversity of the genus *Eumerus* Meigen (Diptera, Syrphidae) on the eastern Mediterranean islands with description of three new species

Ana Grković, Ante Vujić, Snežana Radenković, Antonia Chroni and Thedora Petanidou

Published in Annales de la Société Entomologique de France (N.S.) (2015), 51:4, 361–373.

Abstract

A list of 25 species of the genus *Eumerus* Meigen (Diptera: Syrphidae) from the eastern Mediterranean islands is presented. Descriptions are given for three new species: *Eumerus aurofinis* Grković, Vujić & Radenković sp. n. from Lesvos, Samos, Rhodes islands (Greece) and Bozdağ mountain (Turkey), *E. torsicus* Grković & Vujić sp. n. from Chios Island (Greece) and Cyprus; *E. crassus* Grković, Vujić & Radenković sp. n. from Lesvos Island (Greece). In addition to classical morphological characters, mitochondrial COI barcode sequences were generated for several specimens of two available taxa. The status of *Eumerus alpinus* Rondani, 1857 is revised, and the taxon is resurrected from synonymy of *E. olivaceus* Loew, 1848. The zoogeographical significance of the described endemic taxa to the biodiversity of the Aegean islands is discussed.

Résumé

Une liste de 25 espèces du genre *Eumerus* Meigen (Diptera: Syrphidae) de l'est des îles de la Méditerranée est présentée et trois nouvelles espèces sont décrites: *Eumerus aurofinis* Grković, Vujić & Radenković sp. n. des îles de Lesvos, Samos et Rhodes (Grèce) et des montagnes Bozdağ (Turquie), *E. torsicus* Grković & Vujić sp. n. d'île de Chios (Grèce) et de Chypre; *E. crassus* Grković, Vujić & Radenković sp. n. de l'île de Lesvos Island (Grèce). En plus des caractères de la morphologie classique, des séquences COI de barcoding ont été générées pour plusieurs specimens disponibles de deux taxa. Le statut de *Eumerus alpinus* Rondani, 1857 a été révisé. La signification zoo-géographique des taxa endémiques décrits ont été discuté dans le contexte de la biodiversité des îles Egée.

Keywords: hoverflies; *Eumerus aurofinis*; *Eumerus torsicus*; *Eumerus crassus*; DNA barcoding; COI

Introduction

Genus *Eumerus* is one of the most species-rich hoverfly genera, originating from the Old World with 256 registered species worldwide (Pape & Thompson 2015). It is widely distributed in Palaearctic, Afrotropical, Oriental and Australian regions (Stackelberg 1961). Recently, it has been introduced into the Nearctic and Neotropical regions due to commercialized import of plant bulbs (Marinoni & Morales 2007).

This is one of the largest hoverfly genera in the Palaearctic region, with 140 species listed by Peck (1988). In Europe, there are more than 50 species recorded (Speight 2014), with the highest species richness in the Mediterranean region (Ricarte et al. 2008). Species diagnosis and identification within *Eumerus* is not always feasible and face impediments such as (a) the existing key is not sufficient (Stackelberg 1961); (b) a large number of species are of obscure taxonomic status; and (c) the nomenclature of others is blurred (Peck 1988; Speight 2014). During recent decades, to overcome these shortcomings the traditional morphology-based taxonomy has become more integrative, and includes the use of molecular and biochemical data, morphological features (including morphometric data), ecological indices and biogeographical parameters (Dayrat 2005). One very popular tool in species identification and diagnosis is the generation of DNA barcodes of the mitochondrial gene cytochrome c oxidase I (COI); therefore it was implemented here.

Despite its wide geographical distribution and rich biodiversity, the genus lacks recent and comprehensive studies in systematics, biodiversity, ecology and biogeography. This is not the case for the related genus *Merodon* in the eastern Mediterranean region, for which many studies have been carried out during the last decade revealing its importance in e.g. pollination services, or resulting in descriptions of multiple new taxa (Vujić et al. 2007, 2011, 2013; Popov 2010; Radenković et al. 2011).

Eumerus are either blackish or reddish small to medium-sized hoverflies, usually with white or black markings on tergites. They have a flattened face without prominence. The femur is swollen and simple, without projections. The apical part of the ventral surface of the hind femur has two rows of stout spines, usually one row anterolateral, the other row posterolateral. The M1 wing vein is recurved.

Early stages of *Eumerus* can be found in underground storage organs of plants, as is also the case in the genus *Merodon* (Ricarte et al. 2008). Based on the morphological characters established for the mouthparts of the larval stages, Rotheray (1993) indicated that *Eumerus* larvae are fed on semi-liquid food and partially decaying plant bulbs and that their survival rate increases when fungal decay is present. Rotheray and Gilbert (1999) inferred the phylogeny of the Palaearctic Syrphidae by applying 187 larval morphological characters and considered that the genus *Eumerus* is the basal hoverfly taxon. There is a lack of more detailed information about the larval stages of the genus *Eumerus*, with only a few descriptions and observations available, primarily regarding economically important species (Pérez-Bañon & Marcos-García 1998).

Eumerus adults usually prefer warm and sunny places for resting, while they visit a range of different flowers, from families Apiaceae, Euphorbiaceae, Asteraceae and Ranunculaceae (Speight 2014). *Eumerus* species are usually fast flying and easily overlooked insects, and can be found near to the ground in association with their preferred flowers. Their ecological role is crucial, e.g. in pollination and nutrient cycles (Rotheray & Gilbert 2011).

In the present study, we aimed to: (a) document the diversity and distribution of *Eumerus* species in the eastern Mediterranean region (i.e. islands and adjacent regions); (b) describe three new species recorded in the eastern Mediterranean islands, both morphologically and genetically by generating DNA barcodes for the available taxa.

Materials and Methods

The present study is based on examination of newly collected specimens deposited in the collections of the Faculty of Sciences in the Department of Biology and Ecology at the University of Novi Sad (Serbia (FSUNS)) and in the Melissotheque of the Aegean at the University of the Aegean (Mytilene, Greece (MAegean)). The sampling method employed was hand netting pan-trapping, and Malaise trap. Sampling was carried out from spring 2010 to autumn 2014 and covered 28 islands in the eastern Mediterranean (Fig. 1) and several sites adjacent to the surveyed islands on the Greek and Anatolian mainland. Islands and mainland localities were sampled for a minimum of three times during *Eumerus* adult flight season and for a minimum of two collecting days per visit. The total number of specimens was 2192.

Additionally, we studied collections deposited in the following European museums: MZUF – Museum of Zoology and Natural History of Firenze (Museo Zoologico "La Specola"), Italy; RMNH – Nationaal Natuurhistorisch Museum, Leiden, the Netherlands; ZHMB – Museum für Naturkunde, Von Humboldt Universität of Berlin, Germany; and ZMUC – Zoological Museum, Copenhagen University, Denmark. All available types of western Palaearctic species were checked and material from the collections of ZMHB and MZUF were considered here (types of *Eumerus alpinus* Rondani 1857 and *E. olivaceus* Loew, 1848). Identity of particular species was confirmed by A. Ricarte, D. Doczkal, and J. Smith as mentioned in Table 1.

The morphological characters used in descriptions and drawings were based on the terminology established by Thompson (1999), and those relating to male genitalia by Hurkmans (1993) and Doczkal (1996). Colour characters are described from dry mounted specimens. To study male genitalia, specimens were relaxed in a closed pot with a high level of humidity and the genitalia were extracted using an entomological pin with a hooked tip. Genitalia were stored in microvials containing glycerol after clearing in warm 10% potassium hydroxide (KOH) for a few minutes and washing in distilled water. Drawings were created by using photographs of characters taken with a Leica DFC 320 (Wetzlar, Germany) camera attached to a Leica MZ16 binocular stereomicroscope and then processed in Adobe Photoshop CS3 V 10.0 software (Adobe Systems, San Jose, CA, USA), using drawing tablet EasyPen i405 (Genius, KYE Systems America Corporation, Miami, FL, USA).

Each specimen subjected to molecular analysis was labeled as a DNA voucher specimen and deposited in the insect collections of the FSUNS, the MZH (Insect collection of the Zoology unit, Finnish Museum of Natural History, Helsinki, Finland) or the MAegean. Table S1 (online supplementary information) provides the list of the specimens used for the species description, their collection data and the GenBank accession numbers of the generated DNA barcodes for *E. aurofinis* sp. n. and *E. torsicus* sp. n.

DNA analyses

Total genomic DNA was extracted using two or three legs from each specimen, performing the Chen et al. (2010) protocol for SDS extraction, slightly modified: (a) RNase A solution not added; (b) 40 mg ml–1 concentration of proteinase K solution;

and (c) two additional steps of chloroform/isoamyl alcohol (24:1). DNA samples were re-suspended in 30 µl of TAE buffer.

A standard primer pair was used to amplify the DNA barcodes of the mitochondrial cytochrome c oxidase subunit I gene fragment (COI, cox1); LCO-1490 (5′-GGTCAACAAATCATAAAGATATTGG-3′) and HCO-2198 (5′-TAAACTTCAGGGTGACCAAAAAATCA-3′) (Folmer et al. 1994). PCR amplifications were performed in a total volume of 25 µl, containing 25 ng µl–1 template of DNA, 5 pmol µl–1 of each primer, 0.08 mM of dNTPs, 1× reaction buffer (Fermentas, Thermo Fisher Scientific, Kent, UK) and 1.25 units of Polymerase (Dream Taq poly, Fermentas). We performed touchdown PCRs in an authorized PCR thermal cycler (Mastercycler®personal, Eppendorf, Hamburg, Germany), comprised of four steps: (a) initial denaturation at 94°C for 5 min; (b) denaturation at 94°C for 30 s, annealing at 60°C for 30 s with 0.5°C decrease per cycle and extension at 72°C for 1 min (total repetition of 18 cycles); (c) denaturation at 94°C for 30 s, annealing at 51°C for 30 s, extension at 72°C for 1 min (total repetition of 14 cycles); and (d) a final extension at 72°C for 10 min. Amplified products were visually inspected on 1.5% agarose gels. The ExoSap-IT kit (USB, Cleveland, OH, USA) was used for the PCR products purification and clean products were thereafter Sanger sequenced in both directions on an ABI 3730 DNA analyser (Applied Biosystems™, Thermo Fisher Scientific, Waltham, MA, USA) at the Sequencing Service laboratory of the Finnish Institute for Molecular Medicine (http://www.fimm.fi).

The obtained sequences were edited by eye, where required, using BioEdit 7.2.5 software (Hall 1999). The dataset included 12 DNA barcode sequences (eight sequences of *E. aurofinis* sp. n. and four sequences of *E. torsicus* sp. n.) with final length 601 nt. Pairwise distances between the species *E. aurofinis* sp. n. and *E. torsicus* sp. n. were conducted in MEGA version 6 (Tamura et al. 2013) and the computations were run by default using the p-distances model with 1000 bootstrap replicates. Basic parameters of intra and interspecific genetic diversity were calculated in DNASP v5 (Librado and Rosas, 2009).

Table 1. *Eumerus* species on eastern Mediterranean islands (species described here are not included).

Πίνακας 1. Τα είδη *Eumerus* των νησιών της Ανατολικής Μεσογείου (δεν συμπεριλαμβάνονται τα είδη τα οποία περιγράφονται για πρώτη φορά στην παρούσα έρευνα).

	Species	Type(s)	Distribution	Endemics
1	*Eumerus alpinus* Rondani, 1857	Studied (MZUF)	Corfu, Lesvos	no
2	*Eumerus amoenus* Loew, 1848	Studied (ZMHB)	Aegina, Anafi, Crete, Chios, Corfu, Euboea, Iraklia, Karpathos, Lesvos, Peloponnese, Rhodes, Samos, Thassos	no
3	*Eumerus argyropus* Loew, 1848	Studied (ZMHB)	Chios, Corfu, Crete, Peloponnese	no
4	*Eumerus armatus* Ricarte & Rotheray, 2012	Not studied, identity confirmed by A. Ricarte	Lesvos, Peloponnese, Rhodes, Samos	yes (limited to mentioned islands)
5	*Eumerus basalis* Loew, 1848	Studied (ZMHB)	Aegina, Anafi, Chios, Crete, Folegandros, Ikaria, Ios, Iraklia, Karpathos, Lesvos, Naxos, Peloponnese, Rhodes, Samos	no
6	*Eumerus claripennis* Coe, 1957	Not studied, identity confirmed by A. Ricarte	Lesvos	yes (Balkan endemic)
7	*Eumerus clavatus* Becker, 1921	Studied (ZMHB)	Corfu	no
8	*Eumerus consimilis* Šimić &t Vujić, 1996	Studied (FSUNS)	Peloponnese	no
9	*Eumerus emarginatus* Loew, 1848	Not studied, identity confirmed by D. Doczkal	Corfu, Crete, Lesvos, Peloponnese, Rhodes, Samos	no
10	*Eumerus lucidus* Loew, 1848	Studied (ZMHB)	Aegina, Chios, Lesvos	no
11	*Eumerus minotaurus* Claussen & Lucas, 1988	Studied (RMNH)	Corfu, Crete, Peloponnese	yes (Balkan endemic)
12	*Eumerus niehuisi* Doczkal, 1996	Studied (ZMHB)	Chios, Lesvos, Samos	no
13	*Eumerus niveitibia* Becker, 1921	Studied (ZMHB)	Crete, Lesvos, Peloponnese, Zakynthos	yes (limited to mentioned islands)
14	*Eumerus obliquus* (Fabricius, 1805)	Studied (ZMUC)	Corfu	no

15	*Eumerus pulchellus* Loew, 1848	Studied (ZMHB)	Aegina, Anafi, Andros, Chios, Corfu, Crete, Folegandros, Ios, Iraklia, Karpathos, Kea, Lesvos, Mykonos, Naxos, Paros, Rhodes, Samos, Samothraki, Santorini	no
16	*Eumerus pusillus* Loew, 1848	Studied (ZMHB)	Aegina, Anafi, Andros, Chios, Crete, Euboea, Ios, Iraklia, Karpathos, Kea, Lesvos, Mykonos, Naxos, Paros, Rhodes, Samos, Santorini, Sifnos	no
17	*Eumerus sogdianus* Stackelberg, 1952	Not studied, identity confirmed by D. Doczkal	Peloponnese	no
18	*Eumerus strigatus* (Fallen, 1817)	Not studied, identity confirmed by D. Doczkal	Peloponnese	no
19	*Eumerus sulcitibius* Rondani, 1868	Studied (MZUF)	Andros, Chios, Crete, Ikaria, Lesvos, Paros, Peloponnese, Samos	no
20	*Eumerus tricolor* (Fabricius, 1798)	Types destroyed (ZMUC), identity confirmed by D. Doczkal	Corfu, Euboea, Lefkada, Peloponnese	no
21	*Eumerus truncatus* Rondani 1868	Studied (MZUF)	Crete, Lesvos, Naxos	no
22	*Eumerus vestitus* Bezzi, 1912	Not studied, identity confirmed by J. Smith	Santorini	no

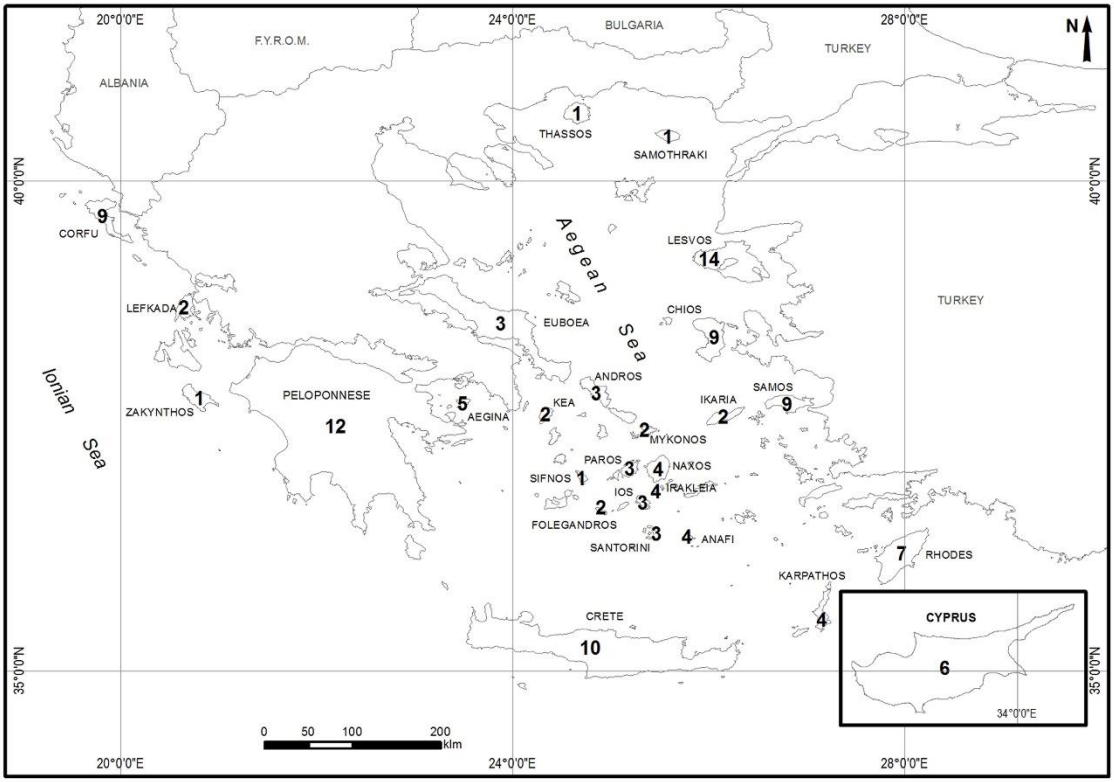

Fig. 1. Map of Eastern Mediterranean with investigated islands and number of *Eumerus* species per island.

Σχήμα 1. Χάρτης της Ανατολικής Μεσογείου με τα υπό μελέτη νησιά. Δίνεται ο αριθμός των ειδών *Eumerus* ανά νησί.

Results

Diversity of the genus Eumerus on the eastern Mediterranean islands

We recorded 25 species in the 28 islands of the eastern Mediterranean. Of these, 22 species are previously known taxa (Table 1), whereas the three additional species are new and are described here. Moreover, regarding the two new species *E. aurofinis* sp. n. and *E. torsicus* sp. n., the pairwise distance computations showed a clear differentiation between them (0.115). Seven species are recorded for the first time for Greece: *Eumerus alpinus* Rondani, 1857, *Eumerus clavatus* Becker, 1921, *Eumerus consimilis* Šimić et Vujić, 1996, *Eumerus obliquus* (Fabricius, 1805), *Eumerus sogdianus* Stackelberg, 1952, *Eumerus truncatus* Rondani, 1868 and *Eumerus vestitus* Bezzi, 1912.

Islands with the highest diversity of *Eumerus* species are (Table 1): Lesvos (14 species), Peloponnese (12), Crete (10), Chios, Corfu, Samos (all with nine), Rhodes (seven) and Cyprus (six). Endemics are recorded on nine islands: Lesvos (four),

Peloponnese (three), Crete, Rhodes and Samos (all with two) and Cyprus, Chios, Corfu, and Zakynthos (all with one endemic taxon).

Taxonomy

Eumerus alpinus Rondani, 1857 n. stat.

Based on our study of type specimens of West Palaearctic species of the genus *Eumerus* a new valid species is proposed from the list of synonyms of *Eumerus olivaceus* Loew, 1848.

Peck (1988) has cited *E. alpinus* Rondani, 1857 as a synonym of *E. olivaceus*. It was described from Piedmont in Italy as *E. alpinus* Bellardi (in litt.) in the paper of Rondani (1857). In the Rondani collection (MZUF) there is one male specimen with the original name label and corresponding data (as mentioned in the original description, this specimen was received from Professor Bellardi). We accept this specimen as the holotype. We also studied types of *E. olivaceus* in the Loew collection from ZMHB described from an unspecified number of males and female from Sicily in Italy. The morphological characters of examined types of these two taxa are clearly different, and we accepted *E. alpinus* as a name for populations on other parts of Apennine and Balkan peninsulas (*E. olivaceus* of authors). *E. olivaceus* remains as the name of the endemic species of Sicily.

Description of new species

Eumerus aurofinis *Grković, Vujić & Radenković sp. n.*

***Material examined*. Holotype. Greece** (Samos Island): 1 male, Koumaradhei, coll. 06.VI.2012, Vujić & Likov. Holotype is deposited in University of Novi Sad (FSUNS). **Paratypes. Greece**: Samos, Kosmadei, 1 male, 1 female, coll. 10.VI.2010, Rojo, Vujić & Ståhls; 1 male, coll. 12.VI.2010, Rojo, Vujić & Ståhls, 1 male, 1 female, coll. 07.VI.2012, Vujić; Koumaradhei, 1 male, 3 females, coll. 06.VI.2012, Vujić & Likov; Chora, 1 female, coll. 06.VI.2012, Vujić; Manolates, 1 female, coll. 15.V.2010, Ståhls; near Manolates, 1 male, coll. 08.VI.2010, Rojo, Vujić & Ståhls; Marathokambos, 1 female, coll. 06.VI.2012, Vujić & Likov; near Kastanea, 1 male, 1 female, coll. 12.VI.2010, Rojo, Vujić & Ståhls; near Kondeika, 2 males, coll. 09.VI.2010, Rojo, Vujić & Ståhls; near Leka, 1 male, 2 females, coll. 10.VI.2010, Rojo, Vujić & Ståhls; near Neochori, 2 males, coll. 17. V.2010, Ståhls & Rättel; 1 male, 1 female, coll. 07.VI.2012, Ståhls & Rättel; near Platanos, 3 males, 1 female,

coll. 09.VI.2010, Rojo, Vujić & Ståhls; near Stavrinides, 2 males, 3 females, coll. 08.VI.2010, Rojo, Vujić & Ståhls; Pyrgos, 1 male, 1 female, coll. 06.VI.2012, Vujić; 3 males, 2 females, coll. 08.VI.2012, Vujić & Likov; Rhodos, Kalathos, 1 male, 1 female, coll. 29.V.2014, Vujić; Lesvos, Skala Kallonis, 1 female, coll. 10.V.2006, Hull; **Turkey**: Mountain Bozdağ, near Çamurhamamı Köyü, 6 females, coll. 07.VI.2014, Vujić & Ačanski; Muğla, 1 male, 1 female, coll. 06.III.2014, Vujić & Ačanski (FSUNS).

General description. Robust species (9–11 mm), with very short body hairs, dark appearance, and golden reflection on top of abdomen (Fig. 2A, B).

Male. Head: Eyes (Fig. 3A) dichoptic, three ommatidia spaced, eye contiguity bare, black colour. Eye with sparse hairs of medium length. Eye margin slightly broadening ventrally. Lower facial margin anteromedially not protruding in lateral view (Fig. 3C). Anterior ocellus more distant from posterior ocelli than the later are from each other (Fig. 3E). Distance from posterior ocellus to the upper eye corner is slightly longer than to anterior ocellus. Face and frons black with whitish and gold pollinosity, especially along the posterior eye margin. Posterolateral eye margin with white pollinosity. Vertex and postocular orbit black with gold socket at the hair bases. Dense white hairs on face and more yellow on the frons. Ommatidia closed to the eye contiguity enlarged. Hairs on vertex yellow except on ocellar triangle, where they are black. Hairs denser and shorter anterior of anterior ocellus. Posterior of anterior ocellus obscure groove which extends behind posterior ocelli. Antenna rounded, brown to reddish. Sensory pit rounded, located in the centre of outer side of distal part of antennal third segment. Long ventral hairs of pedicel length about half depth of pedicel, inner side with short pale hairs. First flagellomere little deeper than pedicel. Arista dark brown.

Thorax. Scutum and scutellum black with blue metallic lustre and dense punctuation, short pale hairs, little longer on anterior margin of presutural area. Prescutum with bronze pruinosity. Anterior part of presutural area with two white triangles of pruinescence and short white line in the middle, shorter than the length of triangle. Triangles sometimes extend behind the transverse suture. Posterior margin of scutellum broad with serration. Subscutellum small. In the middle of scutellum small depression. Presence of groove on scutellum parallel with its posterior margin. Pleurae black with gold pruinosity. Anepisternum with yellow hairs, posteriorly with longer yellow bristles directed backwards. Presutural cali with few yellow bristles.

Katepisternum with pale hairs, slightly longer in posterior part. Halter yellow. Wing with brownish tinge with gradual shadows in the area posterior of intersection of Rs1 + 2 and Rs3 + 4. Wing entirely microtrichose. Calypter white in contrast to the dark appearance of the body. Legs dark, basal half and apical part of tibia, ventral side of tarsus red. Two rows of black spines on ventral preapical part of femora. Hind trochanter simple, hind femora thick (Fig. 4E).

Abdomen. Twice as long as wide. Tergites black with metallic blue reflection medially and metallic green laterally. Punctuated, interspaces bigger than the puncture diameters, on tergite 3–4 denser punctuation. Tergites 2–4 with pairs of white pruinose lunules, separated in the middle. Abdomen pale haired, laterally with longer erect hairs. Sternites 2 and 3 with white hairs. Abdomen with gold pollinosity laterally. Tergite 4 with gold hairs laterally and on posterior part.

Male genitalia. (Fig. 4A–D). Cercus small, rounded, recurved (Fig. 4A). Interior accessory lobe of posterior surstyle lobe covered with dense microtrichia. Posterior surstyle lobe elongated, simple, on ventral apical ridge with short bristles, on dorsal side with longer sparse microtrichia. Hypandrium broad, curved, on dorsal side with sparse microtrichia (Fig. 4B). Ctenidion situated apically. Aedeagus (Fig. 4C, D: ae) and associated structures shown in Fig. 4C, D: lateral sclerite of aedeagus (Fig. 4C, D: ls); ejaculator apodeme (Fig. 4C, D: ea) narrow and elongated; aedeagal apodeme very expanded, kite shaped in ventral view (Fig. 4C, D: ap).

Female. Similar to the male except normal sexual dimorphism and for the following characteristics: *Head*. Face and frons (Fig. 3B) black, covered with white and gold pollinosity. Short yellow hairs from anterior ocellus to antennal socket and brighter hairs from antennae to mouth edge. From anterior ocellus obscure groove which extends to antennal socket. Ocelli in equilateral triangle (Fig. 3F). Antenna oval, red (Fig. 3D). Eye sparse haired. Abdomen. Wide as thorax. Tergites black, tergites 2–4 with a pair of grey pollinose lunules, tergite 4 entirely covered with short yellow hairs.

Diagnosis. It differs from the all the other species of the genus in having very short body hairs, golden reflections and short golden hairs on the top of the abdomen. Male genitalia with specific shape of surstyle lobe (Fig. 4A) and aedeagal apodeme (Fig. 4C, D: ap); sternum 4 in male simple without any additional structure.

Etymology. The epithet is derived from the Latin words aurum (gold) and finis (end) and refers to the golden reflection of the tip of abdomen.

DNA voucher specimen. All DNA voucher specimens are deposited in the DNA voucher specimen collection of FSUNS, and specimens voucher, GenBank accession numbers as well as locality information can be found in Table S1 (online supporting information).

In total three different haplotypes were recorded for *E. aurofinis* (Table 2). Basic indices of genetic diversity are given in Table 2. The most frequent haplotype was found in four specimens from Samos Island and one from Turkey (Mt Bozdag). One haplotype was also detected in Samos Island (1 specimen), while the third occurred exclusively on Rhodes Island.

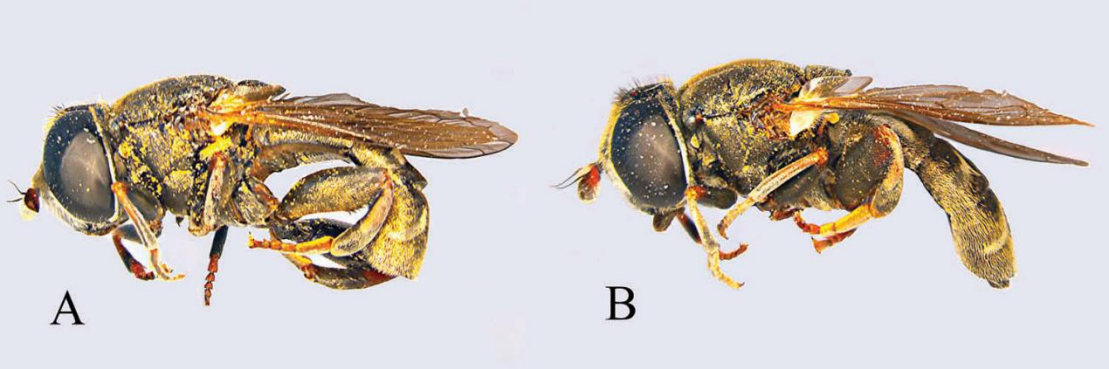

Fig. 2. *Eumerus aurofinis* sp. n. (A) male; (B) female. Photo: A. Grković.
Σχήμα 2. *Eumerus aurofinis* sp. n. (A) άρρεν· (B) θήλυ. Φωτογραφία: A. Grković.

Table 2. Basic genetic diversity indices for *Eumerus aurofinis* sp. n. and *E. torsicus* sp. n. based on DNA barcode sequences.
Πίνακας 2. Βασικοί δείκτες γενετικής ποικιλότητας για τα είδη *Eumerus aurofinis* sp. n. και *E. torsicus* sp. n. με βάση τον γενετικό γραμμωτό κώδικα (DNA barcode).

Parameter	*E. aurofinis*	*E. torsicus*	Total
N	8	4	12
h	3	2	5
Hd	0.607	0.667	0.803
π	0.0039	0.0022	0.059
k	2.036	1.333	35.227

N – number of specimens; h – number of haplotypes; Hd – haplotype diversity; π – nucleotide diversity; k – average number of nucleotide differences.

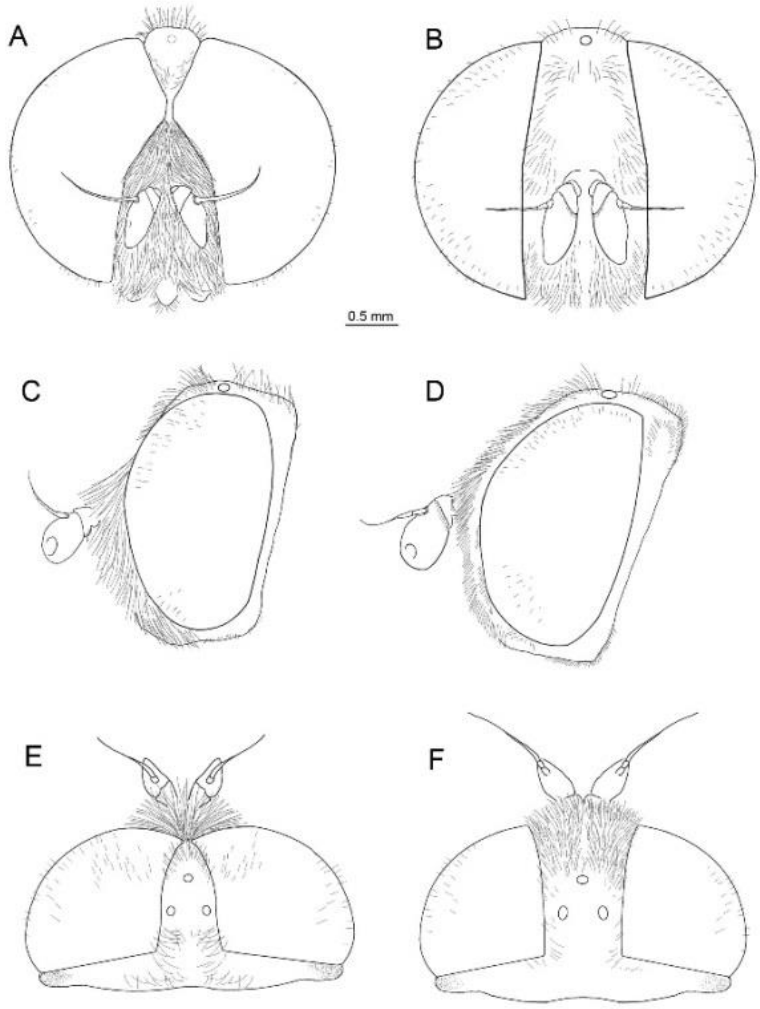

Fig. 3. *Eumerus aurofinis* sp. n., head. Frontal view: (A) male; (B) female. Lateral view: (C) male, (D) female. Dorsal view: (E) male, (F) female.

Σχήμα 3. *Eumerus aurofinis* sp. n., κεφαλή. Μετωπική όψη: (A) άρρεν· (B) θήλυ. Πλευρική όψη: (C) άρρεν, (D) θήλυ. Ραχιαία όψη: (E) άρρεν, (F) θήλυ.

Eumerus torsicus *Grković & Vujić sp. n.*

Material examined. Holotype. Greece (Chios Island): 1 male, Elinta, coll. 9–11.XI.2012, Nakas. Holotype is deposited in University of Novi Sad (FSUNS**). Paratypes. Greece**: Chios, Elinta, 2 males, coll. 9–11.XI.2012, Nakas. **Cyprus**: Troodos Mountains, Almirolivado, 4 females, coll. 18.IX.2011, Hionistra, Xióni, 6 males, 12 females, coll. 18.IX.2011, Kakopetria, 1 male, 17.IX.2011; Makria Kondarka, 1 male, 3 females, 18.IX.2011.

General description. Large species (9–11 mm), with long and narrow abdomen (Fig. 5A, B).

Male. *Head*. Eyes bare, holoptic, 10–11 ommatidia long contiguity. Eye margin almost parallel. Lower facial margin flattened. Vertex and postocullar orbit black with

white pollinosity anterior of anterior ocellus and posterior of posterior ocelli, to upper eye margin (Fig. 6A). Ocelli form an equilateral triangle. Anterior ocellus smaller than the posterior two. Vertex and postocullar orbit with long white hair, except on ocellar triangle, which are black. White pollinosity behind upper eyes margins. Face black with white pollinosity and long white hairs. Antenna fanshaped, slightly elongated on ventral corner, reddishbrown (Fig. 6C). Scape and pedicel dark, except distal margin of pedicel which is reddish. Sensory pit on brighter area, at the ventral base of third antennal segment. Long white ventral hairs of pedicel are longer than depth of pedicel, dorsal hairs black and white, as long as depth of pedicel. Arista dark brown.

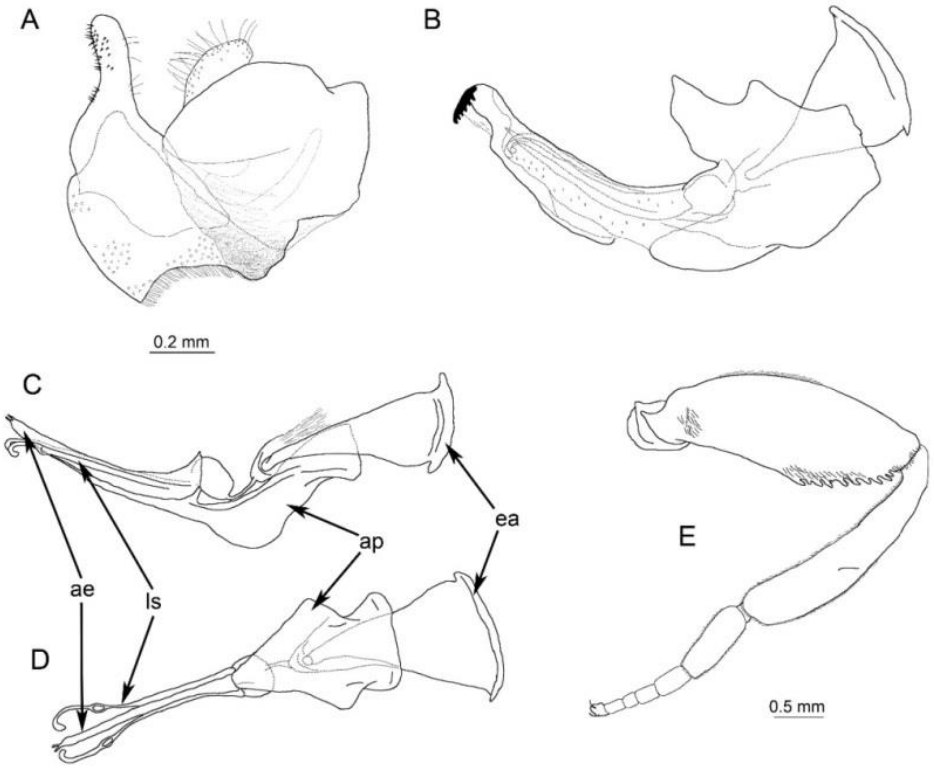

Fig. 4. *Eumerus aurofinis* sp. n., (A–D) male genitalia: (A) epandrium, lateral view; (B) hypandrium, lateral view; (C) aedeagus and accessory structures, lateral view; (D) aedeagus and accessory structures, ventral view (ae – aedeagus, ls – lateral sclerite of aedeagus, ap – aedeagal apodeme, ea – ejaculator apodeme). (E) Hind leg, male. **Σχήμα 4**. *Eumerus aurofinis* sp. n., (A–D) γεννητικός οπλισμός άρρενος: (A) επάνδριο (τελευταίος νωτιαίος τεργίτης), πλευρική όψη· (B) υπάνδριο (9ος κοιλιακός στερνίτης), πλευρική όψη· (C) αιδοιαγός και βοηθητικά εξαρτήματα, πλευρική όψη· (D) αιδοιαγός και βοηθητικά εξαρτήματα, κοιλιακή όψη (ae – αιδοιαγός, ls – πλευρικός σκληρίτης του αιδοιαγού, ap – απόδεμα του αιδοιαγού, ea – εκσπερματικό απόδεμα). (E) Πίσω πόδι, άρρεν.

Thorax. Scutum and scutellum black with gold-green lustre, with dense punctuation and short pale hairs which are a little longer on the scutellum. Scutum with two pairs of white stripes, the pair in the middle spreading toward the full-length of the scutum, the lateral pair of shorter stripes extending from the transverse suture to the posterior margin of the scutum. Posterior margin of scutellum with narrow edge. Pleurae black with gold pollinosity and long yellow pilose. Halter pale yellow. Wing entirely transparent; vena spuria well expressed, ending at rm crossvein. Legs dark, yellow haired. Ventral side of hind tarsus yellow-gold, apical part of femora and basal part of tibia reddish. Fore and middle tarsi entirely gold. Hind trochanter slightly tapered ventrally, femora thick. Hind tibia twisted in apical fifth (Fig. 6E). Hind basitarsus long, as long as half of hind tibia; tarsal segments 2–5 extremely short (Fig. 6E).

Abdomen. Three times as long as wide, with dense punctuation, white haired. Tergite 1 with white pollinosity laterally. Tergites 2–4 with pairs of white pruinose lunules separated in the middle. Posterior margin of tergite 4 colourless. Sternite 2–3 with pale hairs in the middle. Sternite 4 in specific form (Fig. 7E).

Male genitalia. (Fig. 7A–D). Cercus small, rounded. Interior accessory lobe of posterior surstyle lobe covered with dense microtrichia. Posterior surstyle lobe very elongated, narrowing toward the top, slightly recurved with short bristles laterally and few long bristles dorsally (Fig. 7A). Hypandrium narrow, simple, ctenidion situated apically (Figu. 7B). Aedeagus (Fig. 7C, D: ae) and associated structures shown in Fig. 7C, D: lateral sclerite of aedeagus (Fig. 7C, D: ls), aedeagal apodeme three-pointed on the top, keel-shaped ventrally (Fig. 7C, D: ap); ejaculator apodeme broad, with narrow edge (Fig. 7C, D: ea).

Female. Similar to the male except normal sexual dimorphism and for the following characteristics: *Head*. Face and frons black with white pollinosity toward eye margin and behind posterior ocelli, except in the area of vertex (Fig. 6B). Gold pollinosity from vertex to antennal socket. Face from antennae to mouth densely covered with white pollinosity and white hairs. Antenna oval, almost round, reddish-brown (Fig. 6D). *Abdomen*. Tergites black covered with white hairs and with pairs of white lunules on tergites 2–4.

Diagnosis. The male differs from all the other species of the genus in the twisted apical fifth of the hind tibia andextremely short tarsal segments 2–5 on hind leg (Fig. 6E); male genitalia with very long and two timescurved posterior surstyle lobe (Fig.

7A); sternum 4 with two broad apical prolongations (Fig. 7E). In female, pollinose areas on frons with black undusted dots (Fig. 6B); sternites 2–3 very narrow, about 5 times longer than broad (Fig. 6F).

Etymology. The epithet is derived from the Latin verb torqueo and relates to the twisted apical part of hind tibia in male.

DNA voucher specimen. All DNA voucher specimens are deposited in the DNA voucher specimen collection of FSUNS, and specimens voucher, GenBank accession numbers as well as locality information can be found in Table S1 (online supporting information).

Two haplotypes were found for *Eumerus torsicus* (Table 2). Basic indices of genetic diversity are given in Table 2. One haplotype is exclusive for Cyprus (2 specimens), and the other for Chios Island (2 specimens).

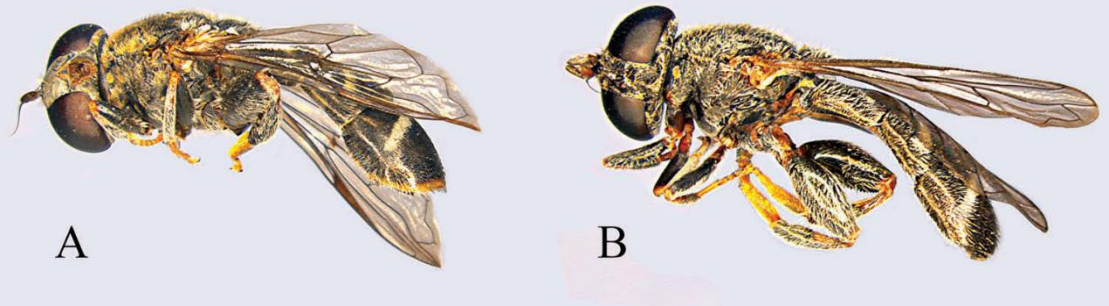

Fig. 5. *Eumerus torsicus* sp. n. (A) male; (B) female. Photo: A. Grković.
Σχήμα 5. *Eumerus torsicus* sp. n. (A) άρρεν· (B) θήλυ. Φωτογραφία: A. Grković.

Eumerus crassus *Grković, Vujić & Radenković sp. n.*

Material examined. Holotype. Greece (Lesvos Island): Ag. Ermogenis Beach, 1 male, coll. 02.V.2008, Vujić (antennae lacking, only right scape and pedicel present). Holotype is deposited in University of Novi Sad (FSUNS).

General description. **Male**. (Fig. 8A) *Head*. Eyes holoptic, covered with dense hairs, with 3–4 ommatidia long contiguity. Eye margins almost parallel, slightly broadening ventrally. Face and frons black with sparse gold and white pollinosity except on ocellar triangle. Ocelli in almost equilateral triangle, anterior ocellus only slightly farther from posterior ocelli than the latter are from each other (Fig. 9G). Face and frons with dense white hairs. Lower facial margin protruding (Fig. 9F). Pedicel elongated, longer than deep. Ventral hairs of pedicel a little longer than dorsal hairs.

Thorax. Scutum and scutellum black with gold lustre, covered with dense pale hairs. Scutum with a pair of white pruinose triangles which are expanding in obscure lines extending almost to the end of scutum. White pinstripe with grey pollinosity in the middle of the scutum. Pleura black with very short yellow dense microtrichia and longer pale hairs on katepisternum, anepisternum and anepimeron. Wing transparent with dense brown to yellow microtrichia. *Leg*. Hind femur black with long yellow hairs and covered with gold pollinosity; hind tibia black and yellow at the base. Tarsus with silver pollinosity.

Abdomen. Abdomen oval, slightly tapering toward the top, wide as the width of the thorax, with white short hairs (Fig. 8B). Tergites 2–3 with pairs of white pollinose lunules. Tergite 4 as long as wide, covered with white dense hairs, quite longer than those of the tergites 2 and 3.

Male genitalia. (Fig. 9A, C). Most similar to genitalia of *Eumerus sogdianus*, Stackelberg, 1952 (Fig. 9B). Cercus rounded, with the notch on posterodorsal margin. Posterior surstyle lobe elongated, with folded dorsal margin covered with hairs. Ventral margin inside with dense long hairs. Interior accessory lobe of posterior surstyle lobe covered with microtrichia. Hypandrium simple (Fig. 9C). Aedeagal apodeme ray-shaped in ventral view.

Female. Unknown.

Diagnosis. Morphologically related to "*strigatus*" group of species (sensu Speight et al. 2013), differs from all related species of the genus in more robust body (Fig. 8B, C), clear differences in structure of male genitalia and shape of sternite 4. Male genitalia similar to *Eumerus sogdianus* from which it differs in cerci with the notch on posterodorsal margin, broad posterior surstyle lobe with straight margins, narrower and bent in *E. sogdianus* (Fig. 9A, B); and broad sternite 4, with two apical prolongations, narrower in *E. sogdianus* (Fig. 9D, E).

Etymology. The epithet is derived from the Latin word *crassus* (solid) demonstrating the body habitus more robust comparing to the related taxon.

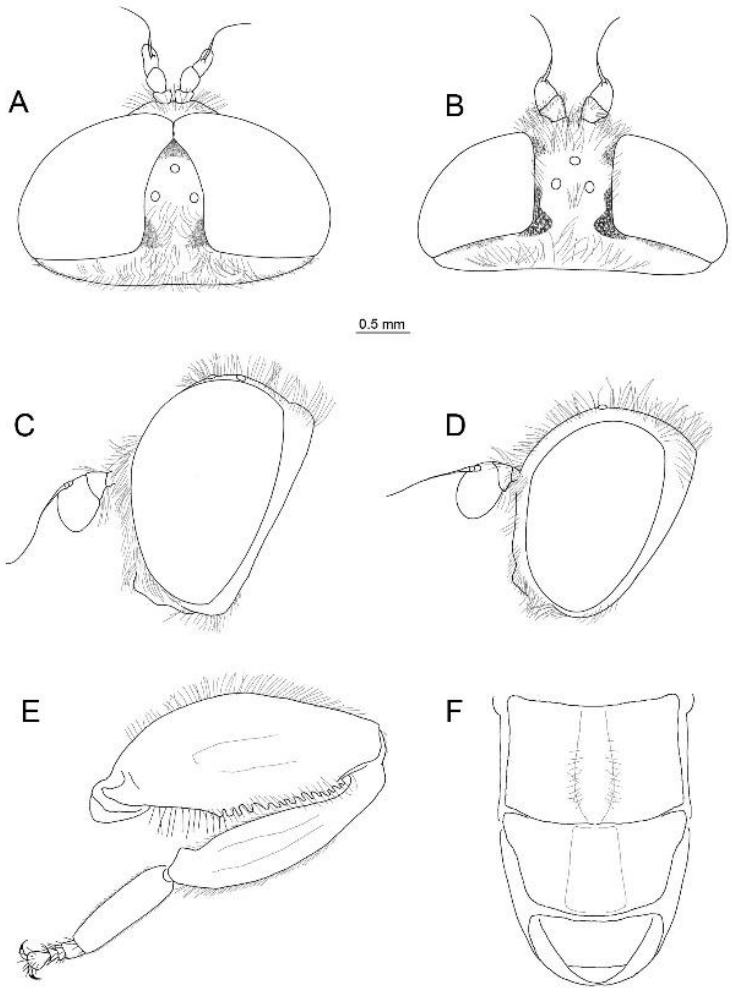

Fig. 6. *Eumerus torsicus* sp. n., head, dorsal view: (A) male; (B) female. Head, lateral view: (C) male; (D) female. (E) Hind leg, male. (F) Sternites 2–4, female.

Σχήμα 6. *Eumerus torsicus* sp. n., κεφαλή, ραχιαία όψη: (A) άρρεν· (B) θήλυ. Κεφαλή, πλευρική όψη: (C) άρρεν· (D) θήλυ. (E) Πίσω πόδι, άρρεν. (F) Στερνίτες θήλεος 2–4.

Discussion

We present a survey of the diversity and distribution of *Eumerus* species in the eastern Mediterranean region, where a high number of species, i.e. 25, was recorded (see Table 1). This is almost three quarters (71%) of all *Eumerus* species known for south-eastern Europe accounting for 35 species in total (Vujić et al. 2015). The latter highlights the significance of the eastern Mediterranean region as a hotspot for the genus. Indeed, our findings support the expectation of Petanidou et al. (2013) to encounter a considerable number of species new to science in the Aegean Islands. Among the 25 species in the eastern Mediterranean, seven are endemic as their geographical distribution is limited to the Balkan Peninsula and/or only to the eastern

Mediterranean islands. Four species out of the 25 were previously known (*Eumerus armatus* Ricarte and Rotheray, 2012, *E. claripennis* Coe, 1957, E. *minotaurus* Claussen & Lucas, 1988, *E. niveitibia* Becker, 1921) and three species are new to science and are described here (*E. aurofinis* sp. n., *E. torsicus* sp. n. and *E. crassus* sp. n.). Islands with the highest number of recorded species belonged to the group of large islands (area >420 km2, based on Vujić et al. Forthcoming 2016). Islands with the highest diversity of *Eumerus* species usually harbour endemics as well (Crete, Cyprus, Lesvos, Peloponnese, Rhodes and Samos), although two islands with high diversity (Chios and Corfu) lack endemic species. Among the small islands (area <420 km2), it was only on Zakynthos where we registered one endemic taxon (*E. niveitibia*).

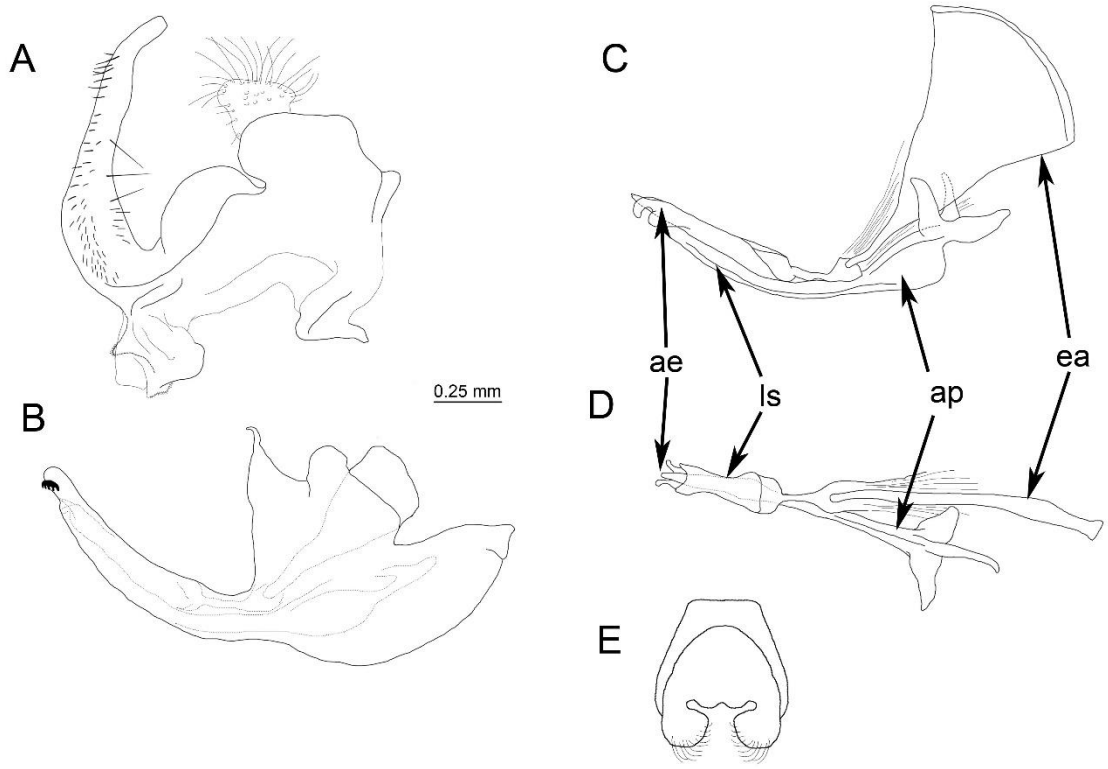

Fig. 7. *Eumerus torsicus* sp. n., (A–D) male genitalia: (A) epandrium, lateral view; (B) hypandrium, lateral view; (C) aedeagus and accessory structures, lateral view; (D) aedeagus and accessory structures, ventral view (ae – aedeagus, ls – lateral sclerite of aedeagus, ap– aedeagal apodeme, ea – ejaculator apodeme). (E) Male sternite 4.

Σχήμα 7. *Eumerus torsicus* sp. n., (A–D) γεννητικός οπλισμός άρρενος: (A) επάνδριο (τελευταίος νωτιαίος τεργίτης), πλευρική όψη· (B) υπάνδριο (9ος κοιλιακός στερνίτης), πλευρική όψη· (C) αιδοιαγός και βοηθητικά εξαρτήματα, πλευρική όψη· (D) αιδοιαγός και βοηθητικά εξαρτήματα, κοιλιακή όψη (ae – αιδοιαγός, ls – πλευρικός σκληρίτης του αιδοιαγού, ap – απόδεμα του αιδοιαγού, ea – εκσπερματικό απόδεμα). (E) Στερνίτης άρρενος 4.

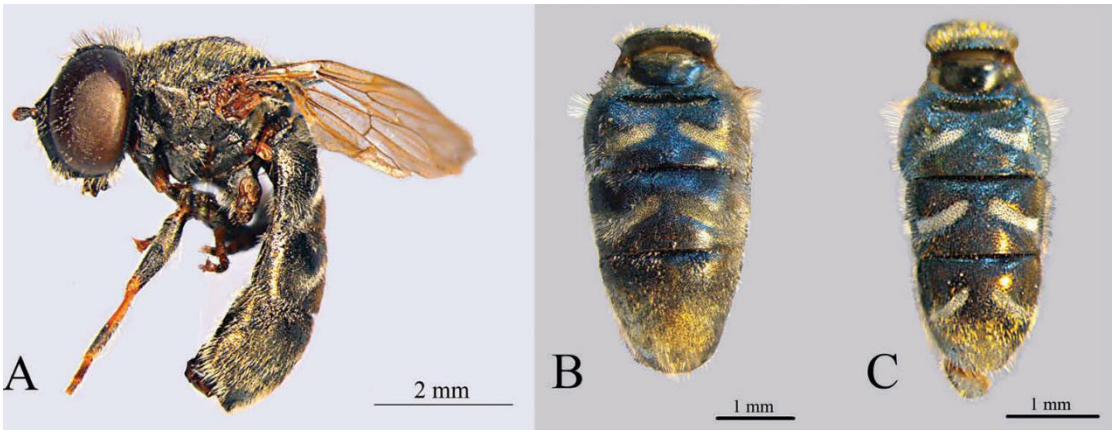

Fig. 8. *Eumerus crassus* sp. n. (A) male; (B) tergites; (C) *Eumerus sogdianus*, tergites. Photo: A. Grković.

Σχήμα 8. *Eumerus crassus* sp. n. (A) άρρεν· (B) τεργίτες· (C) *Eumerus sogdianus*, τεργίτες. Φωτογραφία: A. Grković.

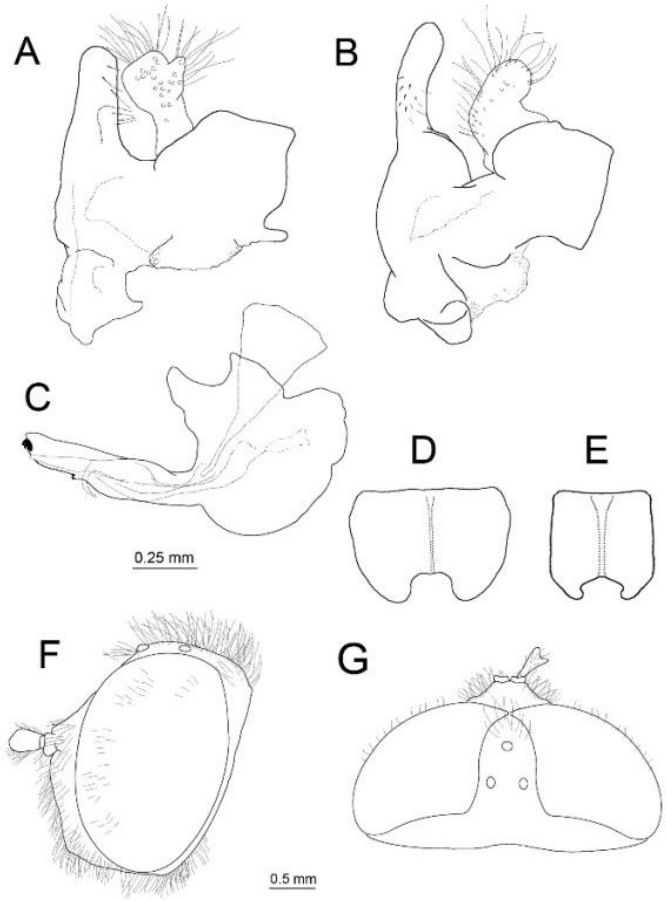

Fig. 9. Epandrium: (A) *E. crassus* sp. n.; (B) *E. sogdianus*. (C) *E. crassus* sp. n. hypandrium. (D, F) Sternite 4: (D*) Eumerus crassus* sp. n.; (E) *E. sogdianus*. (F, G) *E. crassus* sp. n., head, male: (F) lateral view; (G) dorsal view.

Σχήμα 9. Επάνδριο (τελευταίος νωτιαίος τεργίτης): (A) *E. crassus* sp. n.· (B) *E. sogdianus*. (C) *E. crassus* sp. n. υπάνδριο (9ος κοιλιακός στερνίτης). (D, F) Στερνίτης 4: (D*) Eumerus crassus* sp. n.· (E) *E. sogdianus*. (F, G) *E. crassus* sp. n., κεφαλή, άρρεν: (F) πλευρική όψη· (G) ραχιαία όψη.

Only three species are restricted to particular island(s) (and thus can be considered as island endemics): *E. niveitibia* (Crete, Lesvos, Peloponnese and Zakynthos), *E. torsicus* sp. n. (Chios and Cyprus) and *E. crassus* sp. n. (Lesvos). Comparing the percentage of the island endemic species (12%) with recent results for the hoverfly genus *Merodon* (12.3%) in eastern Mediterranean islands (Vujić et al. submitted), the level of endemicity is essentially the same, and twice the percentage of the endemic butterfly fauna reported by Dennis et al. (2000).

Considering the species richness of the genus and its great significance to ecosystems, many studies should have been published, but this is not the case for *Eumerus*; few taxonomical studies exist, and DNA barcodes are deficient or absent; very few *Eumerus* sequences can be found in GenBank. The latter is an issue as the species delimitation within *Eumerus* has proven a challenge, and there is no appropriate key for identification of the European *Eumerus* species, so DNA barcodes would be useful in species identification in addition to diagnostic features and figures of the important morphological characters. This could be even more useful when it comes to newly described species, as in the present study for *E. aurofinis* sp. n. and *E. torsicus* sp. n. For these two species an integrative approach, i.e. a blend of morphological characters and DNA sequences, was applied to achieve and confirm species delimitation. The determined pairwise distance (0.115) and average number of nucleotide differences between these two species (70.625) significantly contribute to species delimitation and also reveal slight intraspecific divergence. For an island endemic species *E. torsicus* sp. n., recorded haplotypes also showed exclusive occurrence for each island (Chios and Cyprus).

Acknowledgments

This research has been co-financed by the European Union (European Social Fund – ESF) and Greek national funds through the Operational Program "Education and Lifelong Learning" of the National Strategic Reference Framework (NSRF) – Research Funding Program: THALES. "Investing in knowledge society through the European Social Fund". We are also grateful to A. Ricarte, D. Doczkal, and J. Smith for confirmation of identity of some species.

References

Chen H, Rangasamy M, Tan SY, Wang HC, Siegfried BD. 2010. Evaluation of five methods for total DNA extraction from western corn rootworm beetles. Plos One. 5(8):1–6.

Dayrat B. 2005. Towards integrative taxonomy. Biological Journal of the Linnean Society. 85:407–415.

Dennis RLH, Shreeve T, Olivier A, Coutsis JG. 2000. Contemporary geography dominates butterfly diversity gradients within the Aegean archipelago (Lepidoptera: Papilionoidea, Hesperioidea). Journal of Biogeography. 27:1365–1383.

Doczkal D. 1996. Description of two new species of the genus *Eumerus* Meigen (Dipt., Syrph.) from Corsica. Volucella.2:3–19.

Folmer O, Black M, Hoeh W, Lutz R, Vrijenhoek R. 1994. DNA primers for amplification of mitochondrial cytochrome c oxidase subunit I from diverse metazoan invertebrates. Molecular Marine Biology and Biotechnology. 3:294–299.

Hall TA. 1999. BioEdit: a user-friendly biological sequence alignment editor and analysis program for Windows 95/98/NT. Nucleic Acids Symposium Series. 41:95–98.

Hurkmans W. 1993. A monograph of *Merodon* (Diptera: Syrphidae) part 1. Tijdschrift Voor Entomologie. 136:147–234.

Librado P, Rozas J. 2009. DnaSP v5: a software for comprehensive analysis of DNA polymorphism data. Bioinformatics. 25:1451–1452.

Marinoni L, Morales M. 2007. The second record of the Genus *Eumerus* Meigen, 1822 (Diptera: Syrphidae) for the neotropical region and the first for Brazil. Proceedings of the Entomological Society of Washington. 109:493–495.

Pape T, Thompson FC, editors. 2015. Systema Dipterorum. Version 1.5. [cited 2015 Sep 18]. Available from: http://www.diptera.org/.

Peck LV. 1988. Syrphidae. In: Soos A, Papp L, editors. Catalogue of Palaearctic Diptera. Akadémiai Kiadó: Budapest; p. 11–230.

Pérez-Bañon C, Marcos-García MÁ. 1998. Life history and description of the immature stages of *Eumerus purpurariae* (Diptera: Syrphidae) developing in *Opuntia maxima*. European Journal of Entomology. 95:373–382.

Petanidou T, Ståhls G, Vujić A, Olesen JM, Rojo S, Thrasyvoulou A, Sgardelis S, Kallimanis AS, Kokkini S, Tscheulin T. 2013. Investigating plant–pollinator relationships in the Aegean: the approaches of the project POLAEGIS (The pollinators of the Aegean archipelago: diversity and threats). Journal of Apicultural Research. 52:106–117.

Popov GV. 2010. *Merodon alexandri* spec. nov. – a new species of hoverfly (Diptera: Syrphidae) from the nothern Black Sea Region. Studia Dipterologica. 16:133–151.

Radenković S, Vujić A, Ståhls G, Pérez-Bañon C, Rojo S, Petanidou T, Šimić S. 2011. Three new cryptic species of the genus *Merodon* Meigen (Diptera: Syrphidae) from the island of Lesvos (Greece). Zootaxa. 2735:35–56.

Ricarte A, Marcos-García MÁ, Rotheray GE. 2008. The early stages and life histories of three *Eumerus* and two *Merodon* species (Diptera: Syrphidae) from the Mediterranean region. Entomologica Fennica. 19:129–141.

Rondani C. 1857. Dipterologiae Italicae Prodromus. 2. Species italicae ordinis Dipterorum in genera characteribus definita, ordinatim collectae, methodo analitica distinctae, et novis vel minus cognitis descriptis. Pars prima. Oestridae: syrphidae [sic!]: Conopidae. Parmae [= Parma]. 1–264.

Rotheray GE. 1993. Colour guide to hoverfly larvae (Diptera, Syrphidae) in Britain and Europe. Dipterists Digest. 9:156.

Rotheray GE, Gilbert FS. 1999. Phylogeny of Palaearctic Syrphidae (Diptera): evidence from larval stages. Zoological Journal of the Linnean Society. 127:1–112.

Rotheray GE, Gilbert FS. 2011. The Natural History of Hoverflies. Forrest Text, Swn y Nant. xiv + 333 pp. [before 2011.06.12 according to Rotheray]

Speight MCD. 2014. Species accounts of European Syrphidae (Diptera). Syrph the Net, the database of European Syrphidae. Dublin.78: Syrph the Net publications; p. 321.

Speight MCD, Hauser M, Withers P. 2013. *Eumerus narcissi* Smith (Diptera, Syrphidae), presence in Europe confirmed, with a redescription of the species. Dipterist Digest. 20:17–32.

Stackelberg AA. 1961. Palaearctic species of the genus *Eumerus* Mg. (Diptera, Syrphidae). Trudy Vsesojuznogo Entomologiceskogo Obscestva. 48:181–229.

Tamura K, Stecher G, Peterson D, Filipski A, Kumar S. 2013. MEGA6: molecular evolutionary genetics analysis version 6.0. Molecular Biology and Evolution. 30:2725–2729.

Thompson CF. 1999. A key to the genera of the flower flies (Diptera: Syrphidae) of the Neotropical Region including descriptions of new genera and species and a glossary of taxonomic terms. Contributions on Entomology International. 3:319–378.

Vujić A, Marcos-García MÁ, Sarıbıyık S, Ricarte A. 2011. New data on the *Merodon* Meigen 1803 fauna (Diptera: Syrphidae) of Turkey including description of a new species and changes in the nomenclatural status of several taxa. Annales de la Société Entomologique de France (N.S.). 47:78–88.

Vujić A, Perez-Banon C, Radenković S, Ståhls G, Rojo S, Petanidou T, Šimić S. 2007. Two new species of genus *Merodon* Meigen, 1803 (Syrphidae, Diptera) from the island of Lesvos (Greece), in the eastern Mediterranean. Annales de la Societe Entomologique de France. 43:319–326.

Vujić A, Petanidou T, Tscheulin T, Ståhls G, Radenković S, Baturan Ž, Mijatović G, Rojo S, Pérez-Bañón C, Devalez J, et al. Forthcoming 2016. Biogeographical patterns of the genus *Merodon* Meigen, 1803 (Diptera: Syrphidae) in islands of the eastern Mediterranean and adjacent mainlands. Insect Conservation and Diversity.

Vujić A, Radenković S, Grković A. 2015. Taxonomic status of *Eumerus* Meigen, 1822 (Diptera, Syrphidae) species in South-East Europe. In: Poster session presented at: 8th International Symposium on the Syrphidae; 2015 Jun 4–8; Monschau: Zoologisches Forschungsmuseum Alexander Koenig; p. 69.

Vujić A, Radenković S, Likov L, Trifunov S, Nikolić T. 2013. Three new species of the *Merodon nigritarsis* group (Diptera: Syrphidae) from the Middle East. Zootaxa. 3640:442–464.

CHAPTER 4

Taxonomy and systematics of three species of the genus *Eumerus* Meigen, 1822 (Diptera: Syrphidae) new to southeastern Europe

Taxonomy and systematics of three species of the genus *Eumerus* Meigen, 1822 (Diptera: Syrphidae) new to southeastern Europe

Ana Grković, Ante Vujić, Antonia Chroni, Jeroen van Steenis, Mihajla Đan and Snežana Radenković

Published in Zoologischer Anzeiger (2017), 270, 176–192.

Abstract

The genus *Eumerus* Meigen (Diptera: Syrphidae) is considered one of the most species-rich hoverfly genera. Here, we present two new species, *E. montanum* Grković, Radenković & Vujić sp. n. (Montenegro, Greece) and *E. rubrum* Grković & Vujić sp. n. (Greece), and one species, *E. uncipes* Rondani, 1850, recorded for the first time in southeastern Europe. The species are members of three different taxon groups, respectively *E. strigatus* sensu Speight et al. (2013), *E. tricolor* sensu Chroni et al. (2017) and *E. clavatus* as defined here. Diagnostic characters for each of the three taxon groups and descriptions of the two new species are provided. In addition, we employed morphological and molecular data for available taxa of the *E. strigatus* taxon group in order to corroborate their taxonomical status and systematic position. Finally, we discuss the diversity of these taxon groups (*E. clavatus*, *E. strigatus* and *E. tricolor*) and give a detailed overview of the differences between closely-related species.

Keywords: *Eumerus*, new species, *Eumerus strigatus* group; *Eumerus tricolor* group; *Eumerus clavatus* group; DNA barcoding

Introduction

During the last glaciations, southeastern Europe, including all countries south of Alpine region and Pannonian plain, harboured a tremendous number of animal species, serving as a center of biodiversity and endemism (Džukić and Kalezić, 2004; Gaston and David, 1994; Hewitt, 1999; 2000, 2011; Poulakakis et al., 2014, Schmitt, 2007). Various projects have explored the biodiversity, ecology and biogeography of southern parts of Europe, revealing the conservation and evolutionary statuses of different species; amphibians and reptiles (Džukić and Kalezić, 2004; Marzahn et al.

2016), beetles (Drees et al., 2016), flies (Vujic et al., 2016; Ståhls et al., 2016), molluscs (Psonis et al., 2015), spiders (Sagonas et al., 2014) to name a few. One very species-diverse target group of such studies is the family of hoverflies (Speight, 2014). Thompson et al. (2010) stated that hoverflies consisted of 6100 species worldwide whereas, five years previously, only 6000 species were known (Thompson, 2005). Studies on hoverfly taxonomy and systematics have increased tremendously over recent years; an assessment of Web of Science records (keywords: hoverflies/syrphidae and taxonomy or systematics) on 07 November 2016 revealed that the number of papers produced during the last decade is almost equal to the number produced from 1970 to 2005. Besides the vast amount of papers the number of newly described species is even higher during the last decade compared with the 35 years period mentioned before. This is partly a consequence of new methods (e.g. DNA barcoding) and approaches (e.g. integrative taxonomy) that have assisted and facilitated species diagnoses and delimitations where species identifications were previously complicated (Chroni et al., 2017; Jordaens et al., 2015; Nedeljković et al., 2015; Ståhls et al., 2008; Suk & Han, 2013; Young et al., 2016).

The genus *Eumerus* Meigen, 1822 is an example of high hoverfly species diversity (Speight, 2014) and endemism (Grković et al., 2015; Ricarte et al., 2012) in southeastern Europe. To date, the European fauna of *Eumerus* comprises more than 50 described species (Speight, 2014; van Steenis, pers. comm.), of which 31 listed by Speight (2016) occur in southeastern Europe (as well as an additional three species that are not on that list, Grković et al., 2015). Notwithstanding the considerable species diversity of *Eumerus*, the genus faces taxonomic challenges posed by the lack of an up-to-date European identification key. In addition, there are still uncertainties about nomenclature (e.g. synonyms) and unclarified taxonomic statuses to be resolved before a clear view of the genus' species diversity can be perceived.

Eumerus species exhibit considerable morphological variability; they are generally medium-sized flies, with a distinctive habitus showing strong metalegs and a narrow or broadly oval abdomen (Doczkal et al., 2016). Doczkal and Pape (2009) studied the adult morphology of the tribe Eumerini (*Eumerus* Meigen, 1822, *Azpeytia* Walker, 1865, *Lyneborgimyia* Doczkal and Pape, 2009, *Merodon* Meigen, 1803, *Platynochaetus* Weidemann, 1830) and provided strong support for Eumerini monophyly, but not for the genus *Eumerus*. Doczkal and Pape (2009) concluded that *Eumerus* is paraphyletic, but did not assign any taxon groups (hereafter called as

'group') except for the *Eumerus maculipennis* group. Following this, Speight et al. (2013) presented the "*E. strigatus* group" of morphologically similar species. Doczkal (1996) had previously mentioned the *E. tuberculatus* group, with some species that were subsequently covered by the *E. strigatus* group sensu Speight et al. (2013). Recently, DNA sequences were used to infer species delimitation within *Eumerus* (Chroni et al., 2017), and that analysis suggested the presence of two major clades and seven groups within the genus based on tree inference approaches. One clade, named as *Eumerus tricolor* group, consisted of species with red parts on the tergites to an entirely red abdomen: *E. armatus* Ricarte and Rotherey, 2012, *E. grandis* Meigen, 1822, *E. sinuatus* Loew, 1855, *E. tricolor* (Fabricius, 1798), as well as *E. niveitibia* Becker, 1921 (a species with a blue appearance), and *E. aurofinis* Grković, Vujić & Radenković, 2015 (a species endemic to eastern Mediterranean islands) (Grković et al., 2015). The remaining species formed the second clade, in which six groups were assigned: *E. basalis* Loew, 1848, *E. minotaurus* Claussen & Lucas, 1988, *E. ornatus* Meigen, 1822, *E. pulchellus* Loew, 1848, *E. strigatus* (Fallen, 1817) and *E. sulcitibius* Rondani, 1868 (Chroni et al., 2017).

In the current study, we present two new species (*E. montanum* sp. n. and *E. rubrum* sp. n.) and one new record (*E. uncipes* Rondani, 1850) for southeastern Europe. These species are members of three different groups: *E. strigatus* sensu Speight et al. 2013, *E. tricolor* sensu Chroni *et al.* 2017 and a *E. clavatus* group defined here (for more details on *Eumerus* groupings, see Chroni et al., 2017; Doczkal and Pape, 2009; Speight et al., 2013). Our objectives are to: (a) provide descriptions for the new species; (b) revise the geographic distribution of *E. uncipes*; and (c) discuss and overview the assignments of the aforementioned species to groups based on morphological and molecular data for the available taxa.

Material and methods

2.1 Taxon sampling

The insect material that we considered in this study was collected over the past few decades from Southeastern Europe, including the following countries: Bulgaria, Croatia, Greece, Romania, Serbia, Slovenia and FYR Macedonia. Insects were collected by researchers from the Laboratory for Biodiversity Research and Conservation of the University of Novi Sad, using hand nets. Specimens belonging to

new species (*E. montanum* sp. n. and *E. rubrum* sp. n.) were collected from continental parts of the Balkan Peninsula (on Mt Pindos in Greece and Mt Durmitor in Montenegro) and in the Peloponnese (Mt Chelmos and Mt Taygetos, Greece), respectively. Specimens of *E. uncipes* were collected in Greece (Corfu Island). Several specimens of each assessed taxon were studied, and these have mainly been deposited in the collections of the Department of Biology and Ecology of the University of Novi Sad. We also considered the female holotype of *E. tauricus* Stackelberg, 1952, from Crimea, coll. 10.V.1905, leg. Kirichenko.

For molecular analyses, we examined DNA barcodes (mitochondrial cytochrome c oxidase subunit I, COI/cox1) for *E. montanum* sp. n. and *E. uncipes* with 13 additional *Eumerus* species. We were unable to obtain DNA barcodes for *E. rubrum* sp. n. The sequenced material originated mainly from Greece and Turkey, as well as from Germany, Italy, Montenegro, Russia and Serbia (for more details see Table S1). The sequence used for *E. funeralis* Meigen, 1822 (Accession No. GMGMJ702-14) was retrieved from GenBank. Outgroup taxa consisted of *Megatrigon tabanoides* Doczkal et al. (2016) (Accession No. KX083393), *Merodon erivanicus* Paramonov, 1925 (Accession No. KX083391) and *Platynochaetus setosus* (Fabricius), 1794 (Accession No. KM224512).

All specimens studied are deposited in the collections of the following institutions: FSUNS − Department of Biology and Ecology, Faculty of Sciences, University of Novi Sad, Serbia; NBC − Natural Biodiversity Centre, Leiden, The Netherlands and MAegean − The Melissotheque of the Aegean, University of the Aegean, Mytilene, Greece.

2.2 Morphological characters

The morphological characters used in the descriptions and drawings are based on the terminology established by Thompson (1999), and those related to the male genitalia by Hurkmans (1993) and Doczkal (1996). Colour characters are described from dry-mounted specimens. Male genitalia were extracted from specimens using standard methods for studying male hoverfly genitalia, as explained in detail in Grković et al., 2015. Drawings were created by using photographs of characters taken with a Leica DFC 320 (Wetzlar, Germany) camera attached to a Leica MZ16 binocular

stereomicroscope and then processed in Adobe Photoshop CS3 V 10.0 software (Adobe Systems, San Jose, CA, USA).

2.3. DNA extraction and PCR amplification

Total genomic DNA was extracted using 2 to 3 legs from each specimen and following the Chen et al. (2010) protocol for DNA extractions, with slight modifications (Grković et al., 2015).

DNA barcodes were generated by amplifying the mitochondrial COI gene fragment, using the primer pair LCO-1490 (5'-GGTCAACAAATCATAAAGATATTGG-3') and HCO-2198 (5'-TAAACTTCAGGGTGACCAAAAAATCA-3') (Folmer et al. 1994). PCR amplifications and DNA sequencing were performed as described in Grković et al. (2015).

2.4. Molecular analyses

We used BioEdit 7.2.5 (Hall, 1999) to edit sequences by eye and to trim to their final length of 612 bp. Multiple sequence alignments were implemented in MAFFT version 7 by employing the L-INS-i algorithm (Katoh et al., 2005; available at http://mafft.cbrc.jp/alignment/server/index.html). We implemented K2P genetic distance analyses in MEGA6 (Tamura et al., 2013) to corroborate species delimitation for *E. montanum* sp. n. (15 species, outgroups were excluded from the analyses; Table S2).

In order to resolve the phylogenetic positions of *E. montanum* sp. n. and *E. uncipes*, we produced a dataset of 41 *Eumerus* DNA sequences plus three outgroup sequences (the 'total' dataset). All trees were rooted based on the *P. setosus* sequence. We employed Neighbor-Joining (NJ), Maximum likelihood (ML) and Maximum parsimony (MP) phylogenetic methods. The NJ analysis was performed in MEGA6 (Tamura et al., 2013) with the Tamura-Nei nucleotide substitution model with a Gamma distribution, which was the second-best nucleotide substitution model (the first one was GTR+G+I) proposed by the Akaike Information Criterion (AIC 5601.91). Evolutionary distances were computed using the Maximum Composite Likelihood method (Tamura et al., 2004) and are presented in units of number of base substitutions per site. All positions containing gaps and missing data were eliminated, resulting in a total of 601 positions in the final dataset. The ML analysis was executed

in RAxML 8.0.9 (Stamatakis, 2006; Stamatakis et al., 2008) in the Cipres Science Gateway (Miller et al., 2010) under the general time-reversible (GTR) evolutionary model with a gamma distribution (GTR+G) (Rodriguez et al., 1990) with 1000 bootstrap replicates. The MP analysis was performed in NONA (Goloboff, 1999), spawned in WINCLADA version 1.00.08 (Nixon, 2002). A heuristics search algorithm with 1000 random addition replicates (mult x 1000) was performed, holding 100 trees per round (hold ⁄ 100), max trees set to 100 000 and applying TBR branch swapping.

The generated NJ and ML trees were merged into a split network in order to extract a united tree topology. The split network was produced in SplitsTree4 4.14.3 (Huson and Bryant, 2006) (http://www.splitstree.org/) under SuperTree, Z-closure super-network from partial trees and heuristic analysis (number of runs: 1000).

Additional MP analyses were performed in order to further evaluate species systematic positions (tree topology) within the *E. strigatus* group with reference to species morphology. We included seven species from within that group (for which DNA sequences were available): *E. amoenus* Loew, 1848, *E. consimilis* Šimić and Vujić (1996), *E. montanum* sp. n., *E. funeralis*, *E. pannonicus* Ricarte, Vujić & Radenković, 2016, *E. sogdianus* Stackelberg, 1952 and *E. strigatus*, and 21 additional *Eumerus* specimens (plus the three outgroup sequences). We performed MP analyses (with run settings as described above) separately and in combination for the morphological and DNA sequence datasets. The morphological matrix scored 24 male characters, related to size, head, thorax and genitalia (Table S3), which was created in Mesquite v2.73 (Maddison and Maddison, 2011).

Results

3.1. The *E. clavatus* group

Diagnosis. Medium-sized species, dark-coloured, with parallel-sided elongated abdomen having lunulate shaped oblique maculae of silver-to-white pollinosity on tergites II–IV (Fig. 4C, D). Distinctive processus on distal margin of abdominal sternite III in males (Fig. 4A, B). Male abdominal sternite IV with characteristic pliers-like shape. Antenna in females oval with more or less noticeable groove medially (Fig. 2D).

Male. *Head.* Eyes holoptic, eye contiguity 8–10 omattidia long. Eye with very scattered and short pile. Eye margins slightly broadening ventrally. Face black,

covered with white pollinosity and long white or yellow pile. Frons and postocular orbit black with long yellow pile, except ocellar triangle with black pile. Ocelli forming an equilateral triangle, longer than wide (Fig. 2A). Antenna yellowish-brown. Basoflagellomere slightly longer than broad (Fig. 2C), with straight anterior margin and deep central incision (sensory pit). Long ventral pile of pedicel yellow to white.

Thorax. Thorax black with golden lustre. Mesoscutum covered with short golden-yellow pile, reclined posteriorly, medially with two vittae of silvery pollinosity. Scutellum black with short yellow pile, pile slightly longer along posterior margin. Pleurae black with metallic golden lustre and covered with golden pollinosity. Anepisternum, posterior katepisternum and anepimeron covered with long yellow pile. Wing transparent, entirely microtrichose. Calypter and halter white to yellow. Metafemur swollen, black with metallic lustre. Long white pile on hind femur ventrally, as long as three-quarters the depth of the femur (Fig. 2E). Metatibia dark-coloured, yellow in proximal part.

Abdomen. Abdomen elongated, black with short white pile, tergites II–IV with pairs of white to silver pollinose lunulate shaped oblique maculae (Fig. 4C, D). Tergite IV long, almost twice the length of tergite III. Sternite III with medial prominence, covered with long whitish pile, and a characteristic processus ventro-medial of the posterior margin (Fig. 4A, B). Sternite IV with a specific pliers-like shape.

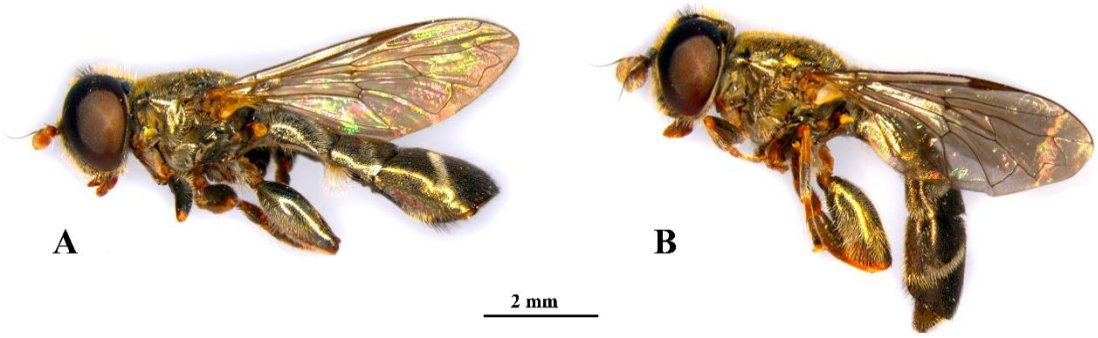

Fig. 1. *E. uncipes*: A) male; B) female. Photo: A. Grković.
Σχήμα 1. *E. uncipes*: A) άρρεν· B) θήλυ. Φωτογραφία: A. Grković.

Genitalia. Cerci oval, flattened laterally, with a row of strong setae dorsally (Fig. 3A, B). Interior accessory lobe of posterior surstylar lobe densely covered in pilosity. Posterior surstylar lobe simple, tapered, with short spines laterally and on apicoventral

ridge. Hypandrium broad, curved, and simple (Fig. 3C, D). Aedeagal apodeme with dorsal processus (Fig. 3E, F).

***Female*.** Similar to the male, except for usual sexual dimorphism (Figs. 1B, 2B, D, F) and the following characteristics: face and frons black and covered with yellow to golden pile, white and golden pollinosity on the face; frons flattened; silver pollinosity along eye margin anterior to ocellar triangle and at the eye corner posterior to ocellar triangle (Fig. 2B).

3.1.1. Species of the E. clavatus group in southeastern Europe

The following two species belonging to the *E. clavatus* group have been recorded on the Balkan Peninsula and on eastern Mediterranean islands: *E. clavatus* Becker, 1923 (Bradescu, 1991; Vujić and Šimić, 1999) and *E. uncipes* recorded during research presented here.

Taxonomic notes about *Eumerus uncipes* Rondani, 1850 (Fig. 1)

Remark. This is first record of *E. uncipes* in southeastern Europe. To clarify the relationship between the related species *E. uncipes* and *E. clavatus*, we present here diagnoses and molecular data for both species.

***Material examined*.** 2♂♂, 1♀, Greece [Corfu], Strinilas [39◦44'20.4"N 19◦50'13.2"E], [642 m.a.s.l.] coll. 08.VIII.2014, 1♂, 2♀♀ coll. 10.VIII.2014,; 1♀, Stroggili [39◦30'43.7"N 19◦55'00.2"E], [153 m.a.s.l.], 10.VIII.2014. leg. Vujić A. (FSUNS).

Diagnosis. This species is closely related to *Eumerus clavatus*, from which it clearly differs in the shape of the processus on abdominal sternite III (Fig. 4A, B); quadratic in *E. uncipes* and as a triangular thorn in *E. clavatus*. In addition, *E. uncipes* has a pointed triangular extension apico-ventrally on the metatibia (Fig. 2G), which is absent in *E. clavatus*. Male genitalia of both species are very similar (Fig. 3). The posterior surstyle lobes are slightly differently shaped (Fig. 3A, B). Dorsal spines on the posterior surstyle lobe of *E. clavatus* are longer than in *E. uncipes*. A row of strong bristles is present dorsally on the cercus of *E. uncipes* (Fig. 3A); in *E. clavatus*, the pile on the cercus is not so distinctive (Fig. 3B). Aedeagal apodeme in *E. clavatus* has a spine-like process dorsally (Fig. 3F), whereas in *E. uncipes* the same process is keel-shaped (Fig. 3E).

Females are very similar, but in *E. uncipes* antennae are more reddish-brown than in *E. clavatus* (which are more yellowish-brown) and basoflagellomere with a noticeable arced groove medially.

In both sexes, the abdomen of *E. clavatus* is more robust and broad with noticeable silvery-white pollinose lunulate oblique maculae, which contrasts with *E. uncipes* that has a narrower abdomen with grey maculae on its tergites (Fig. 4C, D).

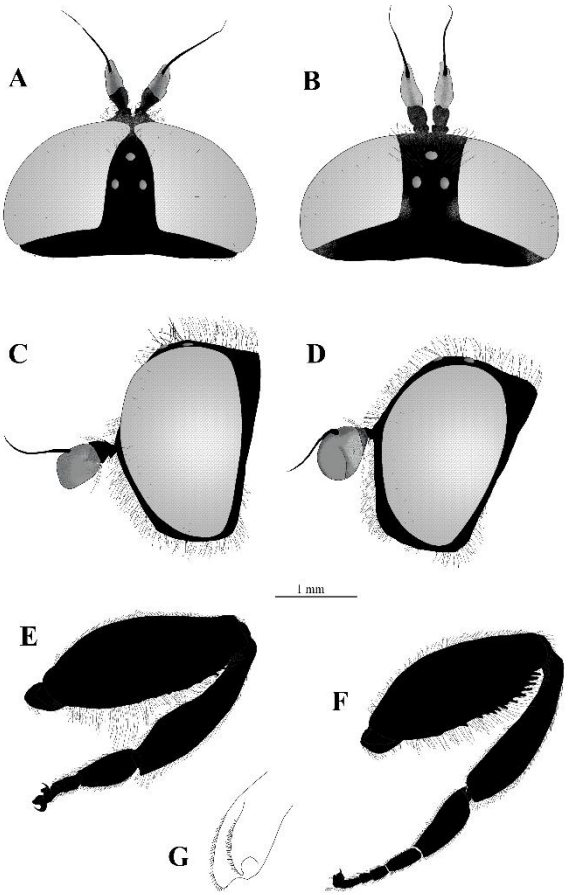

Fig. 2. *E. uncipes*, head: Dorsal view: (A) male; (B) female. Lateral view: (C) male; (D) female. Leg: (E) male; (F) female; (G) Apicoventral part of male metatibia with conspicuous notch.

Σχήμα 2. *E. uncipes*, κεφαλή: Ραχιαία όψη: (A) άρρεν· (B) θήλυ. Πλευρική όψη: (C) άρρεν· (D) θήλυ. Πόδι: (E) άρρεν· (F) θήλυ· (G) Ακροκοιλιακή περιοχή της κνήμης των αρσενικών, με εμφανή εγκοπή.

3.2. The E. strigatus group

Diagnosis. The *E. strigatus* group was named by Speight et al. (2013) in assigning a group of species related to *E. strigatus*. Chroni et al. (2017) presented the same group in their studies based on molecular data. The *E. strigatus* group comprises relatively small, inconspicuous species with usually a bronze shine and without coloured

markings on their tergites; basoflagellomere usually rectangular and from reddish to dark-brown or black coloured; sternites simple, without distinct apomorphic structures (as in the *E. clavatus* group − Fig. 4); legs connections, apex of femora and basal thirds of tibiae bright yellow; abdominal sternite IV in males differently shaped but always with a v-shaped notch on the posterior margin (Fig. 8); cerci elongated (Fig. 7A, D–H). The main diagnostic character is the shape of the male genitalia: epandrium in all examined species has an elongated, posterior surstyle lobe with species-specific shape (Fig. 7A, D–H).

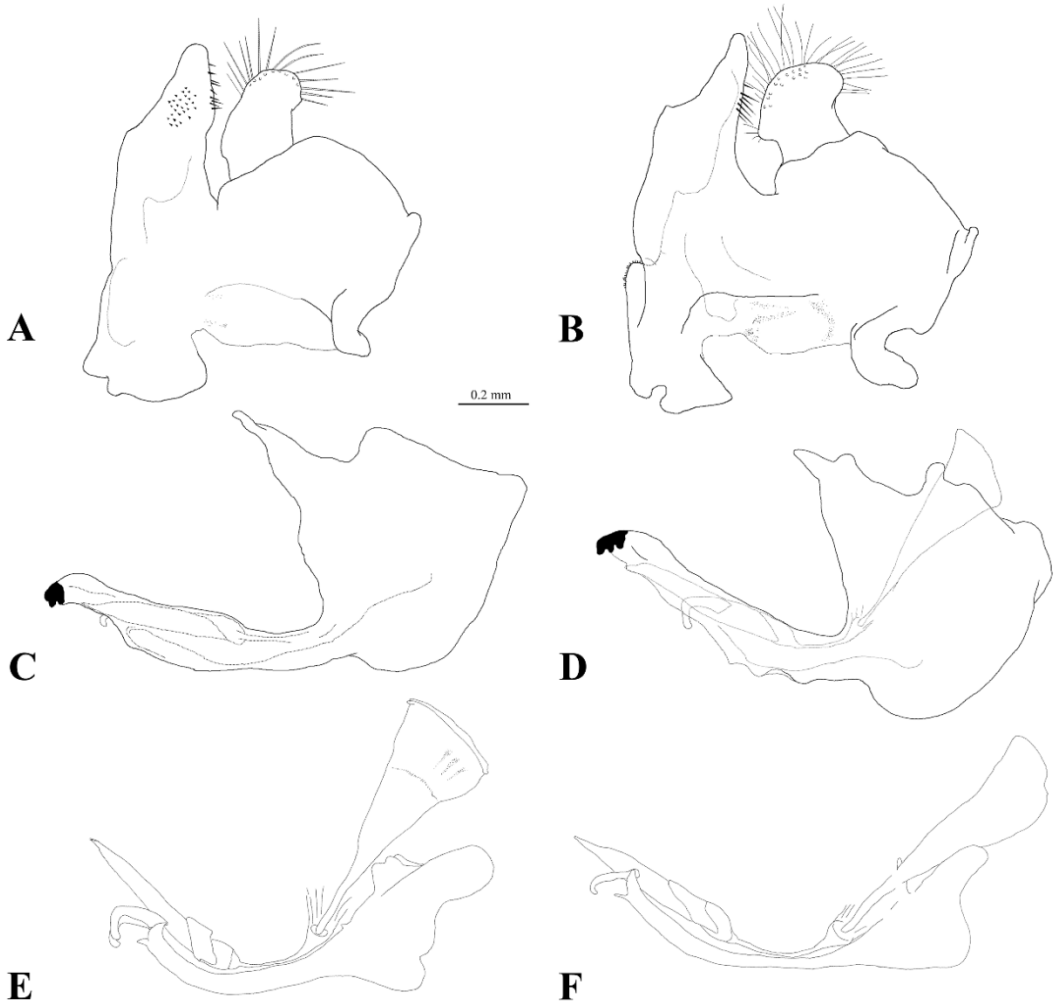

Fig. 3. Male genitalia. Epandrium: (A) *E. uncipes*; (B) *E. clavatus*. Hypandrium: (C) *E. uncipes*; (D) *E. clavatus*. Aedeagus and accessory structures: (E) *E. uncipes*; (F) *E. clavatus*.

Σχήμα 3. Γεννητικός οπλισμός άρρενος. Επάνδριο (τελευταίος νωτιαίος τεργίτης): (A) *E. uncipes*· (B) *E. clavatus*. Υπάνδριο (9ος κοιλιακός στερνίτης): (C) *E. uncipes*· (D) *E. clavatus*. Αιδοιαγός και βοηθητικά εξαρτήματα: (E) *E. uncipes*· (F) *E. clavatus*.

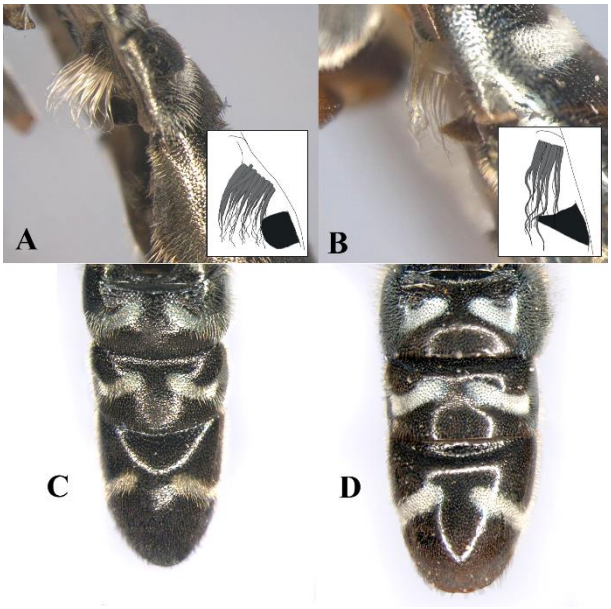

Fig. 4. Third abdominal sternite in male: (A) *E. uncipes*; (B) *E. clavatus*. Male tergites: (C) *E. uncipes*; (D) *E. clavatus*. Photo: A. Grković.

Σχήμα 4. Τρίτος κοιλιακός στερνίτης άρρενος: (A) *E. uncipes*· (B) *E. clavatus*. Τεργίτες άρρενος: (C) *E. uncipes*· (D) *E. clavatus*. Φωτογραφία: A. Grković.

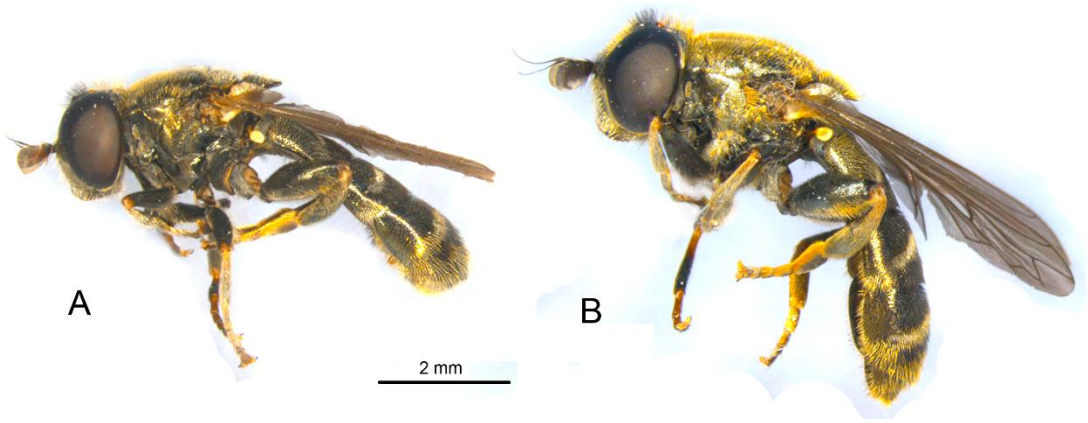

Fig. 5. *E. montanum* sp. n.: (A) male; (B) female. Photo: A. Grković.

Σχήμα 5. *E. montanum* sp. n.: (A) άρρεν· (B) θήλυ. Φωτογραφία: A. Grković.

Male. *Head*. Eyes holoptic, eye contiguity 7–9 ommatidia long. Eye with 2–4 ommatidia-long scattered pile. Distance from anterior ocellus to posterior ocellus approximately equal to the distance from posterior ocellus to eye corner. Distance between posterior ocellus and eye margin is equal to the diameter of ocellus or less. Face with white to yellow pile and silver to grey pollinosity (in some species, ranging to golden). Vertex black with metallic shine (in some species with pollinose maculae from posterior ocellus to upper eye corner along eye margin and sometimes in front of anterior ocellus). Basoflagellomere slightly longer than wide, oval to rectangular with

ventral margin pointed, reddish to dark brown coloured. Depth of pedicel is about four-fifths the depth of the basoflagellomere medially. Longest pile on pedicel as long as the depth of pedicel.

Thorax. Black, weakly punctuated, with bronze to golden shine. Pile of thorax from white to yellow, ranging to golden, slightly longer on scutellum than pile of mesonotum. Mesonotum with two vittae of silvery-white pollinosity, which extend almost its entire length or are clearly visible only on the anterior part of mesonotum. Pleurae black with bluish or bronze to golden metallic shine and pale pile, longer than pile on scutum. Metafemur enlarged, 1.5 to 2 times wider than metatibia, black with yellow apex. Metatibia black, yellow to yellowish-brown in basal quarter to third. Metatrochanter simple, metafemur with anterolateral row of 6–7 spines and posterolateral row of 10–12 spines. Pilosity on legs from white to yellow, ranging to golden.

Abdomen. Tergites entirely shiny black with bluish or bronze tinge, weakly punctuated. Pairs of white to grey lunules of pollinosity on tergites II–IV, usually more grey-coloured in the middle of the tergite and white to silver laterally. Posterior margin of sternite IV with a sharp to shallow v-shaped notch and sometimes with two spatulate or sharp projections laterally (Fig. 8).

Genitalia. Hypandrium simple, with apically-situated ctenidion (Fig. 7B). Cerci simple, more or less curved posteriorly (Fig. 7A, D–H). Posterior surstyle lobe more or less elongated and always spatulate in some way (Fig. 7A, D–F, H), with the exception of species related to *E. bactrianus* Stackelberg, 1952 that has a specifically-shaped surstylus (bifurcated apically, Fig. 7G). Anterior lobe of surstylus is well-developed (Figs. 7A, D–H, 11I).

Female. *Head*. Head. Pile on face and frons white-yellow to golden, black in region of ocellar triangle, this contrast in pile colour is more distinctive than in males (Fig. 5B). Face covered with silver-grey to bronze pollinosity (Fig. 6D). Frons with dense vitta of bronze-green pollinosity from face anteriorly to anterior ocellus, along eye margin. Some species have a triangular macula of pollinosity adjacent to the dorsal eye corner and posterior to the posterior ocellus, usually with pollinosity along the dorsal eye margin.

Thorax. Black with metallic bronze to golden shine. Two vittae of grey pollinosity on mesoscutum, extending from half to almost the entire length of the mesoscutum.

Scutellum black with bronze to golden reflection. Metafemur black with yellow apex. Metatibia black, yellow in basal quarter to a third. Pile of legs yellow to golden.

Abdomen. Tergites with two or three pairs of white lunulate shaped oblique maculae of pollinosity. Tergite IV posteriorly with slightly longer white to yellow pilosity.

3.2.1. Species from the E. strigatus group in southeastern Europe

The species belonging to the *E. strigatus* group that have been recorded from the Balkan Peninsula and eastern Mediterranean islands are: *E. amoenus*, *E. consimilis* (Figs. 7D, 8C), *E. funeralis* (Figs. 6H, 7H, 8D), *E. montanum* sp. n. (species described below; Figs. 5, 6A–G, 7A–C, 8A), *E. strigatus* (Figs. 7F, 8B), *E. sogdianus* (Figs. 7E, 8E, 11I) and *E. pannonicus* (Fig. 7G) (Bradescu, 1991; Šimić and Vujić, 1996; Vujić & Šimić, 1999; Ricarte et al., 2012; Markov et al., 2016).

3.2.2. Description of Eumerus montanum Grković, Radenković & Vujić sp. n.

Material examined. **Holotype.** 1♂, Montenegro [Durmitor Mountain], Komarnica, beside Pošćensko Lake [42◦58’39.2“N 19◦04’15.9“E], [1045 m.a.s.l.], coll. 16.VIII.2015, leg. Vujić A. (FSUNS). **Paratypes**. 1♂, Greece [Epirus], Pindos, Mt Smolikas, Paleoselli [1365 m.a.s.l.], coll. 04.VIII.1994, leg. Renema W. (NBC); 4♂♂, 2♀♀, Montenegro [Durmitor Mountain]: Komarnica, coll. 23.VII.2014, 1♂, 1♀, Pošćensko Lake, [42◦58’39.2“N 19◦04’15.9“E], [1045 m.a.s.l.], coll. 16.VIII.2015, leg. Vujić A., 5♂♂, 3♀♀, coll. 1–04.VI.2016, leg. Vujić A. et al., 1♂, coll. 08.VII.2016, leg. Grković A., 21♂♂, 5♀♀, coll. 30.VII.2016, leg. Vujić A., 23♂♂, coll. 31.VII.2016, leg. Vujić A.; Canyon Sušica, Skakala, 1♂, coll. 13.VIII.2015, legs. Vujić A. and Veličković N.; 6♂♂, 3♀♀, coll. 06.VII.2017, legs. Vujić A. et al. (all in FSUNS).

Diagnosis. It differs from other species of the *E. strigatus* group in the shape of sternite IV in the male: posterior margin of sternite IV with v-shaped, shallow notch with two spatulate projections laterally with tufts of golden pile (Fig. 8A). The new species has distinctive golden pilosity on the posterior ventral part of its metafemur (Figs. 5, 6E, F). Despite these differences, *E. montanum* sp. n. can easily be confused with similar species, so the most valid identification character is that of the male genitalia; the epandrium has cerci curved backwards and an elongated posterior surstylar lobe (Fig. 7A). Females of *E. montanum* sp. n. are extremely similar to

females of other species of the group, differing by a darker appearance and golden pile particularly noticeable on the posteroventral side of the metafemur and the posterior half of tergite IV. Further, females of this species have similar antenna to the males, i.e., slightly elongated and dark (Fig. 6C–D). More detailed differences between females of this group are given below in the taxonomic notes.

***General description*.**

Male. *Head*. Eyes holoptic, eye contiguity 9–11 omattidia long (Fig. 6A). Face, frons and postocular orbit black with long yellow pile except on ocellar triangle where the pile is black. Face with white pollinosity anterior to antennal socket, golden pollinosity posteriorly. Ocelli making an isosceles triangle, slightly longer than wide (Fig. 6A). Distance from anterior ocellus to posterior ocellus equal to distance from posterior ocellus to eye corner. Face margin slightly protruding (Fig. 6C). Antenna dark; basoflagellomere brown to brownish-red, slightly elongated, covered with white velvet pollinosity. Arista dark-brown, inserted dorsomedially of basoflagellomere, thickened basally. Ventral pile of pedicel yellow on median side, dark on lateral side, and as long as depth of pedicel. Dorsal pile of pedicel short, yellow and dark.

Thorax. Black, weakly punctuated, with golden metallic lustre, entirely covered with yellow pile and with two vittae of white pollinosity, sometimes barely visible. Anepisternum and anepimeron yellow pilose, katepisternum posteriorly with white pile. Scutellum simple, black, with yellow pile. Pleurae with metallic golden shine. Wing with brownish tinge, entirely trichose; halters white. Calypter white to bright yellow. Legs dark, with connections, basal thirds of tibiae and basal tarsi brown. Metatrochanter angular, in distinctive characteristic shape (Fig. 6G), metafemur black with reddish to black tip, covered with long white to yellow pile, longer at inner side, posteriorly with distinctive golden pile (Figs. 5A, 6E). Metatibia black, brown in basal quarter to third. Tarsi with golden pile ventrally.

Abdomen. Black, white pilose with golden lustre. Tergites II–IV with pairs of lunulate shaped oblique maculae of pollinosity. Tergite IV apically with slightly longer grey to golden pile (Fig. 5A). Abdominal sternite IV on posterior margin with two spatulate projections (Fig. 8A). Distal margin of sternite IV with longer erect golden pile laterally.

Genitalia. Cerci oval, elongated backwards (Fig. 7A). Interior accessory lobe of posterior surstyle lobe covered with dense pile. Posterior surstylar lobe very long, expanded like a paddle, with dense pile, particularly in the lateromedial part (Fig. 7A).

Hypandrium simple, broad, curved (Fig. 7B). Ctenidion situated apically. Lateral sclerite of aedeagus slightly enlarged (Fig. 7C). Aedeagal apodeme without dorsal processus.

Female. Similar to the male (Figs. 5B, 6B, D, F–G). Antenna dark, basoflagellomere oval, slightly darker apically. Arced groove extends transversally to the apical fourth of basoflagellomere. Face metallic bronze with white pollinosity (Fig. 6D). Frons with dense white to yellow pollinosity along eye margin (Fig. 6B). Ocelli making an isosceles triangle, longer than wide (Fig. 6B). Distance from anterior ocellus to posterior ocellus twice as long as distance from posterior ocellus to upper eye corner. Thorax with golden lustre and golden pile, anepisternum posteriorly with a fringe of longer golden pile. Metatrochanter not rounded, angular. Metafemur ventrally and postero-laterally with golden pile, as in males but more distinctive (Fig. 6F). Tergite IV with bronze shine and golden pile in the posterior one third.

Taxonomic notes. Since females of *E. montanum* sp. n. are very similar to females of related species, we summarize in Table 1 the differences between females of *E. amoenus*, *E. consimilis*, *E. strigatus*, *E. montanum* sp. n., *E. sogdianus* and *E. funeralis*. Females of *E. montanum* sp. n. have a more robust abdomen, a distinctive bronze-golden shine on the posterior third of tergite IV (the anterior margin of which forms a reversed v and has distinctive golden-yellow pile), and narrow pollinose markings on tergites. In *E. montanum* sp. n., the ocellar triangle is clearly isosceles and pollinosity behind the posterior ocelli is absent or almost invisible in this species (Fig. 6B). What is also characteristic of the species is the rectangular shape of the metatrochanter, but this feature is not always as clearly visible as it is in males (Fig. 6G). Females of *E. amoenus* can be quite easily distinguished from *E. montanum* sp. n. and the other species by the lunules of tergite IV that are clearly visible but short, tear-shaped, mid-positioned, and about half the length of the lunules on tergite III. Both males and females of *E. amoenus* have a pair of shallow depressions on tergite IV, in an area of white spots, which are more conspicuous than in other species where this feature is present. Also, females of *E. pannonicus* are easy to distinguish by the absence of pollinose markings on T4, the elongated basoflagellomere and the small ocellar triangle. In contrast to *E. montanum* sp. n., females of *E. sogdianus* have moderately narrow pollinose markings on the tergites, an almost equilateral ocellar triangle, and pollinose patches behind the posterior ocelli that extend behind the eye line. Females of *E. sogdianus* have characteristic antenna, similar to those in males,

which are slightly peaked ventrally. Females of *E. strigatus* have a characteristic ocellar triangle that is always equilateral or even wider than long. Pollinosity near and behind the posterior ocelli in this species is usually limited to the eye line and the pollinose markings on the tergites are quite broad.

More problematic is to distinguish females of *E. montanum* sp. n. and *E. consimilis* by morphological characters. Females of *E. consimilis* have broad lunulate-shaped oblique maculae on tergites II–IV, and the width of the crescent-shaped spots on tergite III are approximately a quarter of the length of the tergite and wider than the distance between two lunules of the same tergite. However, this feature is quite variable, with some females of *E. consimilis* having narrower markings; although, in that case, the distance between two markings of the same tergite is not larger than the width of the markings. In *E. montanum* sp. n., the maculae on the tergites are more linear, and the width of the spots on tergite III are about 5–6 times shorter than the length of the tergite and they are shorter than the distance between lunules of the same tergite. Although the morphology is very similar between the species, molecular data clearly defined all analyzed taxa.

Etymology. The name reflects that the species is found in mountain habitat.

3.3. The E. tricolor group

Diagnosis. Chroni et al. (2017) defined the *E. tricolor* group based on DNA sequencing and named the group after *E. tricolor*. Species belonging to the group are large-sized, predominantly black and usually with red markings on the tergites, but sometimes with a metallic blue shine. The basoflagellomere is characteristic by: square shaped with more or less marked wrinkles; sometimes it is very small and oval, but in some females oval, extremely enlarged. Eyes dichoptic or only slightly holoptic. The main synapomorphic character connecting all analyzed species is the poorly developed anterior surstyle lobe of the male genitalia (Fig. 11E–H) and the usually large wing-shaped interior accessory lobe of the posterior surstylar lobe which is densely pilose (Fig. 11E–H). The less pronounced differentiation of the male genitalia is characteristic of the group.

Male. *Head*. Eyes dichoptic to holoptic. If holoptic usually slightly dichoptic with a space of 1–4 ommatidia in breadth between eye margins and an eye contiguity of 3–7 ommatidia long. Eyes with long dense pile or almost bare. Ocelli in an equilateral or isosceles triangle. Antenna usually dark brown to black, but yellow in some species.

Basoflagellomere more or less square distally with a flattened ellipsoidal area and more or less wrinkled from the base to the top. Face, frons and postocular orbit black, but with a blue shine in some species.

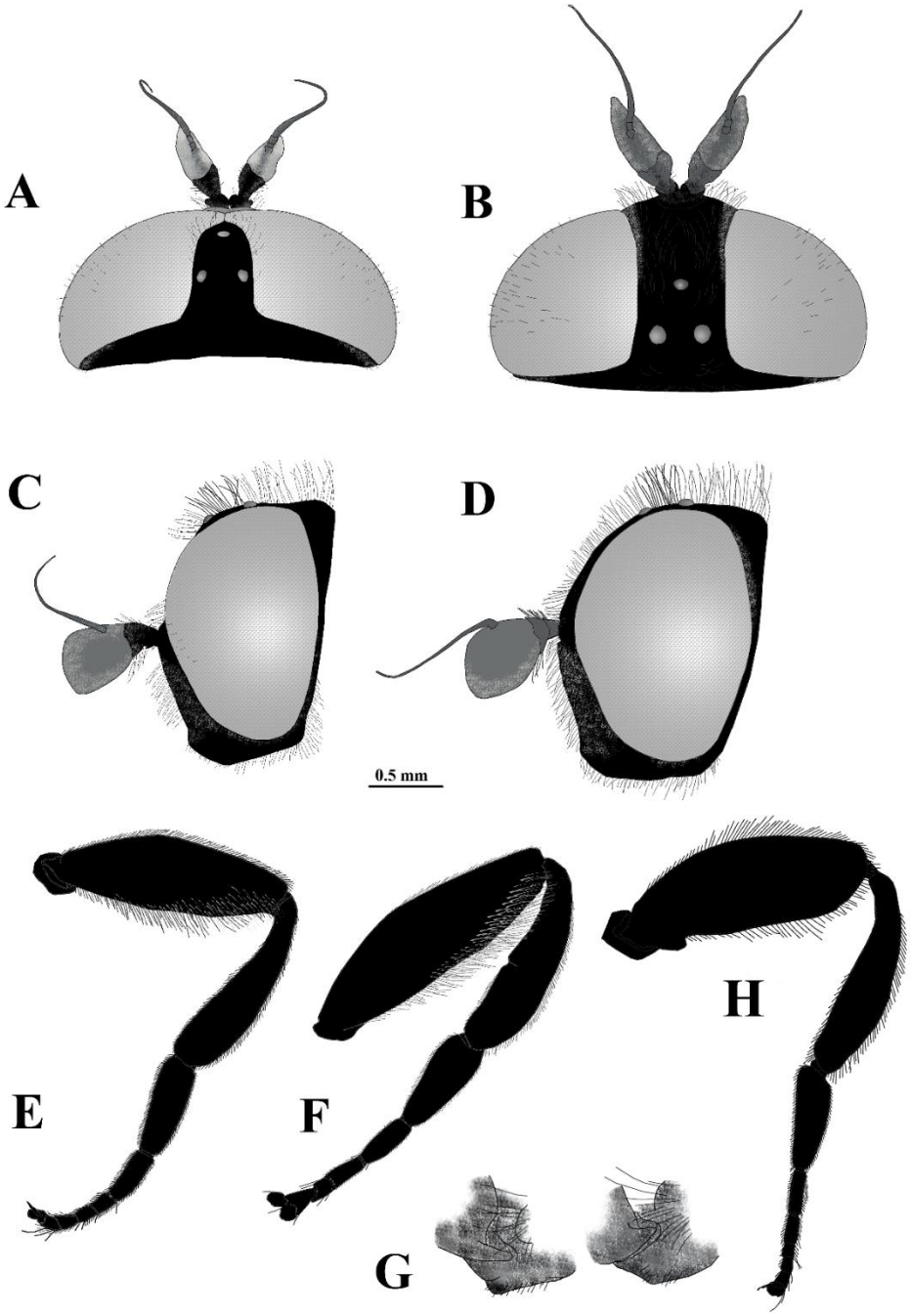

Fig. 6. *E. montanum* sp. n., head. Dorsal view: (A) male; (B) female. Lateral view: (C) male; (D) female. Leg: (E) male; (F) female. (G) Metatrochanter, lateral view, in this order: male, female; (H) Leg of *E. funeralis*.

Σχήμα 6. *E. montanum* sp. n., κεφαλή. Ραχιαία όψη: (A) άρρεν· (B) θήλυ. Πλευρική όψη: (C) άρρεν· (D) θήλυ. Πόδι: (E) άρρεν· (F) θήλυ. (G) Metatrochanter, πλευρική όψη, με αυτή την σειρά: άρρεν, θήλυ· (H) Πόδι του *E. funeralis*.

Thorax. Black, sometimes with a golden or metallic blue shine. Legs usually dark-coloured. Metafemur moderately swollen, postero-ventrally with two rows of 7–9 distinctive sharp spines.

Abdomen. Black, tergites II–IV usually red-coloured to differing degrees (Fig. 10), but entirely black or with metallic blue shine in some species.

Genitalia. Posterior surstylar lobe of epandrium simple, oval to square with strong bristles dorsally. Genitalia do not differ much between species, but they remain the best diagnostic character for species identification (Fig. 11A–H).

Female. Similar to the male, except for normal sexual dimorphism. In some species, basoflagellomere strongly enlarged (for instance in *E. armatus*).

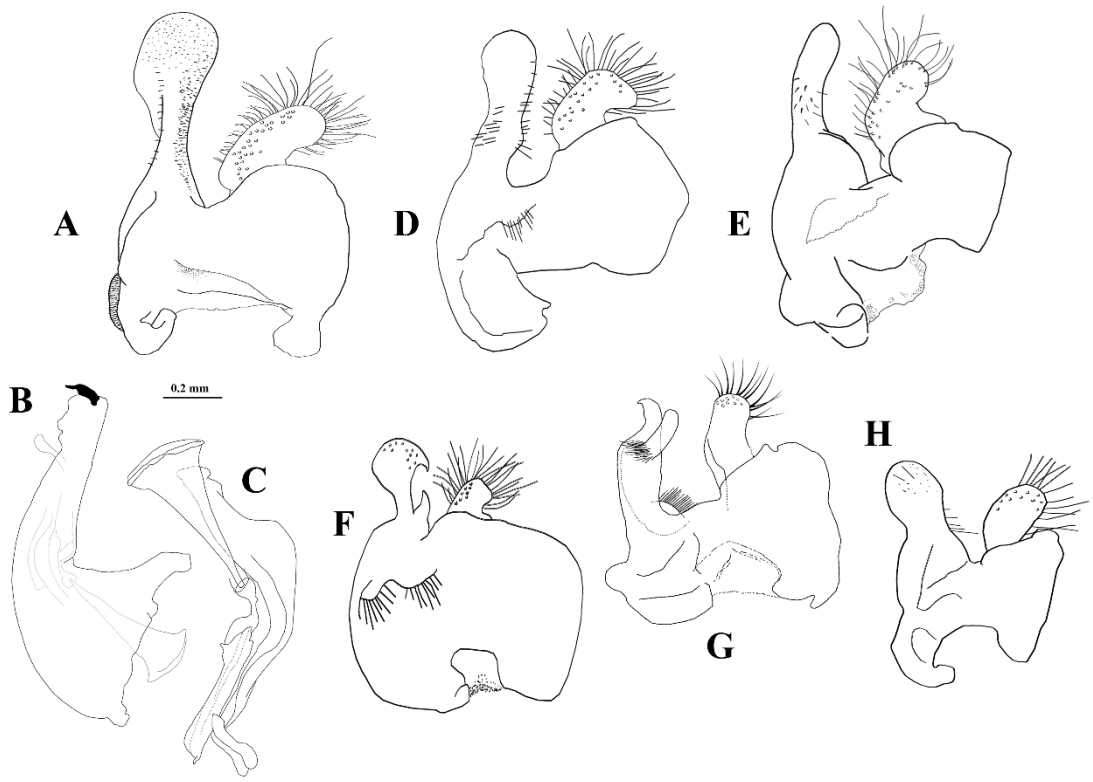

Fig. 7. Male genitalia, *E. strigatus* group. *Eumerus montanum* sp. n.: (A) epandrium, (B) hypandrium, (C) aedeagus and accessory structures; epandrium: (D) *E. consimilis*, (E) *E. sogdianus*, (F) *E. strigatus*, (G) *E. panonnicus*, (H) *E. funeralis*.

Σχήμα 7. Γεννητικός οπλισμός άρρενος της ομάδας ειδών *E. strigatus*. *Eumerus montanum* sp.n.: (A) επάνδριο (τελευταίος νωτιαίος τεργίτης), (B) υπάνδριο (9ος κοιλιακός στερνίτης), (C) αιδοιαγός και βοηθητικά εξαρτήματα· επάνδριο: (D) *E. consimilis*· (E) *E. sogdianus*, (F) *E. strigatus*, (G) *E. panonnicus*, (H) *E. funeralis*.

3.3.1. Species of the E. tricolor group in southeastern Europe

Eleven species belonging to the *E.tricolor* group have been recorded from the Balkan Peninsula and eastern Mediterranean islands: *E. armatus* (Figs. 10D, 11C, G), *E. aurofinis*, *E grandis*, *E. richteri* Stackelberg, 1960, *E. niveitibia*, *E. sinuatus*, *E. ovatus* Loew, 1848, *E. tarsalis* Loew, 1848 (Figs. 10B, 11B, F), *E. tauricus*, *E. tricolor* (Figs. 10C, 11D, H) and *Eumerus rubrum* sp. n., described below (Vujić and Šimić, 1999; Ricarte et al., 2012; Grković et al., 2015).

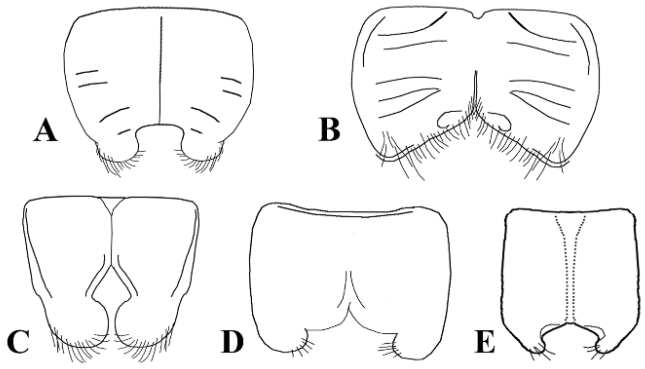

Fig. 8. Males 4th abdominal sternite: (A) E. *montanum* sp. n., (B) *E. strigatus*, (C) *E. consimilis*, (D) *E. funeralis*, (E) *E. sogdianus*.

Σχήμα 8. Τέταρτος κοιλιακός στερνίτης άρρενος: (A) *E. montanum* sp. n., (B) *E. strigatus*, (C) *E. consimilis*, (D) *E. funeralis*, (E) *E. sogdianus*.

3.3.2. Description of Eumerus rubrum Grković & Vujić sp. n.

Material examined. **Holotype.** 1♂, Greece [Peloponnese], Achaia, from Chelmos Mountain above Kalavryta [38◦00'30.9"N 22◦07'08.3"E], [1700 m.a.s.l.], coll. 16.V.2007; legs. Dils, Faes and Langemark (NBC). **Paratype**. Laconia: 1♀ from Varvara, shelter of Taygetos, [37◦02'12.4"N 22◦23'00.8"E], [843 m.a.s.l.], 02.VI.1993; leg. Den Hollander G. (NBC).

***Diagnosis*.** Belongs to the *E. tricolor* group. *E. rubrum* sp. n. is clearly different from all other European species of the *E. tricolor* group by having an almost entirely reddish-yellow abdomen (more extensively red coloured and brighter than in other similar species) (Fig. 10), with a small yellow basoflagellomere (Fig. 9B), and by the long pile of abdominal sternite IV in males that are longer than half the length of the metabasitarsus and the long yellow ventral pile of the metafemur. Male genitalia are different in all similar species (Fig. 11A–H), except in *E. tauricus*, the genitalia of which are identical to those of a new species (see Barkalov, 1990, as *E. carasukensis*

sp. n.). Excluding *E. tauricus*, the genitalia of *E. rubrum* sp. n. and *E. tarsalis* are the most similar, which suggests that these too are closely related species (Fig. 11A, B, E, F). In contrast to *E. tarsalis* (Fig. 11B), the setae of the posterior lobe of the surstylus in *E. rubrum* sp. n. are very strong, more dense and almost transparent, and the posterior lobe is entirely covered with alveolae (Fig. 11A). Since the male genitalia of *E. rubrum* sp. n. and *E. tauricus* are practically identical, the features that distinguish these two species are the following: pile on the ocellar triangle are yellow in *E. rubrum* sp. n. and black in *E. tauricus*; ventral pile on the metafemur in *E. tauricus* are denser and longer compared to the new species; and, most distinctively, tergite I in *E. rubrum* sp. n. is broadly yellow at the posterior margin (Figs. 10A, 12D), whereas in *E. tauricus* tergite I is black or only narrowly orange-red in the posterolateral corner. This last feature is also present in females. In addition, females of these two species can be distinguished by the wide ocellar triangle in *E. rubrum* sp. n. (wider than long and with the anterior angle greater than 90◦) (Fig. 9D, 12A), whereas in females of *E. tauricus* the anterior angle of the ocellar triangle is closer to 80^{o} (Fig. 12B), and by the conspicuous transverse suture in *E. rubrum* that envelops the whole metafemur anteriorly (Figs. 9F, 12C).

***General description*.**

Medium-sized species (10–11 mm) with a characteristic reddish-yellow abdomen.

Male. *Head.* Eyes bare, slightly dichoptic, spaced two ommatidia apart, eye contiguity 3–4 ommatidia long, almost bare; ocelli form an isosceles triangle, slightly wider than long (Fig. 9A). Face and frons black with long pale pile. Eye margins broadening ventrally. Scape and pedicel brownish-yellow, bristles of pedicel pale; basoflagellomere small, yellow, oval with rough margin, slightly extended ventrally (Fig. 9B). Arista dark, basally thickened.

Thorax. Scutum, scutellum and pleurae entirely black with barely visible golden shine, densely and roughly punctuated. Scutum and scutellum with dense yellowish pile. Pleurae with longer yellowish pile. Legs dark with bases of tibiae and basal tarsi of front and mid legs paler. Metafemur slightly swollen (Fig. 9C), simple with long white to gold pile, ventrally as long as the depth of femur. Antero-laterally with barely visible transverse suture. Metafemur apically with a row of 9–10 sharp black spines on anterior ridge and a row of 7–8 spines on the posterior ridge. Tarsi with golden pile ventrally. A row of dense black spinulae on mesonotum above the wing. Wing

entirely microtrichose, transparent with gentle shading apically. Calypter white to gold. Halter whitish, almost transparent.

Abdomen. Tergite I black with broadly reddish-yellow posterior margin; tergites II and III entirely reddish-yellow, tergite IV dark brown with reddish anterior and lateral part (Fig. 10A). Tergite II and III with pairs of barely visible lunulate shaped oblique maculae of white pollinosity, covered with white pile. The rest of the tergites covered with very short black pile, except the postero-lateral part of tergite II which is covered with long white pile. Abdominal sternites reddish-yellow covered with pale pile. Sternite IV darker, covered with long white pile, particularly on lateral margins.

Genitalia. Posterior lobe of surstylus slightly pointed posteriorly and with strong long, almost transparent setae, almost entirely covered in alveolae (Fig. 11A). Inner accessory lobe of surstylus with short dense pile (Fig. 11E). Hypandrium simple and thin (Fig. 11A).

Female. *Head*. Eyes bare (Fig. 9D–E). Frons moderately wide, almost two times wider than the width of basoflagellomere. Ocelli arranged in an isosceles triangle, wider than long (Fig. 9D). Anterior angle of ocellar triangle in female paratype is about 95◦ (Fig. 12A). Face, frons and postocular orbit shiny black with shorter yellow pile. Pronounced longitudinal notch from antennal socket to anterior ocellus. Scape and pedicel brownish-yellow. Basoflagellomere moderately small, oval, yellow (Fig. 9E). Arista dark, basally thickened.

Thorax. Mesonotum and pleurae black, densely punctuated, with short, yellow pile. Mesonotum anteriorly with rudiments of three vittae of white pollinosity. A row of dense black spinulae on mesonotum above the wing, more pronounced than in males. Scutellum black, striated transversely. Legs predominantly brown with yellowish coxae, yellow to translucent metafemur (Figs. 9F, 12C), tips of tibiae and ventral side of tarsi yellowish. Metafemur anteriorly with conspicuous transversal suture that envelops the whole femur (Figs. 9F, 12C). Metafemur apico-ventrally with rows of sharp black spines, 9–10 on anterior row and 7–8 on posterior row. Pile on legs short and yellow, only slightly longer ventrally on metafemur.

Abdomen. Tergite I black with broadly reddish-yellow posterior margin (Fig. 12D), as in males. Tergites II–III completely and tergite IV anteriorly reddish-yellow. Tergites with short yellow pile with intermingled brown pile and three pairs of crescent-shaped lunules of pollinosity on tergites II–IV. Tergite V dark with brown

pile. Sternites I–IV reddish with short sparse yellow pile. Sternite V dark with brown pile.

Etymology. The Latin adjective "rubrum" indicates that it is a species with a ruby appearance.

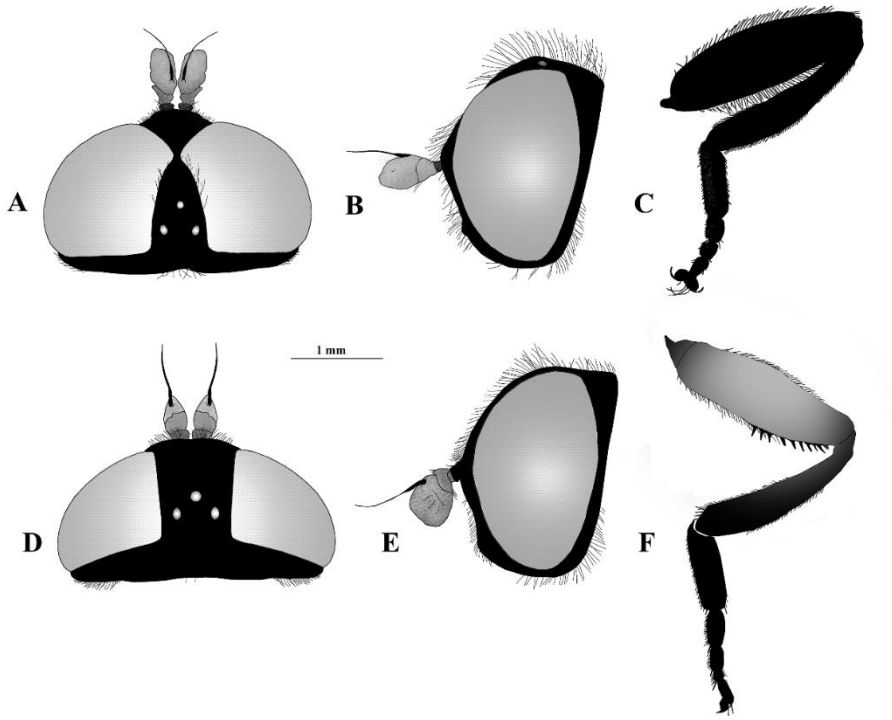

Fig. 9. *E. rubrum* sp. n., Male: head: (A) dorsal view, (B) lateral view. Leg: (C); Female: head: (D) dorsal view, (E) lateral view. Leg: (F).

Σχήμα 9. *E. rubrum* sp. n., Άρρεν: κεφαλή: (A) ραχιαία όψη, (B) πλευρική όψη. Πόδι: (C)· Θήλυ: κεφαλή: (D) ραχιαία όψη, (E) πλευρική όψη. Πόδι: (F).

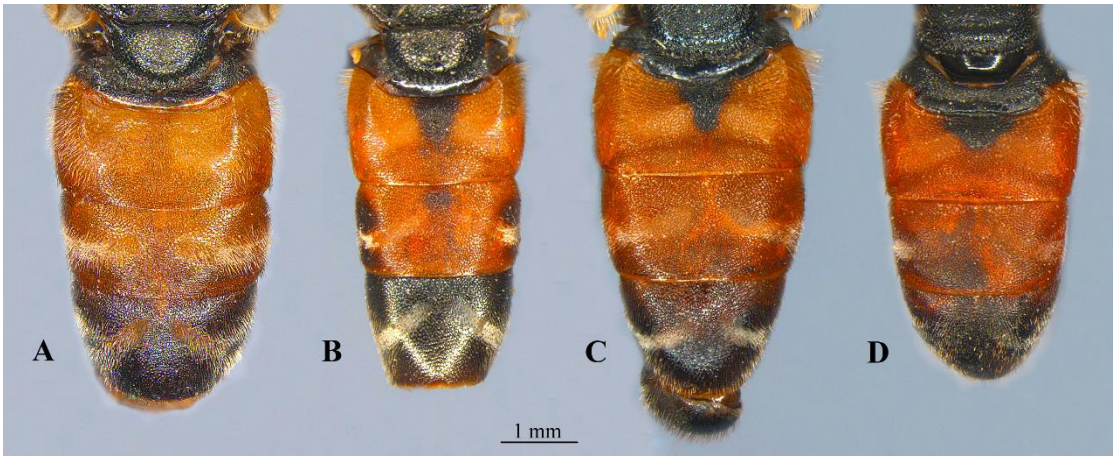

Fig. 10. Male tergites of the *E. tricolor* group: (A) *E. rubrum* sp. n.; (B) *E. tarsalis*; (C) *E. tricolor*; (D) *E. armatus*. Photo: A. Grković.

Σχήμα 10. Τεργίτες αρρένων της ομάδας ειδών *E. tricolor*: (A) *E. rubrum* sp. n.· (B) *E. tarsalis*· (C) *E. tricolor*· (D) *E. armatus*. Φωτογραφία: A. Grković.

Table 1. Characters to distinguish adult females of *E. amoenus* Loew, 1848, *E. consimilis* Šimić & Vujić (1996), *E. strigatus* (Fallen, 1817), *E. montanum* sp. n., *E. sogdianus* Stackelberg, 1952 and *E. funeralis* Meigen, 1822.

Πίνακας 1. Ειδοποιοί χαρακτήρες των ενήλικων θηλυκών για τα είδη *E. amoenus* Loew, 1848, *E. consimilis* Šimić & Vujić, 1996, *E. strigatus* (Fallén, 1817), *E. montanum* sp. n., *E. sogdianus* Stackelberg, 1952 και *E. funeralis* Meigen, 1822.

E. amoenus	*E.consimilis*	*E. strigatus*	*E. montanum sp. n.*	*E. sogdianus*	*E. funeralis*
Tergite 4 sharply tapering to the top	Tergite 4 slightly tapering to the top	Tergite 4 sharply tapering to the top	Tergite 4 slightly tapering to the top	Tergite 4 slightly tapering to the top	Tergite 4 sharply tapering to the top
Tergite 4 black with short white pile	Tergite 4 with bronze shine in posterior half, below lunules, golden-yellow pile slightly longer posteriorly	Tergite 4 with barely visible bronze shine and golden-yellow pile slightly longer in posterior half	Tergite 4 in posterior 1/3 with bronze-gold shine which anterior margin forms reversed v-shape and distinctive golden-yellow pile in that part, other parts with dark pile mixed with yellow	Tergite 4 sharp pointed with bronze shine in posterior half, below lunules, golden-yellow pile slightly longer posteriorly	Tergite 4 black with short white pile
Tergite 5 black with pale pilosity	Tergite 5 bronze with yellow pilosity	Tergite 5 bronze with pale pilosity	Tergite 5 bronze with yellow to gold pilosity	Tergite 5 bronze with pale pilosity	Tergite 5 black with pale pilosity
Abdomen black, sometimes with a blue tinge and with a bronze shine on lateral margins, short white pile	Abdomen black with bronze shine and blurry blue tinge, pale to yellow pile	Abdomen black with bronze shine and blurry blue tinge, pale to yellow	Abdomen black with bronze-gold shine, particulary on lateral parts of tergites with pale to yellow ranged to	Abdomen black with bronze shine and blurry blue tinge, pale to yellow pile	Abdomen black with blurred blue tinge and unobtrusive bronze shine, pale short

			pile	gold pile		sparse pile
Scutum with bronze-shine and pale short pilosity			Scutum with gold shine and yellow to gold pilosity	Scutum with gold shine and yellow to gold pilosity	Scutum with gold to bronze shine and dense gold pilosity	Scutum with gold shine and pale to yellow pile	Scutum with bronze shine and pale to yellow pilosity
Pleural pile pale to white			Pleural pile from pale to gold	Pleural pile from pale to gold	Pleural pile from white to very gold	Pleural pile from white to yellow	Pleural pile pale to yellow
Ventral pile of hind femur white, long about 1/4 of depth of the femur			Ventral pile of hind femur yellow, long about 1/3 of depth of the femur	Ventral pile of hind femur yellow, long about 1/3 of depth of the femur	Ventral pile of hind femur yellow to gold, long about half of depth of the femur	Ventral pile of hind femur pale, long about 1/3 of depth of the femur	Ventral pile of hind femur pale, long more then half of depth of the femur
Ocelli making isoscale triangle, longer then wide	Ocelli making almost equilateral triangle	Ocelli making equilateral triangle	Ocelli making isoscale triangle, longer then wide	Ocelli making almost equilateral triangle		Ocelli making equilateral triangle	
Space between posterior ocellus and eye margin is about 2 ocelli wide	Space between posterior ocellus and eye margin is about 1 ocellus wide	Space between posterior ocellus and eye margin is about 1 ocellus wide	Space between posterior ocellus and eye margin is about 1 ocellus wide	Space between posterior ocellus and eye margin is about 1 ocellus wide		Space between posterior ocellus and eye margin is about 1 ocellus wide	

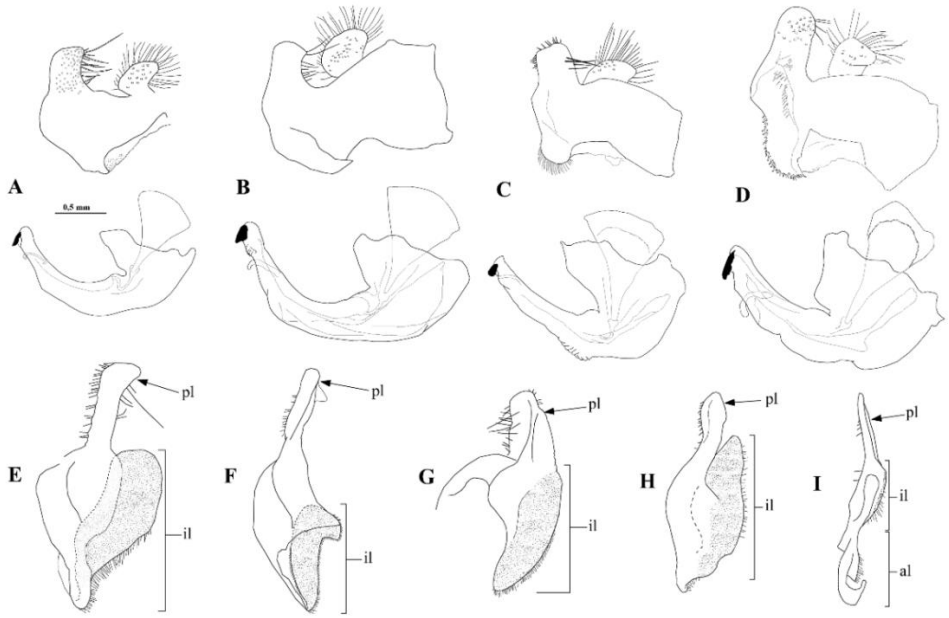

Fig. 11. Male genitalia of the *E. tricolor* group, lateral view: upper- epandrium, lower-hypandrium: (A) *E. rubrum* sp. n.; (B) *E. tarsalis*; (C) *E. armatus*; (D) *E. tricolor*; ventral view of epandrium: (E) *E. rubrum* sp. n., (F) *E. tarsalis*, (G) *E. armatus*, (H) *E. tricolor*; (I) *E. sogdianus*. Abbreviations: pl, posterior lobe of surstylus; il, interior accessory lobe of surstylus; al, anterior lobe of surstylus.

Σχήμα 11. Γεννητικός οπλισμός αρρένων της ομάδας ειδών *E. tricolor*, πλευρική όψη: άνω-επάνδριο (τελευταίος νωτιαίος τεργίτης), κάτω-υπάνδριο (9ος κοιλιακός στερνίτης): (A) *E. rubrum* sp. n.· (B) *E. tarsalis*· (C) *E. armatus*· (D) *E. tricolor*, κοιλιακή όψη του επανδρίου (τελευταίος νωτιαίος τεργίτης): (E) *E. rubrum* sp. n., (F) *E. tarsalis*, (G) *E. armatus*, (H) *E. tricolor*· (I) *E. sogdianus*. Συντομογραφίες: pl, οπίσθιος λοβός στύλου· il, εσωτερικός βοηθητικός λοβός στύλου· al, πρόσθιος λοβός στύλου.

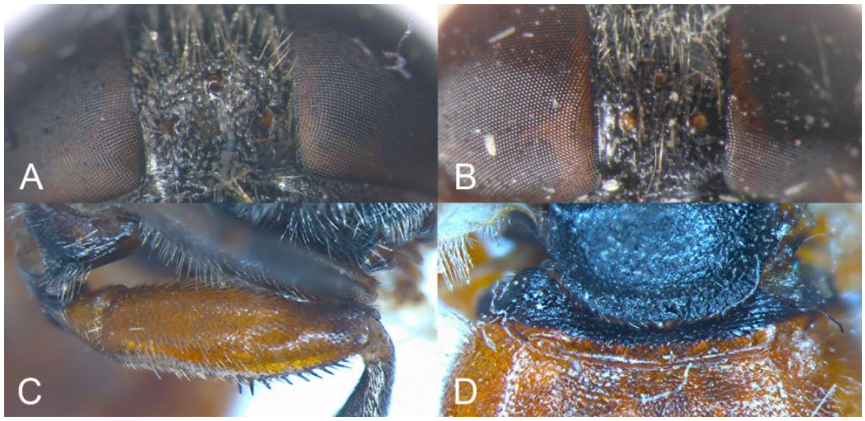

Fig. 12. Some diagnostic characters of females: ocellar triangle: (A) *E. rubrum*, (B) *E. tauricus*; (C) metafemur, lateral view: *E. rubrum*; (D) tergite I: *E. rubrum*. Photo: A. Grković.

Σχήμα 12. Ειδοποιοί χαρακτήρες των ενήλικων θηλυκών: τρίγωνη περιοχή των ομματιδίων: (A) *E. rubrum*, (B) *E. tauricus*· (C) metafemur, πλευρική όψη: *E. rubrum*; (D) Τεργίτης I: *E. rubrum*. Φωτογραφία: A. Grković.

3.4. Molecular analyses

The ML alignment of the 'total' dataset contained 0.06% gaps and completely undetermined characters, and 164 distinct alignment patterns. The NJ, ML and MP tree topologies can be viewed in the Supplementary material (Figs. S1 and S3) and in Fig. 13, respectively. The genetic distance (K2P) computed for the different species of *Eumerus* in the 'total' dataset was found to be 0.023-0.107 (Table S2).

In all phylogenetic trees, *E. uncipes* was clustered with *E. clavatus* (*E. clavatus* group) and together these taxa were highly differentiated, with bootstrap support values of 87 (ML) and 85 (MP). *E. montanum* sp. n. was clustered within the *E. strigatus* group and close to *E. strigatus*, with bootstrap support values of 75 (ML) and 59 (MP). The split network analysis identified the *E. strigatus* and *E. clavatus* groups, indicating the phylogenetic relationships between the species constituting these groups (Fig. 14). Regarding the *E. strigatus* group, the MP tree topologies showed a clear clustering of the seven studied species (Figs. 15–17), with separate and combined DNA/morphological analyses supporting the affinity between the species *E. montanum* sp. n. and *E. strigatus*.

Discussion

To date *Eumerus* has been considered as encompassing 34 species in southeastern Europe. Here, we introduce and provide descriptions of two new species (*E. montanum* sp. n. and *E. rubrum* sp. n.). We revise the geographic distribution of *E. uncipes*, thereby increasing the total number of *Eumerus* species to 37 in southeastern Europe. In addition, the assignment of *Eumerus* species into groups is discussed and, where feasible, based on an integrative approach.

Based on morphology, we found that *E. montanum* sp. n. belongs to the group defined as *E. strigatus* which consists of species "closely similar morphologically in the adult stage to *E. strigatus*", sensu Speight et al. (2013). Based on the study of Speight et al. (2013), in Europe, the *E. strigatus* group includes five species: *E. consimilis*, *E. funeralis*, *E. narcissi* Smith, 1928, *E. sogdianus* and *E. strigatus*.

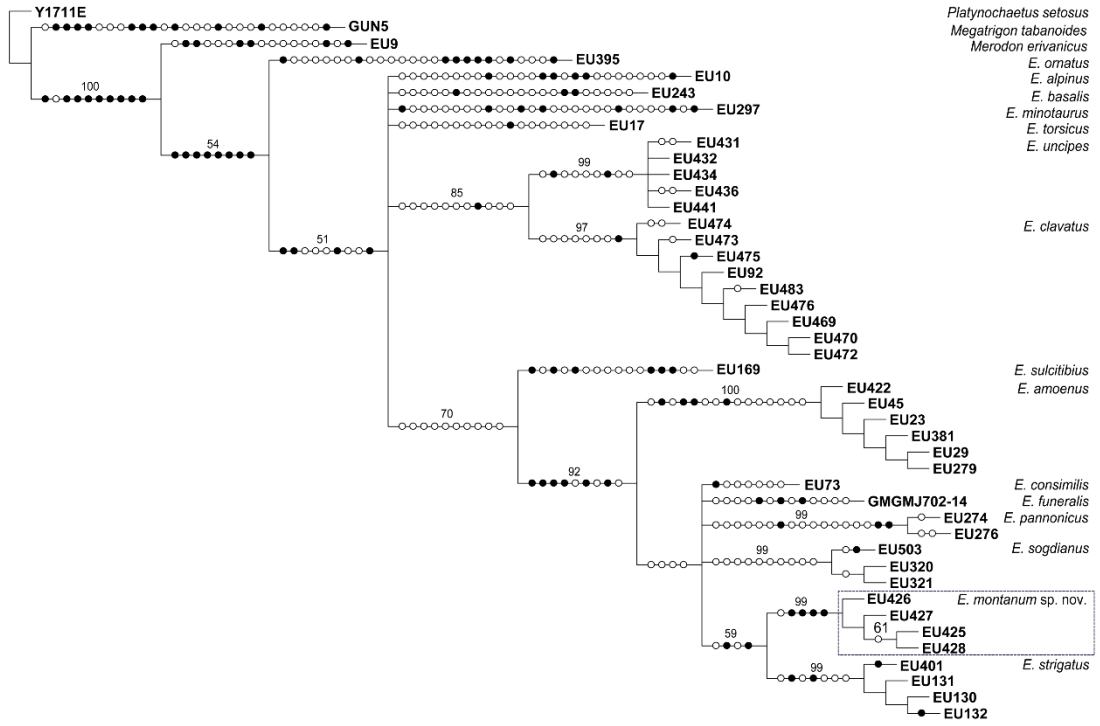

Fig. 13. Maximum parsimony analysis for the 'total' dataset (total length 612 bp); 27 equally parsimonious trees were produced from which the consensus tree is illustrated here. Length 442 steps, Consistency index (CI) = 48, Retention index (RI) = 76; filled circles denote unique changes, open circles non-unique. Bootstrap support values are illustrated above the branches.

Σχήμα 13. Αποτελέσματα ανάλυσης με την μέθοδο της μέγιστης φειδωλότητας (MP) επί των συνολικών δεδομένων (συνολικού μήκους αλληλουχιών 612 bp), η οποία παρήγαγε 27 εξίσου φειδωλά δέντρα· εδώ δίνεται το συναινετικό δένδρο. Μήκος 442 εξελικτικά βήματα, Δείκτης Ομοπλασίας (CI) = 48, Δείκτης Retention (εκφράζει το ποσοστό των taxa τα οποία δεν εμφανίζουν ομοπλασία, RI) = 76. Οι μοναδικές νουκλεοτιδικές υποκαταστάσεις σημειώνονται με μαύρο κύκλο, και οι μη-μοναδικές με απλή περιφέρεια κύκλου. Για να ελεγχθεί η στατιστική στήριξη των κλάδων, πραγματοποιήθηκαν 1000 επαναλήψεις bootstrap, των οποίων οι τιμές παρουσιάζονται πάνω από τους κλάδους του MP δέντρου.

According to the same study, the similarity between species of the *E. strigatus* group was based on morphology not on phylogenetic hypotheses. Here, we found that the aforementioned species belong to one monophyletic group that also encompasses *E. montanum* sp. n. Besides our species description of *E. montanum* sp. n., we attempted to morphologically define the *E. strigatus* group after corroborating through DNA barcoding that all species considered by Speight et al. (2013), with the addition of *E. amoenus* (Chroni et al., 2017) and *E. pannonicus*, really belong to one monophyletic group. We have included neither *E. narcissi* nor *E. vanderbergei* Doczkal, 1996 in our molecular analyses due to lack of available DNA barcodes, but we have considered them part of the *E. strigatus* group based on morphological similarity. *E. narcissi* was

initially described from North America (Santa Cruz, California). Speight et al. (2013) recorded *E. narcissi* for the first time in Europe (France) and redescribed the species, both males and females. We have used the detailed description of Speight et al. (2013) to compare *E. narcissi* with other species of the group. We have also assigned *E. vanderberghei* to the same group based on Doczkal (1996), who described *E. vandenberghei* as an endemic species to Corsica and Sardinia and mentioned its affinity to *E. funeralis*.

In order to conclude phylogenetic positioning and clustering, as well as to confirm species assignments within the *E. strigatus* group, we conducted various analyses (separately and combined for morphological characters and DNA sequences). Analyses with morphological characters alone did not cluster *E. montanum* sp. n. with *E. strigatus*, probably due to the insufficient number of morphological features considered. However, DNA sequences alone and the combined analyses did reveal the strong similarity between *E. montanum* sp. n. and *E. strigatus*. After examining more thoroughly the morphology of adults of these two species, we found considerable similarity in the shapes of the fourth abdominal sternite in males (Fig. 8A, B). Our analyses showed *E. amoenus* and *E. pannonicus* to be the most distinct from the other species of the *E. strigatus* group, which is indeed reflected in the morphology of the males (specific shapes of sternite IV and distinctive morphology of the genitalia). According to Speight et al. (2013), *E. narcissi* can be distinguished from other species of the group by the arrangement of the ocelli that form an equilateral triangle, whereas in other species the ocelli form an isosceles triangle. We found that this feature is also present in *E. strigatus*, but in this species it has a tendency to be wider than long. As mentioned previously, species related to *E. bactrianus* (such as *E. pannonicus*) also belong to the *E. strigatus* group, but since the shape of the surstylar lobe of the epandrium of those species is so distinct, we suspect that they probably form a separate subgroup (Fig. 7G).

We present a new record for the species *E. uncipes* occurring in Greece. *E. uncipes* is related and morphologically similar to *E. clavatus*; a species with a relatively wide range in Europe (northeast France south to Spain, Germany, Danube floodplain of Romania, the former Yugoslavia, Ukraine and the Caucasus; Speight, 2014). According to Speight (2014), the range of *E. clavatus* overlaps with that of *E. uncipes* (whose range is imperfectly known: from the Rhine valley south to the

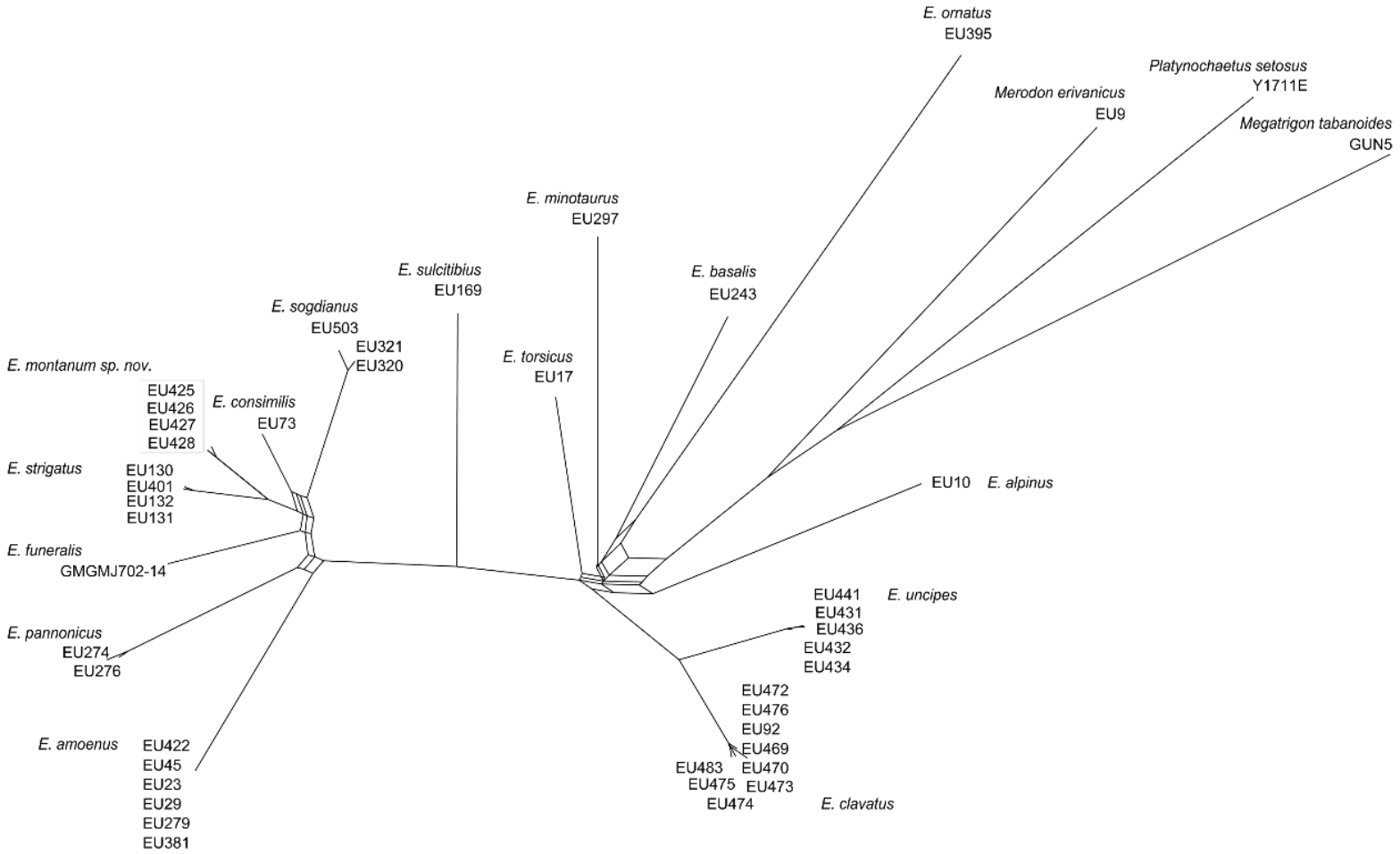

Fig. 14. A phylogenetic network from NJ and ML tree results of the ‘total’ dataset.

Σχήμα 14. Φυλογενετικό δίκτυο, προϊόν των NJ και ML δέντρων επί των συνολικών δεδομένων.

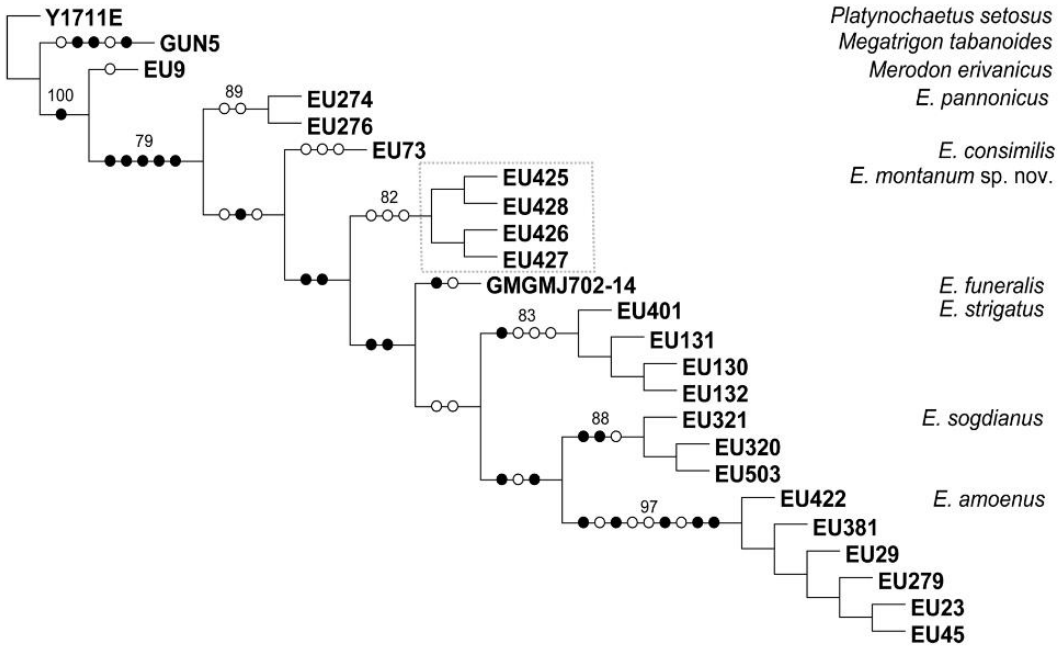

Fig. 15. Maximum parsimony analysis for the dataset of 21 *Eumerus* plus the 3 outgroups; 24 morphological characters were included (characters numbered 0 to 23). One tree was produced and is illustrated here. Length 79 steps, Consistency index (CI) = 68, Retention index (RI) = 86; filled circles denote unique changes, open circles non-unique. Bootstrap support values are illustrated above the branches.

Σχήμα 15. Αποτελέσματα ανάλυσης με την μέθοδο της μέγιστης φειδωλότητας (MP) για την ομάδα δεδομένων με τα 21 είδη *Eumerus* και τις 3 εξωομάδες. Συμπεριλήφθηκαν 24 μορφολογικοί χαρακτήρες (χάρακτηρες 0 εώς 23). Παρήχθη ένα δέντρο, το οποίο και παρουσιάζεται εδώ. Μήκος 79 εξελικτικά βήματα, Δείκτης Ομοπλασίας (CI) = 33, Δείκτης Retention (εκφράζει το ποσοστό των taxa τα οποία δεν εμφανίζουν ομοπλασία, RI) = 86. Οι μοναδικές νουκλεοτιδικές υποκαταστάσεις σημειώνονται με μαύρο κύκλο, και οι μη-μοναδικές με απλή περιφέρεια κύκλου. Για να ελεγχθεί η στατιστική στήριξη των κλάδων, πραγματοποιήθηκαν 1000 επαναλήψεις bootstrap, των οποίων οι τιμές παρουσιάζονται πάνω από τους κλάδους του MP δέντρου.

Mediterranean in France, Germany, northern and central Italy, Romania), but also extends to North Africa. We found that Corfu Island (Greece) probably represents the southeasternmost point of the distribution of *E. uncipes*. Our phylogenetic analyses clustered these two species together, highlighting that they form one monophyletic group that we named *E. clavatus*. From a morphological point of view, this group contains species with a distinctive projection on the posterior margin of abdominal sternite III of males.

In summary, our study contributes to systematic studies of the genus *Eumerus* in Europe by introducing two new species and one new record for a species in southeastern Europe, thereby increasing the total number of *Eumerus* species in this region to 37. We make further conclusions regarding genus clustering and species assignments, with the existence of a new group (*E. clavatus*, defined here) and two other groups being discussed based on morphological and molecular features. An overview of the morphological characters that cluster species into specific groups is provided.

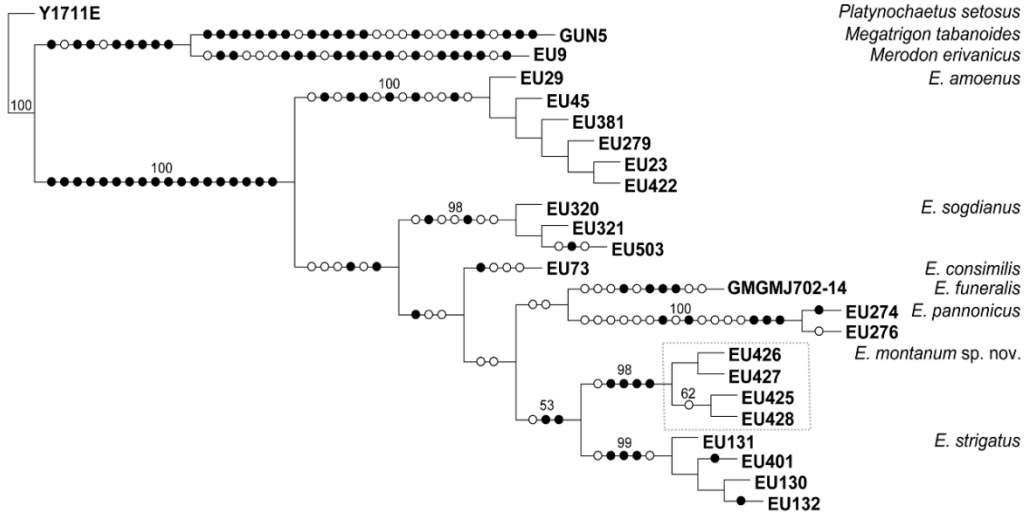

Fig. 16. Maximum parsimony analysis for the dataset of 21 *Eumerus* plus the 3 outgroups (total length 612 bp). One tree was produced and is illustrated here. Length 233 steps, Consistency index (CI) = 71, Retention index (RI) = 81; filled circles denote unique changes, open circles non-unique. Bootstrap support values are illustrated above the branches.

Σχήμα 16. Αποτελέσματα ανάλυσης με την μέθοδο της μέγιστης φειδωλότητας (MP) για την ομάδα δεδομένων με τα 21 είδη *Eumerus* και τις 3 εξωομάδες (συνολικού μήκους αλληλουχιών 612 bp). Παρήχθη ένα δέντρο, το οποίο και παρουσιάζεται εδώ. Μήκος 233 εξελικτικά βήματα, Δείκτης Ομοπλασίας (CI) = 71, Δείκτης Retention (εκφράζει το ποσοστό των taxa τα οποία δεν εμφανίζουν ομοπλασία, RI) = 81. Οι μοναδικές νουκλεοτιδικές υποκαταστάσεις σημειώνονται με μαύρο κύκλο, και οι μη-μοναδικές με απλή περιφέρεια κύκλου. Για να ελεγχθεί η στατιστική στήριξη των κλάδων, πραγματοποιήθηκαν 1000 επαναλήψεις bootstrap, των οποίων οι τιμές παρουσιάζονται πάνω από τους κλάδους του MP δέντρου.

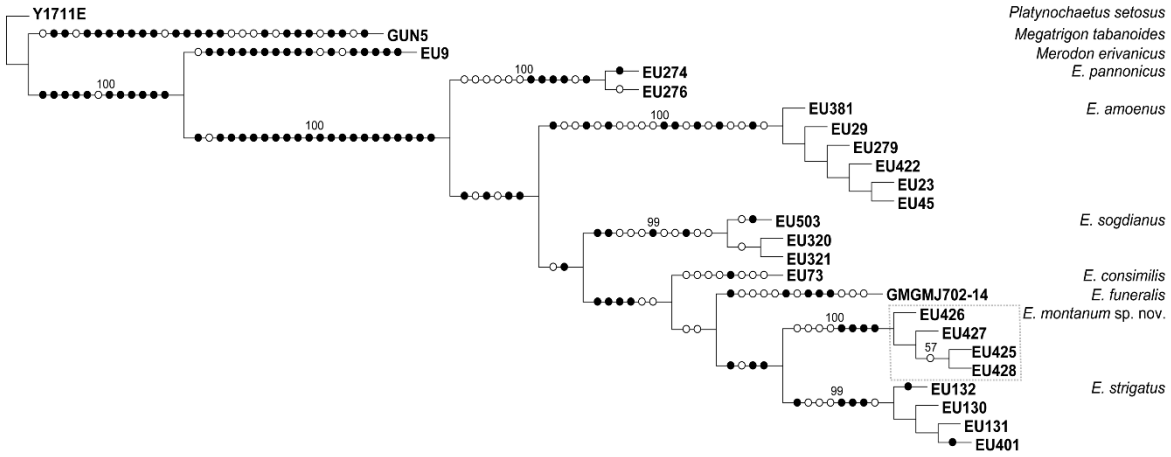

Fig. 17. Maximum parsimony analysis for the dataset of 21 *Eumerus* plus the 3 outgroups; 24 morphological (character states 1-24) and 612 molecular characters (character states 25-636) were included. One tree was produced and is illustrated here. Length 317 steps; filled circles denote unique changes, open circles non-unique. Bootstrap support values are illustrated above the branches.

Σχήμα 17. Αποτελέσματα ανάλυσης με την μέθοδο της μέγιστης φειδωλότητας (MP) για την ομάδα δεδομένων με τα 21 είδη *Eumerus* και τις 3 εξωομάδες. Συμπεριλήφθησαν 24 μορφολογικοί χαρακτήρες (χάρακτηρες 1-24) και οι 612 μοριακοί (χαρακτήρες 25-636). Παρήχθη ένα δέντρο, το οποίο και παρουσιάζεται εδώ. Μήκος 317 εξελικτικά βήματα. Οι μοναδικές νουκλεοτιδικές υποκαταστάσεις σημειώνονται με μαύρο κύκλο, και οι μη-μοναδικές με απλή περιφέρεια κύκλου. Για να ελεγχθεί η στατιστική στήριξη των κλάδων, πραγματοποιήθηκαν 1000 επαναλήψεις bootstrap, των οποίων οι τιμές παρουσιάζονται πάνω από τους κλάδους του MP δέντρου.

Acknowledgments

The authors would like to thank Grigory Popov for his helpful advice and cooperation and the anonymous reviewer for his/her valuable comments and suggestions to improve the quality of the paper. The authors wish to thank Ben Brugge and Pasquale Ciliberti (Leiden, the Netherlands) for loaned material. We thank John O'Brien for proof reading and making constructive suggestions to the text.

Financial support for this research was provided by the Serbian Ministry of Education, Science and Technological Development (Projects OI173002 and III43002), the Provincial Secretariat for Science and Technological Development (Project 'Genetic resources of agro-ecosystems in Vojvodina and sustainable agriculture'). Also, this research was co-financed by the European Union (European Social Fund−ESF) and Greek national funds through the Operational Program "Education and Lifelong Learning" of the National Strategic Reference Framework (NSRF) − Research Funding Program:"Thales. Investing in knowledge society through the European Social Fund." Part of the financial support was provided by the Transnational Access to Research Infrastructures activity in the 7th Framework Programme of the EC under the ExpeER project.

References

Bradescu, V., 1991. Les Syrphides de Roumanie (Diptera, Syrphidae), Clés de détermination et répartition. Trav. Mus. Hist. nat. Grigore Antipa, 31, 7–83.

Chen, H., Rangasamy, M., Tan, S.Y., Wang, H., Siegfried, B.D., 2010. Evaluation of five methods for total DNA extraction from western corn rootworm beetles. PLoS One 5, http://dx.doi.org/10.1371/journal.pone.0011963.

Chroni, A., Djan, M., Vidaković, D.O., Petanidou, T., Vujić, A., 2017. Molecular species delimitation in the genus *Eumerus* (Diptera: Syrphidae). Bull. Entomol. Res. 107, 126–138, http://dx.doi.org/10.1017/S0007485316000729.

Doczkal, D., 1996. Description of two new species of the genus *Eumerus* Meigen (Diptera, Syrphidae) from Corsica. Volucella. 2, 3–19.

Doczkal, D., Radenković, S., Lyneborg, L., Pape, T., 2016. Taxonomic revision of the Afrotropical genus *Megatrigon* Johnson, 1898 (Diptera: Syrphidae). Eur. J. Taxon. 238, 1–36, http://dx.doi.org/10.5852/ejt.2016.238.

Doczkal, D., Pape, T., 2009. *Lyneborgimyia magnifica* gen. et sp. n. (Diptera: Syrphidae) from Tanzania, with a phylogenetic analysis of the Eumerini using new morphological characters. Syst. Entomol. 559–573, http://dx.doi.org/10.1111/j.1365-3113.2009.00478.x.

Drees, C., Husemann, M., Homburg, K., Brandt, P., Dieker, P., Habel, J.C., von Wehrden, H., Zumstein, P., Assmann, T., 2016. Molecular analyses and species distribution models indicate cryptic northern mountain refugia for a forest-dwelling ground beetle. J. Biogeogr. 119, 455–476, http://dx.doi.org/10.1111/jbi.12828.

Džukić, G., Kalezić, M.L., 2004. The Biodiversity of Amphibians and Reptiles in the Balkan Peninsula. In: Griffiths, H.I. (Ed.), Balkan Biodiversity. Kluwer Academic Publishers: Dordrecht. pp. 167–792.

Folmer, O., Black, M., Hoeh, W., Lutz, R., Vrijenhoek, R., 1994. DNA primers for amplification of mitochondrial cytochrome c oxidase subunit I from diverse metazoan invertebrates. Mol. Mar. Biol. Biotechnol., 3 (5), 294–299.

Gaston, K.J., David, R., 1994. Hotspots across Europe. Biodivers. Lett. 2, 108–116.

Grković, A., Vujić, A., Radenković, S., Chroni, A., Petanidou, T., 2015. Diversity of the genus *Eumerus* Meigen (Diptera, Syrphidae) on the eastern Mediterranean islands with description of three new species. Ann. la Société Entomol. Fr. 51, 361–373, http://dx.doi.org/10.1080/00379271.2016.1144483.

Goloboff, P. (1999) NONA (no name), version 2. Published by the author, Tucuman, Argentina.

Hall, T., 1999. BioEdit: a user-friendly biological sequence alignment editor and analysis program for Windows 95/98/NT. Nucleic Acids Symp. Ser.

Hewitt, G.M., 1999. Post-glacial re-colonization of European biota. Biol. J. Linn. Soc. 68 (1-2), 87–112, http://dx.doi.org/10.1111/j.1095-8312.1999.tb01160.x.

Hewitt, G.M., 2000. The genetic legacy of the Quaternary ice ages. Nature 405, 907–913, http://dx.doi.org/10.1038/35016000.

Hewitt, G.M., 2011. Mediterranean Peninsulas: The Evolution of Hotspots, in: Zachos, F.E., Habel, J.C., (Eds.), Biodiversity Hotspots. Springer Publishers, Berlin Heidelberg. pp. 123–47.

Hurkmans, W., 1993. A monograph of *Merodon* (Diptera : Syrphidae). Part 1. Tijdschr. Voor Entomol. 234, 147–234.

Huson, D.H., Bryant, D., 2006. Application of Phylogenetic Networks in Evolutionary Studies, Mol. Biol. Evol. 23 (2), 254–267, http://dx.doi.org/10.1093/molbev/msj030.

Jordaens, K., Goergen, G., Virgilio, M., Backeljau, T., Vokaer, A., De Meyer, M., 2015. DNA barcoding to improve the taxonomy of the Afrotropical Hoverflies (Insecta: Diptera: Syrphidae). PLoS ONE 10 (10), e0140264, http://dx.doi.org/10.1371/journal.pone.0140264.

Katoh, K., Kuma, K.I., Toh, H., Miyata, T., 2005. MAFFT version 5: Improvement in accuracy of multiple sequence alignment. Nucleic Acids Res. 33, 511–518, http://dx.doi.org/10.1093/nar/gki198.

Maddison, W.P., Maddison, D.R., 2011. Mesquite: a modular system for evolutionary analysis. Version 3.03, http://mesquiteproject.org.

Markov, Z., Nedeljković, Z., Ricarte, A., Vujić, A., Jovičić, S., Józan, Z., Mudri-Stojnić, S., Radenković, S., Ćetković, A., 2016. Bee (Hymenoptera: Apoidea) and hoverfly (Diptera: Syrphidae) pollinators in Pannonian habitats of Serbia, with a description of a new *Eumerus* Meigen species (Syrphidae). Zootaxa. 4154 (1), 027–050, http://doi.org/10.11646/zootaxa.4154.1.2.

Marzahn, E., Mayer, W., Joger, U., Ilgaz, Ç., Jablonski, D., Kindler, C., Kumlutaş, Y., Nistri, A., Schneeweiß, N., Vamberger, M., Žagar, A., Fritz, U., 2016. Phylogeography of the *Lacerta viridis* complex: mitochondrial and nuclear markers provide taxonomic insights. J. Zool. Syst. Evol. Res. 54, 85–105, http://doi.org/10.1111/jzs.12115.

Miller, M.A., Pfeiffer, W., Schwartz, T., 2010. Creating the CIPRES Science Gateway for inference of large phylogenetic trees, in: 2010 Gateway Computing Environments Workshop, GCE 2010, http://doi.org/10.1109/GCE.2010.5676129.

Nedeljković, Z., Ačanski, J., Dan, M., Obreht-Vidaković, D., Ricarte, A., Vujić, A., 2015. An integrated approach to delimiting species borders in the genus *Chrysotoxum* Meigen, 1803 (Diptera: Syrphidae), with description of two new species. Contr. Zool. 84 (4), 285–304.

Nixon, K.C., 2002. WinClada ver. 1.00.08. Publ. by author, Ithaca, NY 8.

Poulakakis, N., Kapli, P., Lymberakis, P., Trichas, A., Vardinoyiannis, K., Sfenthourakis, S., Mylonas, M., 2014. A review of phylogeographic analyses of animal taxa from the Aegean and surrounding regions. J. Zool. Syst. Evol. Res. 53, 18–32, http://doi.org/10.1111/jzs.12071.

Psonis, N., Vardinoyannis, K., Mylonas, M., Poulakakis, N., 2015. Unraveling the evolutionary history of the *Chilostoma* Fitzinger, 1833 (Mollusca, Gastropoda, Pulmonata) lineages in Greece. Mol. Phylogenet. Evol. 91, 210, http://doi.org/10.1016/j.ympev.2015.05.019.

Ricarte, A., Nedeljković, Z., Rotheray, G.,E., Yszkowski, R., M., Hancock, E., G., Watt, K., Hewitt, S., M., Horsefield, D., Wilkinson, G., 2012. Syrphidae (Diptera) from the Greek island of Lesvos, with description of two new species. Zootaxa. 3175, 1–23, http://doi.org/10.15468/jggcg8.

Rodriguez, F., Oliver, J.L., Marin, A., Medina, J.R., 1990. The general stochastic-model of nucleotide substitution. J. Theor. Biol. 142, 485–501, http://dx.doi.org/10.1016/S0022-5193(05)80104-3.

Sagonas, K., Poulakakis, N., Lymberakis, P., Parmakelis, A., Pafilis, P., Valakos, E.D., 2014. Molecular systematics and historical biogeography of the green lizards (Lacerta) in Greece: insights from mitochondrial and nuclear DNA. Mol. Phyl. Evol. 76 (1), 144–154, http://doi.org/10.1016/j.ympev.2014.03.013.

Schmitt, T., 2007. Molecular biogeography of Europe: Pleistocene cycles and postglacial trends. Front. Zool. 4, 1–13, http://dx.doi.org/10.1186/1742-9994-4-11.

Suk, S.W., Han, H.Y., 2013. Clarification of previously confused *Chrysotoxum sapporense* and *Chrysotoxum graciosum* (Insecta: Diptera: Syrphidae) in East Asia based on morphological and molecular data. Anim. Cells Syst. 17 (4), 277–289, http://dx.doi.org/10.1080/19768354.2013.814588.

Speight, M.C.D., Hauser, M., Withers, P., 2013. *Eumerus narcissi* Smith (Diptera, Syrphidae), presence in Europe confirmed, with a redescription of the species. Dipterists Dig. 20, 17–23.

Speight, M.C.D., 2014. Species accounts of European Syrphidae (Diptera). Syrph the Net, the database of European Syrphidae. Syrph the Net publications, Dublin. 78, pp. 321.

Speight, M.C.D., 2016. Species accounts of European Syrphidae (Diptera). Syrph the Net, the database of European Syrphidae. Syrph the Net publications, Dublin. 93, pp. 288.

Ståhls, G., Vujić, A., Milankov, V., 2008. *Cheilosia vernalis* (Diptera, Syrphidae) complex: molecular and morphological variability. Ann. Zool. Fennici. 45, 149–159.

Ståhls, G., Vujić, A., Petanidou, T., Cardoso, P., Radenković, S., Ačanski, J., Pérez-Bañon, C., Rojo, S., 2016. Phylogeographic patterns of *Merodon* hoverflies in the Eastern Mediterranean region: revealing connections and barriers. Ecol. Evol. 6, 2226–2245, http://dx.doi.org/10.1002/ece3.2021.

Stamatakis, A., 2006. RAxML-VI-HPC: Maximum likelihood-based phylogenetic analyses with thousands of taxa and mixed models. Bioinformatics. 22, 2688–2690, http://dx.doi.org/10.1093/bioinformatics/btl446.

Stamatakis, A., Hoover, P., Rougemont, J., 2008. A rapid bootstrap algorithm for the RAxML Web servers. Syst. Biol. 57, 758–771, http://dx.doi.org/10.1080/10635150802429642.

Šimić, S., Vujić, A., 1996. A new species of the genus *Eumerus* Meigen, 1822 (Diptera: Syrphidae). Acta entomol. Serb. 1 (½),1–4.

Tamura, K., Stecher, G., Peterson, D., Filipski, A., Kumar, S., 2013. MEGA6: Molecular Evolutionary Genetics Analysis version 6.0. Mol. Biol. Evol. 30, 2725–2729, http://dx.doi.org/ 10.1093/molbev/mst197.

Tamura, K., Nei, M., Kumar, S., 2004. Prospects for inferring very large phylogenies by using the neighbor-joining method. Proc. Natl. Acad. Sci. U. S. A. 101, 11030–11035, http://dx.doi.org/10.1073/pnas.0404206101.

Thompson, C.F., 1999. A key to the genera of the flower flies (Diptera: Syrphidae) of the Neotropical Region including descriptions of new genera and species and a glossary of taxonomic terms. Contrib. Entomol. Int. 3, 319–378.

Thompson, F.C., 2005. Biosystematic Database of World Diptera. Version 7.5 [WWW document]. URL http://www.sel.barc.usda.gov/Diptera//biosys.htm [accessed on 30 November 2011].

Thompson, F.C., Rotheray, G.E., Zimbado, M.A., 2010. Syrphidae (flower flies), in: Brown, B.V., Borkent, A., Cumming, J.M., Wood, D.M., Woodley, Norman, E., Zumbado, M.A. (Eds.), Manual of Central American Diptera. Ottawa, NRC Research Press. pp. 763–792.

Vujić, A., Petanidou, T., Tscheulin, T., Cardoso, P., Radenković, S., Ståhls, G., Baturan, Ž., Mijatović, G., Roho, S., Pérez-Bañón, C., Devalez, J., Andrić, A., Jovičić, S., Krašić, D., Markov, Z., Radišić, D., Tataris, G., 2016. Biogeographical patterns of the genus *Merodon* Meigen, 1803 (Diptera: Syrphidae) in islands of the Eastern Mediterranean and adjacent mainlands. Insect Conserv. Divers. 9 (3), 181–191, http://dx.doi.org/10.1111/icad.12156.

Vujić, A., Šimić, S., 1999. Genus *Eumerus* Meigen 1822 (Diptera: Syrphidae) in area of former Jugoslavia. Glasn. Prir. Muz. u Beogradu, B49–50, 173–190.

Young, A.D., Marshall, S.A., Skevington, J.H., 2016. Revision of *Platycheirus* Lepeletier and Serville (Diptera: Syrphidae) in the Nearctic north of Mexico. Zootaxa 4082 (1), 001–317, http://dx.doi.org/10.11646/zootaxa.4082.1.1.

CHAPTER 5

Is there more out there? Disentangling cryptic species complex and new species within *Eumerus minotaurus* group (Diptera: Syrphidae) based on integrative taxonomy and Aegean palaeogeography

Is there more out there? Disentangling cryptic species complex and new species within *Eumerus minotaurus* group (Diptera: Syrphidae) based on integrative taxonomy and Aegean palaeogeography

Antonia Chroni, Ana Grković, Jelena Ačanski, Ante Vujić, Snežana Radenković, Nevena Veličković, Mihajla Djan and Theodora Petanidou

Paper under revision in Contributions to Zoology.

Abstract

This study provides an overview of the *Eumerus minotaurus* taxon group, by diagnosing a new species, *E. anatolicus* Grković, Vujić & Radenković sp. n. (Muğla, Turkey), and unravelling three cryptic species within *E. minotaurus*: *E. karyates* Chroni, Grković & Vujić sp. n. (Peloponnese, Greece), *E. minotaurus* Claussen & Lucas, 1988 (Crete and Karpathos, Greece) and *E. phaeacus* Chroni, Grković & Vujić sp. n. (Corfu and Mt Olympus, Greece; Mt Rumija, Montenegro). We applied an integrative taxonomic approach based on molecular, morphological and wing geometric morphometry data to corroborate and delimit the cryptic species within the complex. In addition, we studied and discussed the latent biogeographic patterns and speciation processes leading to the configuration of the *E. minotaurus* group based on the palaeogeographic evolution in the Aegean. Mitochondrial phylogeographic analysis suggested that the formation of the mid-Aegean Trench and the Messinian Salinity Crisis are accountable for the speciation within the *E. minotaurus* group, which was integrated at the Pleistocene. We showed that more accurate estimations of divergence times may be accounted based on geological events rather than on the standard arthropod mtDNA substitution rate.

Keywords: hoverflies; geometric morphometry; DNA sequences; MAT; Aegean

Introduction

Integrative taxonomy is a multisource approach that takes advantage of complementarity among disciplines and tends to gain ground more and more in species delimitation and diagnosis of cryptic diversity (Dayrat, 2005; Padial *et al*., 2010; Schlick-Steiner *et al*., 2010). Single-method approaches in taxonomic and

systematic studies pose many limitations especially in diagnosis of cryptic species and, as a result, (two or more) distinct species are erroneously classified (and hidden) under one species name (Bickford *et al.*, 2007; Pfenninger and Schwenk, 2007). Cryptic species are morphologically indistinguishable with genetically distinct lineages, and a combination of molecular, biological and morphological approaches, as well phylogeographic and population genetic analyses have been proposed (and are required) as a framework to diagnose and separate cryptic species (Pérez-Ponce de León and Nadler, 2010). Mitochondrial (DNA barcodes; Hebert *et al.*, 2003) and nuclear molecular markers (e.g. 28S, Belshaw *et al.*, 1998) have added to the effort to tally up the total species diversity, leading to the prosperity of integrative taxonomy (e.g. hoverflies, Mengual *et al.*, 2008) and the detection of new species (beetles, Soldati *et al.*, 2014; butterflies, Kirichenko *et al.*, 2015; cone snails, Puillandre *et al.*, 2014; flies, Diaz *et al.*, 2015) as well as cryptic species complexes (earthworms, Martinsson and Erséus, 2017; flies, Dias *et al.*, 2016; Šašić *et al.*, 2016; lizards, Rato *et al.*, 2016; plants, Perez *et al.*, 2016; rotifers, Papakostas *et al.*, 2016).

The hoverfly genus *Eumerus* Meigen, 1822 (Diptera: Syrphidae) accounts of its great diversity (256 species recorded worldwide, Pape and Thompson, 2015, of which 37 occur in southeastern Europe, Grković *et al.*, 2017), yet we know little about its fauna (unknown total species number as e.g. new species are constantly being described: Doczkal, 1996; Speight *et al.*, 2013; Grković *et al.*, 2015, 2017; Markov *et al.*, 2016), habitat preferences (Speight, 2016), life cycle (often strictly connected to plant species, Arzone, 1971, 1973; Pérez-Bañón and Marcos-García, 1998; Speight, 2016), and foraging behaviour (pests of vegetables, Doczkal, 1996; Pérez-Bañón and Marcos-García, 1998; flower visitors, Petanidou *et al.*, 2011; Speight, 2016). In addition, the nomenclatural history and the unclarified taxonomic status within the genus are complicated, pointing out the need of a revision of the genus taxonomy. Considering the importance of hoverflies in ecosystems (as pollinators, predators of plant pests, herbivores, etc.; Rotheray and Gilbert, 2011), and subsequently of *Eumerus*, further ecological and biogeographic studies are required; there might be more out there that we are missing which should be taken into account in, e.g. conservation outlines.

Heretofore, few studies revisit unresolved problems of the genus *Eumerus* with DNA barcoding, let alone integrative taxonomy that has rarely been employed; new species, some of them endemics, have been described during the past decade

(Doczkal, 1996; Ricarte *et al.*, 2012; Grković *et al.*, 2015, 2017; Markov *et al.*, 2016), and several taxon groups (hereafter named as 'group') have been proposed within the genus (Chroni *et al.*, 2017). The latter study suggested the configuration of the *Eumerus minotaurus* group with two related species: *E. crassus* Grković, Vujić & Radenković, 2015 (species range: Lesvos Island, Greece; originally identified as *E. niehuisi* Doczkal, 1996, and treated as such in the relevant publication; specimen EU37) and *E. minotaurus* Claussen & Lucas, 1988 (species range: Crete and Thessaly, Greece; and parts of the former Yugoslavia; Speight, 2016) (Fig. 1A). Doczkal (1996) had discussed the issue, and suggested an affinity for *E. longicornis* Loew, 1855 (species range, requiring confirmation: southern and central Germany, Slovakia, Hungary and the Mts Caucasus; Speight, 2016), *E. minotaurus*, *E. niehuisi* (species range: Corsica and Sardinia; Doczkal, 1996) and *E. sibiricus* Stackelberg, 1952 (species range: Siberia; drawn by Stackelberg, 1961; Doczkal, 1996; Fig. 1B). Within the frame of this study, we also considered all aforementioned species (Doczkal, 1996; Chroni *et al.*, 2017) to belong to the *E. minotaurus* group (Fig. 1C), and we intended to study the species and specimens (collected and available in our disposition) that originated from southeastern Europe. We have contemplated an integrative approach of molecular, morphological and wing morphometric data (*E. crassus* and *E. minotaurus*) or morphological data (*E. longicornis*, due to unavailability of DNA sequences). Our current analyses denoted a cryptic species complex within *E. minotaurus* and one undescribed species within *E. minotaurus* group. Cryptic diversity is not something new when dealing with hoverflies as such examples exist in the genera *Chrysotoxum* (Nedeljković *et al.*, 2013, 2015), *Merodon* (*M. aureus* group, Šašić *et al.*, 2016; *M. avidus*, Popović *et al.*, 2015, Ačanski *et al.*, 2016; *M. nanus* group, Vujić *et al.*, 2014), *Microdon* (*M. myrmicae*, Bonelli *et al.*, 2011) and *Pipiza* (Vujić *et al.*, 2013).

The Aegean archipelago and its adjacent regions (Balkan Peninsula, Greek mainland and Anatolian coast) are well-known for the high diversity of both cryptic and endemic species (Poulakakis *et al.*, 2015), as well as for the multiple and complex alterations that have occurred since the Miocene (23 Mya) until Holocene (0.0117 Mya to present) (Poulakakis *et al.*, 2015; Gkontas *et al.*, 2016; Kougioumoutzis *et al.*, 2017; Sfenthourakis and Triantis, 2017). In the Aegean region, four major geological events are considered liable for the important species dispersal barriers: (1) the formation of the mid-Aegean Trench (MAT) at the middle Miocene (12–9 Mya)

during which a sea interference separated the eastern from the central-western regions (Sfenthourakis and Triantis, 2017); (2) the isolation of Crete from Peloponnese (5.5–5 Mya) after the Messinian Salinity Crisis (MSC) in the late Miocene (5.96–5.33 Mya) when the Mediterranean Sea almost desiccated allowing every species to travel anywhere wanted; (3) an extensive segregation and widening of the Aegean Sea and the separation of Karpathos–Kassos island group from Rhodos in the Pliocene (5–2 Mya); and (4) orogenetic and eustatic sea-level changes during the Pleistocene (2-0 Mya) (Kougioumoutzis *et al.*, 2017; Sfenthourakis and Triantis, 2017). A series of phenomena including geological (geotectonic forces), climatic events (sea-level oscillations) and human pressure (first evidence of human settlement in Palaeolithic, ca.130.000 years ago, Strasser *et al.*, 2010) have shaped everything as known today; the configuration or isolation of landmasses allowed or impeded the dispersal of organisms, driving speciation or species extinction (Poulakakis *et al.*, 2005; Parmakelis *et al.*, 2006; Poulakakis and Sfenthourakis, 2008; Akin *et al.*, 2010; Simaiakis *et al.*, 2012; Gkontas *et al.*, 2016; Sfenthourakis and Triantis, 2017).

The aims of our paper are threefold: (a) to define and delimit cryptic species within *E. minotaurus* by integrating molecular markers (mtDNA and nDNA), subtle morphological characters and wing geometric morphometrics; (b) to provide an overview of the species in the *E. minotaurus* group and explore the existence of potential new species within the group; and (c) to investigate the speciation processes and suggest a biogeographic pattern for the *E. minotaurus* group.

Materials and Methods

Specimen collection and morphological analysis

The study relies on collections assembled by hand net during the years of 2003 and 2016, deposited in the entomological collections of the Faculty of Sciences of Novi Sad (FSUNS), the Melissotheque of the Aegean (University of the Aegean, Mytilene, Greece, MAegean) and the Finnish Museum of Natural History (Zoological Museum, Helsinki, Finland, MZH). The specimens of *E. anatolicus* sp. n. were collected by Malaise trap and belong to Miroslav Barták collection (Faculty of Agrobiology, Food and Natural Resources, Czech University of Life Sciences, Prague). A total of 52 specimens belonging to 19 species of *Eumerus*, representing 33 sampling localities, were used for the molecular analyses (Fig. 2; Appendix): 15 specimens of representative *Eumerus* species and 37 of *E. minotaurus* group. The number and

provenance of the *E. minotaurus* group study specimens used in morphological/ molecular/ wing morphometry analyses were, respectively, as follows (Fig. 2): *E. crassus* (Greece: Chios, Evros, Lesvos, Mt Rhodope, Samos, Thassos; Turkey: Mt Bozdag; 40/ 4/ - specimens), *E. anatolicus* sp. n. (Turkey: Muğla; 7/ -/ - specimens), *E. karyates* sp. n. (Greece: Peloponnese; 8/ 8/ 9 specimens), *E. minotaurus* (Greece: Crete, Karpathos; 11/ 7/ 7 specimens) and *E. phaeacus* sp. n. (Greece: Corfu, Mt Olympus; Montenegro: Mt Rumija; 24/ 18/ 17 specimens). The additional material of representative *Eumerus* species used in the molecular analyses derived from four countries (for more details see Appendix). Furthermore, we have borrowed two paratypes of *E. minotaurus* from the Zoological Museum of Amsterdam (The Netherlands, ZMAN) and studied one specimen from Austria determined by Schiner (FSUNS) as a representative of *E. longicornis* (which possesses two labels, "longicornis det. Schiner" and "Austria Alte Sammlung"). Outgroup taxa used in the phylogenetic analyses consisted of *Platynochaetus setosus* Fabricius, 1794 (Accession No. KY865491, KY865444, KM224496), *Merodon erivanicus* Paramonov, 1925 (Accession No.LN890909, KY865445, KY865575) and *Megatrigon tabanoides* Johnson, 1898 (Accession No. KY865492, KX083393, KY865574). Two sequences used for *P. setosus* (28S) and *M. tabanoides* (COI) were retrieved from GenBank. More details regarding the locality information and GenBank accession numbers for the specimens employed in the molecular analyses are enlisted in the Appendix.

The morphological characters used in the descriptions and drawings are based on the terminology established by Thompson (1999), and those related to the male genitalia by Doczkal (1996). Colour characters are described from dry-mounted specimens. Male genitalia were extracted from specimens using standard methods for studying male hoverfly genitalia, as explained in detail in Grković *et al.* (2015). Figures as well as drawings were created by using photographs of characters taken with a Leica DFC 320 (Wetzlar, Germany) camera attached to a Leica MZ16 binocular stereomicroscope and then processed in Adobe Photoshop CS3 v10.0 (Adobe Systems, San Jose, CA, USA). An ocular micrometer attached to a stereomicroscope has been used for measurements. All measurements were carried out in such a way that both ends of all distances bound to the same view are situated in the same plane. The width of the face and the width of the head have been measured in line with the lower margin of the antennal sockets, in frontal view. The proportions of the antennal segments have been measured from the outside. The width

of the vertex is defined as the distance between the eyes at the posterior margins of the posterior ocelli. The length of the frons has been measured from eyes to upper margin of antennal socket. The widths of tergites 3 and 4 have been measured in line with anterior margin and the width of abdomen in widest part. The lengths of the tergites have been measured in medium line, as well as the length of abdomen. Abbreviations used in descriptions are: T - tergite, S - sternite, IL - interior accessory lobe of posterior surstyle lobe.

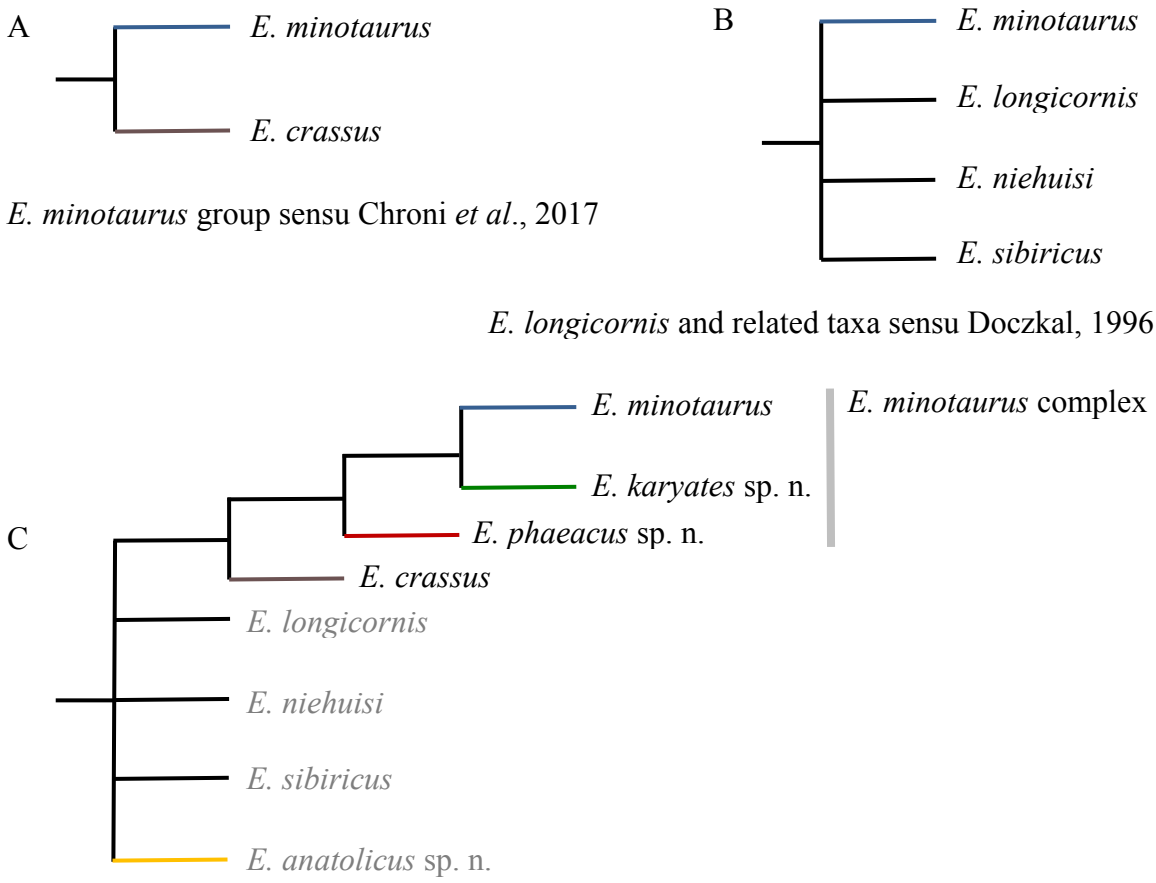

Fig. 1. (A) *E. minotaurus* group sensu Chroni et *al.*, 2017; (B) *E. longicornis* and related taxa sensu Doczkal, 1996; and (C) *E. minotaurus* group sensu Chroni et *al.*, 2017 presented here (species in grey were not included in integrative taxonomy approach due to unavailability of DNA sequences). The branches of species discussed in the present study are marked with different colours: *E. anatolicus* sp. n. (orange), *E. crassus* (grey), *E. karyates* sp. n. (green), *E. minotaurus* (blue) and *E. phaeacus* sp. n. (red) (for interpretation of the references to color in this figure legend, the reader is asked to refer to the web version of this article).

Σχήμα 1. (A) Ομάδα ειδών *E. minotaurus* sensu Chroni et *al.*, 2017· (B) *E. longicornis* και σχετικά taxa sensu Doczkal, 1996· και (C) ομάδα ειδών *E. minotaurus* sensu Chroni et *al.*, 2017 όπως παρουσιάζεται στην παρούσα έρευνα (τα είδη με γκρι

δεν έχουν αναλυθεί σύμφωνα με την προσέγγιση της ενοποιητικής ταξινομικής λόγω μη διαθεσιμότητας αλληλουχιών DNA). Οι κλάδοι των ειδών τα οποία μελετώνται στην παρούσα έρευνα σημειώνονται με διαφορετικό χρώμα: *E. anatolicus* sp. n. (πορτοκαλί), *E. crassus* (γκρί), *E. karyates* sp. n. (πράσινο), *E. minotaurus* (μπλε) και *E. phaeacus* sp. n. (κόκκινο) (για την ερμηνεία των χρωματικών αναφορών του σχήματος αυτού, ο αναγνώστης παραπέμπτεται στην ηλεκτρονική έκδοση του άρθρου).

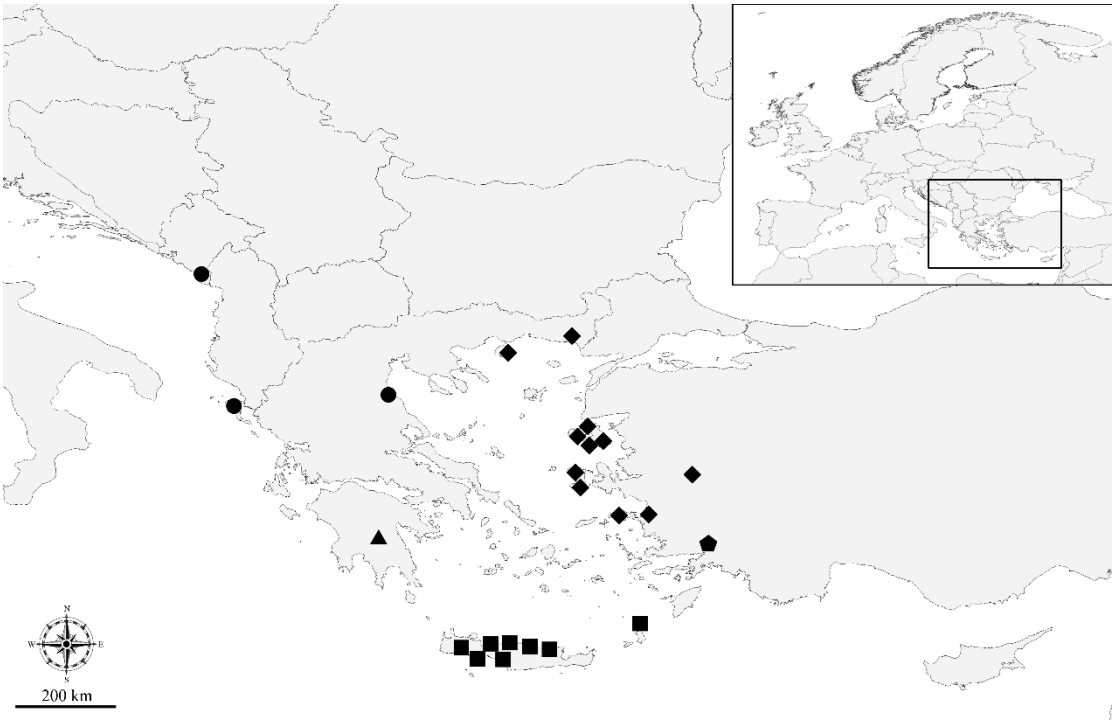

Fig. 2. Distribution of all the specimens used for the morphological, molecular and wing morphometry analyses. ■ *E. minotaurus*, ▲ *E. karyates* sp. n., ● *E. phaeacus* sp. n., ◆ *E. crassus*, ⬟ *E. anatolicus* sp. n.

Σχήμα 2. Γεωγραφική κατανομή των δειγμάτων εντόμων, που χρησιμοποιήθηκαν στις μορφολογικές και μοριακές αναλύσεις, καθώς και στην γεωμετρική μορφομετρία πτερύγων. ■ *E. minotaurus*, ▲ *E. karyates* sp. n., ● *E. phaeacus* sp. n., ◆ *E. crassus*, ⬟ *E. anatolicus* sp. n.

Sequence analysis

Raw sequences were examined and proofread by employing BioEdit v7.2.5 (Hall, 1999). The multiple sequence alignments were implemented in the MAFFT v7 by employing the L-INS-i algorithm (see supplementary information, Data S1, S2; Katoh *et al*., 2005; available at http://mafft.cbrc.jp/alignment/server/index.html). Polymorphic sites, parsimony informative sites and number of haplotypes were calculated using DnaSP v5.10.01 (Librado and Rozas, 2009).

Phylogenetic analyses and tree-based species delimitation

We have constructed three datasets to elucidate and corroborate the phylogenetic position of the four species (*E. anatolicus* sp. n. was not included due to unavailability of DNA sequences) within the *E. minotaurus* group: (1) COI dataset, based on concatenated 3' and 5' fragment of COI gene (19 *Eumerus* taxa, 1238 bp); (2) 28S dataset, based on 28S gene fragment (4 *Eumerus* taxa, 510 bp); and (3) COI subset, based on concatenated 3' and 5' fragment of COI gene (only species of the *E. minotaurus* group, 4 *Eumerus* taxa, 1238 bp) (for more details see Table 2). Representatives of other species of *Eumerus* (15 species) were only considered for COI dataset in order to properly display the phylogenetic position and relationships of the species encompassing the *E. minotaurus* group. The phylogenetic position and species delimitation of these 15 species have been confirmed and discussed in Chroni *et al*. (2017) and Grković *et al.* (2017), and thus we argue that the singletons used here do not jeopardize the phylogenetic inferences. The morphology of these species were also accounted in species delimitation (confirmation by the taxonomists Ante Vujić and Ana Grković).

Regarding the COI dataset, we have inferred Maximum parsimony (MP), Maximum likelihood (ML), Neighbor joining (NJ), Bayesian inference (BI) and split network analyses. MP analyses were performed in NONA (Goloboff, 1999), spawned in WINCLADA v1.00.08 (Nixon, 2002). A heuristics search algorithm with 1000 random addition replicates (mult x 1000) was performed with holding 100 trees per round (hold/100), max trees set to 100 000 and applying TBR branch swapping. The ML analyses were executed in RAxML v8.0.9 (Stamatakis, 2006; Stamatakis *et al.*, 2008) in the Cipres Science Gateway (Miller *et al.*, 2010) with 1000 bootstrap replicates. ML analysis was implemented under the general time-reversible (GTR) evolutionary model with gamma distribution (GTR+G; Rodriguez *et al.*, 1990) since it is the most accurate substitution model for datasets with approximately 50 taxa. The estimation of the best-fit substitution model for COI dataset in MEGA v6.06 (Tamura *et al*., 2013) resulted to GTR+G+I model as proposed by the Bayesian Information Criterion (BIC). We employed MEGA v6.06 (Tamura *et al*., 2013) to perform NJ analyses, but under the Tamura-Nei (TN93) nucleotide substitution model with a Gamma distribution (second-best nucleotide substitution model proposed by BIC; GTR model is not included in MEGA for NJ trees), and with a bootstrap test of 1000 replicates. We assessed BI tree in MrBayes v3.2.6 (Huelsenbeck and Ronquist, 2001)

at the Cipres Science Gateway (Miller *et al.*, 2010) under the GTR+G+I model as proposed by the BIC (Rodriguez *et al.*, 1990). We have partitioned by codon (2 partitions: positions 1st+2nd; 3rd) as it is recommended for protein encoding genes and considered the third codon position to be susceptible in higher mutational rates (Shapiro *et al.*, 2006; Simmons *et al.*, 2006; Bofkin and Goldman, 2007). The settings for the Bayesian Markov chain Monte Carlo (MCMC) process included two runs of 10*10e-6 MCMC generations (×4 chains) with a sampling frequency of 1000 generations and a relative burn-in of 10%. MCMC results were checked with TRACER v1.6 (http://tree.bio.ed.ac.uk/software/tracer/; Rambaut *et al*., 2014) and the tree was displayed in FigTree v1.4.2 (http://tree.bio.ed.ac.uk/software/figtree/; Rambaut, 2013). The generated ML, NJ and BI trees were merged into a split network in order to extract a united tree topology. The split network was produced in SplitsTree4 v4.14.3 (Huson and Bryant, 2006) (http://www.splitstree.org/) under SuperTree, Z-closure super-network from partial trees and heuristic analysis (number of runs: 1000). Regarding the 28S dataset, we employed MP analysis, as described above. All phylogenetic trees were rooted on *P. setosus*.

In addition, Poisson tree processes (PTP) models were implemented in order to highlight putative molecular species clusters (Zhang *et al.*, 2013; also Chroni *et al.*, 2017 for a minor review) based on the best ML tree resulting from the RA×ML analysis of the COI dataset; PTP analyses were conducted on the web server for PTP (available at http://species.h-its.org/ptp/).

Non-tree-based species delimitation

The average pairwise Kimura 2-parameter (K2P) distances between the taxa of the COI dataset and the overall sequence divergence (under the TN93+G+I model in COI dataset and in COI subset, and the Tamura 3-parameter in 28S; estimated in MEGA v6.06 and proposed by BIC, Tamura *et al*., 2013) for both datasets was estimated and performed in MEGA v6.06 (Tamura *et al.*, 2013). We have considered a threshold of 2% sequence divergence (the barcode gap) while assessing the species delimitation (outgroups were excluded; Ratnasingham and Hebert, 2013).

Network approaches can be more effective than classical phylogenetic ones for representing intraspecific evolution (Posada and Crandall, 2001). In this sense, the genealogical relationships between haplotypes of the COI subset were assessed with haplotype networks constructed using the statistical parsimony algorithm

implemented in the program TCS v1.21 (Clement *et al.*, 2000) under the 95% connection limit of parsimony (gaps treated as missing data).

Table 1. Primers used for the amplification of the mtDNA and nDNA gene fragments.
Πίνακας 1. Εκκινητές ενίσχυσης θραυσμάτων των μιτοχονδριακών και πυρηνικών γονιδίων.

	Primer pair	**Primer sequence**	**Source**
3'-end fragment of *COI*	C1-J-2183 (alias Jerry)	5'-CAACATTTATTTTGATTTTTTGG-3'	Simon *et al.*, 1994
	TL2-N-3014 (alias Pat)	5'-TCCAATGCACTAATCTGCCATATTA-3'	Simon *et al.*, 1994
5'-end fragment of *COI*	LCO-1490	5'-GGTCAACAAATCATAAAGATATTG-3'	Folmer *et al.*, 1994
	HCO-2198	5'-TAAACTTCAGGGTGACCAAAAAATCA-3'	Folmer *et al.*, 1994
28s *D2 rDNA*	28S (F2)	5'-AGAGAGAGTTCAAGAGTACGTG-3'	Belshaw *et al.*, 1998
	28S (3DR)	5'-TAGTTCACCATCTITCGGGTC-3'	Belshaw *et al.*, 1998

Table 2. Characteristics for each analysed dataset; in the 'Sequences no' the number of outgroups is not considered.
Πίνακας 2. Χαρακτηριστικά για την κάθε ομάδα δεδομένων· στον αριθμό αλληλουχιών δεν συνθεωρήθηκαν οι εξωομάδες.

Dataset	**COI**	**28S**	**subset COI**
Gene fragment(s)	3'- and 5'-end fragment of COI	28s D2 rDNA	3'- and 5'-end fragment of COI
Taxa no	19	4	4
Sequences no	52	29	37
Sequence length (bp)	1238	510	1238
Singleton variable sites	86	11	18
Parsimony informative sites	258	2	100
Sequence divergence (%)	6.1	0.3	2.8
Haplotypes no (with gaps/missing data: not considered)	41	3	26
Geographical clusters no (BBM analysis)	-	-	4

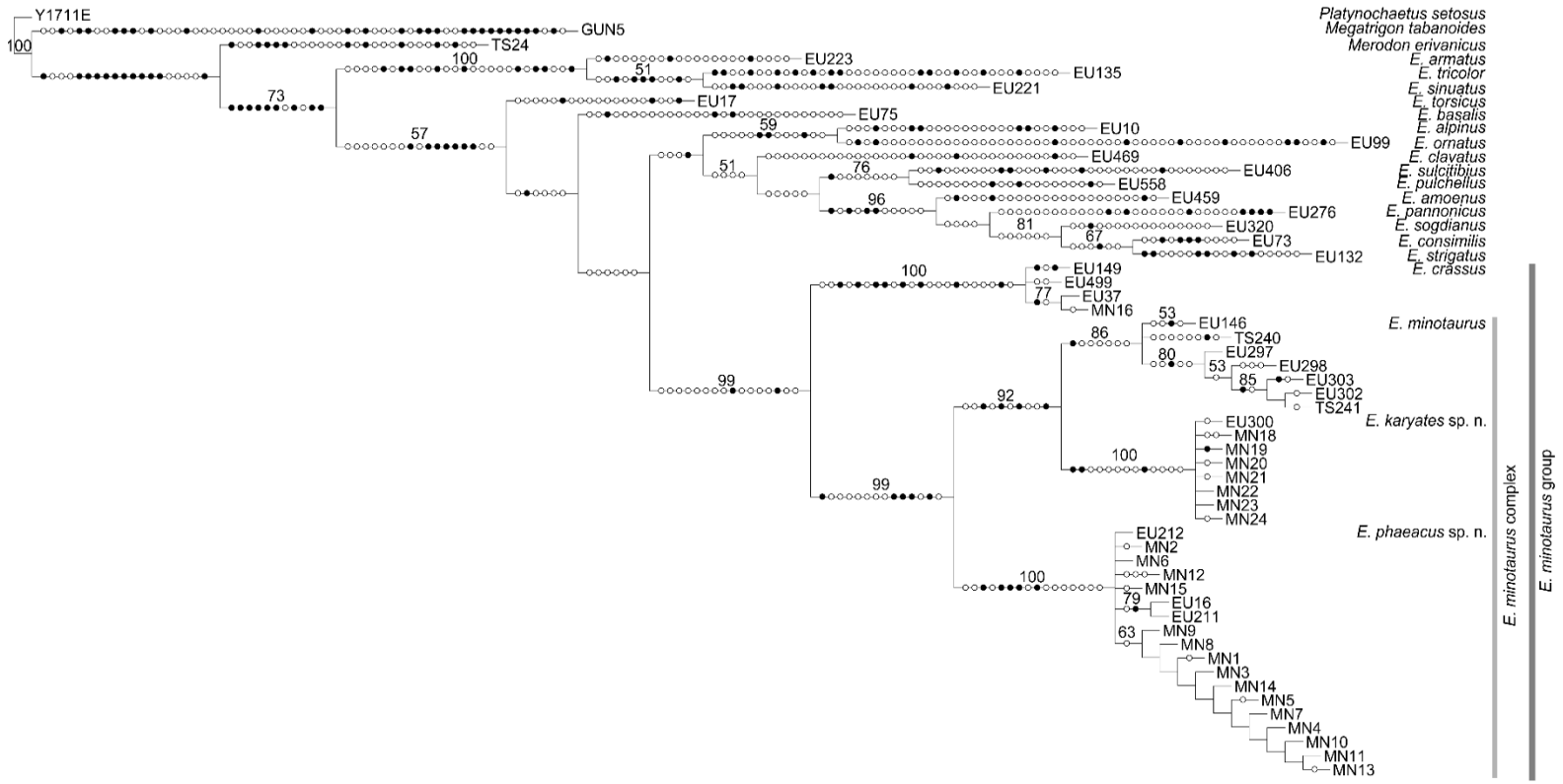

Fig. 3. Maximum parsimony analyses for the concatenated 3' and 5' fragment of COI gene fragment (COI dataset). Only the condensed tree is illustrated here. Filled circles denote unique changes and open circles non-unique. Bootstrap support values are illustrated above the branches: 60 trees, Length 1122 steps, CI=44, RI=72.

Σχήμα 3. Αποτελέσματα ανάλυσης με την μέθοδο της μέγιστης φειδωλότητας (MP) για την ομάδα δεδομένων COI, η οποία συμπεριλάμβανε τα συζευγμένα θραύσματα του COI γονιδίου. Δίνεται το συναινετικό δέντρο. Οι μοναδικές νουκλεοτιδικές υποκαταστάσεις σημειώνονται με μαύρο κύκλο, και οι μη-μοναδικές με απλή περιφέρεια κύκλου. Για να ελεγχθεί η στατιστική στήριξη των κλάδων, πραγματοποιήθηκαν 1000 επαναλήψεις bootstrap, των οποίων οι τιμές παρουσιάζονται πάνω από τους κλάδους του MP δέντρου. 60 δέντρα, Μήκος 1122 εξελικτικά βήματα, CI=44, RI=72.

Molecular divergence time estimates

A COI subset was created in order to estimate a time-calibrated species tree, and reconstruct the biogeographic history for the species encompassing the *E. minotaurus* group: *E. crassus*, *E. karyates* sp. n., *E. minotaurus* and *E. phaeacus* sp. n.

Initially, we explored the temporal structure in the COI subset, a necessary prerequisite for the reliable estimation of substitution rates, by performing a regression of root-to-tip genetic distances in TempEst program (Rambaut *et al.*, 2016). As input file we have used the NJ tree (NJ analysis for the COI subset was conducted as described above).

Subsequently, we estimated the divergence times using BEAST v1.8.4 (Drummond *et al.*, 2012). The input file (xml) was created using BEAUti v1.8.4, and we integrated the BEAGLE library (Ayres *et al.*, 2012) into BEAST runs to achieve high-performance computing. Prior specifications applied were as follows: Relaxed Uncorrelated Lognormal Clock; Birth Death process of speciation; TN93 model with G rate heterogeneity. We have also partitioned by codon (2 partitions: positions 1st+2nd; 3rd, Shapiro *et al.*, 2006; Simmons *et al.*, 2006; Bofkin and Goldman, 2007). To calibrate the molecular clock, we have considered three approaches, with employment of: (a) one calibration point based on MAT event that separated the Aegean archipelago to its western and eastern parts (10.5 ± 1.5 My, MAT analysis, Papadopoulou *et al.*, 2010); (b) two calibration points where the root height was based on MAT event and the prior of the taxon subset *E. karyates* sp. n./*E. minotaurus* was based on the end of the MSC event that represents the permanent isolation of Crete from the Greek mainland (5.3 ± 0.3 My, MAT&MSC analysis, Kasapidis *et al.*, 2005; Kamilari *et al.*, 2014); and (c) 2.3% pairwise evolutionary rate per million years (My), the standard arthropod substitution rate for the mtDNA (mtDNA-rate analysis, Brower, 1994). We have also created: (i) four taxon subsets based on the estimation of the four species within the *E. minotaurus* group for the MAT and mtDNA-rate analyses; and (ii) two taxon subsets, one with *E. crassus* sequences and one with the *E. karyates* sp. n./*E. minotaurus*, for the MAT&MSC analysis, in order to log the time to the most common ancestor tMRCA for each taxon subset and also to set the prior distributions on the corresponding divergence times. Three independent runs were performed with a chain length of 10*10e-6 iterations for the MAT and MAT&MSC analyses and of 5*10e-6 iterations for the mtDNA-rate analysis, sampled every 1000 generations. The program TRACER v1.6 (http://tree.bio.ed.ac.uk/software/tracer/;

Rambaut *et al*., 2014) was employed to confirm stationarity. Independent runs were combined using Logcombiner v1.8.4 (in BEAST). The final tree with divergence time estimates was summarized with TreeAnnotator v1.8.4 (in BEAST; 10% of trees were discarded as burn-in; Maximum clade credibility tree; and Mean heights) and visualized with FigTree v1.4.2 (http://tree.bio.ed.ac.uk/software/figtree/; Rambaut, 2013).

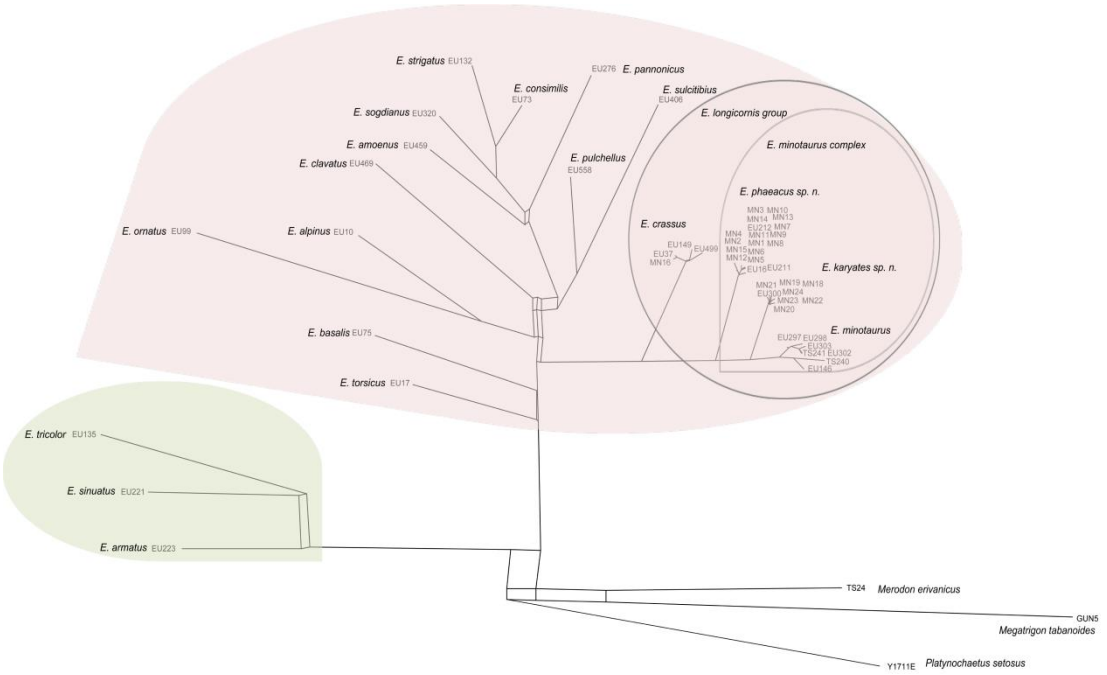

Fig. 4. A phylogenetic network from ML, NJ and BI tree results of the concatenated 3' and 5' fragment of COI gene fragment (COI dataset).

Σχήμα 4. Φυλογενετικό δίκτυο, προϊόν των ML, NJ και BI δέντρων της ομάδας δεδομένων COI, το οποίο συμπεριελάμβανε τα συζευγμένα θραύσματα του COI γονιδίου.

Biogeographic analyses

To reconstruct the biogeographic history and to predict biogeographic ancestral ranges of the *E. minotaurus* group (COI subset), we conducted the statistical approach of Bayesian Binary MCMC (BBM) Method For Ancestral State (Ronquist and Huelsenbeck, 2003), as employed in RASP v3.2 (Yu *et al.*, 2015). The MCMC chains were run by default, and the annotated trees from the BEAST analyses were used as input tree files. Four geographical areas were defined based on the clustering and distribution of the *E. minotaurus* group lineages as well as on the (recorded) plant distributions (Brummitt *et al.*, 2001; Strid, 2016): (A) Crete and Karpathos, (B)

Peloponnese, (C) Balkan Peninsula, and (D) East Aegean islands (Appendix). Ancestral ranges were assumed to include from one to four areas.

Geometric morphometric analysis

Geometric morphometric analysis of wing shape was conducted on 33 specimens of the *E. minotaurus* complex (Table S1). To reduce the statistical errors due to the low number of specimens (Arnqvist and Mårtensson, 1998), each wing was digitized three times. The right wing of each specimen was taken off by means of micro-scissors and then mounted in Hoyer's medium on a microscopic slide. Wings are archived and labeled with a unique code in the FSUNS collection, together with other data relevant to the specimens. High-resolution photographs of the wings were made using a Leica DFC320 video camera attached to a Leica MZ16 stereomicroscope. Twelve homologous landmarks at vein intersections or terminations, –that could be reliably identified– were selected using TpsDig v2.05 (Rohlf, 2006). Generalised least squares Procrustes superimposition was performed to minimise non-shape variations in location, scale and orientation of wings, and to superimpose the wings in a common coordinate system (Rohlf and Slice, 1990; Zelditch *et al.*, 2004) by employing CoordGen v7.14 (part of IMP package, Sheets, 2012). Regarding the wing shape analysis, we calculated partial warp scores (thin plate spline coefficients, Rohlf and Slice, 1990) in CVAgen v7.14a (part of IMP package, Sheets, 2012). MorphoJ v2.0 was used to visualize the thin-plate spline deformation (Klingenberg, 2011).

To explore wing shape variation among the specimens, we employed principal component analysis (PCA) without *a priori* defining groups. Analysis of variance (ANOVA) conducted on principal components (PC) was used to explore whether observed variations were connected with shape differences between taxa. Additionally, canonical variate (CVA) and discriminant function (DA) analyses were employed to test the significance in wing shape differences, to produce distance matrices and to graph results. Thereupon, we determined the phenetic relationships among taxa by UPGMA analysis based on squared Mahalanobis distances computed from the DA applied to wing variables and graphically represented using GenGIS v2.4.1 (Parks *et al.*, 2013) All statistical analyses were performed in Statistica for Windows (Dell Statistica, 2015).

Correlation among wing shape, genetic, spatial and environmental differentiation

We have addressed the correlation between squared Mahalanobis distances of wing, as well as geographic, environmental and genetic distances (uncorrected p distance, for more details see above) by employing Mantel test (Mantel, 1967) with 10.000 permutations in PaSSaGe (Rosenberg and Anderson, 2011). The two tailed Mantel tests were performed to test pairwise correlation among four distance matrices, while partial Mantel tests were used to explore relationship between (i) wing shape and genetic differentiation while holding the effect of geographical distance and separately environmental distances and (ii) wing shape and geographical distances while holding the genetic distance. Geographic distance was calculated as the minimum distance between two species using QGIS (Quantum GIS Development Team, 2012). Environmental distances were represented as Euclidean distances of the factor scores calculated based on 19 bioclim variables generated for each locality from WorldClim dataset (2.5 arc-minutes resolution) (Hijmans *et al.*, 2005).

Results

Molecular analyses

Phylogenetic analyses: tree-based and non-tree-based species delimitation

All tree-based (MP, ML, NJ, BI, split network and PTP models, high bootstrap and probability support values; Figs 3, S1, S2, S3 and 4, respectively) and non-tree-based (K2P, TCS) species delimitation analyses of the COI dataset (1238 bp) indicated four, well-supported, clusters-species within the *E. minotaurus* group and three species within *E. minotaurus*, revealing the *E. minotaurus* complex. The PTP analysis returned an estimation of 22 to 26 lineages, with four within the *E. minotaurus* group. The interspecific genetic distance (K2P) for the COI dataset was found to be 0.025-0.117 (except for the specimen TS241, 0.014). The sequence divergence was calculated for both COI and 28S datasets, as well for COI subset (Table 2). The TCS analysis for the COI subset led to four independent networks, one for each species within the *E. minotaurus* group (Fig. S4).

The nuclear molecular marker (28S dataset) did not duly distinguish the evolutionary lineages as denoted from the mitochondrial marker (COI dataset; Fig. S5). Adding to this fact the low sample size (4 species, 29 sequences; multiple specimens failed to amplify the 28S marker) and the short length of sequences (510

bp), we considered of no account to further analyse the 28S dataset (as we did for the COI dataset).

Table 3. The morphological differences between *E. minotaurus* complex and *E. longicornis*.

Πίνακας 3. Οι μορφολογικές διαφορές μεταξύ του συμπλέγματος *E. minotaurus* και του είδους *E. longicornis*.

E. longicornis Loew, 1855	*E. minotaurus* complex
Eyes almost bare	Eyes covered with moderately long and dense pile
Ventral margin of basoflagellomere linear	Ventral margin of basoflagellomere slightly convex
Ventral pile of pedicel shorter than the depth of pedicel	Ventral pile of pedicel longer than the depth of pedicel
Ventral pile of scape distinctly longer than ventral pile of pedicel	Ventral pile of scape about the same length as ventral pile of pedicel
Ventral pile on femur short as the dorsal	Ventral pile on femur longer than the dorsal
Pollinose maculae on tergites II–IV wide, well expressed, third pair clearly oblique	Pollinose maculae on tergites II–IV narrow, linear, third pair often absent

Molecular divergence time estimates and biogeographic analyses

Our root-to-tip regression revealed relatively strong temporal structure in the COI subset with correlation coefficients of 0.1586 (R squared= 0.02514), allowing us to implement a molecular clock model. This analysis also indicated that the sequences EU37, EU149 (*E. crassus*) and TS240 (*E. minotaurus*) are less divergent than the rest, while the EU297 (*E. minotaurus*) is the most divergent. The indication of few more or less divergent sequences was not considered as the quality of those sequences was checked and confirmed.

The time-calibrated species tree and results from the BBM analysis are both depicted in Fig. 5. Due to the similar probability values and out of simplicity, the Figure 5 depicts only the results from the BBM analysis based on the annotated tree produced from the MAT analysis. The species-tree topology is congruent with the one inferred by the phylogenetic analyses. Divergence time estimations, as assessed from MAT and MAT&MSC approaches are well-nigh consistent; according to the inferred dates, the diversification of the *E. minotaurus* group dates back to the Miocene, while the speciation start within the *E. minotaurus* complex to be dated approximately during the MSC (Fig. 5). The pairwise substitution rates obtained were 0.882% and

0.706% for MAT and MAT&MSC analyses, respectively. In the case of the mtDNA-rate analysis divergence times were estimated much lower, and placed the diversification of the *E. minotaurus* group and the *E. minotaurus* complex to the Pliocene and Pleistocene, respectively. All obtained posterior probability values per lineage exceeded 0.95 (and were up to 1). The substitution rates were approximately 0.80 based on codon positions 1+2, and 1.36 based on codon position 3.

The BBM analyses from all annotated trees were congruent and suggested that in total six dispersal and three vicariant events have shaped the current distribution of the *E. minotaurus* group, and that speciation events have occurred within areas as follow: A:6, B:7, C:17 and D:3. Dispersal events may have occurred between areas; A to B (Crete and Karpathos to Peloponnese), C to A (Balkan Peninsula to Crete and Karpathos) and D to C (East Aegean Islands to Balkan Peninsula). Three possible dispersal routes are proposed for each node; I: A→BA→B | A, II: C→CA→C | A, III: D→CD→C | D (Fig. 5).

Geometric morphometric evidence

Wing shape variations of entire sample without *a priori* defined groups were studied using PCA, which produced eight PCs with an eigenvalue greater than 1. The ANOVA conducted on factor scores revealed that the observed wing shape variations were linked to shape differences among three species within the *E. minotaurus* complex in six of eight PCs (Table S2). Moreover, DA showed that all species differ highly significantly in wing shape ($p < 0.01$). Importantly, all specimens were correctly classified (100%) to *a priori* defined groups, which confirms wing shape as a reliable character for interspecific discrimination.

The CVA produced two highly significant axes (CV1: Wilks' Lambda = 0.021; $\chi 2 = 359.746$; $p < 0.01$; CV2: Wilks' Lambda = 0.165; $\chi 2 = 166.502$; $p < 0.01$). CV1 described 58% of total shape variation and clearly separated *E. minotaurus* from *E. phaeacus* sp. n. and *E. karyates* sp. n. (Fig. 6). The latter two species were clearly separated by CV2 with 42% of total shape variation (Fig. 6).

Based on the squared Mahalanobis distances produced by DA, *E. minotaurus* has the most distinct wing shape (Fig. 7A). The superimposed outline drawings showed major wing deformations between the three cryptic species, which occur in the central and apical part of the wing (Fig. 7B). *E. minotaurus* has the narrowest apical part, contrary

to *E. phaeacus* sp. n., which has the broadest apical and narrowest basal part of the wing. *E. karyates* sp. n. has the broadest basal part of the wing (Fig. 7B).

Table 4. Results of simple and partial two-tailed Mantel tests for correlation among phenetic distance (wing shape) and genetic, geographic and environmental distances.
Πίνακας 4. Αποτελέσματα συσχέτισης, χρησιμοποιώντας απλό και μερικού αμφίπλευρο Mantel test, μεταξύ φαινετικής απόστασης (σχήμα πτερυγίων) και γενετικής, γεωγραφικής και περιβαλλοντικής απόστασης.

	r	P
Simple Mantel test		
wing - genetic	0.96247	0.1805
wing - geography	0.2724	1
wing - ecology	0.85954	0.4811
Partial Mantel test		
wing - genetic - holding geography	1	0.6677
wing - genetic - holding ecology	1	0.698
wing - geography holding genetic	-1	0.4479

Correlation among wing shape, genetic, spatial and environmental differentiation

Simple Mantel tests revealed that genetic, geographic and environmental distances exhibited no association with wing shape distance among the *E. minotaurus*, *E. karyates* sp. n. and *E. phaeacus* sp. n. (Table 4). Additionally, partial Mantel test showed that genetic distance has no impact on wing shape differentiation while holding geographic and environmental distances, as well as geography while holding genetic distance (Table 4).

Morphological analyses

Eumerus minotaurus group

Diagnosis. Species with elongated pedicel, at least 1.5 times longer than deep. Short body pile. Metafemur moderately swollen. Ventral pile on metafemur not longer than the half of depth of the femur. Abdomen black with bronze to gold tinge laterally, about two times as long as wide. S4 in males flat, with invaginated posterior margin (Fig. 8K), very similar in shape in all species of the group. Posterior surstyle lobe in males genitalia simple, oval (Fig. 8A–C); it does not vary noticeably in shape between species, except in *E. crassus* and *E. niehuisi* (slightly different). The group includes the following species in Europe: *E. crassus* (Fig. 8E), *E. longicornis* (Figs 8B, E, M,

9F), *E. niehuisi* and *E. minotaurus* cryptic species complex (*E. karyates* sp. n., *E. minotaurus* and *E. phaeacus* sp. n.; hereafter called *E. minotaurus* complex); and in Turkey: *E. anatolicus* sp. n. and *E. crassus*.

Eumerus minotaurus cryptic species complex

Diagnosis. Dark appearance, body blackish-bronze. Eyes covered with long white scattered pilosity (Fig. 9G, H), while eyes in *E. longicornis* are almost bare. Second and third antennal segment elongated, with almost the same width (Fig. 9A–C), similar as in *E. longicornis*, while in later one ventral margin of basoflagellomere is linear (Fig. 9F) and in *E. minotaurus* complex is slightly convex. White to grey pollinose maculae on tergites very narrow, linear, often absent on T4, especially for females, while this maculae in *E. longicornis* in particular, but also in other species of the group are well expressed and more lunulate. Females of the *E. minotaurus* complex, can be easily distinguished from the females of *E. crassus* by well-developed and wider pairs of maculae on T2–4 and conspicuously developed pollinosity behind posterior ocellus in *E. crassus*. The Table 3 shows the morphological differences between *E. minotaurus* complex and *E. longicornis*, which are clearly visible. The male genitalia of these two taxa are shown in Figure 2.

Distribution. Eastern Mediterranean (Greece, Montenegro).

General description. *Male*. *Head*. Eyes holoptic. Eyes contiguity about 6 ommatidia long. Eye with scattered long white pilosity, bare near the margins. Face, vertex and occiput black to bronze, moderately punctuated. Face with uneven white to bronze pollinosity, less or more expressed but usually with prominent silver longitudinal median stripe of pollinosity. Ocellar triangle isosceles, longer than wide (Fig. 9G). Face slightly convex, covered with white pile (Fig. 9A). Pile on vertex and occiput yellow, in ocellar triangle mixed with black. Scape and pedicel dark brown covered with yellow pile, ventrally long as the depth of pedicel. Pedicel elongated, long almost as the basoflagellomere (Fig. 9A–C). Basoflagellomere elongated, brown, from almost yellow to dark, covered with grey pollinosity. Sensory pit located ventrally near the distal margin of basoflagellomere. Arista reddish-brown.

Thorax. Scutum, scutellum and pleurae black to bronze, moderately punctuated. Mesonotum anteriorly with fine white pollinosity which extends in two pollinose vittae, reaching 2/3 of the length of scutum. Median vitta present only in anterior part. Pile on thorax yellow to white, short on scutum and scutellum and longer on pleurae.

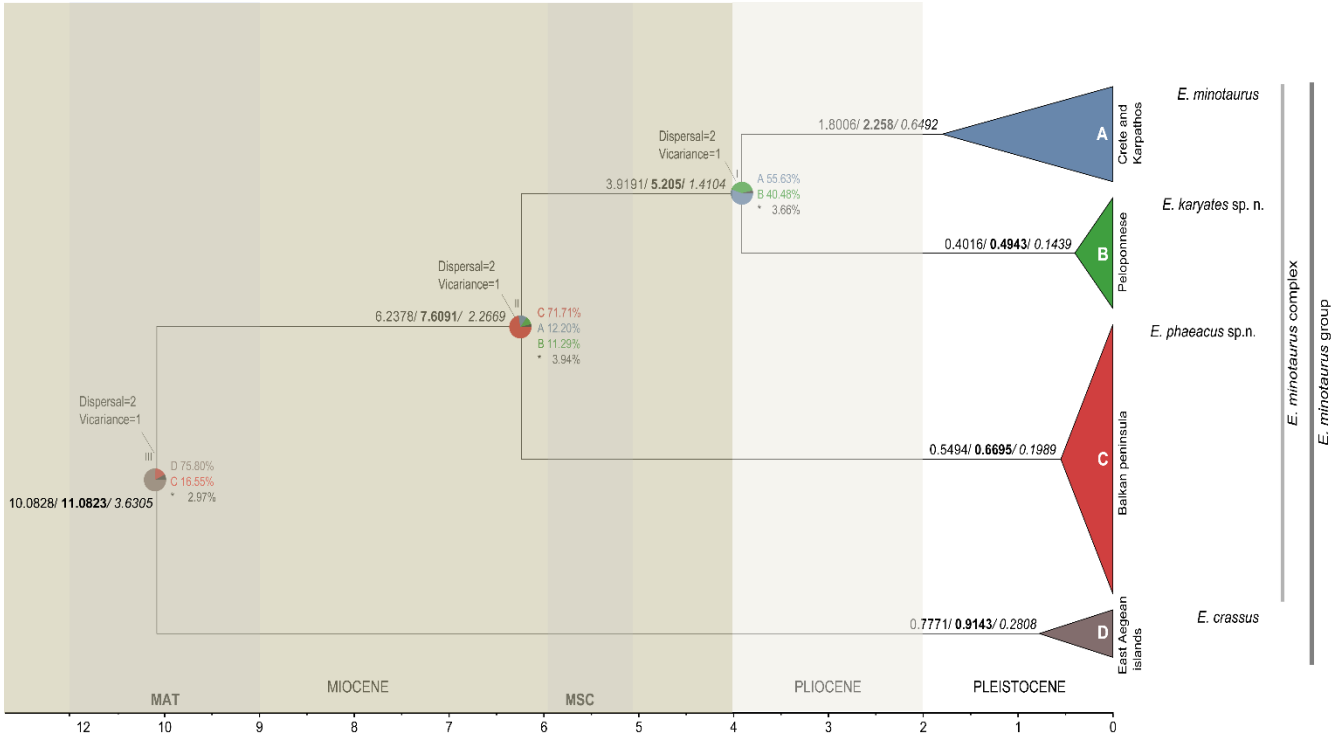

Fig. 5. Trees inferred with BEAST for the concatenated 3' and 5' fragment of COI gene fragment (COI subset) of the *E. minotaurus* group. Values on the left and above of the branches are mean ages as estimated by the uncorrelated lognormal clock based on (a) MAT, (b) MAT&MSC (bold), and (c) 2.3% mtDNA-rate (italics), in Mya (a/b/c). The four defined areas are presented with different colors, percentage values (on the right side of the nodes of the tree) and pie charts at nodes I, II and III; (A) Crete and Karpathos (blue), (B) Peloponnese (green), (C) Balkan Peninsula (red), (D) East Aegean Islands (grey), and (*) Unknown (black) (for interpretation of the references to color in this figure legend, the reader is asked to refer to the web version of this article).

Σχήμα 5. Το χρονόγραμμα προέκυψε από το πρόγραμμα BEAST (υπο-ομάδα δεδομένων COI), και παρουσιάζονται οι φυλογενετικές σχέσεις και οι εκτιμώμενοι χρόνοι απόσχισης των εξελικτικών γραμμών για την ομάδα ειδών *E. minotaurus*. Οι αριθμοί αριστερά και πάνω από τους κόμβους αντιστοιχούν σε χρόνους, υπολογιζόμενοι βάσει του χαλαρού μοριακού ρολογιού (μη συνδεδεμένη λογαριθμοκανονική κατανομή). Η βαθμονόμηση του μοριακού ρολογιού είναι ως εξής: (a) MAT, (b) MAT&MSC (έντονη γραμματοσειρά) και (c) 2.3% mtDNA-rate (πλάγια γραμματοσειρά), και δίνεται σε εκατ. χρόνια (a/b/c). Οι τέσσερις καθορισμένες περιοχές παρουσιάζονται με διαφορετικά χρώματα, ποσοστιαίες τιμές (στα δεξιά των κόμβων) και διαγράμματα πίτας στους κόμβους I, II και III: (A) Κρήτη και Κάρπαθος (μπλε), (B) Πελοπόννησος (πράσινο), (C) Βαλκανική Χερσόνησος (κόκκινο), (D) νησιά του Ανατολικού Αιγαίου (γκρι), και (*) Άγνωστο (μαύρο) (για την ερμηνεία των χρωματικών αναφορών του σχήματος αυτού, ο αναγνώστης παραπέμπτεται στην ηλεκτρονική έκδοση του άρθρου).

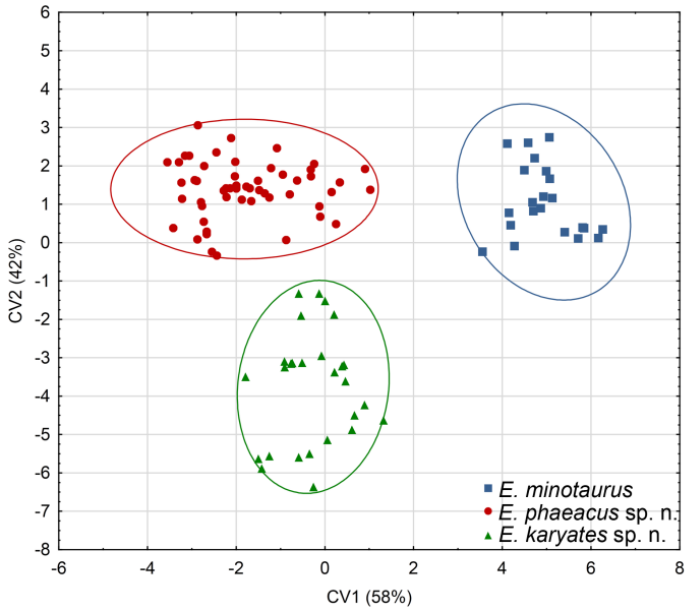

Fig. 6. Scatter plot of individual scores of CV1 and CV2 illustrating wing shape differences among species of the *Eumerus minotaurus* complex.

Σχήμα 6. Διάγραμμα διασποράς μεμονωμένων βαθμολογιών CV1 και CV2, το οποίο παρουσιάζει τις διαφορές στο σχήμα των πτερύγων μεταξύ των ειδών του συμπλέγματος *Eumerus minotaurus*.

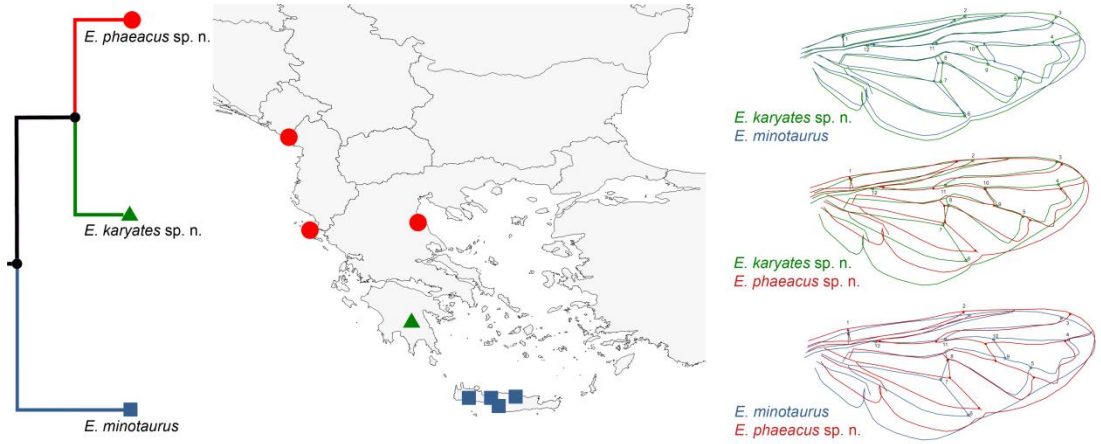

Fig. 7. Wing shape differences among species of the *Eumerus minotaurus* species complex. a) UPGMA geo-phenogram constructed using the squared Mahalanobis distances of wing shape. b) Superimposed outline drawings showing wing shape differences between analysed species. Differences between the species were exaggerated five-fold to make them more visible.

Σχήμα 7. Διαφορές στο σχήμα των πτερύγων μεταξύ των ειδών του συμπλέγματος *E. minotaurus*. a) το γεωμετρικό φαινόγραμμα (geo-phenogram) UPGMA κατασκευάστηκε χρησιμοποιώντας τις τετραγωνικές Mahalanobis διαστάσεις των πτερύγων. b) Επικαλυμμένα σχέδια περιγράμματος, τα οποία παρουσιάζουν τις διαφορές σχήματος των πτερύγων μεταξύ των υπό μελέτη ειδών. Οι διαφορές μεταξύ των ειδών έχουν μεγεθυνθεί πέντε φορές.

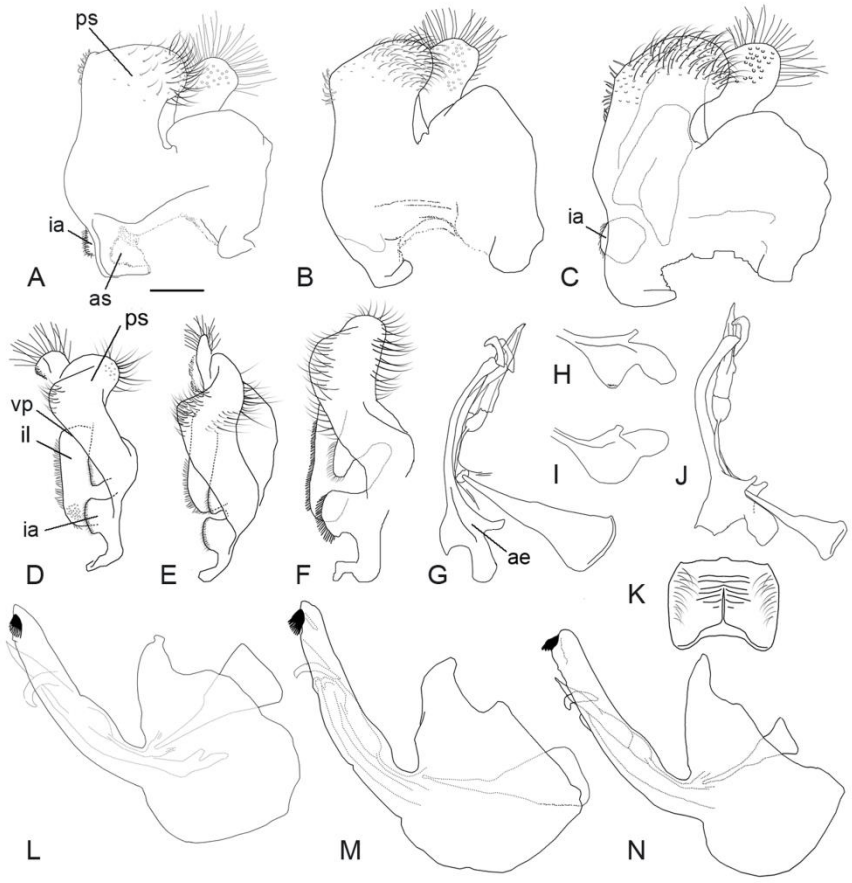

Fig. 8. Male genitalia. Epandrium, lateral view: A) *E. minotaurus* complex, B) *E. longicornis* Loew, 1855, C) *E. anatolicus* sp. n., ventral view: D) *E. minotaurus* complex, E) *E. longicornis*, F) *E. anatolicus* sp. n.; G) *E. minotaurus* Claussen and Lucas, 1988, aedeagus with accessory structures; distal part of aedeagal apodeme: H) *E. karyates* sp. n., I) *E. phaeacus* sp. n., J) *E. anatolicus* sp. n., aedeagus with accessory structures; K) *E. minotaurus* complex, males IV abdominal sternite; hypandrium, lateral view: L) *E. minotaurus* complex, M) *E. longicornis*, N) *E. anatolicus* sp. n. Scale 0.2 mm. ae – aedeagal apodeme, as – anterior lobe of surstylus, il – interior lobe of posterior lobe of surstylus, ia – inner lobe of anterior lobe of surstylus, ps – posterior lobe of surstylus, vp – ventral margin of posterior surstyle lobe.

Σχήμα 8. Γεννητικός οπλισμός αρρένων. Επάνδριο (τελευταίος νωτιαίος τεργίτης), Πλευρική όψη: Α) σύμπλεγμα *E. minotaurus*, Β) *E. longicornis* Loew, 1855, C) *E. anatolicus* sp. n., κοιλιακή όψη: D) σύμπλεγμα *E. minotaurus*, Ε) *E. longicornis*, F) *E. anatolicus* sp. n.· G) *E. minotaurus* Claussen και Lucas, 1988, αιδοιαγός και βοηθητικά εξαρτήματα · η ακραία περιοχή του αποδέματος του αιδοιαγού: Η) *E. karyates* sp. n., Ι) *E. phaeacus* sp. n., J) *E. anatolicus* sp. n., αιδοιαγός και βοηθητικά εξαρτήματα · Κ) σύμπλεγμα *E. minotaurus*, άρρεν, IV κοιλιακός στερνίτης· υπάνδριο (9ος κοιλιακός στερνίτης), Πλευρική όψη: L) σύμπλεγμα *E. minotaurus*, Μ) *E. longicornis*, Ν) *E. anatolicus* sp. n. Κλίμακα 0.2 mm. ae – απόδεμα του αιδοιαγού, as – πρόσθιος λοβός του στύλου, il – εσωτερικός λοβός του οπίσθιου λοβού του στύλου, ia – εσωτερικός λοβός του πρόσθιου λοβού του στύλου, ps – οπίσθιος λοβός του στύλου, vp – κοιλιακό περιθώριο του οπίσθιου στυλικού λοβού.

Pleurae black with bronze to golden sheen, covered in silvery-white pollinosity and long white pile. Scutellum roughly transversely striated. Legs black to brown with reddish connections between segments, covered with gold pollinosity and moderately long white pile (Fig. 9I). Metafemur moderately swollen, ventral pile yellow to white, long about half of the depth of the femur. Metatibia a little narrower than metafemur, slightly curved. Tarsi covered with dense, golden short pile ventrally. Wing with brown tinge, entirely covered with microtrichia.

Abdomen. Length: the width of abdomen = about 0.7. Tergites black, densely punctuated, covered in short white pilosity which turns into yellow in proximal half of T4. T1 with scarce white pollinosity laterally. T2–3 with pairs of silvery-white maculae of pollinosity, narrow, almost straight. Maculae on T4 barely visible, sometimes absent. Sternites light brown, covered with bronze pollinosity and moderately long white to yellow pile. S3 wide, on posterior margin with longer yellow to golden pile. Pregenital segment covered with golden pilosity.

Male genitalia. Posterior surstyle lobe large, covered with long scattered pile (Fig. 8A, D). IL covered with dense short pilosity (Fig. 8D). Hypandrium simple (Fig. 8L). Distal part of aedeagal apodeme with processes that differ in shape in different species of complex (Fig. 8G–I).

Female. Similar to the male with normal sexual dimorphism (Fig. 9B, H, J). Frons less or more longitudinally wrinkled, in narrower part wide approximately as one fourth of the width of the head in dorsal view or twice wider than the width of ocellar triangle. White pollinosity along eye margin less or more expressed. Pollinose maculae on T4 usually absent.

We have resolved three cryptic species within the *E. minotaurus* complex: *E. karyates* sp. n., *E. minotaurus* and *E. phaeacus* sp. n.

Eumerus minotaurus Claussen & Lucas, 1988

Material studied. Paratypes. One male, Greece: Crete, one male, Lasithi, Sissi, 08.iv.1983, leg. Claussen; Heraclion, 7.iv.1975, leg. Lucas, (NBC). Additional material. Greece: one female, Crete, Rethimnon, Bali, 06.v.2003, leg. Tkalcu; one female, Orne-Agia Galini, 25.iv.2014, leg. Vujić; 2 males, Fotinos, 26.v.2014, leg. Vujić; Chania, one male, Armeni, 25.iv.2014, leg. Vujić; one female, Imbors, 27.v.2014, leg. Vujić; one male, one female, Omalos plain, 28.v.2014, leg. Vujić; Karpathos, one male, Avlona, 02-04.v.2012, leg. Vavitsas.

Diagnosis. Differs from other species of *E. minotaurus* complex by shape of distal part of aedeagal apodeme (Fig. 8G), wing morphometric characters (distal ventral part of the wing, Fig. 7B) and molecular data (see accession numbers in Appendix). Basoflagellomere is usually pointed (Fig. 9A).

Distribution. Greece: Crete and Karpathos.

Description. Size: body length 10–11.5 mm; wing length 7–9 mm.

Male. Width of face: the width of head = 0.25 to 0.3. Width of the vertex: the width of the head = from 0.21 to 0.22. Length of contiguity of eyes: length of frons = from 0.47 to 0.62. Basoflagellomere usually conspicuously pointed (Fig. 3A). The width of pedicel: the width of basoflagellomere = about 0.8. The width of pedicel: the length of pedicel = about 0.6. Thorax. Length: the width of scutellum = 0.5.

Female. Width of the frons: width of the head = from 0.24–0.27. The width of pedicel: the width of basoflagellomere = about 0.94. The width of pedicel: the length of pedicel = from 0.5 to 0.8. Abdomen. The height: the width of T4 = 0.7. The height: the width of T3 = 0.46 to 0.49.

Eumerus karyates Chroni, Grković & Vujić sp. n.

Type material. Holotype. Male. Greece: Peloponnese, Karyes, 20.v.2016, legs. Vujić, Nedeljković, Ačanski, Likov, Miličić. Paratypes. Greece: Peloponnese, Karyes, three females, 20.v.2016; one male, 22.v.2016; two males, two females, 23.v.2016, legs. Vujić, Nedeljković, Ačanski, Likov, Miličić.

Diagnosis. Differs from other species of *E. minotaurus* complex by shape of distal part of aedeagal apodeme (Fig. 8H), wing morphometric characters (distal ventral part of the wing, Fig. 7B) and molecular data (see accession numbers in Appendix). Basoflagellomere is slightly pointed, but less pronounced than in *E. minotaurus* (Fig. 9C).

Distribution. Greece: Peloponnese.

Description. Size: body length 10–11 mm; wing length 7–8 mm.

Male. Head. Width of face: the width of head = 0.27 to 0.32. Width of the vertex: the width of the head = from 0.19 to 0.21. Length of contiguity of eyes: length of frons = from 0.29 to 0.42. Basoflagellomere usually slightly pointed (Fig. 9C). The width of pedicel: the width of basoflagellomere = from 0.8 to 0.9. The width of pedicel: the length of pedicel = about 0.7. Thorax. Length: the width of scutellum = 0.6.

Female. Head. Width of the frons: width of the head = from 0.24 to 0.27. The width of pedicel: the width of basoflagellomere = from 0.8 to 1. The width of pedicel: the length of pedicel = about 0.7. Abdomen. The height: the width of T4 = 0.7. The height: the width of T3 = 0.46.

Etymology. Karyatides mainly known as the model figures sculptured as columns of the Erechtheion on the Acropolis of Athens were the priestesses of Artemis at Karyae (today's Karyes) in ancient Laconia, Peloponnese. As all our Peloponnesian specimens derive from Karyes, we considered the male adjective "karyates" to be an adequate name for the species.

Eumerus phaeacus Chroni, Grković & Vujić sp. n.

Type material. Holotype. Male. Greece: Corfu, Ano Korakiana, 24.v.2016, leg. Vujić, Nedeljković, Ačanski, Likov, Miličić. Paratypes. Montenegro, Rumija, one male, 42.11201 Lat., 19.21739 Long., 02.v.2011, leg. Vujić; Greece: Mt Olympos, one male, one female, Ag. Paraskevi, 17.v.2011, leg. Vujić; Corfu, Ano Korakiana, 14 males, 24.v.2016, leg. Vujić, Nedeljković, Ačanski, Likov, Miličić; four males, one female, Liapades, 24.v.2016, leg. Vujić, Nedeljković, Ačanski, Likov, Miličić; one male, Strinilas, 24.v.2016, leg. Vujić, Nedeljković, Ačanski, Likov, Miličić.

Diagnosis. Differs from other species of *E. minotaurus* complex by shape of distal part of aedeagal apodeme (Fig. 8I), wing morphometric characters (distal ventral part of the wing, Fig. 7B) and molecular data (see accession numbers in Appendix). Basoflagellomere is rounded, which is quite stable character in this species (Fig. 9B).

Distribution. Montenegro: Mt Rumija, Greece: Corfu, Mt Olympos.

Description. Size: body length 10–11 mm; wing length 7–8 mm.

Male. Width of face: the width of head = 0.28–0.32. Width of the vertex: the width of the head = from 0.19–0.23. Length of contiguity of eyes: length of frons = from 0.28–0.4. Basoflagellomere almost always rounded (Fig. 9B). The width of pedicel: the width of basoflagellomere = about 0.8. The width of pedicel: the length of pedicel = about 0.8. Thorax. Length: the width of scutellum = 0.5–0.6.

Female. Width of the frons: width of the head = 0.27. The width of pedicel: the width of basoflagellomere = 0.8. The width of pedicel: the length of pedicel = 0.6. Abdomen. The height: the width of T4 = 0.7. The height: the width of T3 = 0.45.

Etymology. The Phaeacians (Φαίακες, in Gr.), the ancient inhabitants of Corfu Island, were famous for their nautical skills, and renowned for their ability to travel

and reach fast any place. We selected this name as to the origin of the majority of the insect specimens (Corfu) and as to their wide geographic range.

Taxonomy notes

Doczkal (1996) denoted the morphological affinity between *E. minotaurus* and *E. longicornis* and their dissimilarity as to *E. niehuisi*, with the latter to be closely related and morphologically similar to *E. crassus*. The first two species can be separated from the latter two based on a slightly shorter body pile, the pruinose supra-alar area without transverse striae and the scutum without black pile. *E. crassus* and *E. niehuisi* have pedicel about 1.5 as long as deep (Fig. 9E), while in *E. longicornis* (Fig. 9F) and *E. minotaurus* complex (Fig. 9A–C) pedicel is about two times as long as deep.

New species for Eumerus minotaurus group

Eumerus anatolicus Grković, Vujić & Radenković sp. n.

Type material. Holotype. Male. Turkey: Muğla, University campus (720 m), iv.2011. leg. Kavak. Paratypes. Muğla, University campus (720 m), one female, 17–22.v.2011. legs. Barták and Kubík, 3 males, iv.2011, 2 males, 26.v.-26.vi.2015 leg. Kavak.

Diagnosis. Species is similar to *E. minotaurus* complex. It can be distinguished by patches of grey to white pollinosity on vertical triangle anteriorly and near the posterior ocelli as well as distinctive pollinose maculae on T2–4. In *E. minotaurus* complex, these markings are linear on T3, while in *E. anatolicus* sp. n. they are more wide and lunulate. This character is also present in females. Additionally, vertex in new species is moderately punctuated and shiny, while in *E. minotaurus* complex, is roughly punctuated and matte. Also in females of *E. minotaurus* complex, frons is wrinkled, covered in white pollinosity along eye margin which is interrupted in front of ocellar triangle, while in *E. anatolicus* sp. n., frons is shinier with continuous line of pollinosity along eye margin, up to wide pollinose patch behind posterior ocelli. Regarding male genitalia, they are very similar with those in *E. minotaurus* complex but with denser pilosity of posterior surstyle lobe (Fig. 8C). Pilosity extends along almost entire length of ventral margin of surstylus (Fig. 8F), while in species of *E. minotaurus* complex, is restricted in upper part, sometimes with only few pile beneath (Fig. 8D). Anterior surstyle lobe is with inner lobe more oval in lateral view than in *E. minotaurus* complex, covered with fine short pilosity (Fig. 8C).

Distribution. Turkey: Muğla.

Description. Size: body length 10–12 mm; wing length 7–8.5 mm.

Male. Head. Width of face: the width of head = 0.30 to 0.33. Width of the vertex: the width of the head = from 0.22 to 0.24. Length of contiguity of eyes: length of frons = from 0.40 to 0.47. Eyes contiguity 6–8 ommatidia long. Eyes covered in long dense white pilosity, bare near posterior margins. Face, frons, vertex and occiput black with bronze sheen. Face and frons covered in very dense silvery-white pollinosity and white pile. Frons laterally often with few long black pile mixed with black. Face convex. Vertex and occiput moderately punctuated. Pile on vertex and occiput yellow mixed with black. Ocelli arranged in isosceles triangle, longer than wide. Scape and pedicel brown, covered in dense yellow pile, ventrally sometimes longer than the depth of the pedicel. Pedicel elongated, long approximately as basoflagellomere, in some specimens even longer (Fig. 9d). The width of pedicel: the width of basoflagellomere = about 0.9. The width of pedicel: the length of pedicel = about 0.7. Basoflagellomere is usually pointed but in some specimens it is oval, with ventral margin quite convex. Thorax. Scutum, scutellum and pleurae black to bronze, densely punctuated. Pleurae, scutum anteriorly and supra-alar area with fine white pollinosity. Mesonotum with two longitudinal vittae of pollinosity extending up to 4/5 of the length. Narrow median vitta present, long almost as lateral vittae. Pile on thorax white to yellow. Scutellum roughly transversely striated. Length: the width of scutellum = 0.5–0.6. Legs black, tips of femora at both sides brownish. Base of tibiae brownish. Metafemur slightly swollen, ventral pile long approximately as half of the depth of the femur. Metatibia curved in the middle. Wings with dark tinge, entirely microtrichose. Abdomen. Tergites black, densely punctuated, covered in short white pilosity which turns into yellow to gold in posterior half of T4. T2–4 with clearly visible, wide, lunulate maculae of pollinosity. Maculae on T4 narrower. Sternites brown with long white to yellow pile. S4 broad, with yellowish pile posterolaterally. Genitalia. Posterior surstyle lobe large, covered in long dense pilosity evenly distributed (Fig. 8C). IL covered with dense short pile (Fig. 8F). Ventral margin of surstylus densely pilose, almost in entire length.

Female. Similar to the male with normal sexual dimorphism. Head. Width of the frons: width of the head = 0.3. Frons shiny, moderately punctuated with continuous line of pollinosity along eye margin, up to wide pollinose patch behind posterior ocelli.

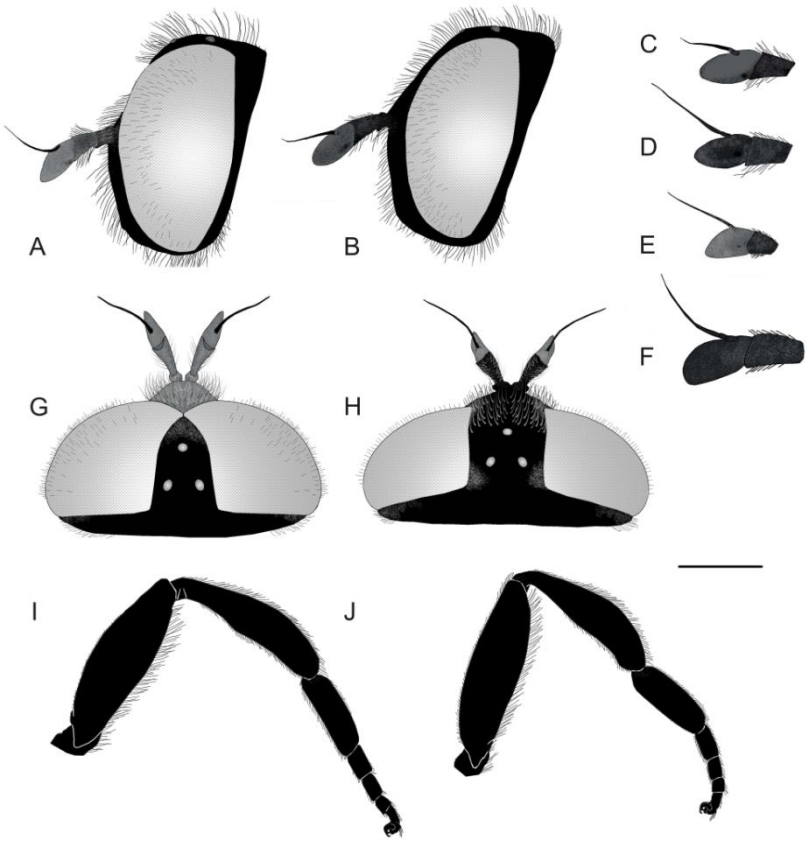

Fig. 9. *E. minotaurus* group, head, lateral view: A) *E. minotaurus* Claussen & Lucas, 1988, male, B) *E. phaeacus* sp. n., female; antenna: C) *E. karyates* sp. n., D) *E. anatolicus* sp. n., E) *E. crassus* Grković, Vujić & Radenković, 2015, F) *E. longicornis* Loew, 1855; dorsal view: G) *E. minotaurus*, male, H) *E. phaeacus* sp. n., female. *E. minotaurus* complex, leg: I) male, J) female. Scale: 1mm.

Σχήμα 9. *E. minotaurus* group, κεφαλή, πλευρική όψη: A) *E. minotaurus* Claussen & Lucas, 1988, άρρεν, B) *E. phaeacus* sp. n., θήλυ· κεραίες: C) *E. karyates* sp. n., D) *E. anatolicus* sp. n., E) *E. crassus* Grković, Vujić & Radenković, 2015, F) *E. longicornis* Loew, 1855· Ραχιαία όψη: G) *E. minotaurus*, άρρεν, H) *E. phaeacus* sp. n., θήλυ. Σύμπλεγμα *E. minotaurus*, πόδι: I) άρρεν, J) θήλυ. Κλίμακα: 1mm.

Discussion

Despite *Eumerus* high species diversity, both described and continuously piling on through new species introduction, and its critical role in ecosystems, there are still taxonomic implications to confront. Studies (Doczkal 1996; Ricarte *et al*., 2012; Grković *et al*., 2015, 2017; Markov *et al*., 2016) have disclosed new species within the genus that should further be considered in phylogenetic and biogeographic studies. To date, only one phylogenetic study (Chroni *et al.*, 2017) exists, and was the first to support the configuration of two major monophyletic lineages and seven ‘molecular’ groups within *Eumerus* based on DNA sequences, with *E. minotaurus* group among them.

The present study is the first to provide conclusions about the *E. minotaurus* group revealing one new species and unveiling *E. minotaurus* cryptic species complex within the genus by employing an integrative framework (Figs 10, 11); evidences for the new species are based on morphological data and cryptic species complex are well supported by mtDNA sequences, discrete features in morphology (antennas, male genitalia), wing morphometry and biogeographic reconstructions. We have also employed a nuclear marker (never used before in *Eumerus*) to infer the phylogenetic relationships between the species of *E. minotaurus* group. Below, we discuss all the above, and further conclude with contingent biogeographic patterns and speciation processes within the *E. minotaurus* group in relation to the palaeogeography of the broad region of the Aegean.

Taxonomical and molecular implications

The first published study that grouped and indicated the affinity of *Eumerus* species with elongated pedicel (*E. minotaurus* group) was of Doczkal (1996) when he described *E. niehuisi*. Taxonomical and phylogenetic analyses of *E. crassus*, *E. anatolicus* sp. n., *E. minotaurus* complex and *E. longicornis* have showed their separate position from other *Eumerus* species (Doczkal, 1996; Chroni *et al.*, 2017). We proffer all the aforementioned species to belong to the same taxon group (*E. minotaurus* group) due to the elongated pedicel and the shape of male genitalia, their major common feature differentiating them for the remaining *Eumerus* species and groups. Our suggestion is based on the finding by Hasson *et al.* (2009) and House *et al.* (2013) that natural and sexual selection and their interaction may promote insect genital evolution.

Our morphology-based results were further tested on the basis of mtDNA and nDNA markers (where DNA sequences were available). The competence of a molecular marker is rendered on the ability to infer a high resolution of phylogenetic relationships of the under study organism(s), an ability related to the mutation rate of the coding region. MtDNA phylogenetic reconstructions (tree-based species delimitation) and molecular putative species limits analyses (non-tree-based) reaffirmed the morphology assignments (species prediction), clustered all these species within the same phylogenetic group with quite high bootstrap and probability values, and supported the configuration of the *E. minotaurus* group. In addition, the employed mtDNA sequences clearly granted three lineages representing three

different species within *E. minotaurus*, proven its suitability to resolve cryptic species. The revealing of the three mitochondrial lineages led us to further examine our specimens and identify the presence of subtle differences on the male genitalia which we considered crucial as to the differentiation of the cryptic species (see above). Tree topologies within the *E. minotaurus* group were consistent; in all cases, *E. crassus* was clustered separately from *E. minotaurus* complex, and within the complex, *E. karyates* sp. n. and *E. minotaurus* were clustered together, apart from *E. phaeacus* sp. n.

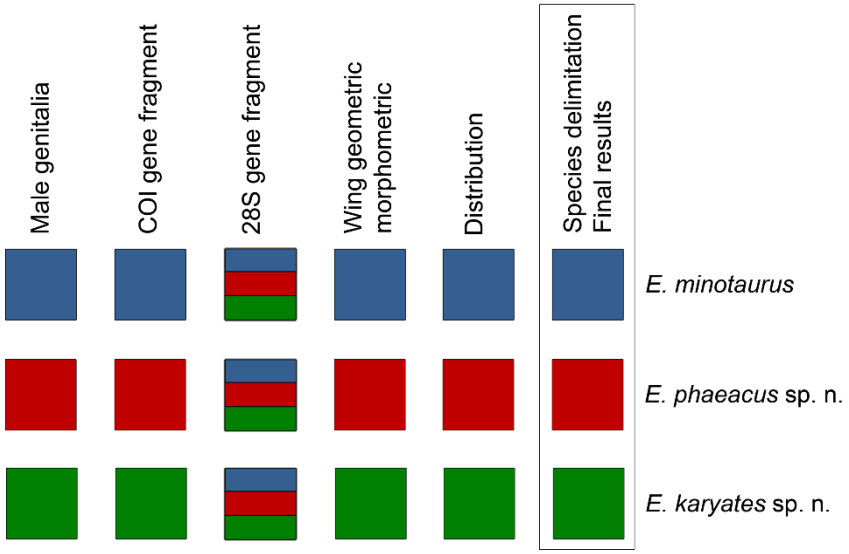

Fig. 10. Summary of the results of the integrative species delimitation within the *Eumerus minotaurus* complex: morphological characters (male genitalia), molecular markers (COI and 28S gene fragments), wing geometric morphometrics and geographical distribution. Each species is presented by different colour; *E. karyates* sp. n. (green), *E. minotaurus* (blue) and *E. phaeacus* sp. n. (red). Solid colour boxes indicate successful species delimitation by particular approach. Multicolor boxes depict clusters formed by multiple species.

Σχήμα 10. Σύνοψη των αποτελεσμάτων της οριοθέτησης ειδών του συμπλέγματος *E. minotaurus* μέσω της ενοποιητικής ταξινομικής: μορφολογικοί χαρακτήρες (γεννητικός οπλισμός άρρενος), μοριακοί δείκτες (θραύσματα των COI και 28S γονιδίων), γεωμετρική μορφομετρία πτερύγων, και γεωγραφική κατανομή. Κάθε είδος αποδίδεται με διαφορετικό χρώμα: *E. karyates* sp. n. (πράσινο), *E. minotaurus* (μπλε) και *E. phaeacus* sp. n. (κόκκινο). Τετράγωνα με συμπαγή χρώματα υποδηλώνουν επιτυχή οριοθέτηση είδους από την συγκεκριμένη μέθοδο, ενώ τα πολύχρωμα εικονίζουν ομάδες πολλαπλών ειδών.

A combination of mitochondrial and nuclear gene fragments is often preferred to discriminate evolutionary lineages, therefore we intended to merge a nuclear marker into our phylogenetic analyses. The 28S nuclear marker has shown genetic divergence

in the hoverflies (Mengual *et al*., 2008), and not only (e.g. Olsen & Woese 1993; Awasthi *et al*., 2016). In our study, the 28S marker resulted in low tree resolution and lineages' admixture. The amplification in most of the *Eumerus* species was not successful, and for those it was successful, the produced topology was not very distinct. We detected a partial (six out of eight sequences) clustering in one species of the *E. minotaurus* complex (*E. karyates* sp. n.) in MP tree, denoting a recent speciation event, most likely not complete yet. Regarding the rest of the species of the *E. minotaurus* complex, 28S marker proved not to be informative as species diagnosis failed. For the *E. minotaurus* group (or any other *Eumerus* species apart of the *E. minotaurus* complex), we had only one 28S sequence (*E. crassus*) which was separated from the *E. minotaurus* complex, but the limitation of the number of sequences did not allow us to further conclude of the significant utility of the 28S marker in species diagnosis within *Eumerus*. We speculate that the differences in the lineages' clustering between the two molecular markers are due to the faster evolutionary (mutation) rate of the employed mitochondrial gene fragment comparing to the nuclear one.

Our molecular and morphological inferences were also supported by high significant morphological wing differentiation for the species within *E. minotaurus* complex. Even though species assignment for the wing shape estimations was established based on phylogenetic inference, we consider wing shape heritability as a part of an integrative approach, and hence a significant and additive contribution to diagnosis of the cryptic species complex. Previous studies on hoverflies have shown that wing shape is a reliable predictor of interspecific discrimination. So far, wing geometric morphometry was mainly carried out on the genus of *Merodon* (Milankov *et al.*, 2009; Francuski *et al.*, 2009, 2011; Ačanski *et al.*, 2016; Šašić *et al.*, 2016), but there were also examples of successful implementation of this method in other hoverfly genera, such as *Cheilosia* (Ludoški *et al.*, 2008) and *Chrysotoxum* (Nedeljković *et al.*, 2013; 2015), as well as the hoverfly tribe Pipizini (Vujić *et al.*, 2013). This is the first study that includes wing shape analyses on the genus *Eumerus*. The most divergent wing shape was detected between *E. karyates* sp. n. and *E. minotaurus*, while the most similar wing shape was between *E. karyates* sp. n. and *E. phaeacus* sp. n. The most obvious wing shape differences occur in central and apical parts of the wing affecting the length and width of the wing. Documented wing shape disparities are not uncommon among hoverfly species (Ačanski *et al.*, 2016; Šašić *et*

al., 2016; Ačanski, 2017) and we can assume that they influence flight ability and male species specific courtship song as shown in some insect species (Cowling and Burnet, 1981; Stubbs and Falk, 1983; Sacchi and Hardersen, 2012; Menezes *et al.*, 2013; Outomuro *et al.*, 2013).

The results from the Mantel test demonstrated that wing shape was not influenced by current environmental factors, which is not surprising considering the high heritability of wing shape (Moraes *et al.*, 2004; Mezey and Houle, 2005; Yeaman *et al.*, 2010). Recently, wing shape conservatism in relation to environmental factors, as well as to geographic proximity, were established within the genus *Merodon* (Šašić *et al.*, 2016; Ačanski, 2017). The lack of correlation between measured phenetic, genetic and geographic distances (in both simple and partial Mantel tests) implies that other factors, as e.g. genetic drift in fragmented ancestral populations, could be liable for wing shape differences among the cryptic species.

Mitochondrial dating, biogeographic history and divergence time estimates

An important issue for the mitochondrial phylogeography of hoverflies (viz *Eumerus*) is the absence of fossil records and/or of an accurate mitochondrial substitution rate per gene fragment that could be treated to calibrate the molecular clock. Here we essayed three different approaches, based on the two major geological events occurred in the Aegean Archipelago (MAT and MSC) and the standard mitochondrial substitution rate existing in literature for arthropods (mtDNA-rate, Brower, 1994). The mtDNA-rate is not always feasible for all insect groups, has been proven to produce unreliable results, and hence, potential pitfalls should be taken into account (Papadopoulou *et al.*, 2010). Indeed, in *Eumerus* case, the assessed values from the mtDNA-rate analysis were rather low and not consistent with any major geological event of the Aegean region that could explain the speciation within the *E. minotaurus* group, confirming its reputation to give 'unrealistic ages'. On the other hand, the MAT and MAT&MSC time estimations were more close, with the latter approach to concur a bit more with the biogeographic events in the region. We posit that the MAT&MSC divergence times (i.e. the two calibration points analysis) might reflect better the occurred diversification times and events. The estimated pairwise substitution rates from the latter two approaches are not negligible of discussion; low COI pairwise substitution rates have been found in other insects as well, in e.g. ants (1.5%, Quek *et al.*, 2004) and *Drosophila* species (1.54%, Nunes *et al.*, 2010),

supporting the conclusion that we should be more cautious while calibrating the molecular clock under the 2.3% rate.

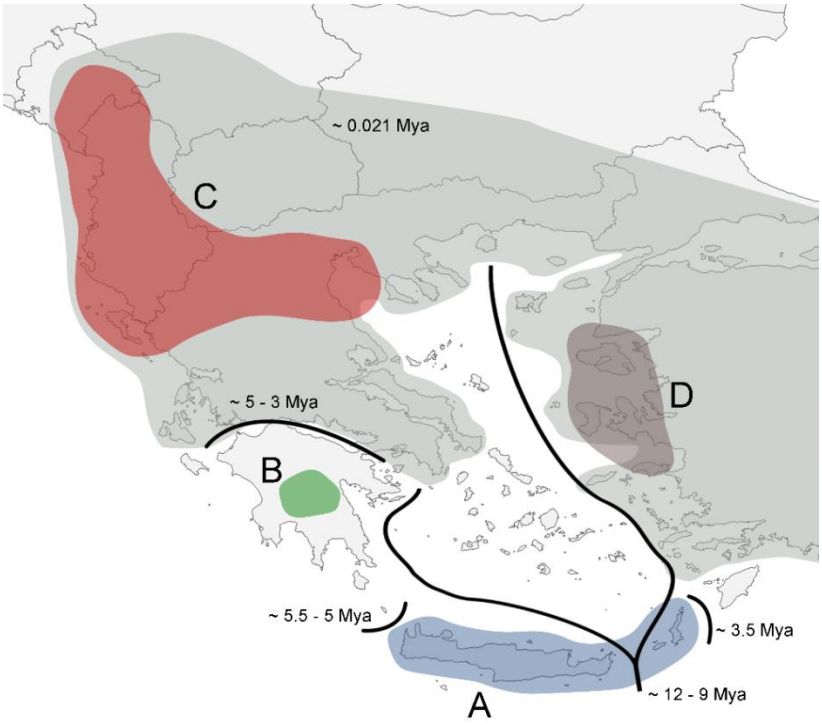

Fig. 11. Mitochondrial phylogeographic pattern of the *E. minotaurus* taxon group. The specimens were grouped corresponding to each species/ geographical cluster: *E. crassus*/East Aegean Islands, D; *E. karyates* sp. n./Peloponnese, B; *E. minotaurus*/Crete and Karpathos, A; and *E. phaeacus* sp. n./Balkan peninsula, C. The major geological events occurred in the Aegean Archipelago, that led on the speciation within the group, are shown, the formation of MAT (12–9 Mya) and separations of Crete from Peloponnese (5.5–5 Mya), Peloponnese from the Greek mainland (5–3 Mya) and Karpathos from Crete (3.5 Mya). Until the end of Pleistocene (0.021 Mya), there are evidences that the Greek mainland, Anatolia and the East Aegean Islands were still consolidated (for interpretation of the references to color in this figure legend, the reader is referred to the web version of this article).

Σχήμα 11. Μιτοχονδριακό φυλογεωγραφικό πρότυπο της ομάδας ειδών *E. minotaurus*. Η ομαδοποιήση των δειγμάτων αντισοιχεί σε κάθε είδος/ γεωγραφική ομάδα: *E. crassus*/νησιά του Ανατολικού Αιγαίου, D· *E. karyates* sp. n./Πελοπόννησος, B· *E. minotaurus*/Κρήτη και Κάρπαθος, A· και *E. phaeacus* sp. n./Βαλκανική Χερσόνησος, C. Παρουσιάζονται τα σημαντικότερα γεωλογικά γεγονότα που συνέβησαν στο Αιγαίο, τα οποία οδήγησαν στον σχηματισμό της MAT (12–9 εκατ. χρόνια) και στους διαχωρισμούς Κρήτη/Πελοπόννησος (5.5–5 εκατ. χρόνια), Πελοπόννησος/Ελληνική Χερσόνησος (5–3 εκατ. χρόνια) και Κάρπαθος/ Κρήτη (3.5 εκατ. χρόνια). Υπάρχουν ενδείξεις ότι η Ελληνικη Χερσόνησος, η Ανατολία και τα νησιά του Ανατολικού Αιγαίου παρέμειναν ενωμένα μέχρι το τέλος του Πλειστόκαινου (0.021 εκατ. χρόνια) (για την ερμηνεία των χρωματικών αναφορών του σχήματος αυτού, ο αναγνώστης παραπέμπτεται στην ηλεκτρονική έκδοση του άρθρου).

Heled and Drummond (2010) have pointed out the necessity of implementing multiple samples per species when inferring speciation times and that 'two or more sequences per species are necessary for a complete estimation of speciation times, given enough loci'. We have employed from 4 to 18 sequences per species, which originated from different localities (except for *E. karyates* sp. n. which has been recorded only in Karyes of Peloponnese, and thus specimens from one locality were used). Since the tree topology obtained from the BEAST was congruent to the ones obtained from the mitochondrial phylogenetic inferences (COI dataset) and the obtained molecular divergence time estimates were close to the geological events occurred in the Aegean region, we claim that the estimations about speciation events of the species of the *E. minotaurus* group most likely reflect to reality. Certainly, more sequences/ taxa or more loci would further assist to elucidate the phylogeography of the *E. minotaurus* group, but unfortunately, insect sampling or gene amplification always remain a challenge.

The phylogenetic assessment of the four species within the *E. minotaurus* group is contingent with their geographic distribution, with each species to occur in specific region and belong to a geographical. As the initial diversification event occurred at 11.08 Mya (hereinafter all values are based on the MAT&MSC analysis), we speculate that there was a single species during the Miocene in Ägäis, which served as the first ancestor for the rest of the species of the *E. minotaurus* group as known today. When the MAT occurred, eastern populations were splitted from the western, and progressively one population dominated the eastern part of the Aegean, leading to the speciation of *E. crassus*. Historical biogeographic reconstruction analyses suggested an east-to-west (from the East Aegean towards the Greek mainland and the Balkan Peninsula) species diversification of *E. crassus*, with dispersal and/or vicariant events to be accounted for, confirming the MAT scenario. In the biogeographic context, the Greek mainland was isolated from Anatolia and the East Aegean Islands at 0.18-0.14 Mya (and were most likely consolidated until the end of Pleistocene at 0.021 Mya), whereas some of the Aegean Islands started to acquire their current configuration ca. 0.03-0.018 Mya and were finally shaped at 0.008 Mya (for a thorough review see Kougioumoutzis *et al.*, 2017). We have estimated the speciation of *E. crassus* at 0.91 Mya (mid Pleiostocene), reflecting that period of momentous geological and climatic occurrences in the Aegean accountable for species speciation and/or extinction.

Another diversification event was detected at 7.6 Mya by our analyses, which led to the separation of the north-western population (Balkan Peninsula) from the south-western one (Peloponnese/ Crete and Karpathos); our biogeographic analyses confirmed that 'north-to-south' division. Distribution patterns in the Aegean Islands are far more complex than those of the Ionian because of their larger numbers and greater topographic, palaeogeographic, and environmental complexity (Gillespie and Clague, 2009; Kougioumoutzis *et al.*, 2017). On the other hand, 'the fauna and flora in the Ionian Islands are expected to be more "harmonic", without profound gaps in their taxonomic composition' (Gillespie and Clague, 2009); there are found to contain few endemic taxa and the existing taxa are more similar to those of the adjacent mainland. Indeed, *E. phaeacus* sp. n. was identified as an insular (Corfu: Ionian Archipelago, Greece) and montane species (Balkan Peninsula: Mt Olympus, Greece; and Mt Rumija, Montenegro). Similar speciation forces that acted on *E. crassus* must have also influenced speciation of *E. phaeacus* sp. n. (which was estimated at 0.67 Mya).

The second major event that acted on the Aegean was of the Messinian Salinity Crisis, during which Crete was isolated from the Greek mainland, but maintained the land connection to the Peloponnese until 5 Mya. During the Pliocene and because of the intense tectonic phenomena, the Aegean region was fragmented and changed considerably. Crete was permanently isolated from the Peloponnese and other inland areas, and a wide sea-barrier (aka the Corinthian channel) separated Peloponnese from the mainland Greece (5–3 Mya, Dermitzakis, 1990). Later on, during the Pleistocene, climatic oscillations and sea-level fluctuations led to repeated connection/ disconnection cycles (8 cycles of glaciation events; for a review see Perissoratis and Conispoliatis, 2003), altered the size and isolation of the areas (e.g. of the islands) by forming temporal land bridges/corridors, and connecting the insular with the mainland during which animals could disperse. These sea-level fluctuations continued until late Pleistocene (0.021 Mya) and Holocene times (Dermitzakis, 1990), and induced species diversification and distribution (Perissoratis and Conispoliatis, 2003). It was then that a diversification event occurred (5.2 Mya) within the southern populations of the *E. minotaurus* complex which gave rise to two species: *E. karyates* sp. n. (Peloponnese cluster) and *E. minotaurus* (Crete and Karpathos cluster), their speciation to be dated at 0.49 Mya and 2.26 Mya, respectively. We speculate that the gene flow between the Peloponnese and Crete and Karpathos populations was

impeded at the end of the MSC, when the Mediterranean Sea was refilled, and the speciation was favoured when the sea level started to stabilize. It is worth mentioning that the disconnection of Crete and Karpathos Islands (5-2 Mya) did not seem to affect the distribution of *E. minotaurus* (the same species was recorded in both islands) and no further speciation has taken place.

Based on other phylogeographic studies carried out in the Aegean in order to explore the driving forces of animal speciation and biogeographic patterns, Poulakakis (2014) highlighted the importance of MAT for the species distribution in the area and categorized the species distribution based on the MAT. According to their classification, the species belonging to the *E. minotaurus* group can be characterized as post-MAT colonizers, i.e. 'species that reached the region after the creation of the MAT, and whose diversification is due to the MSC, intense tectonism during the Pliocene and the climatic oscillations in these periods' (Poulakakis *et al.*, 2014). Molecular clock is not applied very often in insects groups in the Aegean, and when it does, it concerns mostly beetles (Papadopoulou *et al.*, 2009; 2010) or crickets (Allegrucci *et al.*, 2009; 2011) or termites (Luchetti *et al.*, 2005; 2007) or sand fly (Kasap *et al.*, 2015). Here, we present for the first time phylogeographic and mitochondrial dating inferences about the hoverfly genus *Eumerus* in the Aegean, firmly supported by integrative taxonomic data, which may foster similar studies for other hoverflies genera in relation to the palaeogeographic evolution of the Aegean.

Acknowledgments

The authors would like to thank the anonymous reviewers for their valuable comments and suggestions to improve the quality of the paper. We thank John O'Brien for proof reading and making constructive suggestions to the text.

Financial support for this research was provided by the (a) Serbian Ministry of Education, Science and Technological Development (Projects OI173002 and III43002), the Provincial Secretariat for Science and Technological Development (Project 'Genetic resources of agro-ecosystems in Vojvodina and sustainable agriculture') and (b) the European Union (European Social Fund – ESF) and Greek national funds through the Operational Program 'Education and Lifelong Learning' of the National Strategic Reference Framework (NSRF) – Research Funding Program: THALES. Investing in knowledge society through the European Social Fund. We also acknowledge the Program «Grants IKY» of the State Scholarships Foundation of Greece, in the frame of the OP «Education and Lifelong Learning» of the European Social Fund (ESF) – NSRF, 2007–2013 (contract WP2-SHORT TERMS-19348), as a partial financial support of the PhD thesis of AC.

References

Ačanski J, Vujić A, Djan M, Obreht Vidaković D, Ståhls G, Radenković S. 2016. Defining species boundaries in the *Merodon avidus* complex (Diptera, Syrphidae) using integrative taxonomy, with a description of a new species. *European Journal of Taxonomy* 237: 1-25.

Ačanski J. 2017. Taxonomy and distribution of the genus *Merodon* Meigen (Diptera: Syrphidae) in Palearctic. PhD thesis (in Serbian), University of Novi Sad, Novi Sad, pp 209.

Akin C, Can Bilgin C, Beerli P, Westaway R, Ohst T, Litvinchuk SN, Uzzell T, Bilgin M, Hotz H, Guex GD, Plötner J. 2010. Phylogeographic patterns of genetic diversity in eastern Mediterranean water frogs were determined by geological processes and climate change in the Late Cenozoic. *Journal of Biogeography* 37: 2111-2124.

Allegrucci G, Rampini M, Gratton P, Todisco V, Sbordoni V (2009) Testing phylogenetic hypotheses for reconstructing the evolutionary history of *Dolichopoda* cave crickets in the eastern Mediterranean. *Journal of Biogeography* 36: 1785-1797.

Allegrucci G, Trucchi E, Sbordoni V. 2011. Tempo and mode of species diversification in *Dolichopoda* cave crickets (Orthoptera, Rhaphidophoridae). *Molecular Phylogenetics and Evolution* 60: 108-121.

Arnqvist G, Mårtensson T. 1998. Measurement error in geometric morphometrics: empirical strategies to assess and reduce its impact on measures of shape. *Acta Zoologica Academiae Scientiarum Hungaricae* 44: 73-96.

Arzone A. 1973. *Tragopon pratensis* L., ospite naturale di *Eumerus tricolor* Meigen (Dipt. Syrphidae). *Tipografia Vincenzo Bona, Torino* 8:55-66.

Arzone A. 1971. Reperti biologici su *Eumerus tricolor* Meigen, nocivo alle coltivazioni di *Tragopogon porrifolius* L. in Piemonte (Dipt.Syrphidae). Tipografia Vincenzo Bona, Torino 7(1): 17-52.

Ayres DL, Darling A, Zwickl DJ, Beerli P, Holder MT, Lewis PO, Huelsenbeck JP, Ronquist F, Swofford DL, Cummings MP, Rambaut A, Suchard MA. 2012. BEAGLE: an application programming interface and high-performance computing library for statistical phylogenetics. *Systematic Biology* 61: 170-173.

Awasthi, M, Kashyap, A & Serajuddin, M. 2016. Molecular Phylogeny of Four Gouramis Based on Divergent Domain D11 of 28S rRNA Gene. *Advances in Biological Research* 10(6): 351-353. 10.5829/idosi.abr.2016.351.353.

Belshaw R, Fitton M, Herniou E, Gimeno C & Quicke DLJ. 1998. A phylogenetic reconstruction of the Ichneumonoidea (Hymenoptera) based on the D2 variable region of 28s ribosomal RNA. *Systematic Entomology* 23: 109-123.

Bickford D, Lohman DJ, Navjot SS, Ng PKL, Meier R, Winker K, Ingram KK, Das I. 2007. Cryptic species as a window on diversity and conservation. *Trends in Ecology and Evolution* 22: 148-155.

Bofkin L, Goldman N. 2007. Variation in evolutionary processes at different codon positions. *Molecular Biology and Evolution* 24: 513-521.

Bonelli S, Witek M, Canterino, S, Sielezneiew M, Stankiewicz-Fiedurek A, Tartally A, Balletto E, Schonrogge K. 2011. Distribution, host specificity, and the potential for cryptic speciation in hoverfly *Microdon myrmicae* (Diptera: Syrphidae), a social parasite of Myrmica ants. *Ecological Entomology* 36: 135-143.

Brower AVZ. 1994. Rapid morphological radiation and convergence among races of the butterfly *Heliconius erato* inferred from patterns of mitochondrial DNA Evolution. *Proceedings of the National Academy of Sciences* 91: 6491-6495.

Brummitt RK, Pando F, Hollis S, Brummitt NA. 2001. World geographical scheme for recording plant distributions. International Working Group on Taxonomic Databases for Plant Sciences (TDWG).

Chen H, Rangasamy M, Tan SY, Wang HC, Siegfried BD. 2010. Evaluation of Five Methods for Total DNA Extraction from Western Corn Rootworm Beetles. *PLoS One* 5(8): 1-6.

Chroni A, Djan M, Vidaković DO, Petanidou T, Vujić A. 2017. Molecular species delimitation in the genus Eumerus (Diptera: Syrphidae). *Bulletin of Entomological Research* 107(1): 126-138.
Clement M, Posada D, Crandall KA. 2000. TCS: a computer program to estimate gene genealogies. *Molecular Ecology* 9: 1657-1660.
Cowling DE, Burnet B. 1981. Courtship songs and genetic control of their acoustic characteristics in sibling species of the *Drosophila melanogaster* subgroup. *Animal Behaviour* 29: 924-935.
Dayrat B. 2005. Towards integrative taxonomy.*Biological Journal of the Linnean Society* 85: 407-415.
Dell Statistica. 2015. Dell Statistica data analysis software system, version 13. Dell Inc.
Dermitzakis MD. 1990. Paleogeography, geodynamic processes and event stratigraphy during the Late Cenozoic of the Aegean area. *Accademia Nazionale dei Lincei* 85: 263-288.
Dias VS, Silva JG, Lima KM, Petitinga CSCD, Hernández-Ortiz V, Laumann RA, Paranhos BJ, Uramoto K, Zucchi RA, Joachim-Bravo IS. 2016. An integrative multidisciplinary approach to understanding cryptic divergence in Brazilian species of the *Anastrepha fraterculus* complex (Diptera: Tephritidae). *Biological Journal of the Linnean Society* 117(4): 725-746.
Diaz SA, Moncada LI, Murcia CH, Lotta IA, Matta NE, Adler PH. 2015. Integrated taxonomy of a new species of black fly in the subgenus *Trichodagmia* (Diptera: Simuliidae) from the Páramo Region of Colombia. *Zootaxa* 3914(5): 541-57.
Doczkal D. 1996. Description of two new species of the genus *Eumerus* Meigen (Dipt., Syrph.) from Corsica. *Volucella* 2: 3-19.
Drummond AJ, Suchard MA, Xie D, Rambaut A. 2012. Bayesian phylogenetics with BEAUti and the BEAST 1.7. *Molecular Biology and Evolution* 29: 1969-1973.
Folmer O, Black M, Hoeh W, Lutz R, Vrijenhoek R. 1994. DNA primers for amplification of mitochondrial cytochrome c oxidase subunit I from diverse metazoan invertebrates. *Molecular Marine Biology and Biotechnology* 3: 294-299.
Francuski L, Ludoški J, Vujić A, Milankov V. 2009. Wing geometric morphometric inferences on species delimitation and intraspecific divergent units in the *Merodon ruficornis* group (Diptera, Syrphidae) from the Balkan Peninsula. *Zoological Science* 26(4): 301-308.
Francuski L, Ludoški J, Vujić A, Milankov V. 2011. Phenotypic evidence for hidden biodiversity in the *Merodon aureus* group (Diptera, Syrphidae) on the Balkan Peninsula: conservation implication. *Journal of Insect Conservation* 15(3): 379-388.
Gillespie RG, Clague DA. 2009. Encyclopedia of islands. No. 2.Univ of California Press.
Gkontas I, Papadaki S, Trichas A, Poulakakis N. 2016. First assessment on the molecular phylogeny and phylogeography of the species *Gnaptor boryi* distributed in Greece (Coleoptera: Tenebrionidae). *Mitochondrial DNA Part A* 1-8. http://dx.doi.org/10.1080/24701394.2016.1209196
Goloboff PA. 1999. NONA (NO NAME), version 2 [computer program]. Tucumán, Argentina: The Author.
Grković A, Vujić A, Chroni A, van Steenis J, Đan M, Radenković S. (2017) Taxonomy and systematics of three species of the genus Eumerus Meigen, 1822 (Diptera: Syrphidae) new in southeastern Europe. *Zoologischer Anzeiger* 270: 176-192, https://doi.org/10.1016/j.jcz.2017.10.007.
Grković A, Vujić A, Radenković S, Chroni A, Petanidou T. 2015. Diversity of the genus *Eumerus* Meigen (Diptera, Syrphidae) on the eastern Mediterranean islands with description of three new species. *Annales de la Société Entomologique de France* 51: 361-373.
Hall TA. 1999. BioEdit: a user-friendly biological sequence alignment editor and analysis program for Windows 95/98/NT. *Nucleic Acids Symposium Series* 41: 95-98.
Hasson E, Soto IM, Carreira VP, Corio C, Soto EM, Betti M. 2009. Host plants, fitness and developmental instability in a guild of cactophilic species of the genus *Drosophila*. In: Santos EB, editor. Ecotoxicology research developments. New York: Nova Science Publishers 89-109.

Hebert PD, Cywinska A, Ball SL, deWaard JR. 2003. Biological identifications through DNA barcodes. *Proceedings of the Royal Society B* 270: 313-321.

Heled J, Drummond AJ. 2010. Bayesian inference of species trees from multilocus data. *Molecular Biology and Evolution* 27:570-580.

Hijmans RJ, Cameron SE, Parra JL, Jones PG, Jarvis A. 2005. Very high resolution interpolated climate surfaces for global land areas. *International Journal of Climatology* 25: 1965-1978.

House CM, Lewis Z, Hodgson DJ, Wedell N, Sharma MD, Hunt J, Hosken DJ. 2013. Sexual and natural selection both influence male genital evolution. *PLoS One* 8(5): e63807. doi: 10.1371/journal.pone.

Huelsenbeck JP, Ronquist F. 2001. MRBAYES: bayesian inference of phylogenetic trees. *Bioinformatics* 17: 754-755.

Huson DH, Bryant D. 2006. Application of Phylogenetic Networks in Evolutionary Studies, *Molecular Biology and Evolution* 23(2): 254-267.

Kamilari M, Klossa-Kilia E, Kilias G, Sfenthourakis S. 2014. Old Aegean palaeoevents driving the diversification of an endemic isopod species (Oniscidea, Trachelipodidae). *Zoologica Scripta* 43(4): 379-92.

Kasap OE, Dvorak V, Depaquit J, Alten B, Votypka J, Volf P. 2015. Phylogeography of the subgenus *Transphlebotomus Artemiev* with description of two new species, *Phlebotomus anatolicus* n. sp. and *Phlebotomus killicki* n. sp. *Infection, Genetics and Evolution* 34: 467-79.

Kasapidis P, Magoulas A, Mylonas M, Zouros E. 2005. The phylogeography of the gecko *Cyrtopodion kotschyi* (Reptilia: Gekkonidae) in the Aegean Archipelago. *Molecular Phylogenetics and Evolution* 35: 612-623.

Katoh K, Kuma K, Toh H, Miyata T. 2005. MAFFT version 5: improvement in accuracy of multiple sequence alignment. *Nucleic Acids Research* 33: 511-518.

Kirichenko N, Huemer P, Deutsch H, Triberti P, Rougerie R, Lopez-Vaamonde C. 2015. Integrative taxonomy reveals a new species of *Callisto* (Lepidoptera, Gracillariidae) in the Alps. *ZooKeys* 473: 157-176.

Klingenberg CP. 2011. MORPHOJ: an integrated software package for geometric Morphometrics. Ver.2.0. *Molecular Ecology Resources* 11(2): 353-357.

Kougioumoutzis K, Valli AT, Georgopoulou E, Simaiakis S, Triantis KA, Trigas P. 2017. Network biogeography of a complex island system: the Aegean archipelago revisited. *Journal of Biogeography* 44(3): 651-660.

Librado P, Rozas J. 2009. DnaSP v5: a software for comprehensive analysis of DNA polymorphism data. *Bioinformatics* 25: 1451-1452.

Ludoški J, Francuski L, Vujić A, Milankov V. 2008. The *Cheilosia canicularis* group (Diptera: Syrphidae): species delimitation and evolutionary relationships based on wing geometric morphometrics. *Zootaxa* 1825: 40-50.

Luchetti A, Marini M, Mantovani B. 2005. Mitochondrial evolutionary rate and speciation in termites: data on European *Reticulitermes* taxa (Isoptera, Rhinotermitidae). *Insectes Sociaux* 52: 218-221.

Luchetti A, Marini M, Mantovani B. 2007. Filling the European gap: biosystematics of the eusocial system *Reticulitermes* (Isoptera, Rhinotermitidae) in the Balkanic Peninsula and Aegean area. *Molecular Phylogenetics and Evolution* 45: 377-383.

Mantel NA. 1967. The detection of disease clustering and a generalized regression approach. *Cancer Research* 27: 209-220.

Markov Z, Nedeljković Z, Ricarte A, Vujić A, Jovičić S, Józan Z, Mudri-Stojnić S, Radenković S, Ćetković A. 2016. Bee (Hymenoptera: Apoidea) and hoverfly (Diptera: Syrphidae) pollinators in Pannonian habitats of Serbia, with a description of a new *Eumerus* Meigen species (Syrphidae). *Zootaxa* 4154(1): 027-050.

Martinsson S, Erséus C. 2017. Cryptic speciation and limited hybridization within *Lumbricus earthworms* (Clitellata: Lumbricidae). *Molecular Phylogenetics and Evolution* 106:18-27.

Menezes BF, Vigoder FM, Peixoto AA, Varaldi J, Bitner-Mathé BC. 2013. The influence of male wing shape on mating success in *Drosophila melanogaster*. *Animal Behaviour* 85: 1217-1223.
Mengual, X, Ståhls, G & Rojo, S. 2008. First phylogeny of predatory flower flies (Diptera, Syrphidae, Syrphinae) using mitochondrial COI and nuclear 28S rRNA genes: conflict and congruence with the current tribal classification. *Cladistics* 24: 543-562.
Mezey JG, Houle D. 2005. The dimensionality of genetic variation for wing shape in *Drosophila melanogaster*. *Evolution* 59: 1027-1038.
Milankov V, Ludoški J, Ståhls G, Stamenković J, Vujić A. 2009. High molecular and phenotypic diversity in the *Merodon avidus* complex (Diptera, Syrphidae): cryptic speciation in a diverse insect taxon. *Zoological Journal of the Linnean Society* 155(4): 819-833.
Miller MA, Pfeiffer W, Schwartz T. 2010. Creating the CIPRES Science Gateway for inference of large phylogenetic trees, in: 2010 Gateway Computing Environments Workshop, GCE 2010.
Moraes EM, Manfrin MH, Laus AC, Rosada RS, Bomfin SC, Sene FM. 2004.Wing shape heritability and morphological divergence of the sibling species *Drosophila mercatorum* and *Drosophila paranaensis*. *Heredity* 92: 466-473.
Nedeljković Z, Ačanski J, Vujić A, Obreht D, Dan M, Ståhls G, Radenković S. 2013. Taxonomy of *Chrysotoxum festivum* Linnaeus, 1758 (Diptera: Syrphidae) – an integrative approach. *Zoological Journal of the Linnean Society* 169: 84-102.
Nedeljković Z, Ačanski J, Dan M, Obreht-Vidaković D, Ricarte A, Vujić A. 2015. An integrated approach to delimiting species borders in the genus *Chrysotoxum* Meigen, 1803 (Diptera: Syrphidae), with description of two new species. *Contributions to Zoology* 84(4): 285-304.
Nixon KC. 2002. WinClada ver. 1.00.08.Publ. by author, Ithaca, NY 8, Published by the author, Ithaca, NY.
Nunes MD, Orozco-Ter Wengel PA, Kreissl M, Schlötterer C. 2010. Multiple hybridization events between *Drosophila simulans* and *Drosophila mauritiana* are supported by mtDNA introgression. *Molecular Ecology* 19(21): 4695-707.
Olsen, GJ & Woese, CR. 1993. Ribosomal RNA: a relationship between four species using divergent key to phylogeny. Federation of American Societies domain d8 in family: Siluridae. *International Journal for Experimental Biology* 7: 113-123.
Outomuro D, Adams DC, Johansson F. 2013.The evolution of wing shape in ornamented-winged damselflies (Calopterygidae, Odonata). *Evolutionary biology* 40: 300-309.
Padial JM, Miralles A, de la Riva I, Vences M. 2010. The integrative future of taxonomy. *Frontiers in Zoology* 7(1): 16.
Papadopoulou A, Anastasiou I, Keskin B, Vogler AP. 2009. Comparative phylogeography of tenebrionid beetles in the Aegean archipelago: the effect of dispersal ability and habitat preference. *Molecular Ecology* 18: 2503-2517.
Papadopoulou A, Anastasiou I, Vogler AP. 2010. Revisiting the insect mitochondrial molecular clock: the mid-Aegean trench calibration. *Molecular Biology and Evolution* 27: 1659-1672.
Papakostas S, Michaloudi E, Proios K, Brehm M, Verhage L, Rota J, Peña C, Stamou G, Pritchard VL, Fontaneto D, Declerck SAJ. 2016. Integrative Taxonomy Recognizes Evolutionary Units Despite Widespread Mitonuclear Discordance: Evidence from a Rotifer Cryptic Species Complex. *Systematic Biology* 65(3): 508-524.
Pape T, Thompson FC (Eds). 2015. Systema Dipterorum. Version 1.5.Available online at http://www.diptera.org/.
Parks DH, Mankowski T, Zangooei S, Porter MS, Armanini DG, Baird DJ, Langille MGI, Beiko RG. 2013. GenGIS 2: Geospatial analysis of traditional and genetic biodiversity, with new gradient algorithms and an extensible plugin framework. *PLoS One* 8(7): e69885.
Parmakelis A, Stathi I, Chatzaki M, Simaiakis S, Spanos L, Louis C, Mylonas M. 2006. Evolution of *Mesobuthus gibbosus* (Brulle, 1832) (Scorpiones: Buthidae) in the northeastern Mediterranean region. *Molecular Ecology* 15: 2883-2894.

Pérez-Bañón C, Marcos-García A. 1998. Life history and description of the immature stages of *Eumerus purpurariae* (Diptera: Syrphidae) developing in *Opuntia maxima*. *European Journal of Entomology* 95(3): 373-82.
Perez MF, Carstens BC, Rodrigues GL, Moraes EM. 2016. Anonymous nuclear markers data supporting species tree phylogeny and divergence time estimates in a cactus species complex in South America. *Data Brief* 6: 456-460.
Pérez-Ponce de León G, Nadler SA. 2010. What we don't recognize can hurt us: A plea for awareness about cryptic species. *Journal of Parasitology* 96: 453-464.
Perissoratis C, Conispoliatis N. 2003. The impacts of sea-level changes during latest Pleistocene and Holocene times on the morphology of the Ionian and Aegean seas (SE Alpine Europe). *Marine Geology* 196: 145-156.
Petanidou T, Vujić A, Ellis WN. 2011. Hoverfly diversity (Diptera: Syrphidae) in a Mediterranean scrub community near Athens, Greece. *Annales de la Société Entomologique de France* 47(1-2): 168-175.
Pfenninger M, Schwenk K. 2007. Cryptic animal species are homogeneously distributed among taxa and biogeographical regions. *Journal of Evolutionary Biology* 7(1): 121.
Popović D, Ačanski J, Djan M, Obreht D, Vujić A, Radenković S. 2015. Sibling species delimitation and nomenclature of the *Merodon avidus* complex (Diptera: Syrphidae). *European Journal of Entomology* 112(4): 790-809.
Posada D, Crandall KA. 2001. Evaluation of methods for detecting recombination from DNA sequences: computer simulations. *Proceedings of the National Academy of Sciences* 98: 13757-13762.
Poulakakis N, Lymberakis P, Valakos E, Pafilis P, Zouros E, Mylonas M. 2005. Phylogeography of Balkan wall lizard (*Podarcis taurica*) and its relatives inferred from mitochondrial DNA sequences. *Molecular Ecology* 14: 2433-2443.
Poulakakis N, Sfenthourakis S. 2008. Molecular phylogeny and phylogeography of the Greek populations of the genus *Orthometopon* (Isopoda, Oniscidea) based on mitochondrial DNA sequences. *Zoological Journal of the Linnean Society* 152: 707-715.
Poulakakis N, Kapli P, Lymberakis P, Trichas A, Vardinoyiannis K, Sfenthourakis S, Mylonas M. 2015. A review of phylogeographic analyses of animal taxa from the Aegean and surrounding regions. *Journal of Zoological Systematics and Evolutionary Research* 53: 18-32.
Puillandre N, Stöcklin R, Favreau P, Bianchi E, Perret F, Rivasseau A, Limpalaër L, Monnier E, Bouchet P. 2014. When everything converges: Integrative taxonomy with shell, DNA and venomic data reveals *Conus conco*, a new species of cone snails (Gastropoda: Conoidea). *Molecular Phylogenetics and Evolution* 80: 186-92.
Quantum GIS Development Team. 2012. Quantum GIS Geographic Information System. Version 2.12.3 Lyon [Internet]. Open Source Geospatial Foundation Project, available at http://qgis.osgeo.org.
Quek SP, Davies SJ, Itino T, Pierce NE. 2004. Codiversification in an ant-plant mutualism: stem texture and the evolution of host use in *Crematogaster* (Formicidae: Myrmicinae) inhabitants of Macaranga (Euphorbiaceae). *Evolution* 58(3): 554-70.
Rambaut A, Lam TT, Carvalho LM, Pybus OG. 2016. Exploring the temporal structure of heterochronous sequences using TempEst (formerly Path-O-Gen). *Virus Evolution* 2(1): vew007.
Rambaut A, Suchard MA, Xie D, Drummond AJ. 2014. Tracer v1.6. http://tree.bio.ed.ac.uk/software/tracer/
Rambaut A. 2013. FigTree, http://tree.bio.ed.ac.uk/software/figtree/
Ratnasingham S, Hebert PDN. 2013. A DNA-based registry for all animal species: the Barcode Index Number (BIN) System. *PLoS ONE* 8: e66213.
Rato C, Harris DJ, Carranza S, Machado L, Perera A. 2016. The taxonomy of the *Tarentola mauritanica* species complex (Gekkota: Phyllodactylidae): Bayesian species delimitation supports six candidate species. *Molecular Phylogenetics and Evolution* 94: 271-278.

Ricarte A, Nedeljković Z, Rotheray GE, Yszkowski RM, Hancock EG, Watt K, Hewitt SM, Horsefield D, Wilkinson G. 2012. Syrphidae (Diptera) from the Greek island of Lesvos, with description of two new species. *Zootaxa* 317:1-23.

Rodriguez F, Oliver JL, Marin A, Medina JR. 1990. The general stochastic-model of nucleotide substitution. *Journal of Theoretical Biology* 142: 485-501.

Rohlf FJ, Slice DE. 1990. Extensions of the Procrustes method for the optimal superimposition of landmarks. *Systematic Zoology* 39(1): 40-59.

Rohlf FJ. 2006. TpsDig—Digitize landmarks and outlines. Ver.2.05. New York: Department of Ecology and Evolution, State University of New York at Stony Brook.

Ronquist F, Huelsenbeck JP. 2003. MrBayes3: Bayesian phylogenetic inference undermixed models. *Bioinformatics* 19: 1572-1574.

Rosenberg MS, Anderson CD. 2011. PASSaGE: Pattern Analysis, Spatial Statistics and Geographic Exegesis. Version 2. *Methods in Ecology and Evolution* 2(3): 229-232.

Rotheray GE, Gilbert F. 2011. The Natural History of Hoverflies. UK, Ceredigion.

Sacchi R, Hardersen S. 2013. Wing length allometry in *Odonata*: differences between families in relation to migratory behaviour. *Zoomorphology* 132: 23-32.

Šašić L, Ačanski J, Vujić A, Ståhls G, Radenković S, Milić D, Vidaković DO, Đan M. 2016. Molecular and Morphological Inference of Three Cryptic Species within the Merodon aureus Species Group (Diptera: Syrphidae). *PLoS ONE* 11(8): e0160001.

Schlick-Steiner BC, Steiner FM, Seifert B, Stauffer C, Christian E, Crozier RH. 2010. Integrative taxonomy: a multisource approach to exploring Biodiversity. *Annual Review of Entomology* 55: 421-438.

Shapiro B, Rambaut A, Drummond AJ. 2006. Choosing Appropriate Substitution Models for the Phylogenetic Analysis of Protein-Coding Sequences. *Molecular Biology and Evolution* 23: 7-9.

Sheets HD. 2012. IMP software series. Buffalo, New York: Canisius College.

Sfenthourakis S, Triantis KA. 2017. The Aegean archipelago: a natural laboratory of evolution, ecology and civilisations. *Journal of Biological Research-Thessaloniki* 24: 4.

Simaiakis SM, Dimopoulou A, Mitrakos A, Mylonas M, Parmakelis A. 2012. The evolutionary history of the Mediterranean centipede *Scolopendra cingulata* (Latreille, 1829) (Chilopoda: Scolopendridae) across the Aegean archipelago. *Biological Journal of the Linnean Society* 105: 507-521.

Simmons MP, Zhang LB, Webb CT, Reeves A. 2006. How can third codon positions outperform first and second codon positions in phylogenetic inference? An empirical example from the seed plants. *Systematic Biology* 55: 245-58.

Simon C, Frati F, Beckenbach A, Crespi B, Liu H, Flook P. 1994. Evolution, Weighting, and Phylogenetic Utility of Mitochondrial Gene-Sequences and a Compilation of Conserved Polymerase Chain-Reaction Primers. *Annals of the Entomological Society of America* 87: 651-701.

Soldati L, Kergoat GJ, Clamens AL, Jourdan H, Jabbour-Zahab R, Condamine FL. 2014. Integrative taxonomy of New Caledonian beetles: species delimitation and definition of the *Uloma isoceroides* species group (Coleoptera, Tenebrionidae, Ulomini), with the description of four new species. *ZooKeys* 415: 133-167.

Speight MCD, Hauser M, Withers P. 2013. *Eumerus narcissi* Smith (Diptera, Syrphidae), presence in Europe confirmed, with a redescription of the species. *Dipterist Digest* 20: 17-32.

Speight, MCD 2016. Species accounts of European Syrphidae (Diptera). Syrph the Net, the database of European Syrphidae. Dublin. 93: Syrph the Net publications pp. 288.

Stackelberg AA. 1961. Palaearctic species of the genus *Eumerus* Mg. (Diptera, Syrphidae). *Trudy Vsesojuznogo Entomologiceskogo Obscestva* 48, 181-229.

Stamatakis A. 2006. RAxML-VI-HPC: Maximum likelihood-based phylogenetic analyses with thousands of taxa and mixed models. *Bioinformatics* 22: 2688-2690.

Stamatakis A, Hoover P, Rougemont J. 2008.A rapid bootstrap algorithm for the RAxML Web servers. *Systematic Biology* 57: 758-71.

Strasser TF, Panagopoulou E, Runnels CN, Murray PM, Thompson N, Karkanas P, McCoy FW, Wegmann KW. 2010. Stone Age seafaring in the Mediterranean: evidence from the Plakias region for lower palaeolithic and mesolithic habitation of Crete. *Hesperia* 79: 145-190.

Strid A. 2016. Atlas of the Aegean flora. *Englera* 33: 1-578.

Stubbs AE, Falk S. 1983. British hoverflies: an illustrated guide. British Entomological and Natural History Society, London.

Tamura K, Stecher G, Peterson D, Filipski A, Kumar S. 2013. MEGA6: Molecular Evolutionary Genetics Analysis Version 6.0. *Molecular Biology and Evolution* 30: 2725-2729.

Thompson CF. 1999. A key to the genera of the flower flies (Diptera: Syrphidae) of the Neotropical Region including descriptions of new genera and species and a glossary of taxonomic terms. *Contributions on Entomology International* 3: 319-378.

Vujić A, Ståhls G, Ačanski J, Bartsch H, Bygebjerg R, Stefanović A. 2013. Systematics of *Pipizini* and taxonomy of European Pipiza Fallen: molecular and morphological evidence (Diptera, Syrphidae). *Zoologica Scripta* 42: 288-305.

Vujić A, Radenković S, Ačanski J, Grković A, Taylor M, Şenol SG, Hayat R. 2014. Revision of the species of the *Merodon nanus* group (Diptera: Syrphidae) including three new species. *Zootaxa* 4006(3): 439-462.

Yeaman S, Chen Y, Whitlock MC. 2010. No effect of environmental heterogeneity on the maintenance of genetic variation in wing shape in Drosophila melanogaster. *Evolution* 64: 3398-3408.

Yu Y, Harris AJ, Blair C, He XJ. 2015. RASP (Reconstruct Ancestral State in Phylogenies): a tool for historical biogeography. *Molecular Phylogenetics and Evolution* 87: 46-49.

Zelditch ML, Swiderski DL, Sheets HD, Fink WL. 2004. Geometric morphometrics for biologists: a primer. London: Elsevier Academic Press.

Zhang JJ, Kapli P, Pavlidis P, Stamatakis A. 2013. A general species delimitation method with applications to phylogenetic placements. *Bioinformatics* 29: 2869-2876.

Appendix

List of the specimens used for the molecular analyses, their locality information and GenBank accession numbers. GenBank accession numbers of newly-generated sequences (this study) are in boldface, of previously-generated are in normal and of obtained from the GenBank in italics. FSUNS: Faculty of Sciences of Novi Sad, Serbia. MAegean: The Melissotheque of the Aegean, University of the Aegean, Mytilene, Greece. MZH: Finnish Museum of Natural History, Zoological Museum, Helsinki, Finland.

Παράρτημα. Κατάλογος των δειγμάτων εντόμων, τα οποία χρησιμοποιήθηκαν για τις μοριακές αναλύσεις. Δίνονται πληροφορίες σχετικές με την τοποθεσία συλλογής των εντόμων και οι κωδικοί καταχώρησης στη βάση δεδομένων GenBank. Οι κωδικοί GenBank των αλληλουχιών, οι οποίες παρήχθησαν στην παρούσα έρευνα, δίνονται με έντονη γραμματοσειρά, με κανονική δίνονται οι κωδικοί GenBank παλαιότερων αλληλουχιών και με πλάγια αυτών που ανακτήθηκαν από την βάση δεδομένων GenBank. FSUNS: Σχολή Θετικών Επιστημών, Τμήμα Βιολογίας και Οικολογίας, Πανεπιστήμιο του Νόβι Σαντ, Σερβία. M-UAegean: Μελισσοθήκη του Αιγαίου, Πανεπιστήμιο του Αιγαίου, Μυτιλήνη, Ελλάδα. MZH: Εντομολογική συλλογή, Φινλανδικό Μουσείο Φυσικής Ιστορίας, Ελσίνκι, Φινλανδία.

Sequence ID	Specimen voucher	3'-end fragment of *COI*	5'-end fragment of *COI*	*28S*	Species name	Species group	Species subgroup	Sex	Field data
EU10	FSUNS:G1147	**KY865493**	KX083349	none	*Eumerus alpinus* Rondani, 1857	*E. alpinus*	none	F	Italy, Toscana, Mts Apuane, near Orto Botanico, 44.056359, 10.19884
EU132	FSUNS:60653	**KY865499**	KX083380	none	*Eumerus strigatus* (Fallen, 1817)	*E. strigatus*	none	M	Germany, Unknown
EU135	FSUNS:G3018	**KY865500**	**KY865450**	none	*Eumerus tricolor* (Fabricius), 1798	*E. tricolor*	none	F	Italy, Baragazza, 44.13217, 11.19112, 09/06/2013
EU146	FSUNS (loan by Maegean):E078	**KY865501**	**KY865451**	**KY865546**	*Eumerus minotaurus* Claussen & Lucas,	*E. minotaurus*	*E. minotaurus*	M	Greece, Karpathos, Avlona, 35.7689,

	7, UOTA_MEL026180				1988				27.1849, 2-4/05/2012
EU149	FSUNS:G3025	**KY865502**	**KY865452**	none	*Eumerus crassus* Grković, Vujić & Radenković, 2015	*E. minotaurus*	none	M	Greece, Chios, Kambia Gorge, 38.578499, 25.979666, 14/05/2009
EU16	FSUNS:G0278	**KY865494**	**KY865446**	**KY865545**	*Eumerus phaeacus* Chroni, Grković & Vujić, sp. n.	*E. minotaurus*	*E. minotaurus*	M	Greece, Mt Olympus, Ag. Paraskevi, kanjon, 39.8785, 22.5863, 17/05/2011
EU17	MAegean:UOTA_MEL0746, E0746	KT221020	KT221006	none	*Eumerus torsicus* Grković et Vujić, 2016	*torsicus*	none	M	Greece, Chios, Elinda, 38.393, 25.9914, 9-11/11/2012
EU211	FSUNS:G0277	**KY865503**	**KY865453**	**KY865550**	*Eumerus phaeacus* Chroni, Grković & Vujić, sp. n.	*E. minotaurus*	*E. minotaurus*	F	Greece, Mt Olympus, Ag. Paraskevi, kanjon, 39.8785, 22.5863, 17/05/2011
EU212	FSUNS:G0269	**KY865504**	**KY865454**	none	*Eumerus phaeacus* Chroni, Grković & Vujić, sp. n.	*E. minotaurus*	*E. minotaurus*	M	Montenegro, Mt Rumija, okosredine (deokajezeru, uz put), 42.11201, 19.21739, 02/05/2011
EU221	FSUNS:G0271	**KY865505**	**KY865455**	none	*Eumerus sinuatus* Loew, 1855	*E.tricolor*	none	M	Serbia, Fruska Gora, Glavica, 45.153999, 19.834681, 17/06/2011
EU223	FSUNS:G1020	**KY865506**	**KY865456**	none	*Eumerus armatus* Ricarte & Rotheray, 2012	*E.tricolor*	none	M	Greece, Samos, near Platanos, 37.740527, 26.742116, 09/06/2010
EU276	FSUNS:08910	**KY865507**	KY272852	none	*Eumerus pannonicus*	*E.strigatus*	none	F	Serbia, Mokrin,

					Ricarte, Vujić & Radenković, 2016				Pašnjacivelikedroplje, 45.90615, 20.3018, 11/06/2014
EU297	FSUNS:06366	**KY865508**	KX083386	none	*Eumerus minotaurus* Claussen & Lucas, 1988	*E. minotaurus*	*E. minotaurus*	F	Greece, Lassithi, Iraklion, 7 km prePlateau of Lassithi, 35.211883, 25.461649, 22/04/2014
EU298	FSUNS:06452	**KY865509**	**KY865457**	none	*Eumerus minotaurus* Claussen & Lucas, 1988	*E. minotaurus*	*E. minotaurus*	M	Greece, Chania, 3 km pre Armeni, 35.285761, 24.468983, 25/04/2014
EU300	FSUNS:06557	**KY865510**	**KY865458**	**KY865549**	*Eumerus karyates* Chroni, Grković & Vujić, sp. n.	*E. minotaurus*	*E. minotaurus*	M	Greece, Peloponnese, Karyes, 25km N from Sparti, 37.304145, 22.421241
EU302	FSUNS:06710	**KY865511**	**KY865459**	none	*Eumerus minotaurus* Claussen & Lucas, 1988	*E. minotaurus*	*E. minotaurus*	F	Greece, Chania, Imbors, 35.252332, 24.174351, 27/05/2014
EU303	FSUNS:06728	**KY865512**	**KY865460**	**KY865547**	*Eumerus minotaurus* Claussen & Lucas, 1988	*E. minotaurus*	*E. minotaurus*	M	Greece, Chania, Omalos plain, 35.322592, 23.930496, 28/05/2014
EU320	FSUNS:06561	**KY865513**	KX083382	none	*Eumerus sogdianus* Stackelberg, 1952	*E. strigatus*	none	F	Greece, Peloponnese, Karyes2, 25km N from Sparti, 37.30416, 22.42106

EU37	FSUNS:G2286	**KY865495**	**KY865447**	none	*Eumerus crassus* Grković, Vujić & Radenković, 2015	*E. minotaurus*	none	M	Greece, Lesvos, Argennos, 39.357622, 26.254769, 03-04/06/2012
EU406	FSUNS:E1333	**KY865514**	**KY865461**	none	*Eumerus sulcitibius* Róndani, 1868	*E. sulcitibius*	none	F	Greece, Lassithi, Psichro, 35.15, 25.4666667, Unknown
EU459	FSUNS:E1260	**KY865515**	**KY865462**	none	*Eumerus amoenus* Loew, 1848	*E. strigatus*	none	F	Greece, Mt Taygetos, Lok I, 37.066156, 22.265413, 06/08/2014
EU469	FSUNS:07982	**KY865516**	KX083351	none	*Eumerus clavatus* Becker, 1923	*E. clavatus*	none	F	Turkey, Mt Davraz, ski center, 37.781694, 30.75871
EU499	FSUNS:GO290	**KY865517**	**KY865463**	none	*Eumerus crassus* Grković, Vujić & Radenković, 2015	*E. minotaurus*	none	F	Greece, Samos, Neochori, 37.707965, 26.769917, Unknown
EU73	FSUNS:G0292	**KY865496**	KX083373	none	*Eumerus consimilis* Šimić &Vujić, 1996	*E. strigatus*	none	M	Serbia, Djerdap, 44.54104, 22.02024, 01/09/2011
EU75	FSUNS:G0992	**KY865497**	**KY865448**	none	*Eumerus clavatus* Becker, 1923	*E. basalis*	none	M	Greece, Ikaria, near Hristos, 37.601523, 26.084755, 11/06/2010
EU99	FSUNS:G2219	**KY865498**	**KY865449**	none	*Eumerus ornatus* Meigen, 1822	*E. ornatus*	none	M	Montenegro, Boka Kotorska, Morinj Bay, 42.490394, 18.648914, 08/10/2010
GUN5	FSUNS:GUN5	**KY865492**	KX083393	**KY865574**	*Megatrigon tabanoides* Doczkal, Radenković,	Outgroup	none	M	South Africa, Unknown

					Lyneborg & Pape, 2015				
Y1711E	MZH:Y1711	**KY865491**	**KY865444**	*KM224496 (GB)*	*Platynochaetus setosus* Fabricius, 1794	Outgroup	none	M	France, Banyuls-sur-Mer, Pyrenées-Orientales, JardinMediterranéen, 42.474144, 3.117728
EU558	MAegean:UOTA_MEL082471, 10064	**KY865518**	**KY865464**	none	*Eumerus pulchellus* Loew, 1848	*E. pulchellus*	none	M	Greece, Anafi, Helicodrome, 36.3565, 25.7736, 15-17/06/2013
TS240	FSUNS:06666	**KY865520**	**KY865466**	**KY865552**	*Eumerus minotaurus* Claussen & Lucas, 1988	*E. minotaurus*	*E. minotaurus*	M	Greece, Rethymnon, Fotinos, 35.285762, 24.468983, 26/05/2014
TS241	FSUNS:6724	**KY865521**	**KY865467**	none	*Eumerus minotaurus* Claussen & Lucas, 1988	*E. minotaurus*	*E. minotaurus*	F	Greece, Chania, Omalos plain, 35.322592, 23.930496, 28/05/2014
MN1	FSUNS:11413	**KY865522**	**KY865468**	**KY865558**	*Eumerus phaeacus* Chroni, Grković & Vujić, sp. n.	*E. minotaurus*	*E. minotaurus*	M	Greece, Corfu, nr Ano Korakiana, 39.69882, 19.786956, 24/05/2016
MN2	FSUNS:11415	**KY865523**	**KY865469**	**KY865572**	*Eumerus phaeacus* Chroni, Grković & Vujić, sp. n.	*E. minotaurus*	*E. minotaurus*	M	Greece, Corfu, nr Ano Korakiana, 39.69882, 19.786956, 24/05/2016
MN3	FSUNS:11419	**KY865524**	**KY865470**	**KY865565**	*Eumerus phaeacus* Chroni, Grković & Vujić, sp. n.	*E. minotaurus*	*E. minotaurus*	M	Greece, Corfu, nr Ano Korakiana, 39.69882, 19.786956, 24/05/2016

MN4	FSUNS:11458	**KY865525**	**KY865471**	**KY865566**	*Eumerus phaeacus* Chroni, Grković & Vujić, sp. n.	*E. minotaurus*	*E. minotaurus*	M	Greece, Corfu, nr Liapades, 39.673537, 19.756369, 24/05/2016
MN5	FSUNS:11457	**KY865526**	**KY865472**	**KY865570**	*Eumerus phaeacus* Chroni, Grković & Vujić, sp. n.	*E. minotaurus*	*E. minotaurus*	M	Greece, Corfu, nr Liapades, 39.673537, 19.756369, 24/05/2016
MN6	FSUNS:11546	**KY865527**	**KY865473**	**KY865569**	*Eumerus phaeacus* Chroni, Grković & Vujić, sp. n.	*E. minotaurus*	*E. minotaurus*	M	Greece, Corfu, nr Strinilas, 39.739862, 19.837306, 24/05/2016
MN7	FSUNS:11461	**KY865528**	**KY865474**	**KY865555**	*Eumerus phaeacus* Chroni, Grković & Vujić, sp. n.	*E. minotaurus*	*E. minotaurus*	F	Greece, Corfu, nr Liapades, 39.673537, 19.756369, 24/05/2016
MN8	FSUNS:11460	**KY865529**	**KY865475**	**KY865548**	*Eumerus phaeacus* Chroni, Grković & Vujić, sp. n.	*E. minotaurus*	*E. minotaurus*	M	Greece, Corfu, nr Liapades, 39.673537, 19.756369, 24/05/2016
MN9	FSUNS:11448	**KY865530**	**KY865476**	**KY865551**	*Eumerus phaeacus* Chroni, Grković & Vujić, sp. n.	*E. minotaurus*	*E. minotaurus*	M	Greece, Corfu, nr AnoKorakiana, 39.69882, 19.786956, 24/05/2016
MN10	FSUNS:11430	**KY865531**	**KY865477**	**KY865559**	*Eumerus phaeacus* Chroni, Grković & Vujić, sp. n.	*E. minotaurus*	*E. minotaurus*	M	Greece, Corfu, nr Ano Korakiana, 39.69882, 19.786956, 24/05/2016
MN11	FSUNS:11459	**KY865532**	**KY865478**	**KY865561**	*Eumerus phaeacus* Chroni, Grković & Vujić, sp. n.	*E. minotaurus*	*E. minotaurus*	M	Greece, Corfu, nr Liapades, 39.673537, 19.756369, 24/05/2016

MN12	FSUNS:11432	**KY865533**	**KY865479**	**KY86555**	*Eumerus phaeacus* Chroni, Grković & Vujić, sp. n.	*E. minotaurus*	*E. minotaurus*	M	Greece, Corfu, nr Ano Korakiana, 39.69882, 19.786956, 24/05/2016
MN13	FSUNS:11436	**KY865534**	**KY865480**	**KY865567**	*Eumerus phaeacus* Chroni, Grković & Vujić, sp. n.	*E. minotaurus*	*E. minotaurus*	M	Greece, Corfu, nr Ano Korakiana, 39.69882, 19.786956, 24/05/2016
MN14	FSUNS:11426	**KY865535**	**KY865481**	**KY865562**	*Eumerus phaeacus* Chroni, Grković & Vujić, sp. n.	*E. minotaurus*	*E. minotaurus*	M	Greece, Corfu, nr Ano Korakiana, 39.69882, 19.786956, 24/05/2016
MN15	FSUNS:11437	**KY865536**	**KY865482**	**KY865560**	*Eumerus phaeacus* Chroni, Grković & Vujić, sp. n.	*E. minotaurus*	*E. minotaurus*	M	Greece, Corfu, nr Ano Korakiana, 39.69882, 19.786956, 24/05/2016
MN16	FSUNS:11310	**KY865537**	**KY865483**	**KY865573**	*Eumerus crassus* Grković, Vujić & Radenković, 2015	*E. minotaurus*	none	F	Greece, Lesvos, Neochori I, 39.024073, 26.321613, 03/5/2016
MN18	FSUNS:11411	**KY865538**	**KY865484**	**KY865556**	*Eumerus karyates* Chroni, Grković & Vujić, sp. n.	*E. minotaurus*	*E. minotaurus*	M	Greece, Peloponnese, Karyes, 25km N from Sparti, 37.304145, 22.421241
MN19	FSUNS:11412	**KY865540**	**KY865485**	**KY865564**	*Eumerus karyates* Chroni, Grković & Vujić, sp. n.	*E. minotaurus*	*E. minotaurus*	F	Greece, Peloponnese, Karyes, 25km N from Sparti 37.304145, 22.421241
MN20	FSUNS:11572	**KY865539**	**KY865486**	**KY865554**	*Eumerus karyates* Chroni, Grković & Vujić, sp. n.	*E. minotaurus*	*E. minotaurus*	F	Greece, Peloponnese, Karyes, 25km N from Sparti, 37.304145,

									22.421241
MN21	FSUNS:11573	**KY865541**	**KY865487**	**KY865557**	*Eumerus karyates* Chroni, Grković & Vujić, sp. n.	*E. minotaurus*	*E. minotaurus*	F	Greece, Peloponnese, Karyes, 25km N from Sparti, 37.304145, 22.421241
MN22	FSUNS:11574	**KY865542**	**KY865488**	**KY865563**	*Eumerus karyates* Chroni, Grković & Vujić, sp. n.	*E. minotaurus*	*E. minotaurus*	F	Greece, Peloponnese, Karyes, 25km N from Sparti, 37.304145, 22.421241
MN23	FSUNS:11571	**KY865543**	**KY865489**	**KY865571**	*Eumerus karyates* Chroni, Grković & Vujić, sp. n.	*E. minotaurus*	*E. minotaurus*	M	Greece, Peloponnese, Karyes, 25km N from Sparti, 37.304145, 22.421241
MN24	FSUNS:11410	**KY865544**	**KY865490**	**KY865568**	*Eumerus karyates* Chroni, Grković & Vujić, sp. n.	*E. minotaurus*	*E. minotaurus*	F	Greece, Peloponnese, Karyes, 25km N from Sparti, 37.304145, 22.421241
TS24	FSUNS:08451	*LN890909 (GB)*	**KY865445**	**KY865575**	*Merodon erivanicus* Paramonov, 1925	Outgroup	none	M	Turkey, Isparta, Geledost, Yesilkoy, 42.250833, 32.351111, 29/05/2014

CHAPTER 6

Connecting the dots: Bridging genetic to spatial differentiation of the genus *Eumerus* (Diptera: Syrphidae) in the Mediterranean Basin and the Balkans

Connecting the dots: Bridging genetic to spatial differentiation of the genus *Eumerus* (Diptera: Syrphidae) in the Mediterranean Basin and the Balkans

Antonia Chroni, Milomir Stefanović, Mihajla Djan, Ante Vujić, Llilja Šašić Zorić, Nataša Kočiš Tubić and Theodora Petanidou

Abstract

Aim The Mediterranean Basin and the Balkan Peninsula have been recognized as hotspots of a high hoverfly diversity and endemism. Considering, however, the high importance of the region for this insect group, the number of biogeographic and phylogeographic studies conducted therein is very low. Here we (i) explore the intraspecific genetic differentiation of hoverfly species of the genus *Eumerus* in relation to isolation-by-distance, landscape discontinuities, palaeogeological and palaeoclimatic events, (ii) unveil high- and low- genetic divergent regions, and (iii) discuss the potential driving forces which led to observed spatial genetic patterns.

Location Mediterranean Basin (8 countries, and 23 islands included therein); continental Balkan Peninsula (three countries; Bulgaria, FYRO Macedonia, and Serbia).

Methods DNA barcodes for 274 individuals from nine *Eumerus* species sampled from 58 localities were generated. We performed spatially-explicit Bayesian clustering of individuals and tested the correlation between geographic and genetic distances (presence of isolation-by-distance), and constructed Median Joining networks from the haplotypes to examine and corroborate the inferred spatial genetic structure. We employed Landscape Shape Interpolation analyses to visualize areas of high and low genetic distances between individuals within each species.

Results We observed high mtDNA haplotype diversity consisting of unique and shared haplotypes. In four species, the pattern observed by the haplotype network was consistent with species distribution and Bayesian clustering. The Bayesian clustering showed one to three (genetic) clusters membership with high posterior probability values. Mantel tests confirmed there was no presence of isolation-by-distance between the sampling areas (except for two species). In all species, areas with high- and low-genetic divergence were detected through Landscape Shape Interpolation analyses.

Main conclusions Our study represents the first broad- and large-scale study for nine *Eumerus* species in the Mediterranean and the Balkans. It reveals the occurrence of a

spatially genetic clustering in four species, and associates the relative driving forces liable for that such as evolutionary processes (e.g. allopatric), palaeogeological events etc. Five species displayed neither spatial genetic patterns nor isolation-by-distance presence, indicating relict taxa (long term stable populations); for three out of these five species, star-like mtDNA haplotypes were affirmative.

Keywords

Balkans, Bayesian clustering, biogeography, DNA barcode, *Eumerus*, genetic differentiation, isolation-by-distance, Mediterranean, phylogeography, Syrphidae

Introduction

The term of phylogeography was outlined for the first time three decades ago (Avise *et al*., 1987), and ever since, the discipline has flourished considerably, encountering many followers. By conjoining phylogenetics and population genetics, phylogeography is keen to explore the driving forces of the geographical distribution within or among species (Avise, 2009; Hickerson *et al*., 2010; Chan *et al*., 2011). Historical biogeography intends to shed light into the species distribution too, but it does so in the context of evolutionary history such as vicariance and dispersal processes (Ronquist, 1997) or the impact of the Quaternary climatic oscillations (Sanmartín, 2012). Both phylogeography and historical biogeography are complementary to each other, and may contribute to reconstruct and infer the population's demographics through time (gene flow, migration etc.) or to associate the contemporary species distribution to historic evolution of landscape discontinuities (e.g. mountains) and/or isolation-by-distance (Chan *et al*., 2011).

With a high species diversity and a wide distribution worldwide, hoverflies (Diptera: Syrphidae) have a crucial impact on ecosystem structure and functioning (Rotheray & Gilbert, 2011). Hitherto, there are some phylogeographic and biogeographic studies on hoverflies as study organisms (Milankov *et al*., 2013; Šašić *et al*., 2016; Ståhls *et al*., 2016; Vujić *et al*., 2016; Radenković *et al*., 2017; Chroni *et al*., unpubl.). Here, we employ species of the genus *Eumerus* Meigen, 1822, which is noteworthy for its contribution to pollination among other services (e.g. predation of plant pests, nutrient recycling from dead matter; Rotheray & Gilbert, 2011). Further attention to the genus has been drawn recently because of the ingress of DNA barcoding in the arena of *Eumerus* taxonomy (Grković *et al*., 2015, 2017; Chroni *et*

al., 2017, unpubl.). The latter has launched (i) species diagnosis and delimitation, as well as phylogenetic inferences (Chroni *et al.*, 2017); (ii) identification of new species and endemics (e.g. Grković *et al.*, 2015, 2017; Chroni *et al.*, unpubl.); and (iii) exposure of a cryptic species complex with speciation events affiliated to the palaeogeographic evolution of the Aegean (due to the formation of the mid-Aegean Trench and Messinian Salinity Crisis; Chroni *et al.*, unpubl.). Aggregating these findings to the genus species diversity, endemism and role in ecosystems, phylogeographic and biogeographic considerations will be valuable and auxiliary as to identify and comprehend the potential drivers of e.g. species distribution or speciation within the genus.

The Mediterranean Basin and the Balkan Peninsula are both regarded as remarkably diverse in species (including endemic and cryptic taxa), and spatially heterogeneous in their biota. Indeed, the Mediterranean is classified as one of the 36 global biodiversity hotspots (CEPF.net-The Biodiversity Hotspots, www.cepf.net). Such a delineation is explained by the vicinity of three continents representing diverse ecogeographical zones with their own biota, high relief and insularity/peninsularity, (palaeo)geological history (e.g. collision of the African and the European tectonic plates, orogenic processes; Lymberakis & Poulakakis, 2010), and (palaeo)climatic events (climatic oscillations from Quaternary to Holocene; Vogiatzakis *et al*., 2016). In addition to that, a sustained human pressure has acted on the area (for a thorough review see Hewitt, 2011). All aforementioned events have favored the formation/ emersion or loss of land bridges that either connected or isolated areas, or operated as refugia (Hewitt, 2011), and subsequently led to a high landscape heterogeneity (Hughes *et al*., 2006). As a consequence, high species diversity and endemism were ensued in the region for many biota, such as insects and other invertebrates (e.g. Hewitt, 2011), mammals (e.g. Barros *et al*., 2016), and plants (e.g. Médail & Myers, 2004).

The present study is the first endeavorment to (1) assess the intraspecific genetic differentiation in *Eumerus* species in the Mediterranean and the Balkans by employing DNA barcodes; (2) test for a spatially-explicit Bayesian clustering within these nine species, and to evaluate the acquired results based on landscape discontinuities (e.g. Aegean Archipelago, Dinaric Alps & Pindos Mts) and the presence of isolation-by-distance; (3) reveal potential high- or low- genetic divergent

regions within the study area; and (4) discuss and provide more insights regarding the driving forces which led to observed spatial genetic patterns.

Materials and Methods

Taxa and geographic distribution

A total of 274 specimens belonging to 9 *Eumerus* species were used for the analyses. The species were chosen on the basis of their geographic distribution in the entire study area (Anatolia, Apennines, Balkan and Iberian peninsulas) encompassing species of relatively wide or very wide distribution within the study area. The species with their geographical distribution in the Palearctic region are as follows; *E. amoenus* Loew, 1848 from southwestern Mediterranean and central Europe to Asia (our sampling ranged from Italy to Turkey); *E. argyropus* Loew, 1848 from south Mediterranean, central Europe, through the Balkans to Turkey (the Balkans, Turkey); *E. armatus* Ricarte & Rotheray, 2012 has been recorded in Greece so far, but here we had one record from Turkey as well (Greece and Turkey); *E. basalis* Loew, 1848 from south Europe to Turkey and Iran (the Balkans); *E. clavatus* Becker, 1923 from central Europe and southwestern Mediterranean to North Africa (the Balkans, Turkey); *E. phaeacus* Chroni, Grković & Vujić, in litt. in the Balkans (the Balkans); *E. pulchellus* Loew, 1848 from south Mediterranean, the Balkans, Turkey and N. Africa (our sampling covered all these areas); *E. pusillus* Loew, 1848 shows a similar range as *E. pulchellus* (we covered almost all this range); and *E. sulcitibius* Rondani, 1868 from southwestern Mediterranean to Turkey, Asia and to Azerbaijan (our sampling was restricted to the Aegean Islands, Greece). For more details in each species distribution see Grković *et al*., 2015, Speight, 2016, and Chroni *et al*., unpubl. The list of the specimens used, including their field data, GenBank accession numbers and haplotypes codes, are shown in Table S1 (Supporting Information).

All study specimens are deposited in the entomological collections of the Faculty of Sciences of Novi Sad (University of Novi Sad, Serbia, FSUNS) and the Melissotheque of the Aegean (University of the Aegean, Mytilene, Greece, MAegean).

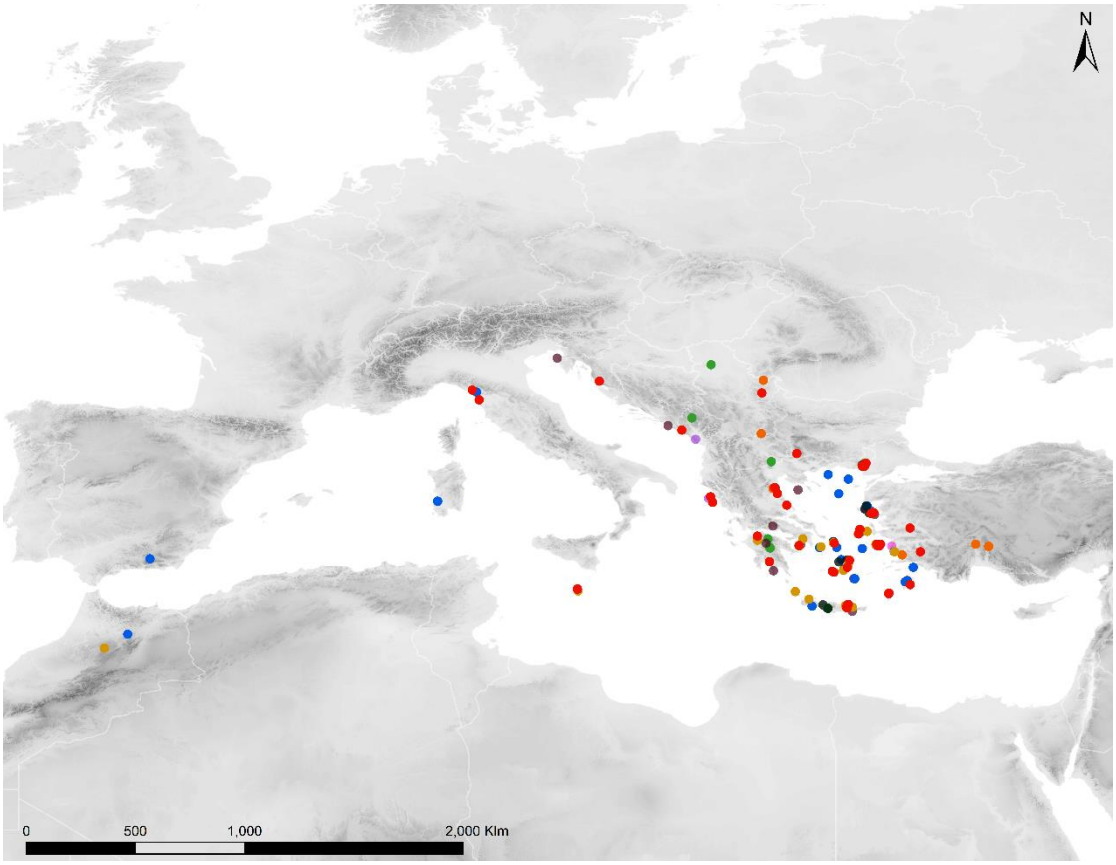

Fig. 1. Sampling sites of the study species: *E. amoenus* (red), *E. argyropus* (green), *E. armatus* (pink), *E. basalis* (brown), *E. clavatus* (orange), *E. phaeacus* (purple), *E. pulchellus* (light blue), *E. pusillus* (olive), and *E. sulcitibius* (black).

Σχήμα 1. Περιοχές προέλευσης των υπο μελέτη ειδών: *E. amoenus* (κόκκινο), *E. argyropus* (πράσινο), *E. armatus* (ροζ), *E. basalis* (καφέ), *E. clavatus* (πορτοκαλί), *E. phaeacus* (μωβ), *E. pulchellus* (γαλάζιο), *E. pusillus* (λαδί) και *E. sulcitibius* (μαύρο).

MtDNA data analyses

We performed DNA extractions after the Chen *et al.* (2010) protocol, with slight modifications as described in Grković *et al.* (2015). We sequenced the 5'-end fragment of the mitochondrial gene Cytochrome c oxidase subunit I (COI, DNA barcode). For the PCR amplification and sequencing, we employed the primers LCO-1490 (5′-GGTCAACAAATCATAAAGATATTGG-3′) and HCO-2198 (5′-TAAACTTCAGGGTGACCAAAAAATCA-3′) (Folmer *et al.*, 1994). PCR reactions and purification of the PCR products were carried out as Grković *et al.* (2015). DNA sequencing was performed at Sequencing Service Laboratory of the Finnish Institute for Molecular Medicine (http://www.fimm.fi/) and at Macrogen Inc. (The Netherlands; http://www.macrogen.com/eng/).

We created nine datasets, each corresponding to the aforementioned species and named after them, e.g. dataset *E. amoenus* and so forth. The multiple sequence alignments were performed in the MAFFT 7 (Katoh *et al.*, 2005; available at http://mafft.cbrc.jp/alignment/server/index.html). The sequences were edited where needed (by eye) by using BioEdit 7.2.5 (Hall, 1999). We have implemented DnaSP 5.10.01 (Librado & Rozas, 2009) to calculate singleton and parsimony informative sites, as well as the number of haplotypes and to generate the haplotypes files per dataset. We have inferred Median Neighbor Joining networks for each dataset based on the haplotypes by implementing PopART (mtDNA haplotype networks; Bandelt *et al*., 1999, http://popart.otago.ac.nz).

Spatial genetic structure analyses

The genetic structure of each dataset individuals (viz. genetic clusters) was examined in relation to their geographic locations by performing a spatially-explicit Bayesian cluster membership (hereinafter cluster membership) of individuals in the GENELAND 4.0.5 (Guillot *et al.*, 2005) of the R-package. We implemented the uncorrelated model based on multinomial distribution of genotypes, population memberships and linkage equilibrium. We estimated the K value with the following settings: 5 replicates of 1,000,000 iterations, thinning interval of 100 and range of genetic clusters' number K from 1 to 5 and 1 to 10. Then we assessed the consistency of suggested number of genetic clusters inferred from each replicate for each dataset. The final assignment of individuals (conclusion for the cluster membership) was performed in a separate run with the fixed (suggested) K value to the inferred number of clusters membership under the same parameters, but with three replicates conducted.

Safner *et al.* (2011) have pointed out the importance of the evaluation of the cluster membership in order to avoid detection of incorrect barriers, and suggested testing the cluster membership as a potential consequence of isolation-by-distance, i.e. to test whereas genetic differentiation increases with the increase in geographic distance (Wright, 1943). Thus, the relationship between the genetic and geographic distances was tested by a Mantel test (Mantel, 1967) and implemented in ALLELES IN SPACE (AIS; Miller, 2005), with 1,000 permutations for accessing the significance of the correlation coefficient.

To visualize spatial patterns of genetic diversity, we produced a Landscape Shape Interpolation analysis (LSI), where, in a three-dimensional surface plot, the geographic coordinates (X and Y) can be related to the genetic distances (surface plot heights, Z). Peaks represent areas of high genetic distances between individuals, and therefore they can be considered areas of restricted gene flow (likewise troughs point out low genetic distances). The Landscape Shape Interpolation analyses were performed in AIS, with distance weighting parameter (α) of 1 and grid settings of 150x150. For all the analyses implemented in AIS, we have used sequences as input matrix (raw genetic distances), and coordinates in UTM system.

The ArcMap 10.2.2 (Gorr & Kurland, 2012) was implemented to construct the maps per each dataset, and the information of the cluster membership was incorporated into the visualization of the sampling points of individuals (Figs 2a–10a).

Table 1. Characteristics for each analyzed dataset per species; cluster membership as assigned from Geneland; Mantel test results and the relative p values.

Πίνακας 1. Χαρακτηριστικά των υπό μελέτη ομάδων δεδομένων ανά είδος· οι ομάδες (cluster membership) όπως ταυτοποιήθηκαν από το πρόγραμμα Geneland· Αποτελέσματα των Mantel test και οι σχετικές τιμές p.

Dataset	No sequences	Singleton variable sites	Parsimony informative sites	No polymorphic sites	Haplotype (gene) diversity, Hd	No Haplotypes	Cluster membership	Presence of IBD	IBD (Mantel test) r	IBD (Mantel test) p
E. amoenus	59	16	25	41	0.942	39	1	no	**0.14**	0.0429570430
E. argyropus	36	4	8	12	0.83	12	3	**yes**	0.28	0.000999001
E. armatus	10	7	3	10	0.8	5	2	no	**0.04**	0.236763237
E. basalis	43	11	6	17	0.449	10	1	no	**0.03**	0.198801199
E. clavatus	13	7	3	10	0.795	7	1	no	**0.40**	0.024975025
E. phaeacus	18	4	0	4	0.314	4	1	no	**-0.18**	0.128871129
E. pulchellus	41	63	16	79	0.902	26	2	no	**0.06**	0.240759241
E. pusillus	33	1	3	4	0.665	6	2	**yes**	0.38	0.000999001
E. sulcitibius	21	7	3	10	0.614	6	2	no	**-0.03**	0.403596404

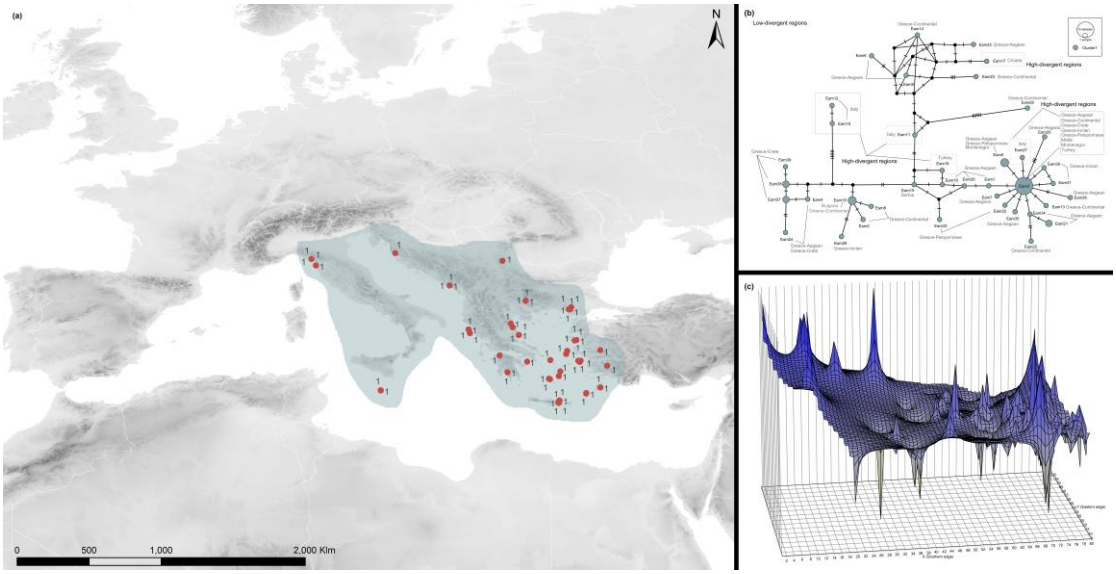

Fig. 2. Analyses of the *E. amoenus* dataset: (a) geographic distribution of the identified clusters, numbers above the circles indicate the cluster membership; (b) median-joining network analysis based on the haplotypes, colours of the circles are according to the cluster membership, circle sizes are proportional to haplotype frequencies, number of mutational steps is depicted by lines; and (c) genetic landscape interpolation plot depicting the areas with high- or low-genetic differentiation in relation to the geographic coordinates using a 150×150 grid and a distance weighting parameter α=1. Darker shading and higher peaks show areas of greater genetic diversity.

Σχήμα 2. Αναλύσεις της ομάδας δεδομένων *E. amoenus*: (a) γεωγραφική κατανομή των ταυτοποιημένων κλάδων, οι αριθμοί πάνω από τους κύκλους υποδηλώνουν τον κλάδο· (b) δίκτυα Σύνδεσης Γειτόνων (NJ) των απλοτύπων, τα χρώματα των κύκλων είναι σύμφωνα με τον κλάδο στον οποίο ανήκουν, το μέγεθος κάθε κύκλου είναι ανάλογο με τη συχνότητα του απλοτύπου (αριθμός ατόμων που έχουν αυτόν τον απλότυπο), ο αριθμός των εξελικτικών βημάτων δίνεται ανά ζεύγος απλοτύπων· και (c) γραφική απεικόνιση του γενετικού τοπίου (genetic landscape interpolation plot) που απεικονίζει περιοχές υψηλής- και χαμηλής-γενετικής διαφοροποίησης σε συσχέτιση με τις γεωγραφικές συντεταγμένες χρησιμοποιώντας 150×150 πλέγμα και παράμετρο σταθμιστικής απόστασης α=1. Οι σκοτεινότερες σκιάσεις δείχνουν περιοχές μεγαλύτερης γενετικής ποικιλότητας.

Results

Genetic diversity and mtDNA haplotype network

Each dataset was of total length 610 bp, and numbers of sequences per dataset ranged from 10 to 59. The alignments did not comprise gaps. Based on polymorphic sites, we observed a range of genetic polymorphism from 4 to 79 (for more information to each dataset's characteristics see Table 1).

We detected high mitochondrial haplotype diversity (≥ 50%) in all species apart of *E. basalis* and *E. phaeacus* (Table 1). As shown in Figs 2b–10b, unique and shared

haplotypes appeared across the entire study area. There were shared mtDNA haplotypes between different sampling areas (*E. amoenus*, *E. basalis*, *E. phaeacus*, *E. pusillus* and *E. sulcitibius*) or multiple (unique) haplotypes for one area (*E. argyropus*, *E. armatus*, *E. clavatus*, *E. phaeacus*, *E. pulchellus*, *E. pusillus* and *E. sulcitibius*). For the datasets *E. argyropus*, *E. armatus*, *E. pulchellus* and *E. pusillus*, the observed distribution of the mtDNA haplotypes corresponded to the clustering membership as indicated from GENELAND (Figs 3a–b, 4a–b, 8a–b & 9a–b, respectively). The dataset *E. argyropus* presented one shared haplotype (Earg7) for three specimens originated from Corfu Island (Ionian Islands), Pieria (Central Greece), and Mt Davraz (Turkey). Finally, 13 specimens of the dataset *E. sulcitibius* showed one shared haplotype (Es1) originating from three islands of the Aegean (Andros, Lesvos and Paros) and Crete (Greece).

Spatial genetic structure

Spatially-explicit Bayesian clustering of individuals identified one to three clusters membership with high posterior probability values: one genetic cluster in *E. amoenus*, *E. basalis*, *E. clavatus* and *E. phaeacus*; two genetic clusters in *E. armatus*, *E. pulchellus*, *E. pusillus* and *E. sulcitibius*; and three genetic clusters in *E. argyropus* (Table 1 and Figs 2a–10a). There was an exception for three sequences, for which uncertainty has risen as to these individuals' appropriate clustering: EU307 (*E. argyropus*), EU438 (*E. pulchellus*) and EU67 (*E. sulcitibius*).

Mantel tests revealed the correlation of genetic divergence to geographic distance in two out of the nine species (*E. argyropus* and *E. pusillus*), raising questions about the observed clustering of these two species ($p < 0.01$; Table 1). Based on Jenkins *et al*. (2010), the probability of isolation-by-distance presence can be increased in respect to a rather large sample size than to e.g. selection of molecular marker (for more details on sampling size per species see Table 1). This deduction is partially corroborated by *E. pusillus*, where two sequences were included from western Mediterranean (Malta and Morocco), a sample rather low comparing to the very distant eastern Mediterranean (29 sequences; the Balkans and Anatolia), indicating an uneven proportion of the samples between west and east. In the other case of species with similar wide range (*E. pulchellus*), we did not observe isolation-by-distance (the number of sequences was 7 from the west and 34 from the east). The sequences of these two species were derived from different peninsulas (e.g. Anatolia, Apennines

etc), known also for their differences in species. Considering this, we claim that the clustering of *E. pusillus* is genuine, and discuss below its spatial genetic patterns ascribed to landscape discontinuities, and not to isolation-by-distance. We argue that the presence of isolation-by-distance in *E. pusillus* might be blunt by increasing the sampling size of the west, and certainly, further studying for this species is encouraged. In the case of *E. argyropus*, things were a little bit different. Again, we had a more condensed sampling size for the west and center (>15 sequences per each, the Balkans) than for the east (3 sequences, Anatolia). An uneven sampling occurred in *E. amoenus* in similar sampling area, however there, we observed one genetic cluster (which was not correlated to presence of isolation-by-distance). The latter fact made us sceptical, and thus, for *E. argyropus*, even that GENELAND analyses indicated three genetic clusters, we consider that there is one genetic cluster due to presence of isolation-by-distance. As for the rest of the datasets, sampling between areas was more equal.

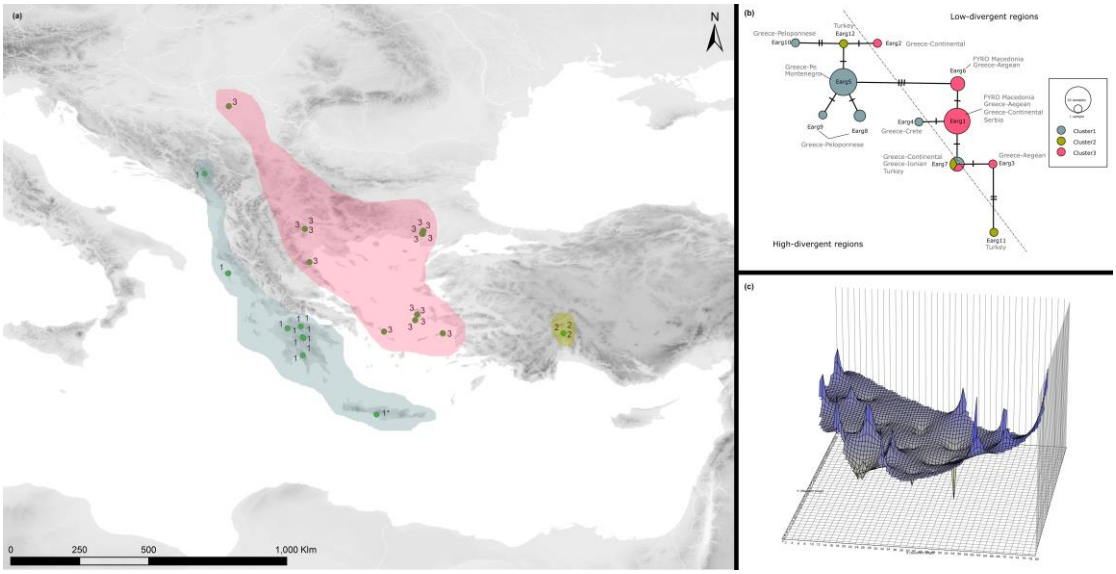

Fig. 3. Analyses of the *E. argyropus* dataset: (a) geographic distribution of the identified clusters, numbers above the circles indicate the cluster membership (asterisk represents individual with low posterior probability clustering, EU307); (b) median-joining network analysis based on the haplotypes, colours of the circles are according to the cluster membership, circle sizes are proportional to haplotype frequencies, number of mutational steps is depicted by lines; and (c) genetic landscape interpolation plot depicting the areas with high- or low-genetic differentiation in relation to the geographic coordinates using a 150×150 grid and a distance weighting parameter α=1. Darker shading and higher peaks show areas of greater genetic diversity.

Σχήμα 3. Αναλύσεις της ομάδας δεδομένων *E. argyropus*: (a) γεωγραφική κατανομή των ταυτοποιημένων κλάδων, οι αριθμοί πάνω από τους κύκλους υποδηλώνουν τον

κλάδο (με αστερίσκο φαίνεται το δείγμα EU307 για το οποίο εξήχθηκε χαμηλή στατιστική υποστήριξη σχετικά με την ομαδοποίησή του)· (b) δίκτυα Σύνδεσης Γειτόνων (NJ) των απλοτύπων, τα χρώματα των κύκλων είναι σύμφωνα με τον κλάδο στον οποίο ανήκουν, το μέγεθος κάθε κύκλου είναι ανάλογο με τη συχνότητα του απλοτύπου (αριθμός ατόμων που έχουν αυτόν τον απλότυπο), ο αριθμός των εξελικτικών βημάτων δίνεται ανά ζεύγος απλοτύπων· και (c) γραφική απεικόνιση του γενετικού τοπίου (genetic landscape interpolation plot) που απεικονίζει περιοχές υψηλής- και χαμηλής-γενετικής διαφοροποίησης σε σχέση με τις γεωγραφικές συντεταγμένες χρησιμοποιώντας 150×150 πλέγμα και παράμετρο σταθμιστικής απόστασης α=1. Οι σκοτεινότερες σκιάσεις δείχνουν περιοχές μεγαλύτερης γενετικής ποικιλότητας.

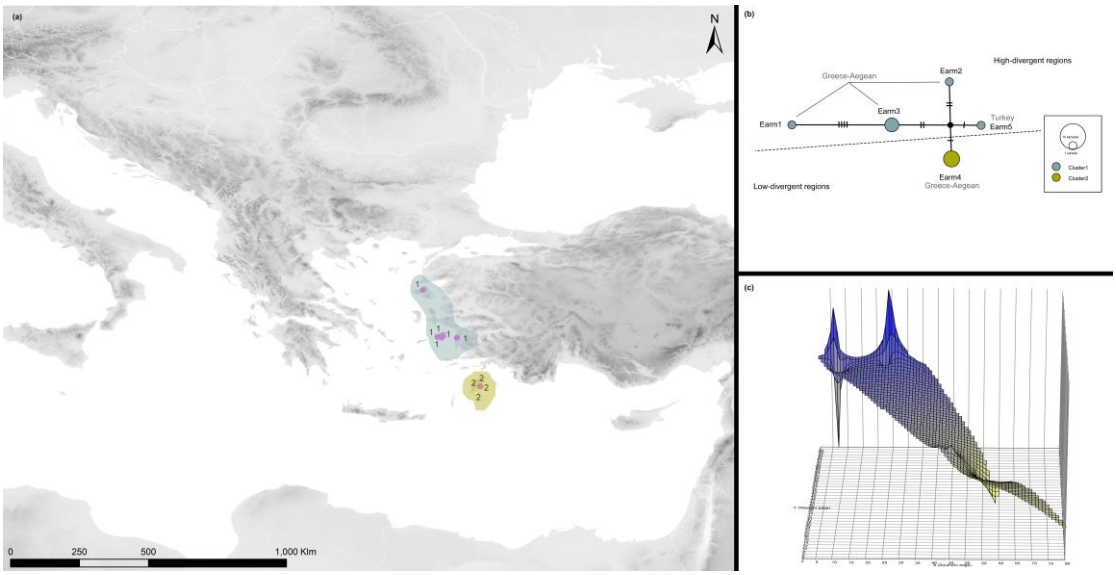

Fig. 4. Analyses of the *E. armatus* dataset: (a) geographic distribution of the identified clusters, numbers above the circles indicate the cluster membership; (b) median-joining network analysis based on the haplotypes, colours of the circles are according to the cluster membership, circle sizes are proportional to haplotype frequencies, number of mutational steps is depicted by lines; and (c) genetic landscape interpolation plot depicting the areas with high- or low-genetic differentiation in relation to the geographic coordinates using a 150×150 grid and a distance weighting parameter α=1. Darker shading and higher peaks show areas of greater genetic diversity.

Σχήμα 4 Αναλύσεις της ομάδας δεδομένων *E. armatus*: (a) γεωγραφική κατανομή των ταυτοποιημένων κλάδων, οι αριθμοί πάνω από τους κύκλους υποδηλώνουν τον κλάδο· (b) δίκτυα Σύνδεσης Γειτόνων (NJ) των απλοτύπων, τα χρώματα των κύκλων είναι σύμφωνα με τον κλάδο στον οποίο ανήκουν, το μέγεθος κάθε κύκλου είναι ανάλογο με τη συχνότητα του απλοτύπου (αριθμός ατόμων που έχουν αυτόν τον απλότυπο), ο αριθμός των εξελικτικών βημάτων δίνεται ανά ζεύγος απλοτύπων· και (c) γραφική απεικόνιση του γενετικού τοπίου (genetic landscape interpolation plot) που απεικονίζει περιοχές υψηλής- και χαμηλής-γενετικής διαφοροποίησης σε σχέση με τις γεωγραφικές συντεταγμένες χρησιμοποιώντας 150×150 πλέγμα και παράμετρο σταθμιστικής απόστασης α=1. Οι σκοτεινότερες σκιάσεις δείχνουν περιοχές μεγαλύτερης γενετικής ποικιλότητας.

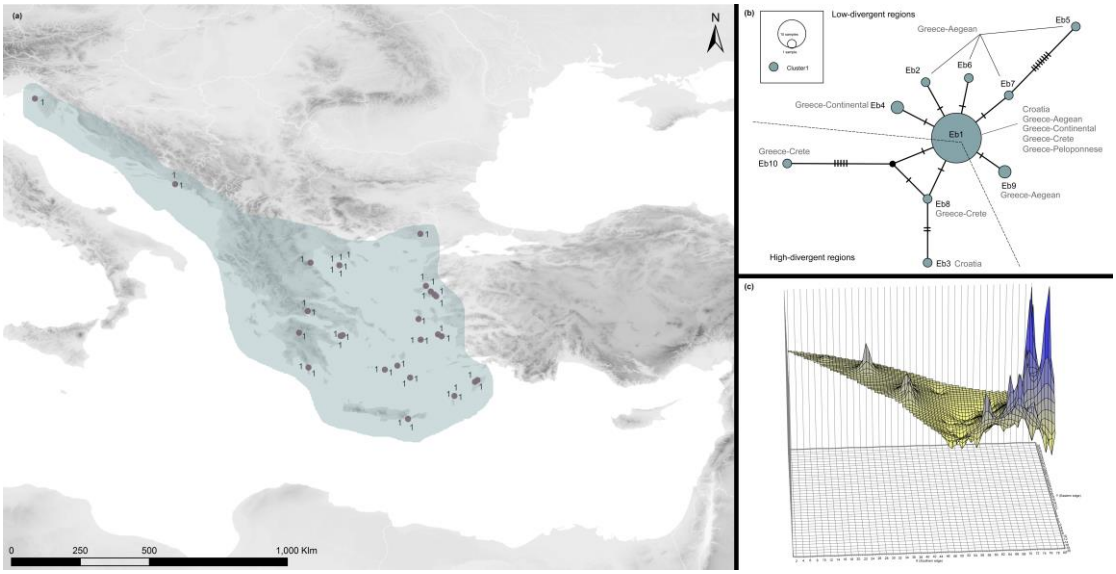

Fig. 5. Analyses of the *E. basalis* dataset: (a) geographic distribution of the identified clusters, numbers above the circles indicate the cluster membership; (b) median-joining network analysis based on the haplotypes, colours of the circles are according to the cluster membership, circle sizes are proportional to haplotype frequencies, number of mutational steps is depicted by lines; and (c) genetic landscape interpolation plot depicting the areas with high- or low-genetic differentiation in relation to the geographic coordinates using a 150×150 grid and a distance weighting parameter α=1. Darker shading and higher peaks show areas of greater genetic diversity.

Σχήμα 5. Αναλύσεις της ομάδας δεδομένων *E. basalis*: (a) γεωγραφική κατανομή των ταυτοποιημένων κλάδων, οι αριθμοί πάνω από τους κύκλους υποδηλώνουν τον κλάδο· (b) δίκτυα Σύνδεσης Γειτόνων (NJ) των απλοτύπων, τα χρώματα των κύκλων είναι σύμφωνα με τον κλάδο στον οποίο ανήκουν, το μέγεθος κάθε κύκλου είναι ανάλογο με τη συχνότητα του απλοτύπου (αριθμός ατόμων που έχουν αυτόν τον απλότυπο), ο αριθμός των εξελικτικών βημάτων δίνεται ανά ζεύγος απλοτύπων· και (c) γραφική απεικόνιση του γενετικού τοπίου (genetic landscape interpolation plot) που απεικονίζει περιοχές υψηλής- και χαμηλής-γενετικής διαφοροποίησης σε σχέση με τις γεωγραφικές συντεταγμένες χρησιμοποιώντας 150×150 πλέγμα και παράμετρο σταθμιστικής απόστασης α=1. Οι σκοτεινότερες σκιάσεις δείχνουν περιοχές μεγαλύτερης γενετικής ποικιλότητας.

The Landscape Shape Interpolation analyses yielded different levels of genetic divergence, indicating high- and low-genetic divergent regions per each species. The genetic diversity appeared to: (1) be homogeneously plain (*E. phaeacus*, Fig. 7c); (2) decrease from (a) northwest (NW) to southeast (SE) (*E. armatus* and *E. clavatus*, Figs 4c & 6c) and (b) SE to NW (*E. basalis*, *E. pulchellus* and *E. pusillus*, Figs 5c, 8c & 9c); (3) present high peaks on east (E) and west (W) with troughs in the center (*E. amoenus* and *E. argyropus*, Figs 2c & 3c); or (4) present high peaks in the center with troughs on E and W (*E. sulcitibius*, Fig. 10c).

Discussion

Notwithstanding the importance of hoverflies in the Mediterranean, the evolutionary processes that stimulated speciation and shaped species distribution are still largely unknown. This brings in the foreground the need for studies in the context of phylogeography and biogeography that could elucidate the role of the Mediterranean on spatial genetic patterns of hoverflies. The current study intends to fill this gap, using for the first time (so far known to the authors) a broad- and large-scale data analysis on the hoverfly genus *Eumerus*. We have implemented DNA barcodes for nine *Eumerus* species sampled throughout the Mediterranean including continental Balkans. Our results show that intraspecific genetic differentiation was successfully related to species distribution. The survey of spatial genetic patterns was confirmed (in four species), and potential high- and low-divergent regions within each of the nine species considered. MtDNA haplotype networks were consistent to spatial patterns and unveiled cases of star-like structuring expansions. Finally, we documented all the results in relevance to landscape discontinuities, presence of isolation-by-distance, evolutionary processes, palaeogeological and palaeoclimatic events.

Spatial genetic patterns

Most variations in genetic cluster structure of the species distributed in the Mediterranean can be anticipated as a consequence of landscape discontinuities that may have facilitated or impeded gene flow, species migration, or species dispersal between individuals from adjacent populations. Species distribution may depend on landscape topography, rendering species prone to population subdivision. The implementation of the spatially-explicit Bayesian clustering of individuals is a powerful tool to indicate contingent genetic clusters. When inferring genetic cluster structure, it is also essential to regard whether the geographical/ physical distance between obtained divides into genetic clusters have affected the pattern of the genetic variation (presence of isolation-by-distance), and to identify the landscape features elevating the 'genetic' barriers.

In order to understand the obtained species population divides into genetic clusters, we firstly need to take a glance in the Mediterranean's history. A blend of palaeogeological and palaeoclimatic events have endured in the Mediterranean and rendered the relief and landscape of the region as complex, with various habitats,

mountain ranges and a plethora of islands and islets (Hewitt, 2011). Everything started with the collision of the African and European plates (65 Mya), where a series of eustatic and tectonic motions generated phenomena of orogenesis (formation of Alps, Dinaric Alps etc), land bridges, sea straits, land configurations and fragmentations (Hewitt, 2011). At the onset of the mid-Miocene (~ 16-12 Mya), the Balkans were connected to Anatolia through the Hellenic Peninsula (Ägäis) (Hewitt, 2011). Four major geological events, from the Miocene (23 Mya) to Holocene (0.0117 Mya to present), are rendered for the fragmentation of Ägäis and consolidation of the Aegean as known today (including the islands of the Archipelago; Lymberakis & Poulakakis, 2010; Kougioumoutzis *et al*., 2017; Sfenthourakis & Triantis, 2017).

The Mediterranean peninsulas played an important role as refugia and natural barriers for species dispersal and colonization during the Pleistocene glaciations, as suggested by a large number of studies postulating the impact of the Quaternary climatic oscillations on species diversity and distribution in the area (e.g. Taberlet *et al*., 1998; Hewitt, 2011; Feliner, 2014). During the glaciations, Central Europe was hostile to most of the species as a cold and dry climate was prevailing. Species relocated towards the southern peninsulas, where the Balkans served as the main refugium, and Apennines and Iberian as subsidiaries (Hewitt, 2011). The peninsulas were isolated during the glacial maxima due to the extended and icy mountain chains, whereas during the warm periods species could move to Central and Northern Europe (Taberlet *et al*., 1998). For example, the Alps caused difficulties to the northward species expansion, isolated species and arise endemism (Taberlet *et al*., 1998) or the Pyrenees have been accused for the same regarding the Iberian populations, even though in a lower extent, in contradistinction to the Balkans (Hewitt 1999, 2000). In the Balkans, species expansion did not face great obstacles, populations could easily move back and forward to the north and hence, many northern populations of today own their origin in the Balkans.

The biogeographical and evolutionary history of all *Eumerus* species studied herewith follows the history of the natural environment. The genetic structure of *E. armatus* was divided in one northern genetic cluster (Lesvos and Samos, East Aegean Islands, Greece; Asia Minor, Turkey) and one southern (Rhodes Island, Greece). The northern genetic cluster can be explained by the fact that East Aegean Islands have been continuously connected to Anatolia until their recent separation (approx. 0.04 Mya; Kougioumoutzis *et al*., 2017). On the other hand, Rhodes was permanently

isolated from Anatolia and all surrounding islands between Pliocene and Pleistocene (Kuss, 1975). We presume that allopatric processes have acted on *E. armatus*, and that genetic degradation of Rhodes' genetic cluster might imply presence of the founder effect or genetic drift.

E. sulcitibius consisted of one western genetic cluster with sequences from two islands of the East Aegean (Lesvos and Chios), three of Cyclades (Andros, Naxos and Paros) and western Crete (Chania and Rethymnon provinces); and one eastern genetic cluster with one sequence from one island of the East Aegean (Samos) and few sequences of eastern Crete (Lasithi province). Considering that the support values inferred from GENELAND for Samos sequence were low, two explanatory scenarios are probable: one that agrees with the GENELAND clustering of the Samos' sequence to the eastern genetic cluster, and one that rejects the clustering, assigning the sequence to the western genetic cluster. There is no landscape or seascape feature that could corroborate the first scenario (i.e. separate Samos from the other East Aegean Islands). We claim that the genetic cluster structure of *E. sulcitibius* is not that apparent, and the pattern might be rectified, and further clarified by adding more sequences derived from Samos and/or from Crete, as well as the in between islands (where/ if the species occurs). We argue that there might be two genetic clusters within Crete (western – eastern), isolated and formed due to the mountains and peripatric processes; evolutionary processes may shape a species genetic structure (e.g. on hedgehogs, Bolfíková *et al*., 2017). At the Pliocene, Crete was composed of at least six islands that corresponded to the current island's mountains which appeared when the island lifted up (during the Pleistocene; Fassoulas, 2001), a palaeogeographical event causing a west-east divide of the populations of *E. sulcitibius* within the island.

The disjunction of *E. pulchellus* and *E. pusillus* into two genetic clusters with a west-east divide was congruent to the expected division of the Mediterranean considering other species distributions (Blondel & Aronson, 1999; Vigna Taglianti *et al.*, 1999). Even though these studies disagree for a strict, accurate delimitation of the Mediterranean, they do agree in the division of the area into two chorotypes: the Eastern part (eastern countries of the Mediterranean, east to the Black Sea and the east of the Italian Peninsula and the Gulf of Sirte) and the Western (western countries of the Mediterranean and west of the Italian Peninsula and the Gulf of Sirte; for more

details see Vigna Taglianti *et al.*, 1999). Here, the Quaternary climatic oscillations might be responsible for the species' divide into two genetic clusters.

Contrary to the aforementioned species, *E. amoenus*, *E. argyropus*, *E. basalis*, *E. clavatus* and *E. phaeacus* displayed one genetic cluster, even though their sampling covered wide and complex geographic regions. The genetic clustering in four of the five species (i.e. except for *E. argyropus*) was not affected from isolation-by-distance between the sampling areas. We postulate that the absence of spatial genetic pattern reflects long term stable populations of these species, and indicate relict or remnant taxa that persisted through all palaeogeological and palaeoclimatic alterations. Relicts, defined by Grandcolas *et al*. (2014) as ''the survivors of clades with a large proportion of extinct members'', can be designated from the perspective of phylogeny (as an indication of long-branch-attraction) or biogeography (once a widespread species, but now with a narrower distribution, often due to the frequent allopatric events).

An important issue to discuss is the sampling size for each dataset. We may not have succeeded to involve specimens from all the regions of each species range (except for *E. phaeacus*), but a thorough insect sampling is often a challenge for scientists. Uncertainty due to low support values was raised in only three specimens (one per species: *E. argyropus*, *E. pulchellus* and *E. sulcitibius*). We entrust the assignment of cluster membership in *E. argyropus* and *E. pulchellus* because they are in accordance to the haplotype networks and to the expectancy of biogeography, but not for *E. sulcitibius*, as explained above.

Are there high- and low- divergent regions?

Disentangling potential spatial genetic patterns in *Eumerus*, we came across with areas of different genetic differentiation of the identified genetic clusters that suggested high- and low- divergent regions (Landscape Shape Interpolation analyses). On the one hand, the Aegean Islands (in particular the East Aegean), Anatolia (except for *E. clavatus*), Croatia (except for *E. basalis*), Malta, Montenegro and Serbia were identified as high-divergent regions in all study species. These are insular and montane regions that are featured with great fragmentation and isolation, both liable factors of restriction of gene flow and increased genetic variability. On the other hand, the Balkans (in particular the Hellenic Peninsula), northern Italy, Morocco and Spain were acknowledged as low-divergent regions for *Eumerus*. The Apennines and the

Balkans are two continental peninsulas where the species movements and gene flow might have been facilitated therein. In both high- and low-divergent regions, landscape discontinuities due to palaeogeological and palaeoclimatic events appear to have impacted the genetic diversity within these nine species of *Eumerus*.

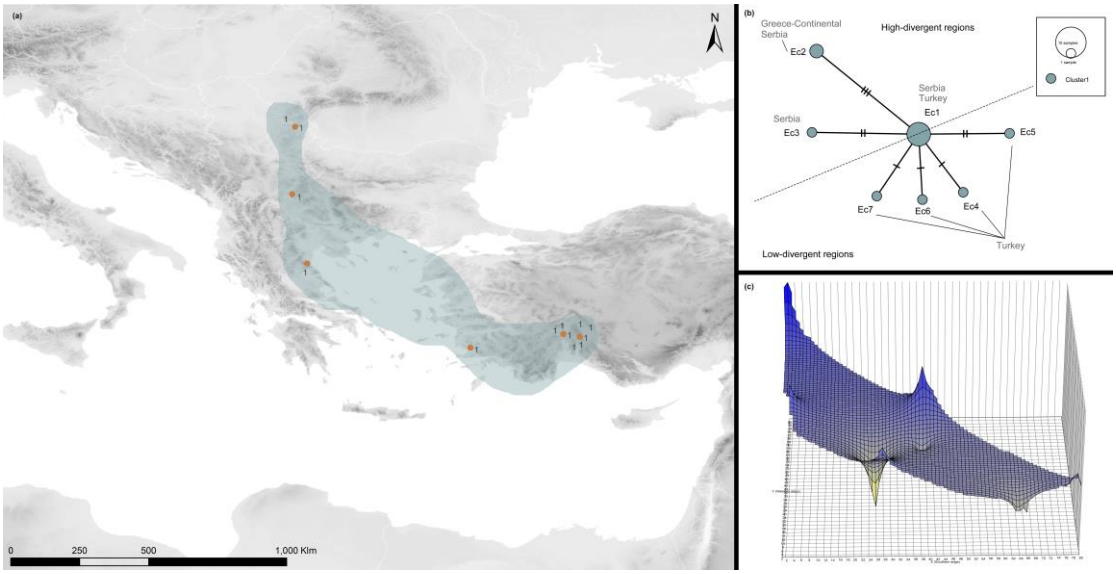

Fig. 6. Analyses of the *E. clavatus* dataset: (a) geographic distribution of the identified clusters, numbers above the circles indicate the cluster membership; (b) median-joining network analysis based on the haplotypes, colours of the circles are according to the cluster membership, circle sizes are proportional to haplotype frequencies, number of mutational steps is depicted by lines; and (c) genetic landscape interpolation plot depicting the areas with high- or low-genetic differentiation in relation to the geographic coordinates using a 150×150 grid and a distance weighting parameter α=1. Darker shading and higher peaks show areas of greater genetic diversity.

Σχήμα 6. Αναλύσεις της ομάδας δεδομένων *E. clavatus*: (a) γεωγραφική κατανομή των ταυτοποιημένων κλάδων, οι αριθμοί πάνω από τους κύκλους υποδηλώνουν τον κλάδο· (b) δίκτυα Σύνδεσης Γειτόνων (NJ) των απλοτύπων, τα χρώματα των κύκλων είναι σύμφωνα με τον κλάδο στον οποίο ανήκουν, το μέγεθος κάθε κύκλου είναι ανάλογο με τη συχνότητα του απλοτύπου (αριθμός ατόμων που έχουν αυτόν τον απλότυπο), ο αριθμός των εξελικτικών βημάτων δίνεται ανά ζεύγος απλοτύπων· και (c) γραφική απεικόνιση του γενετικού τοπίου (genetic landscape interpolation plot) που απεικονίζει περιοχές υψηλής- και χαμηλής-γενετικής διαφοροποίησης σε σχέση με τις γεωγραφικές συντεταγμένες χρησιμοποιώντας 150×150 πλέγμα και παράμετρο σταθμιστικής απόστασης α=1. Οι σκοτεινότερες σκιάσεις δείχνουν περιοχές μεγαλύτερης γενετικής ποικιλότητας.

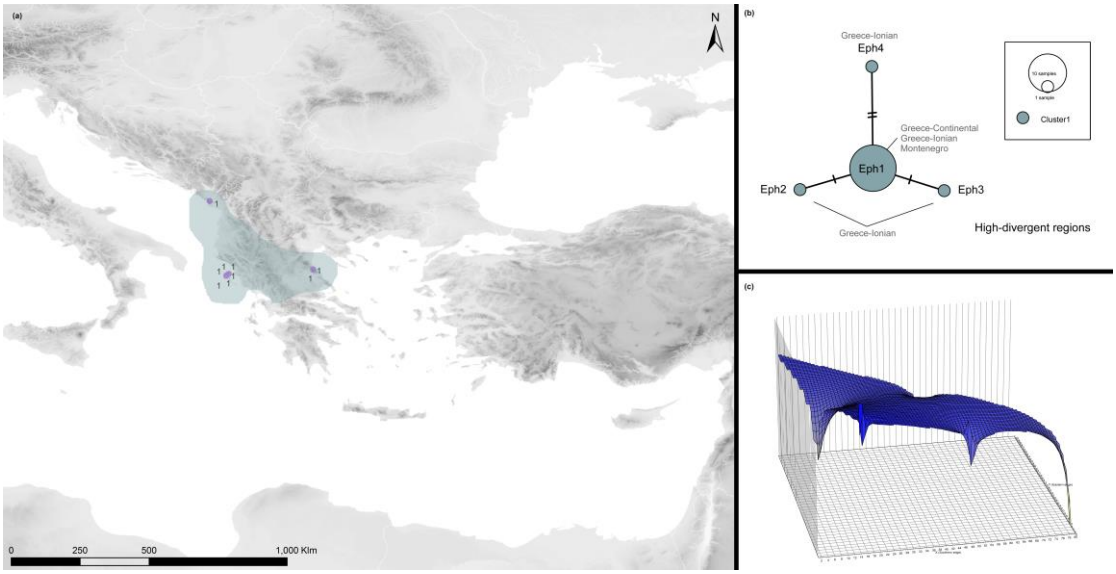

Fig. 7. Analyses of the *E. phaeacus* dataset: (a) geographic distribution of the identified clusters, numbers above the circles indicate the cluster membership; (b) median-joining network analysis based on the haplotypes, colours of the circles are according to the cluster membership, circle sizes are proportional to haplotype frequencies, number of mutational steps is depicted by lines; and (c) genetic landscape interpolation plot depicting the areas with high- or low-genetic differentiation in relation to the geographic coordinates using a 150×150 grid and a distance weighting parameter α=1. Darker shading and higher peaks show areas of greater genetic diversity.

Σχήμα 7. Αναλύσεις της ομάδας δεδομένων *E. phaeacus*: (a) γεωγραφική κατανομή των ταυτοποιημένων κλάδων, οι αριθμοί πάνω από τους κύκλους υποδηλώνουν τον κλάδο· (b) δίκτυα Σύνδεσης Γειτόνων (NJ) των απλοτύπων, τα χρώματα των κύκλων είναι σύμφωνα με τον κλάδο στον οποίο ανήκουν, το μέγεθος κάθε κύκλου είναι ανάλογο με τη συχνότητα του απλοτύπου (αριθμός ατόμων που έχουν αυτόν τον απλότυπο), ο αριθμός των εξελικτικών βημάτων δίνεται ανά ζεύγος απλοτύπων· και (c) γραφική απεικόνιση του γενετικού τοπίου (genetic landscape interpolation plot) που απεικονίζει περιοχές υψηλής- και χαμηλής-γενετικής διαφοροποίησης σε σχέση με τις γεωγραφικές συντεταγμένες χρησιμοποιώντας 150×150 πλέγμα και παράμετρο σταθμιστικής απόστασης α=1. Οι σκοτεινότερες σκιάσεις δείχνουν περιοχές μεγαλύτερης γενετικής ποικιλότητας.

mtDNA haplotype networks

Inferences of mtDNA haplotype networks were congruent to the formation of genetic cluster(s) in the study species of *Eumerus*. An interesting disclosure of the mtDNA haplotype networks (and shared haplotypes) was the delineation of areas where species expansion events and colonizations might have occurred (star-like structuring). The plots from Landscape Shape Interpolation analyses indicated areas with high and low genetic distances, and were auxiliary as to conclude.

More specifically, the mtDNA haplotype network of *E. amoenus* indicated a partial star-like structure (Eam3 haplotype) originated from high-divergent regions (Aegean, the Balkans, Malta and Turkey). Regarding the haplotype network of *E. basalis*, all haplotypes originated from the Eb1 haplotype, which included individuals from the Balkans (Croatia and Hellenic Peninsula; low-divergent regions). Early stages of *E. amoenus* and *E. basalis* have been found to be connected with decayed bulbs or other parts of widely distributed plants, e.g. *E. amoenus* in *Allium* (Alliaceae), potato tubers, watermelon, grapes, rotten paw-paw and damaged rhizomes of *Iris germanica* (Ricarte *et al*., 2008). The shared haplotypes between different sampling areas of *E. amoenus* and *E. basalis* may be the result of trade with their host plants, which can cause gene flow between allopatric populations, and have rendered doubtful to conjecture for the origin of each species expansion.

The star-like structure in the haplotype network of *E. clavatus* resulted from the shared haplotype Ec1 between two distinct geographic areas, with individuals from the Balkans (Serbia) and Turkey (high- and low-divergent regions, respectively). We argue that Turkey may constitute the species origin of *E. clavatus*, and that expansion was promoted towards Central Balkan with the diversification in Turkey to be occurred afterwards. A more extensive sampling that would include more individuals from Greece, and specimens from Bulgaria and Romania could elucidate the migration route of *E. clavatus*, pinpointing whether the migration from Serbia to Turkey has taken place through Greece, Bulgaria or Romania.

Concerning *E. phaeacus*, the star-like structure was due to the Eph1 haplotype with individuals from the Balkans and Ionian Islands (high-divergent regions). Considering that specimens from Ionian displayed higher mitochondrial diversity than specimens from the other two sampling sites (of the Balkan mainland), we posit that the Ionian might be the place of origin of *E. phaeacus*.

The star-like pattern in the haplotype networks can be suggestive of recent or ongoing expansion events (in geological terms) within the genetic cluster/population. In the case of the latter four species, the lack of spatial genetic structure confirms and supports that their dispersal was followed after recent expansion event(s). The high genetic variability reflects a good adaptive potential of the genetic cluster/population. We consider *E. amoenus*, *E. basalis* and *E. phaeacus* as young relicts or neoendemics (a relict is not necessarily an old species or does not always suffer low genetic diversity; Grandcolas *et al*., 2014), a conclusion generated hereabove, whereas we

hesitate to conclude for *E. clavatus* (for reasons explained above). An additional supportive information for *E. phaeacus* as a young relict is that the species is considered of being the source of two more species (speciation event dated at 0.6695 Mya; Chroni *et al*., unpubl.).

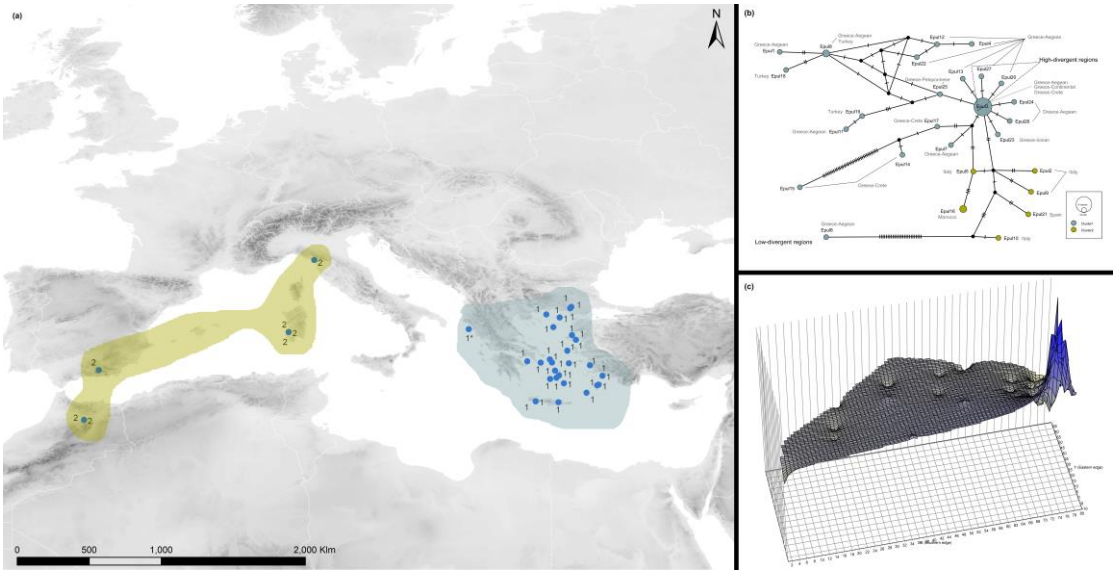

Fig. 8. Analyses of the *E. pulchellus* dataset: (a) geographic distribution of the identified clusters, numbers above the circles indicate the cluster membership (asterisk represents individual with low posterior probability clustering, EU438); (b) median-joining network analysis based on the haplotypes, colours of the circles are according to the cluster membership; circle sizes are proportional to haplotype frequencies, number of mutational steps is depicted by lines; and (c) genetic landscape interpolation plot depicting the areas with high- or low-genetic differentiation in relation to the geographic coordinates using a 150×150 grid and a distance weighting parameter α=1. Darker shading and higher peaks show areas of greater genetic diversity.

Σχήμα 8. Αναλύσεις της ομάδας δεδομένων *E. pulchellus*: (a) γεωγραφική κατανομή των ταυτοποιημένων κλάδων, οι αριθμοί πάνω από τους κύκλους υποδηλώνουν τον κλάδο (με αστερίσκο φαίνεται το δείγμα EU438 για το οποίο εξήχθηκε χαμηλή στατιστική υποστήριξη σχετικά με την ομαδοποίησή του)· (b) δίκτυα Σύνδεσης Γειτόνων (NJ) των απλοτύπων, τα χρώματα των κύκλων είναι σύμφωνα με τον κλάδο στον οποίο ανήκουν, το μέγεθος κάθε κύκλου είναι ανάλογο με τη συχνότητα του απλοτύπου (αριθμός ατόμων που έχουν αυτόν τον απλότυπο), ο αριθμός των εξελικτικών βημάτων δίνεται ανά ζεύγος απλοτύπων· και (c) γραφική απεικόνιση του γενετικού τοπίου (genetic landscape interpolation plot) που απεικονίζει περιοχές υψηλής- και χαμηλής-γενετικής διαφοροποίησης σε σχέση με τις γεωγραφικές συντεταγμένες χρησιμοποιώντας 150×150 πλέγμα και παράμετρο σταθμιστικής απόστασης α=1. Οι σκοτεινότερες σκιάσεις δείχνουν περιοχές μεγαλύτερης γενετικής ποικιλότητας.

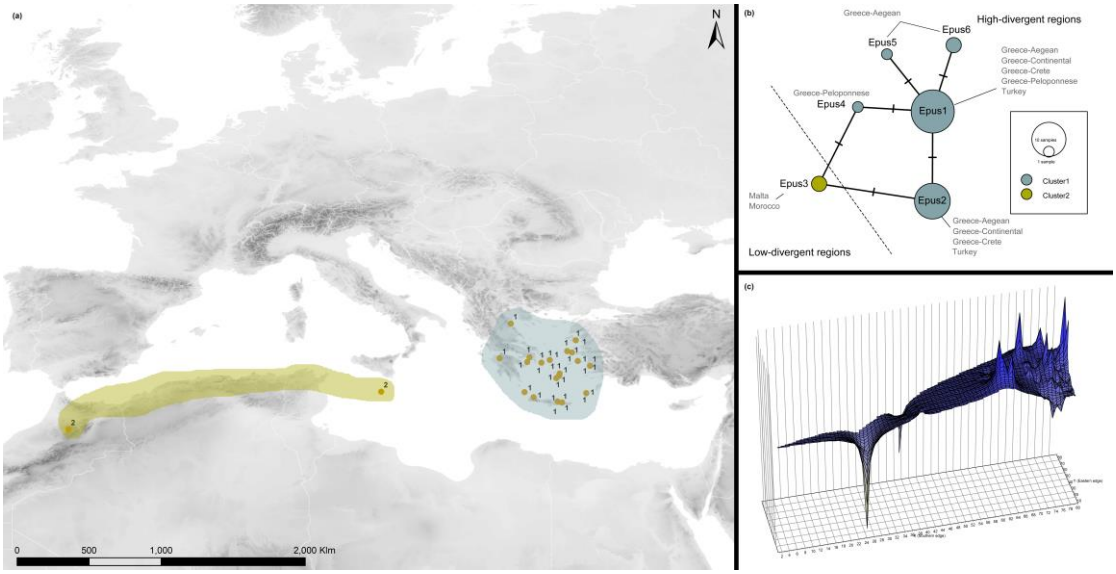

Fig. 9. Analyses of the *E. pusillus* dataset: (a) geographic distribution of the identified clusters, numbers above the circles indicate the cluster membership; (b) median-joining network analysis based on the haplotypes, colours of the circles are according to the cluster membership, circle sizes are proportional to haplotype frequencies, number of mutational steps is depicted by lines; and (c) genetic landscape interpolation plot depicting the areas with high- or low-genetic differentiation in relation to the geographic coordinates using a 150×150 grid and a distance weighting parameter α=1. Darker shading and higher peaks show areas of greater genetic diversity.

Σχήμα 9. Αναλύσεις της ομάδας δεδομένων *E. pusillus*: (a) γεωγραφική κατανομή των ταυτοποιημένων κλάδων, οι αριθμοί πάνω από τους κύκλους υποδηλώνουν τον κλάδο· (b) δίκτυα Σύνδεσης Γειτόνων (NJ) των απλοτύπων, τα χρώματα των κύκλων είναι σύμφωνα με τον κλάδο στον οποίο ανήκουν, το μέγεθος κάθε κύκλου είναι ανάλογο με τη συχνότητα του απλοτύπου (αριθμός ατόμων που έχουν αυτόν τον απλότυπο), ο αριθμός των εξελικτικών βημάτων δίνεται ανά ζεύγος απλοτύπων· και (c) γραφική απεικόνιση του γενετικού τοπίου (genetic landscape interpolation plot) που απεικονίζει περιοχές υψηλής- και χαμηλής-γενετικής διαφοροποίησης σε σχέση με τις γεωγραφικές συντεταγμένες χρησιμοποιώντας 150×150 πλέγμα και παράμετρο σταθμιστικής απόστασης α=1. Οι σκοτεινότερες σκιάσεις δείχνουν περιοχές μεγαλύτερης γενετικής ποικιλότητας.

Conclusion

Overall our study was based on genetic and geographic data, and highlighted the role of allopatric and peripatric evolutionary processes, as well as of landscape discontinuities formed due to palaeogeological events and palaeoclimatic alterations in delineating high- or low-genetic divergent regions in the Mediterranean, and forming spatial genetic clusters within four species (*E. armatus*, *E. pulchellus*, *E. pusillus* and *E. sulcitibius*) of the hoverfly genus *Eumerus*. For the remaining five study species, the identified one genetic cluster pointed into the hypothesis of relict

taxa, and recent or ongoing expansion events were disclosed for these species. We encourage a more comprehensive sampling with more individuals or sampling sites (to corroborate the clustering of *E. clavatus*, *E. pusillus* and *E. sulcitibius*), and further studies, e.g. on demographic and population level, that could assist into clarification of species origin and expansion events.

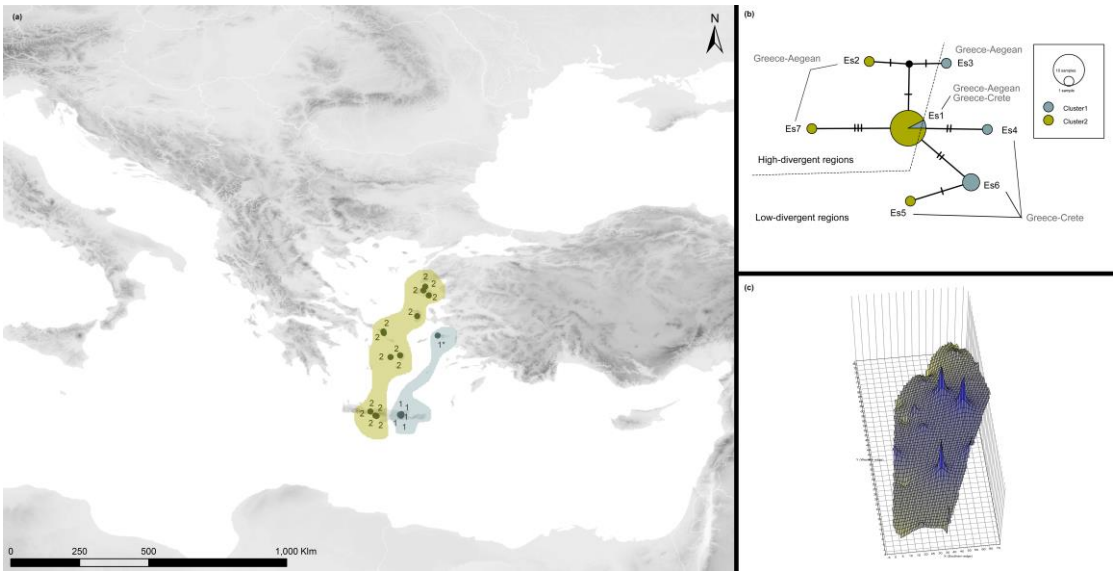

Fig. 10. Analyses of the *E. sulcitibius* dataset: (a) geographic distribution of the identified clusters, numbers above the circles indicate the cluster membership (asterisk represents individual with low posterior probability clustering, EU67); (b) median-joining network analysis based on the haplotypes, colours of the circles are according to the cluster membership, circle sizes are proportional to haplotype frequencies, number of mutational steps is depicted by lines; and (c) genetic landscape interpolation plot depicting the areas with high- or low-genetic differentiation in relation to the geographic coordinates using a 150×150 grid and a distance weighting parameter α=1. Darker shading and higher peaks show areas of greater genetic diversity.

Σχήμα 10. Αναλύσεις της ομάδας δεδομένων *E. sulcitibius*: (a) γεωγραφική κατανομή των ταυτοποιημένων κλάδων, οι αριθμοί πάνω από τους κύκλους υποδηλώνουν τον κλάδο (με αστερίσκο φαίνεται το δείγμα EU67 για το οποίο εξήχθηκε χαμηλή στατιστική υποστήριξη σχετικά με την ομαδοποίησή του)· (b) δίκτυα Σύνδεσης Γειτόνων (NJ) των απλοτύπων, τα χρώματα των κύκλων είναι σύμφωνα με τον κλάδο στον οποίο ανήκουν, το μέγεθος κάθε κύκλου είναι ανάλογο με τη συχνότητα του απλοτύπου (αριθμός ατόμων που έχουν αυτόν τον απλότυπο), ο αριθμός των εξελικτικών βημάτων δίνεται ανά ζεύγος απλοτύπων· και (c) γραφική απεικόνιση του γενετικού τοπίου (genetic landscape interpolation plot) που απεικονίζει περιοχές υψηλής- και χαμηλής-γενετικής διαφοροποίησης σε σχέση με τις γεωγραφικές συντεταγμένες χρησιμοποιώντας 150×150 πλέγμα και παράμετρο σταθμιστικής απόστασης α=1. Οι σκοτεινότερες σκιάσεις δείχνουν περιοχές μεγαλύτερης γενετικής ποικιλότητας.

Acknowledgments

Financial support was provided by the (a) Ministry of Education, Science and Technological Development, Republic of Serbia, Grant No. 43002 and Grant No. 173002, and (b) European Union (European Social Fund – ESF) and Greek national funds through the Operational Program 'Education and Lifelong Learning' of the National Strategic Reference Framework (NSRF) – Research Funding Program: THALES. Investing in knowledge society through the European Social Fund. We also acknowledge the Program «Grants IKY» of the State Scholarships Foundation of Greece, in the frame of the OP «Education and Lifelong Learning» of the European Social Fund (ESF) – NSRF, 2007–2013 (contract WP2-SHORT TERMS-19348), as a partial financial support of the PhD thesis of AC. We kindly thank George Tataris for his assistance in constructing the maps.

References

Avise, J.C. (2009) Phylogeography: retrospect and prospect. *Journal of Biogeography*, **36**(1), 3–15.

Avise, J.C., Arnold, J., Ball, R.M., Bermingham, E., Lamb, T., Neigel, J.E., Reeb, C.A. & Saunders, N.C. (1987) Intraspecific phylogeography: the mitochondrial DNA bridge between population genetics and systematics. *Annual Review of Ecology, Evolution, and Systematics*, **18**, 489–522.

Bandelt, H., Forster, P. & Röhl, A. (1999). Median-joining networks for inferring intraspecific phylogenies. *Molecular Biology and Evolution*, **16**(1), 37–48.

Barros, T., Cushman, S.A., Carvalho, J. & Fonseca, C. (2016) Mediterranean scrubland and elevation drive gene flow of a Mediterranean carnivore, the Egyptian mongoose *Herpestes ichneumo*n (Herpestidae). *Biological Journal of the Linnean Society*, **120**(1), 195–209.

Blondel, J. & Aronson, J. (1999) Biology and wildlife of the Mediterranean region. Oxford University Press, USA.

Bolfíková, B.Č., Eliášová, K., Loudová, M., Kryštufek, B., Lymberakis, P., Sándor, A.D. & Hulva P. (2017) Glacial allopatry vs. postglacial parapatry and peripatry: the case of hedgehogs. *PeerJ*, 5, e3163, https://doi.org/10.7717/peerj.3163.

Chan, L.M., Brown, J.L. & Yoder, A.D. (2011) Integrating statistical genetic and geospatial methods brings new power to phylogeography. *Molecular phylogenetics and evolution*, **59**(2), 523–537.

Chen, H., Rangasamy, M,. Tan, S.Y., Wang, H.C. & Siegfried, B.D. (2010) Evaluation of Five Methods for Total DNA Extraction from Western Corn Rootworm Beetles. *PLoS One*, **5**(8), 1–6.

Chroni, A., Djan, M., Vidaković, D.O., Petanidou, T. & Vujić, A. (2017) Molecular species delimitation in the genus *Eumerus* (Diptera: Syrphidae). *Bulletin of the Entomological Research*, **107**(1), 126–138.

Fassoulas, C. (2001) The tectonic development of a Neogene basin at the leading edge of the active European margin: the Heraklion basin, Crete, Greece. *Journal of Geodynamics*, **31**, 49–70.

Feliner, G.N. (2014) Patterns and processes in plant phylogeography in the Mediterranean Basin. A review. *Perspectives in Plant Ecology, Evolution and Systematics*, **16**(5), 265–278.

Folmer, O., Black, M., Hoeh, W., Lutz, R. & Vrijenhoek, R. (1994) DNA primers for amplification of mitochondrial cytochrome c oxidase subunit I from diverse metazoan invertebrates. *Molecular Marine Biology and Biotechnology*, **3**, 294–299.

Gorr, W.L., & Kurland, K.S. (2012). GIS tutorial for crime analysis. Redlands, CA: Esri Press.

Grandcolas, P., Nattier, R. & Trewick, S. (2014) Relict species: a relict concept?. *Trends in ecology & evolution*, **29**(12), 655–663.
Grković, A., Vujić, A., Chroni, A., van Steenis, J., Đan, M. & Radenković, S. (2017) Taxonomy and systematics of three species of the genus Eumerus Meigen, 1822 (Diptera: Syrphidae) new in southeastern Europe. *Zoologischer Anzeiger*, **270**, 176–192, https://doi.org/10.1016/j.jcz.2017.10.007.
Grković, A., Vujić, A., Radenković, S., Chroni, A. & Petanidou, T. (2015) Diversity of the genus *Eumerus* Meigen (Diptera, Syrphidae) on the eastern Mediterranean islands with description of three new species. *Annales de la Société entomologique de France*, **51**, 361–373.
Guillot, G., Mortier, F. & Estoup, A. (2005) Geneland: a computer package for landscape genetics. *Molecular Ecology Notes*, **5**, 712–715.
Hall, T.A. (1999) BioEdit: a user-friendly biological sequence alignment editor and analysis program for Windows 95/98/NT. *Nucleic Acids Symposium Series*, **41**, 95–98.
Hewitt, G.M. (2011) Mediterranean Peninsulas: The Evolution of Hotspots. In: Zachos F., Habel J. (eds) Biodiversity Hotspots. Springer, Berlin, Heidelberg.
Hewitt, G.M. (2000) The genetic legacy of the Quaternary ice ages. *Nature*, **405**(6789), 907.
Hewitt, G.M. (1999) Post-glacial re-colonization of European biota. *Biological journal of the Linnean Society*, **68**(1-2), 87–112.
Hughes, P.D., Woodward, J.C. & Gibbard, P.L. (2006) Quaternary glacial history of the Mediterranean mountains. *Progress in physical geography*, **30**(3), 334–364.
Jenkins, D.G., Carey, M., Czerniewska, J., Fletcher, J., Hether, T., Jones, A., Knight, S., Knox, J., Long, T., Mannino, M. & McGuire, M. (2010) A meta-analysis of isolation by distance: relic or reference standard for landscape genetics?. *Ecography*, **33**(2), 315–320.
Katoh, K., Kuma, K., Toh, H. & Miyata, T. (2005) MAFFT version 5: improvement in accuracy of multiple sequence alignment. *Nucleic Acids Research*, **33**, 511–518.
Kougioumoutzis, K., Valli, A.T., Georgopoulou, E., Simaiakis, S., Triantis, K.A. & Trigas, P. (2017) Network biogeography of a complex island system: the Aegean archipelago revisited. *Journal of Biogeography*, **44**(3), 651–660.
Kuss, S.E. (1975) Die pleistozanen Hirsche der ostmediterranen Inseln Kreta, Kasos, Karpathos und Rhodos (Griechenland). *Berichte der Naturforschenden Gesellschaft zu Freiburg im Breisgau*, **65**, 25–79.
Librado, P. & Rozas, J. (2009) DnaSP v5: a software for comprehensive analysis of DNA polymorphism data. *Bioinformatics*, **25**, 1451–1452.
Lymberakis, P. & Poulakakis, N. (2010) Three continents claiming an archipelago: the evolution of Aegean's herpetofaunal diversity. *Diversity*, **2**(2), 233–255.
Mantel, N. (1967) The detection of disease clustering and a generalized regression approach. *Cancer Research*, **27**, 209–220.
Médail F. & Myers N. (2004) Mediterranean Basin. In: Mittermeier R.A., Robles Gil P., Hoffmann M., Pilgrim J., Brooks T., Mittermeier C.G., Lamoreux J. & da Fonseca G.A.B. (eds.). Hotspots revisited: Earth's biologically richest and most endangered terrestrial ecoregions. CEMEX (Monterrey), Conservation International (Washington) & Agrupación Sierra Madre (Mexico), pp.144–147.
Milankov, V., Ludoški, J., Francuski, L., Ståhls, G. & Vujić, A. (2013) Genetic and phenotypic diversity patterns in *Merodon albifrons* Meigen, 1822 (Diptera: Syrphidae): evidence of intraspecific spatial and temporal structuring. *Biological Journal of the Linnean Society*, **110**(2), 257–80.
Miller, M.P. (2005) Alleles In Space: Computer software for the joint analysis of interindividual spatial and genetic information. *Journal of Heredity*, **96**, 722–724.
Radenković, S., Šašić Zorić, L., Djan, M., Obreht Vidaković, D., Ačanski, J., Ståhls, G., Veličković, N., Markov, Z., Petanidou, T., Kočiš Tubić, N. & Vujić, A. (2017) Cryptic speciation in the *Merodon luteomaculatus* complex (Diptera: Syrphidae) from the eastern Mediterranean. *Journal of Zoological Systematics and Evolutionary Research*, 1–22.

Ricarte, A., Marcos-García, M.A. & Rotheray, G.E. (2008) The early stages and life histories of three *Eumerus* and two *Merodon* species (Diptera: Syrphidae) from the Mediterranean region. *Entomologica Fennica*, **19**(2).

Ronquist, F. (1997) Dispersal-vicariance analysis: a new approach to the quantification of historical biogeography. *Systematic Biology*, **46**(1), 195–203.

Rotheray, G.E. & Gilbert, F. (2011) The Natural History of Hoverflies. UK, Ceredigion.

Safner, T., Miller, M.P., McRae, B.H., Fortin, M.J. & Manel, S. (2011) Comparison of Bayesian clustering and edge detection methods for inferring boundaries in landscape genetics. *International Journal of Molecular Sciences*, **12**(2), 865–89.

Sanmartín, I. (2012) Historical biogeography: evolution in time and space. *Evolution: Education and Outreach*, **5**(4), 555–568.

Šašić, L., Ačanski, J., Vujić, A., Ståhls, G., Radenković, S., Milić, D., Vidaković, D.O. & Đan M. (2016) Molecular and Morphological Inference of Three Cryptic Species within the *Merodon aureus* Species Group (Diptera: Syrphidae). *PLoS ONE*, **11**(8), e0160001.

Speight, M.C.D. (2016) Species accounts of European Syrphidae (Diptera). Syrph the Net, the database of European Syrphidae. Dublin. 93: Syrph the Net publications pp. 288.

Ståhls, G., Vujić, A., Petanidou, T., Cardoso, P., Radenković, S., Ačanski, J., Pérez Bañón, C. & Rojo, S. (2016) Phylogeographic patterns of *Merodon* hoverflies in the Eastern Mediterranean region: revealing connections and barriers. *Ecology and evolution*, **6**(7), 2226–2245.

Taberlet, P., Fumagalli, L., Wust-Saucy, A.G. & Cosson, J.F. (1998) Comparative phylogeography and postglacial colonization routes in Europe. *Molecular ecology*, **7**(4), 453–464.

Vigna Taglianti, A., Audisio, P.A., Biondi, M., Bologna, M.A., Carpaneto, G.M., De Biase, A., Fattorini, S., Piattella, E., Sindaco, R., Venchi, A. & Zapparoli, M. (1999) A proposal for a chorotype classification of the Near East fauna, in the framework of the Western Palearctic region. *Biogeographia*, 20.

Vogiatzakis, I. N., Mannion, A. M., & Sarris, D. (2016) Mediterranean island biodiversity and climate change: the last 10,000 years and the future. *Biodiversity and conservation*, **25**(13), 2597–2627.

Vujić, A., Petanidou, T., Tscheulin, T., Cardoso, P., Radenković, S., Ståhls, G., Baturan, Ž., Mijatović, G., Rojo, S., Pérez-Bañón, C., Devalez, J. Andrić, A., Jovičić, S., Krašić, D., Markov, Z., Radišić, D. & Tataris, G. (2016) Biogeographical patterns of the genus *Merodon* Meigen, 1803 (Diptera: Syrphidae) in islands of the eastern Mediterranean and adjacent mainland. *Insect Conservation and Diversity*, **9**(3), 181–191.

Wright, S. (1943) Isolation by distance. *Genetics*, **28**, 114–138.

Biosketches

Antonia Chroni is a PhD student at University of the Aegean (Greece). This study is part of her dissertation. AC is interested in molecular taxonomy, phylogenesis, phylogeography, spatial population genetics and biodiversity conservation, currently focusing on the hoverfly genus, *Eumerus* (Diptera: Syrphidae) in the Mediterranean Basin and the Balkans. All authors share a common interest in general evolutionary biology and biogeography.

Author contributions: A.C., A.V., T.P. designed the study; A.C., L.S.Z., N.K.T. conducted the DNA analyses; A.C., M.S., M.D. analysed the data; A.C. wrote the paper; A.V., T.P. directed data collection and collected specimens; and A.V., M.D., T.P., A.C. obtained funding for the project. All authors read, commented on and approved the final version.

Data archiving statement

All sequence data generated in the current study are archived on GenBank (https://www.ncbi.nlm.nih.gov/genbank/) under the accession numbers: KX083350–KX083358, KX083364, KX083366, KX083385, KX083387; KY272853–KY272855; KY865446, KY865448, KY865453, KY865454, KY865456, KY865461, KY865462, KY865464, KY865468–KY865482; and MG559809–MG560043.

Supplementary information

SI CHAPTER 2

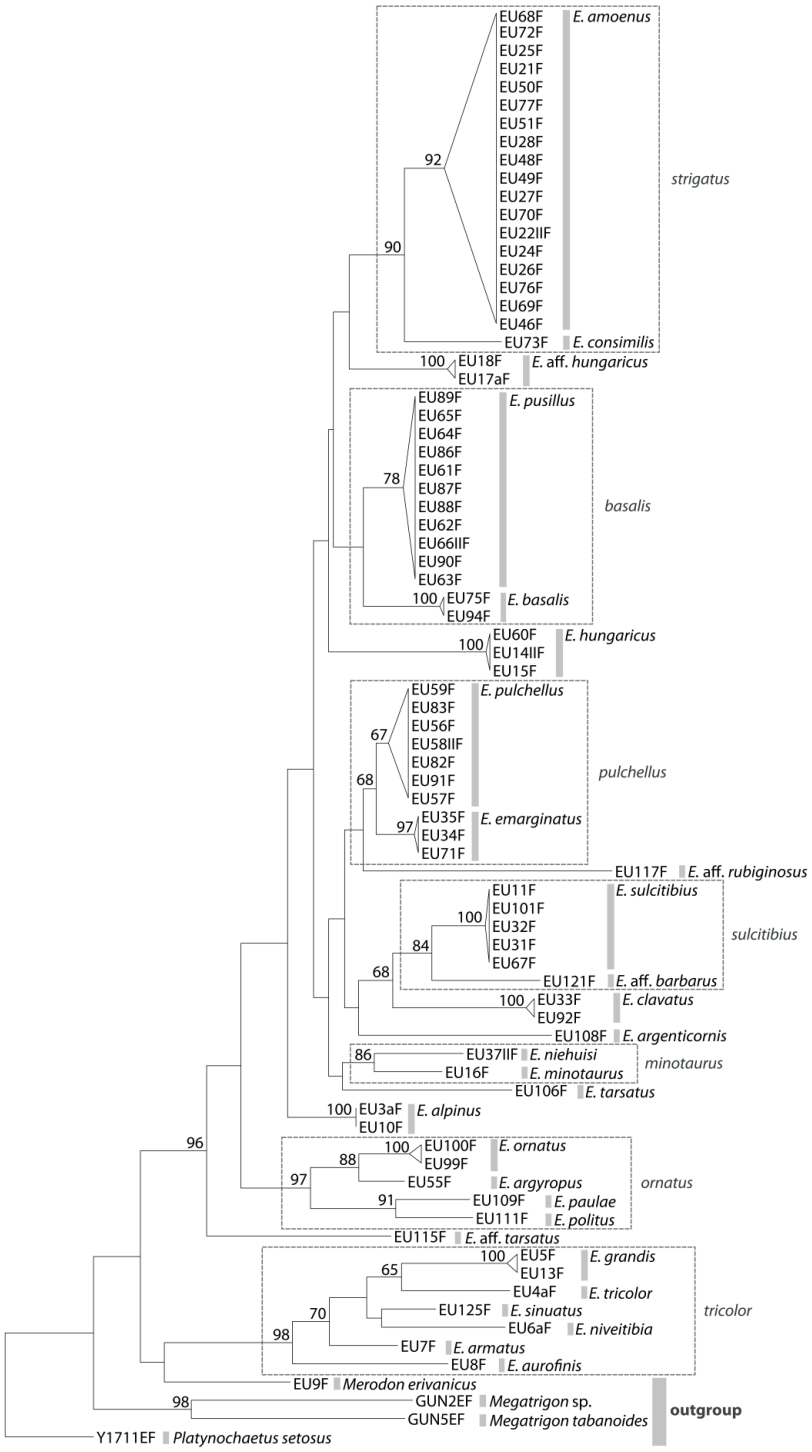

Fig. S1. Maximum likelihood analysis of the dataset A: Forward sequencing of the COI-3' region, 79 sequences, total sequence length 647 bp. Values above branches (>50) indicate bootstrap replicates.

Σχήμα S1. Αποτελέσματα ανάλυσης με την μέθοδο της Μέγιστης Πιθανοφάνειας (ML) για την ομάδα δεδομένων A: αλληλούχιση με εμπρόσθιο εκκινητή της COI-3' κωδικής περιοχής, 79 αλληλουχίες, συνολικό μήκος αλληλουχιών 647 bp. Για να ελεγχθεί η στατιστική στήριξη των κλάδων, πραγματοποιήθηκαν 1000 επαναλήψεις bootstrap, των οποίων οι τιμές παρουσιάζονται πάνω από τους κλάδους του ML δέντρου (μόνον τιμές μεγαλύτερες του 50).

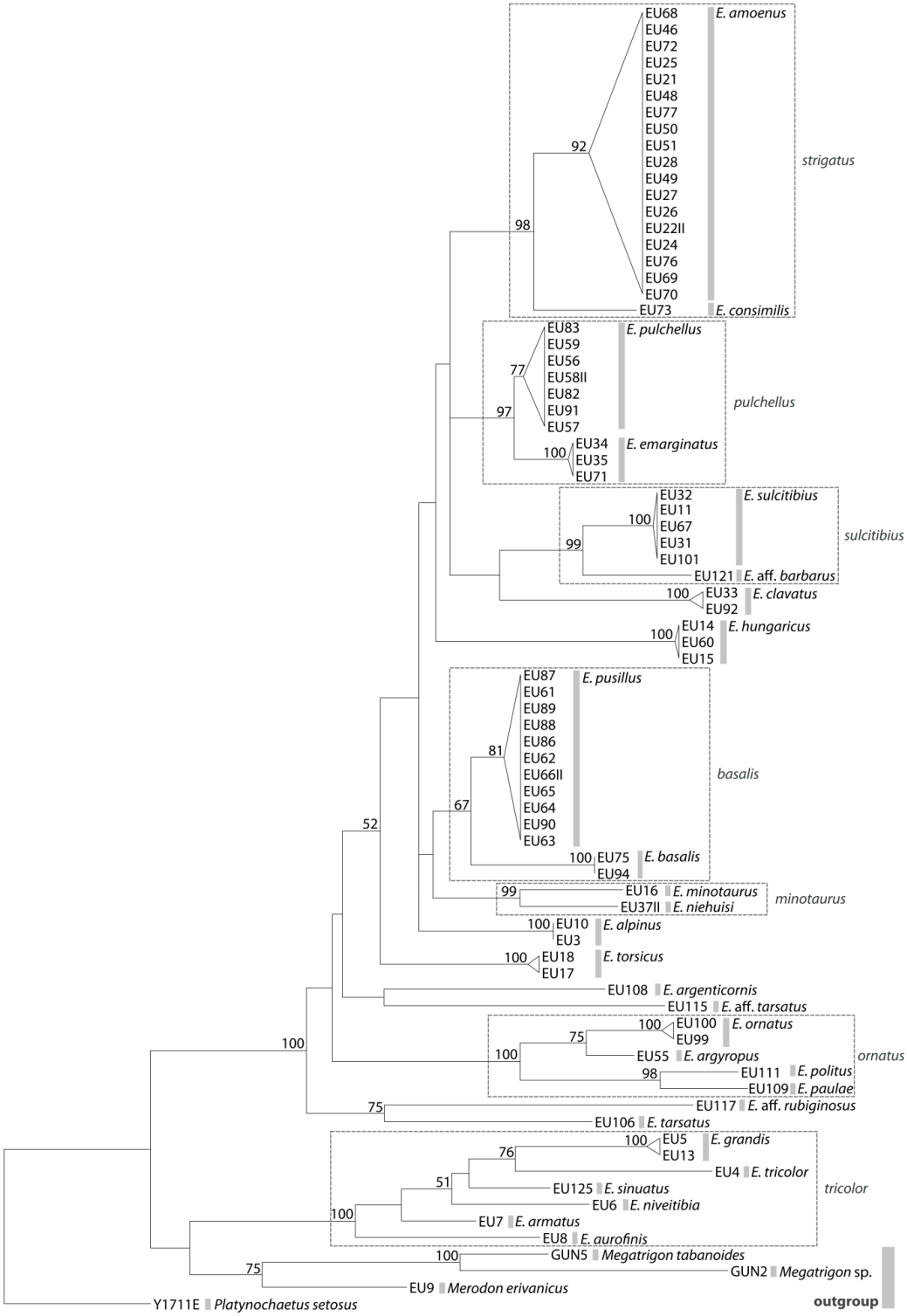

Fig. S2. Maximum likelihood analysis of the dataset B: Bidirectional sequencing of the COI-3' region, 79 sequences, total sequence length 746 bp. Values above branches (>50) indicate bootstrap replicates.

Σχήμα S2. Αποτελέσματα ανάλυσης με την μέθοδο της Μέγιστης Πιθανοφάνειας (ML) για την ομάδα δεδομένων B: αμφίδρομη αλληλούχιση της COI-3' κωδικής περιοχής, 79 αλληλουχίες, συνολικό μήκος αλληλουχιών 746 bp. Για να ελεγχθεί η στατιστική στήριξη των κλάδων, πραγματοποιήθηκαν 1000 επαναλήψεις bootstrap, των οποίων οι τιμές παρουσιάζονται πάνω από τους κλάδους του ML δέντρου (μόνον τιμές μεγαλύτερες του 50).

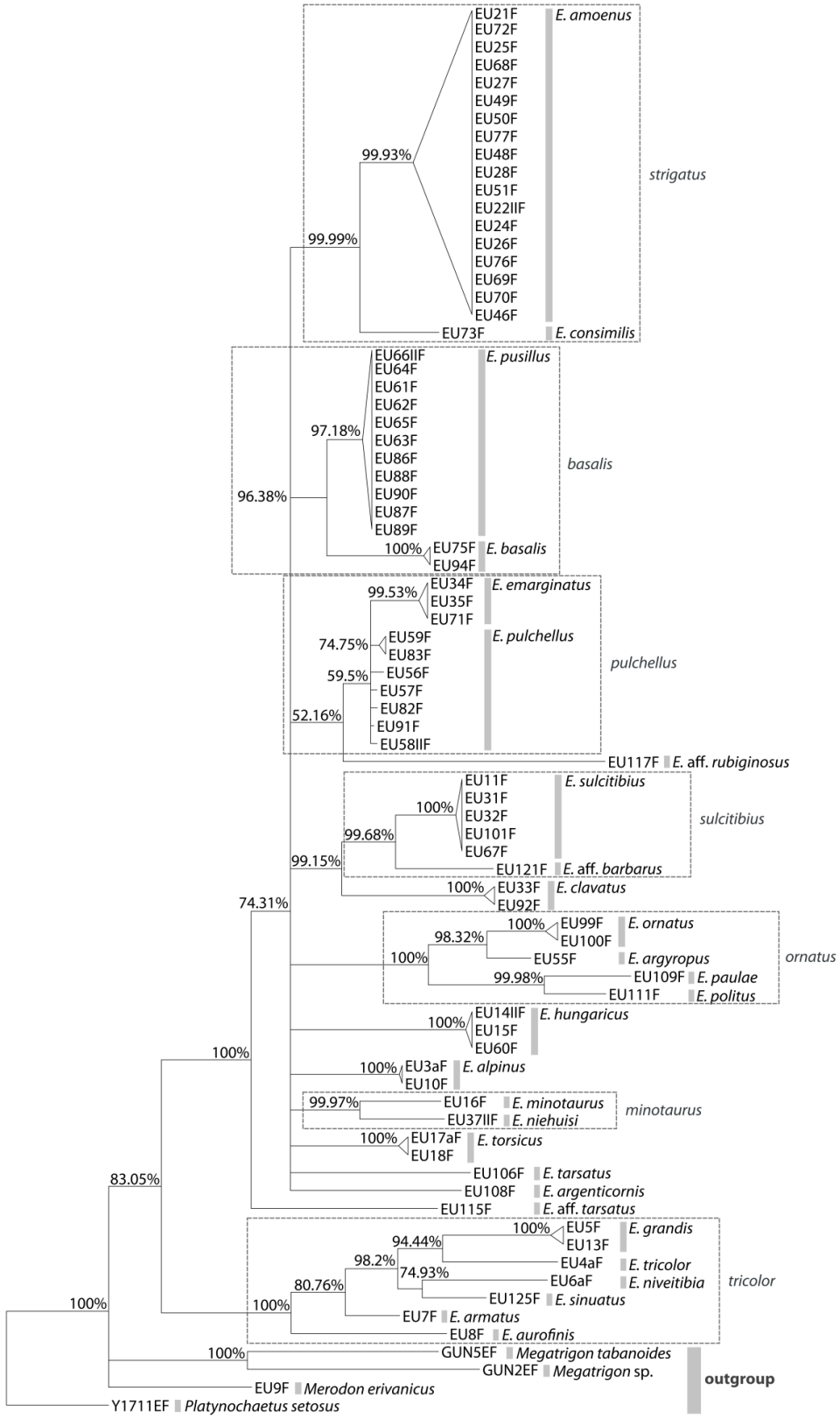

Fig. S3. Bayesian analysis of the dataset A (non-partitioned data). Values indicate Bayesian probability.

Σχήμα S3. Αποτελέσματα ανάλυσης με την μέθοδο της Μπεϊεσιανής Συμπερασματολογίας (BI) για την ομάδα δεδομένων A (μη-διαχωρισμός δεδομένων). Οι αριθμοί στους κλάδους δηλώνουν τις εκ των υστέρων πιθανότητες.

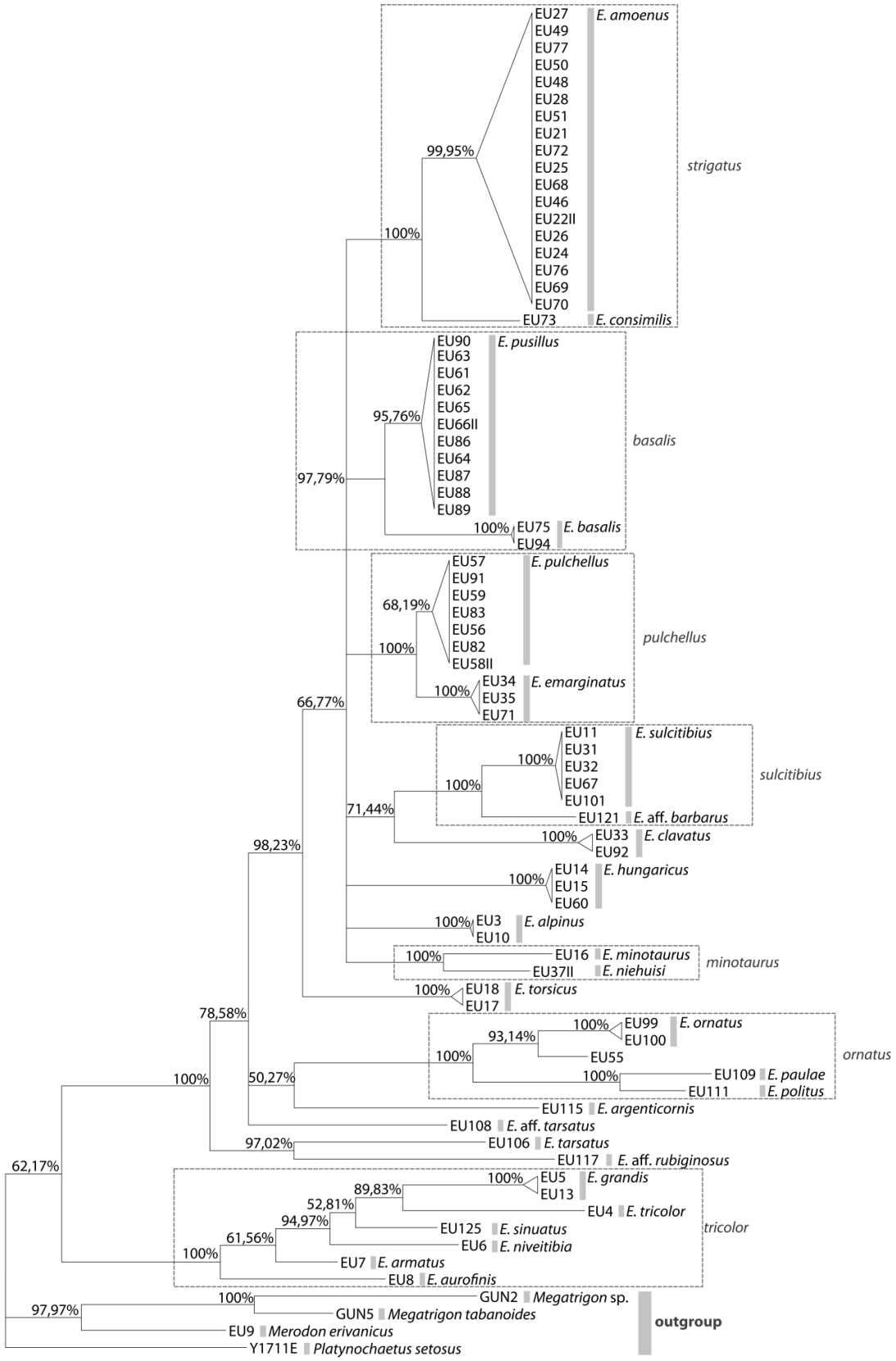

Fig. S4. Bayesian analysis of the dataset B (non-partitioned data). Values indicate Bayesian probability.

Σχήμα S4. Αποτελέσματα ανάλυσης με την μέθοδο της Μπεϊεσιανής Συμπερασματολογίας (BI) για την ομάδα δεδομένων B (μη-διαχωρισμός δεδομένων). Οι αριθμοί στους κλάδους δηλώνουν τις εκ των υστέρων πιθανότητες.

Table S1. List of the study samples: sequence ID and specimen voucher (M-UAegean: collection of the Melissotheque of the Aegean located at the University of the Aegean, Greece; FSUNS: Faculty of Sciences at the Department of Biology and Ecology of the University of Novi Sad, Serbia; and MZH: Insect collection of the Zoology unit, Finnish Museum of Natural History, Helsinki, Finland) together with details on the specimen origin. GenBank accession numbers are also given (in boldface: newly generated sequences within this study).

Πίνακας S1. Κατάλογος των δειγμάτων των εντόμων: κωδικός αριθμός αλληλουχίας, κωδικός αριθμός δείγματος και πληροφορίες σχετικές με την προέλευση του δείγματος (M-UAegean: Μελισσοθήκη του Αιγαίου, Πανεπιστήμιο του Αιγαίου, Μυτιλήνη, Ελλάδα· FSUNS: Σχολή Θετικών Επιστημών, Τμήμα Βιολογίας και Οικολογίας, Πανεπιστήμιο του Νόβι Σαντ, Σερβία· και MZH: Εντομολογική συλλογή, Φινλανδικό Μουσείο Φυσικής Ιστορίας, Ελσίνκι, Φινλανδία). Δίνονται οι κωδικοί καταχώρησης στη βάση δεδομένων GenBank (με έντονη γραμματοσειρά: αλληλουχίες οι οποίες παρήχθησαν στην παρούσα μελέτη).

Sequence ID	Specimen voucher	Accession no	Genus	Species name	Country	Nearest place name
EU10	FSUNS:G1147	**KT157845**	*Eumerus*	*alpinus* Rondani, 1857	Italy	Toscana
EU100	FSUNS:G0279	**KT157904**	*Eumerus*	*ornatus* Meigen, 1822	Montenegro	Boka Kotorska
EU101	FSUNS:G2250	**KT157875**	*Eumerus*	*sulcitibius* Rondani, 1868	Greece	Lesvos
EU106	FSUNS:G2208	**KT157908**	*Eumerus*	*tarsatus* Lyneborg, in litt.	South Africa	KwaZulu-Natal
EU108	FSUNS:05772	**KT157907**	*Eumerus*	*argenticornis* Lyneborg, in litt.	South Africa	KwaZulu-Natal
EU109	FSUNS:G2106	**KT157905**	*Eumerus*	*paulae* Herve-Bazin, 1913	South Africa	KwaZulu-Natal
EU11	FSUNS:G3002	**KT157871**	*Eumerus*	*sulcitibius* Rondani, 1868	Greece	Andros
EU111	FSUNS:G2117	**KT157906**	*Eumerus*	*politus* Lyneborg, in litt.	South Africa	KwaZulu-Natal
EU115	FSUNS:G2104	**KT157915**	*Eumerus*	aff. *tarsatus* Lyneborg, in litt.	South Africa	KwaZulu-Natal
EU117	FSUNS:G2101	**KT157909**	*Eumerus*	aff. *rubiginosus* Lyneborg, in litt.	South Africa	KwaZulu-Natal
EU121	FSUNS:Đ38	**KT157876**	*Eumerus*	aff. *barbarus* Coquebert, 1804	Morocco	Middle Atlas
EU125	M-UAegean:G2735	**KT157917**	*Eumerus*	*sinuatus* Loew, 1855	Serbia	Fruska Gora

EU13	FSUNS:G1919	**KT157912**	*Eumerus*	*grandis* Meigen, 1822	Serbia	Đerdap
EU14	FSUNS:G1920	**KT157899**	*Eumerus*	*hungaricus* Szilady, 1940	Serbia	Đerdap
EU15	FSUNS:G1917	**KT157900**	*Eumerus*	*hungaricus* Szilady, 1940	Serbia	Đerdap
EU16	FSUNS:G0278	**KT157869**	*Eumerus*	*minotaurus* Claussen & Lucas, 1988	Greece	Mt Olympus
EU17	FSUNS:UOTA_MEL0746	**KT157916**	*Eumerus*	*torsicus* Grković & Vujić, 2015	Greece	Chios
EU18	FSUNS:UOTA_MEL0744	**KT157896**	*Eumerus*	*torsicus* Grković & Vujić, 2015	Greece	Chios
EU21	FSUNS:0731	**KT157877**	*Eumerus*	*amoenus* Loew, 1848	Greece	Chios
EU22	FSUNS:1017	**KT157888**	*Eumerus*	*amoenus* Loew, 1848	Greece	Dadia
EU24	FSUNS:0900	**KT157889**	*Eumerus*	*amoenus* Loew, 1848	Greece	Karpathos
EU25	FSUNS:G2220	**KT157887**	*Eumerus*	*amoenus* Loew, 1848	Montenegro	Boka Kotorska
EU26	FSUNS:G2258	**KT157891**	*Eumerus*	*amoenus* Loew, 1848	Greece	Lesvos
EU27	FSUNS:G2260	**KT157879**	*Eumerus*	*amoenus* Loew, 1848	Greece	Lesvos
EU28	FSUNS:G2262	**KT157880**	*Eumerus*	*amoenus* Loew, 1848	Greece	Lesvos
EU3	FSUNS:G1143	**KT157844**	*Eumerus*	*alpinus* Rondani, 1857	Italy	Toscana
EU31	FSUNS:G2292	**KT157872**	*Eumerus*	*sulcitibius* Rondani, 1868	Greece	Lesvos
EU32	FSUNS:G2288	**KT157873**	*Eumerus*	*sulcitibius* Rondani, 1868	Greece	Lesvos
EU33	FSUNS:G1957	**KT157897**	*Eumerus*	*clavatus* Becker, 1923	Serbia	Đerdap
EU34	FSUNS:G2261	**KT157846**	*Eumerus*	*emarginatus* Loew, 1848	Greece	Lesvos

EU35	FSUNS:G2263	**KT157847**	*Eumerus*	*emarginatus* Loew, 1848	Greece	Lesvos
EU37	FSUNS:G2286	**KT157870**	*Eumerus*	*niehuisi* Doczkal, 1996	Greece	Lesvos
EU4	FSUNS:G0297	**KT157910**	*Eumerus*	*tricolor* (Fabricius), 1798	Serbia	Tara
EU46	FSUNS:0753	**KT157893**	*Eumerus*	*amoenus* Loew, 1848	Greece	Chios
EU48	FSUNS:G2268	**KT157878**	*Eumerus*	*amoenus* Loew, 1848	Greece	Samos
EU49	FSUNS:G2218	**KT157881**	*Eumerus*	*amoenus* Loew, 1848	Montenegro	Boka Kotorska
EU5	FSUNS:G0293	**KT157911**	*Eumerus*	*grandis* Meigen, 1822	Serbia	Đerdap
EU50	FSUNS:G0996	**KT157886**	*Eumerus*	*amoenus* Loew, 1848	Greece	Samos
EU51	FSUNS:G0997	**KT157885**	*Eumerus*	*amoenus* Loew, 1848	Greece	Samos
EU55	FSUNS:0994	**KT157902**	*Eumerus*	*argyropus* Loew, 1848	Greece	Dadia
EU56	FSUNS:G3003	**KT157849**	*Eumerus*	*pulchellus* Loew, 1848	Italy	Sardinia
EU57	FSUNS:0742	**KT157850**	*Eumerus*	*pulchellus* Loew, 1848	Greece	Chios
EU58	FSUNS:0797	**KT157855**	*Eumerus*	*pulchellus* Loew, 1848	Greece	Dadia
EU59	FSUNS:G2248	**KT157853**	*Eumerus*	*pulchellus* Loew, 1848	Greece	Lesvos
EU6	FSUNS:G0955	**KT157913**	*Eumerus*	*niveitibia* Becker, 1921	Bulgaria	Nessebar
EU60	FSUNS:G0291	**KT157901**	*Eumerus*	*hungaricus* Szilady, 1940	Serbia	Đerdap
EU61	FSUNS:0912	**KT157856**	*Eumerus*	*pusillus* Loew, 1848	Greece	Karpathos
EU62	FSUNS:0835	**KT157858**	*Eumerus*	*pusillus* Loew, 1848	Greece	Karpathos
EU63	FSUNS:0863	**KT157859**	*Eumerus*	*pusillus* Loew, 1848	Greece	Chios

EU64	FSUNS:0739	**KT157863**	*Eumerus*	*pusillus* Loew, 1848	Greece	Chios
EU65	FSUNS:0879	**KT157860**	*Eumerus*	*pusillus* Loew, 1848	Greece	Naxos
EU66	FSUNS:0861	**KT157861**	*Eumerus*	*pusillus* Loew, 1848	Greece	Naxos
EU67	FSUNS:G0999	**KT157874**	*Eumerus*	sulcitibius Rondani, 1868	Greece	Samos
EU68	FSUNS:G1003	**KT157892**	*Eumerus*	*amoenus* Loew, 1848	Greece	Samos
EU69	FSUNS:G1004	**KT157894**	*Eumerus*	*amoenus* Loew, 1848	Greece	Samos
EU7	FSUNS:G1014	**KT157914**	*Eumerus*	*armatus* Ricarte & Rotheray, 2012	Greece	Samos
EU70	FSUNS:G0282	**KT157890**	*Eumerus*	*amoenus* Loew, 1848	Greece	Samos
EU71	FSUNS:G0283	**KT157848**	*Eumerus*	*emarginatus* Loew, 1848	Greece	Samos
EU72	FSUNS:G0288	**KT157883**	*Eumerus*	*amoenus* Loew, 1848	Greece	Samos
EU73	FSUNS:G0292	**KT157895**	*Eumerus*	*consimilis* Šimić & Vujić, 1996	Serbia	Đerdap
EU75	FSUNS:G0992	**KT157867**	*Eumerus*	*basalis* Loew, 1848	Greece	Ikaria
EU76	FSUNS:G1178	**KT157884**	*Eumerus*	*amoenus* Loew, 1848	Italy	Toscana
EU77	FSUNS:G1202	**KT157882**	*Eumerus*	*amoenus* Loew, 1848	Italy	Toscana
EU8	FSUNS:G1001	**KT157918**	*Eumerus*	*aurofinis* Grković, Vujić & Radenković, 2015	Greece	Samos
EU82	FSUNS:G3005	**KT157851**	*Eumerus*	*pulchellus* Loew, 1848	Greece	Rhodes
EU83	FSUNS:G3006	**KT157854**	*Eumerus*	*pulchellus* Loew, 1848	Greece	Samos
EU86	FSUNS:G3009	**KT157862**	*Eumerus*	*pusillus* Loew, 1848	Greece	Crete

EU87	FSUNS:G3010	**KT157864**	*Eumerus*	*pusillus* Loew, 1848	Greece	Crete
EU88	FSUNS:G3011	**KT157865**	*Eumerus*	*pusillus* Loew, 1848	Greece	Athens
EU89	FSUNS:G3012	**KT157866**	*Eumerus*	*pusillus* Loew, 1848	Greece	Crete
EU90	FSUNS:G3013	**KT157857**	*Eumerus*	*pusillus* Loew, 1848	Greece	Samos
EU91	FSUNS:0836	**KT157852**	*Eumerus*	*pulchellus* Loew, 1848	Greece	Limnos
EU92	FSUNS:G3014	**KT157898**	*Eumerus*	*clavatus* Becker, 1923	Serbia	Pčinja
EU94	FSUNS:G2283	**KT157868**	*Eumerus*	*basalis* Loew, 1848	Greece	Lesvos
EU99	FSUNS:G2219	**KT157903**	*Eumerus*	*ornatus* Meigen, 1822	Montenegro	Boka Kotorska
EU9	FSUNS:G0998	**KT157919**	*Merodon*	*erivanicus* Paramonov, 1925	Greece	Samos
GUN2	FSUNS:GUN2	**KT157920**	*Megatrigon*	sp. Johnson, 1898	South Africa	
GUN5	FSUNS:GUN5	**KT157921**	*Megatrigon*	*tabanoides* Doczkal, Radenković, Lyneborg & Pape, 2015	South Africa	
Y1711E	MZH:Y1711	KM224512	*Platynochaetus*	*setosus* Fabricius, 1794	France	Pyrenées-Orientales

SI CHAPTER 3

Table S1: List of the specimens used for the species description for the taxa *E. aurofinis* sp. n. and *E. torsicus* sp. n.: locality information and GenBank accession numbers for the DNA barcodes of the mtCOI gene. The symbol of (-) represents the non-acquisition of a gene fragment sequence.

Πίνακας S1. Κατάλογος των δειγμάτων των εντόμων, τα οποία χρησιμοποιήθηκαν για την περιγραφή ειδών των *Eumerus aurofinis* sp. n. και *E. torsicus* sp. n. Δίνονται πληροφορίες σχετικές με την τοποθεσία συλλογής και οι κωδικοί αριθμοί GenBank του γενετικού γραμμωτού κώδικα (DNA barcode). Το σύμβολο (-) αναπαριστά την μη-λήψη αλληλουχίας.

DNA specimen voucher	Specimen voucher	Accession no	Disposition	Genus	Species name	Sex	Country	Nearest place name	Locality	Latitude	Longitude	Collection Date
EU138	G2279	KT221008	FSUNS	*Eumerus*	*aurofinis*	Male	Greece	Samos	Kosmadei-Kastanea	37.750271	26.672824	6/7/2012
EU213	G1785	KT221009	FSUNS	*Eumerus*	*aurofinis*	Female	Greece	Samos	Pyrgos 3	37.707809	26.8013	6/7/2012
EU284	06784	(-)	FSUNS	*Eumerus*	*aurofinis*	Female	Turkey	Muğla	near Muğla	37.187559	28.365279	06/03/2014
EU285	06798	KT221011	FSUNS	*Eumerus*	*aurofinis*	Female	Turkey	Mountain Bozdağ	near Çamurhamamı Köyü	38.452905	28.057068	06/07/2014
EU286	06800	KT221012	FSUNS	*Eumerus*	*aurofinis*	Female	Turkey	Mountain Bozdağ	near Çamurhamamı Köyü	38.452905	28.057068	06/07/2014
EU287	06803	KT221013	FSUNS	*Eumerus*	*aurofinis*	Female	Turkey	Mountain Bozdağ	near Çamurhamamı Köyü	38.452905	28.057068	06/07/2014
EU288	06746	KT221014	FSUNS	*Eumerus*	*aurofinis*	Male	Greece	Rhodes	Kalathos	36,116748	28,058878	29/05/2014
EU289	06748	KT221015	FSUNS	*Eumerus*	*aurofinis*	Female	Greece	Rhodes	Kalathos	36,116748	28,058878	29/05/2014
EU8	G1001	KT221005	FSUNS	*Eumerus*	*aurofinis*	Male	Greece	Samos	near Stavrinides	37.797440	26.806723	8/6/2010
EU17	E0746	KT221006	Maegean	*Eumerus*	*torsicus*	Male	Greece	Chios	Elinta	38.399166	25.997776	9-11/11/2012
EU18	E0744	KT221007	Maegean	*Eumerus*	*torsicus*	Male	Greece	Chios	Elinta	38.399166	25.997776	9-11/11/2012
EU208	EO745	(-)	Maegean	*Eumerus*	*torsicus*	Male	Greece	Chios	Elinta	38.399166	25.997776	9-11/11/2012
EU356	E0500	KT221017	Maegean	*Eumerus*	*torsicus*	Female	Cyprus	Mts Troodos	Makria Kondarka	34.909620	32.913370	9/18/2011
EU245	E0489	(-)	Maegean	*Eumerus*	*torsicus*	Male	Cyprus	Mts Troodos	Hionistra	34.935995	32.861964	18/9/2011
EU246	E0493	KT221010	Maegean	*Eumerus*	*torsicus*	Male	Cyprus	Mts Troodos	Makria Kondarka	34.909620	32.913370	18/9/2011

SI CHAPTER 4

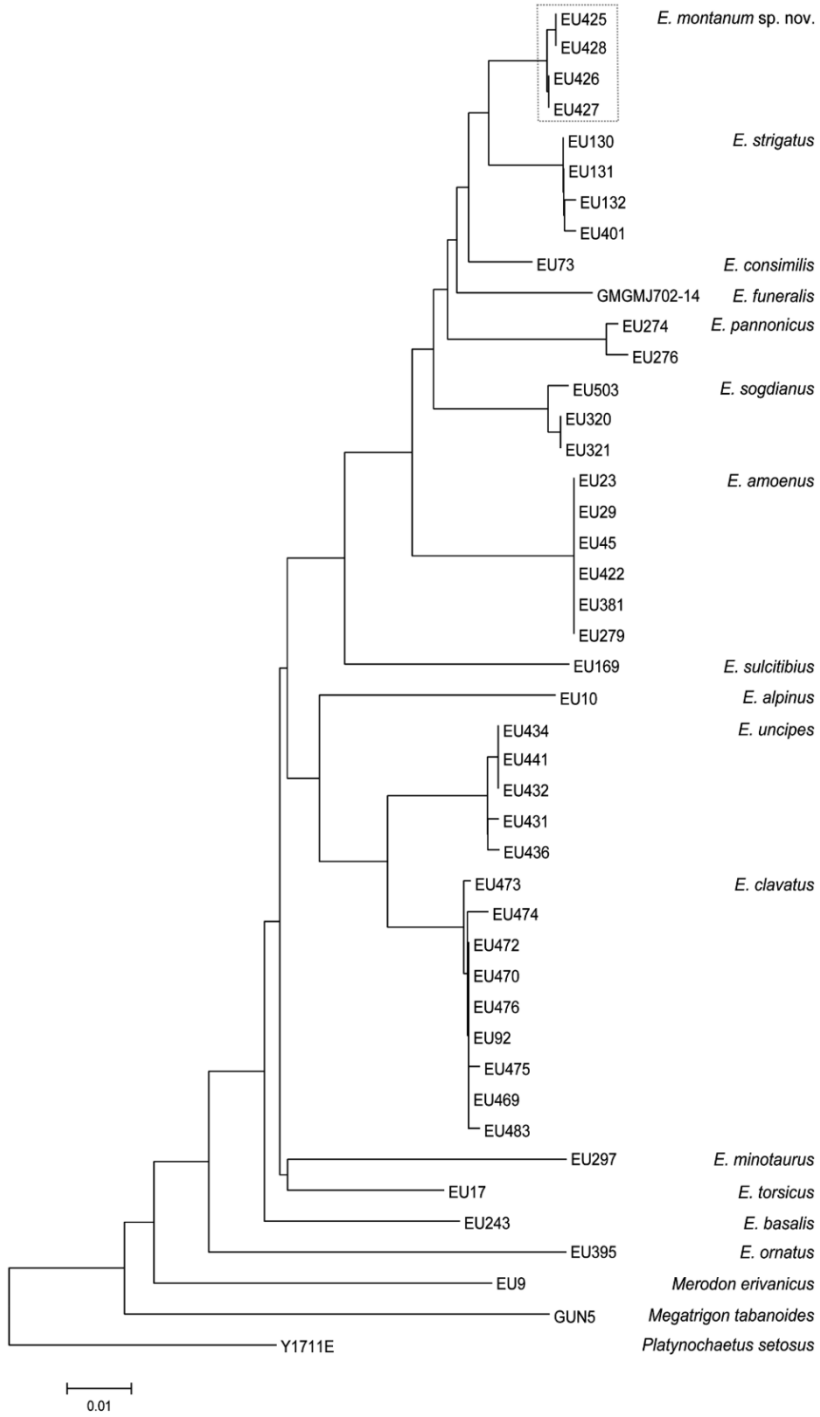

Fig. S1. Neighbor-Joining analysis for the 'total' dataset (total length 612 bp). The optimal tree with the sum of branch lengths = 0.65033298 is shown. The tree is drawn to scale, with branch lengths in the same units as those of the evolutionary distances used to infer the phylogenetic tree.

Σχήμα S1. Αποτελέσματα ανάλυσης με την μέθοδο της Σύνδεσης Γειτόνων (NJ) επί των συνολικών δεδομένων (συνολικού μήκους αλληλουχιών 612 bp). Παρουσιάζεται το βέλτιστο δέντρο (optimal tree) με άθροισμα μηκών βραχιόνων 0.65033298. Το δέντρο αποδίδει την πραγματική κλίμακα, με μήκη βραχιόνων να αντανακλούν τις εξελικτικές αποστάσεις στο φυλογενετικό δέντρο.

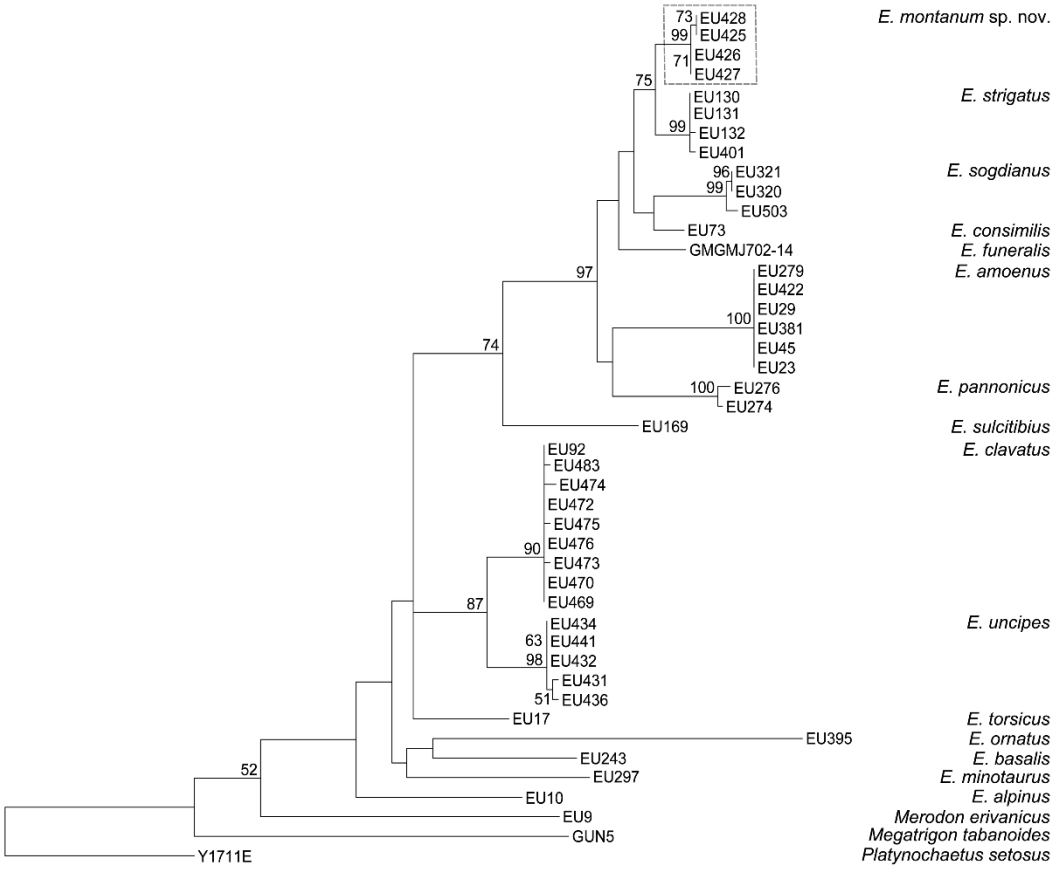

Fig. S2. Maximum likelihood analysis for the 'total' dataset (total length 612 bp). Values above branches indicate bootstrap replicates (only values >50 are illustrated).

Σχήμα S2. Αποτελέσματα ανάλυσης με την μέθοδο της Μέγιστης Πιθανοφάνειας (ML) επί των συνολικών δεδομένων (συνολικού μήκους αλληλουχιών 612 bp). Οι μοναδικές νουκλεοτιδικές υποκαταστάσεις σημειώνονται με μαύρο κύκλο, και οι μη-μοναδικές με απλή περιφέρεια κύκλου. Για να ελεγχθεί η στατιστική στήριξη των κλάδων, πραγματοποιήθηκαν 1000 επαναλήψεις bootstrap, των οποίων οι τιμές παρουσιάζονται πάνω από τους κλάδους του ML δέντρου (μόνον τιμές μεγαλύτερες του 50).

Table S1. List of the specimens used for phylogenetic analyses, their locality information and GenBank accession numbers for DNA barcodes. GenBank accession numbers of newly-generated sequences (this study) are in boldface.

Πίνακας S1. Κατάλογος των δειγμάτων των εντόμων, τα οποία χρησιμοποιήθηκαν για τις φυλογενετικές αναλύσεις, εμπεριέχοντας πληροφορίες σχετικά με την τοποθεσία συλλογής, καθώς και τους κωδικούς καταχώρησης στη βάση δεδομένων GenBank του γενετικού γραμμωτού κώδικα (DNA barcode). Οι κωδικοί GenBank των αλληλουχιών, οι οποίες παρήχθησαν στην παρούσα έρευνα, δίνονται με έντονη γραμματοσειρά.

Sequence ID	Specimen voucher	Accession no LCOF	Disposition	Genus	Species name	Species group	Sex	Country	Nearest place name	Latitude	Longitude	Collection Date
EU10	G1147	**KX083349**	FSUNS	*Eumerus*	*alpinus* Rondani, 1857	*E. alpinus*	F	Italy	Toscana	44.056359	10.198840	12/5/2012
EU130	NJ17	**KX083378**	FSUNS	*Eumerus*	*strigatus* (Fallen), 1817	*E. strigatus*	M	Russia	Mt Altai	51.689	87.562	23-25/06/2013
EU131	42-504	**KX083379**	FSUNS	*Eumerus*	*strigatus* (Fallen), 1818	*E. strigatus*	M	Germany				
EU132	60653	**KX083380**	FSUNS	*Eumerus*	*strigatus* (Fallen), 1819	*E. strigatus*	M	Germany				
EU169	G3034	**KX083387**	FSUNS	*Eumerus*	*sulcitibius* Rondani, 1868	*E. sulcitibius*	M	Greece	Andros	37.845616	24.904967	25/05/2012
EU17	UOTA_ MEL0746	KT221006	MAegean	*Eumerus*	*torsicus* Grković & Vujić, 2016	*E. torsicus*	M	Greece	Chios	38.393	25.9914	9-11/11/2012
EU23	1002	**KX083364**	FSUNS	*Eumerus*	*amoenus* Loew, 1848	*E. strigatus*	M	Greece	Dadia	41.124600	26.238948	10-12/8/2012
EU243	G3054	**KX083385**	FSUNS	*Eumerus*	*basalis* Loew, 1848	*E. basalis*	M	Greece	Rhodes	36.230879	27.852756	16/10/2012
EU274	08909	**KY272851**	FSUNS	*Eumerus*	*pannonicus* Ricarte, Vujić	*E. strigatus*	M	Serbia	Mokrin	45.90615	20.3018	21/5/2014

					& Radenković, 2016							
EU276	08910	**KY272852**	FSUNS	*Eumerus*	*pannonicus* Ricarte, Vujić & Radenković, 2016	*E. strigatus*	F	Serbia	Mokrin	45.90615	20.3018	11/6/2014
EU279	06828	**KY272854**	FSUNS	*Eumerus*	*amoenus* Loew, 1848	*E. strigatus*	F	Turkey	(near Camurhamamı Koyu)	38.452905	28.057068	06/07/2014
EU29	G2265	**KX083365**	FSUNS	*Eumerus*	*amoenus* Loew, 1848	*E. strigatus*	M	Greece	Samos	37.712686	26.79914	15/04/2011
EU297	06366	**KX083386**	FSUNS	*Eumerus*	*minotaurus* Claussen & Lucas, 1988	*E. minotaurus*	F	Greece	Lassithi	35.211883	25.461649	22/04/2014
EU320	06561	**KX083382**	FSUNS	*Eumerus*	*sogdianus* Stackelberg, 1952	*E. strigatus*	F	Greece	Lakonia	37.30416	22.42106	23/05/2014
EU321	06562	**KX083383**	FSUNS	*Eumerus*	*sogdianus* Stackelberg, 1952	*E. strigatus*	F	Greece	Lakonia	37.30416	22.42106	23/05/2014
EU381	E0792	**KY272853**	MAegean	*Eumerus*	*amoenus* Loew, 1848	*E. strigatus*	F	Greece	Evros	40.9943	26.0933	20-22/09/2012
EU395	E0801	**KX083388**	MAegean	*Eumerus*	*ornatus* Meigen, 1822	*E. ornatus*	F	Greece	Evros	41.0296	26.1513	21-23/09/2012
EU401	G0296	**KX083381**	FSUNS	*Eumerus*	*strigatus* (Fallen), 1817	*E. strigatus*	F	Serbia	Stara Planina	43.169254	22.793908	11/07/2011
EU422	E0862	**KY272855**	FSUNS	*Eumerus*	*amoenus*	*E.*	F	Greece	Karpathos	35.741306	27.17488	8-10/06/2012

					Loew, 1848	*strigatus*						
EU425	07522	**KX083374**	FSUNS	*Eumerus*	*montanum* Grković, Radenković & Vujić sp. n.	*E. strigatus*	M	Montenegro	Mt Durmitor	42.98897	19.06862	7/2014
EU426	07519	**KX083375**	FSUNS	*Eumerus*	*montanum* Grković, Radenković & Vujić sp. n.	*E. strigatus*	M	Montenegro	Mt Durmitor	42.98897	19.06862	7/2014
EU427	07518	**KX083376**	FSUNS	*Eumerus*	*montanum* Grković, Radenković & Vujić sp. n.	*E. strigatus*	F	Montenegro	Mt Durmitor	42.98897	19.06862	23/07/2014
EU428	07516	**KX083377**	FSUNS	*Eumerus*	*montanum* Grković, Radenković &Vujić sp. n.	*E. strigatus*	M	Montenegro	Mt Durmitor	42.98897	19.06862	23/07/2014
EU431	E1312	**KX083359**	FSUNS	*Eumerus*	*uncipes* Rondani, 1850	*E. clavatus*	M	Greece	Corfu	39.739862	19.837307	8/8/2014
EU432	E1308	**KX083360**	FSUNS	*Eumerus*	*uncipes* Rondani, 1851	*E. clavatus*	F	Greece	Corfu	39.739862	19.837307	8/8/2014
EU434	E1307	**KX083361**	FSUNS	*Eumerus*	*uncipes* Rondani, 1852	*E. clavatus*	F	Greece	Corfu	39.739862	19.837307	10/8/2014
EU436	E1309	**KX083362**	FSUNS	*Eumerus*	*uncipes* Rondani, 1853	*E. clavatus*	F	Greece	Corfu	39.512151	19.916724	8/8/2014

EU441	E1311	**KX083363**	FSUNS	*Eumerus*	*uncipes* Rondani, 1854	*E. clavatus*	F	Greece	Corfu	39.739862	19.837307	10/8/2014
EU45	0752	**KX083366**	FSUNS	*Eumerus*	*amoenus* Loew, 1848	*E. strigatus*	M	Greece	Chios	38.393	25.9914	9-11/11/2013
EU469	07982	**KX083351**	FSUNS	*Eumerus*	*clavatus* Becker, 1923	*E. clavatus*	F	Turkey	Mt Davraz	37.781694	30.75871	21/07/2014
EU470	07984	**KX083356**	FSUNS	*Eumerus*	*clavatus* Becker, 1923	*E. clavatus*	F	Turkey	Yenisarbademli	37.697777	31.2954	26/07/2014
EU472	07985	**KX083358**	FSUNS	*Eumerus*	*clavatus* Becker, 1923	*E. clavatus*	F	Turkey	Mt Davraz	37.781694	30.75871	21/07/2014
EU473	07986	**KX083357**	FSUNS	*Eumerus*	*clavatus* Becker, 1923	*E. clavatus*	F	Turkey	Yenisarbademli	37.697471	31.29407	04/09/2014
EU474	07987	**KX083353**	FSUNS	*Eumerus*	*clavatus* Becker, 1923	*E. clavatus*	F	Turkey	Mt Davraz	37.782694	30.75925	03/09/2014
EU475	07988	**KX083355**	FSUNS	*Eumerus*	*clavatus* Becker, 1923	*E. clavatus*	F	Turkey	Yenisarbademli	37.697471	31.29407	04/09/2014
EU476	07989	**KX083352**	FSUNS	*Eumerus*	*clavatus* Becker, 1923	*E. clavatus*	M	Turkey	Yenisarbademli	37.697471	31.29407	04/09/2014
EU483	07993	**KX083354**	FSUNS	*Eumerus*	*clavatus* Becker, 1923	*E. clavatus*	F	Turkey	Yenisarbademli	37.697777	31.2954	26/07/2014
EU503	06548	**KX083384**	FSUNS	*Eumerus*	*sogdianus* Stackelberg, 1952	*E. strigatus*	M	Greece	Lakonia	37.30416	22.42106	23/05/2014
EU73	G0292	**KX083373**	FSUNS	*Eumerus*	*consimilis* Šimić &Vujić, 1996	*E. strigatus*	M	Serbia	Djerdap	44.54104	22.02024	01/09/2011
EU9	G0998	**KX083391**	FSUNS	*Merodon*	*erivanicus* Paramonov,	Outgroup	M	Greece	Samos	37.75305	26.735127	9/6/2010

					1925							
EU92	G3014	**KX083350**	FSUNS	*Eumerus*	*clavatus* Becker, 1923	*E. clavatus*	M	Serbia	Pčinja	42.342952	21.92442	06/09/2012
GUN5	GUN5	**KX083393**	MZH	*Megatrigon*	*tabanoides* Doczkal, Radenković, Lyneborg & Pape, 2015	Outgroup	M	Republic of South Africa				
Y1711	MZH: Y1711	KM224512	MZH	*Platynochaetus*	*setosus* Fabricius, 1794	Outgroup	M	France	Banyuls-sur-Mer, Pyrenées-Orientales	42.474144	3.117728	16/04/2012
GMGMJ702-14	BOLD: AAG4654	GMGMJ702-14	BOLD: AAG4654	*Eumerus*	*funeralis* Meigen, 1822	*E. strigatus*	Unknown	Germany	Rhineland-Palatinate	50.552	7.17	02/06/2014

Table S2. The number of base substitutions per site between DNA barcode sequences. Analyses were conducted using the Kimura 2-parameter model on 41 nucleotide sequences. Codon positions included were 1st+2nd+3rd+Noncoding. All positions containing gaps or missing data were eliminated. There were a total of 601 positions in the final dataset. The Table S2 has been trimmed after the 21st column as a matter of convenience, and is continued in the next page.

Πίνακας S2. Ο αριθμός των νουκλεοτιδικών υποκαταστάσεων ανά θέση μεταξύ των αλληλουχιών του γενετικού γραμμωτού κώδικα (DNA barcode). Οι αναλύσεις διεξήχθησαν με βάση το εξελικτικό μοντέλο Kimura 2-parameter σε 41 αλληλουχίες. Οι κωδικές θέσεις συμπεριλάμβαναν τις 1η+2η+3η+Μη κωδικές (1st+2nd+3rd+Noncoding). Οι θέσεις, οι οποίες συμπεριλάμβαναν κενά ή ελλείποντα δεδομένα, καταργήθηκαν. Το σύνολο της ομάδας δεδομένων ήταν 601 θέσεις. Ο Πίνακας S2 έχει κοπεί μετά την 21η στήλη για λόγους ευκρίνειας, και συνεχίζεται στην επόμενη σελίδα.

		1	2	3	4	5	6	7	8	9	10	11	12	13	14	15	16	17	18	19	20
1	EU10LCOF																				
2	EU92LCOF	0.060																			
3	EU469LCOF	0.060	0.000																		
4	EU476LCOF	0.060	0.000	0.000																	
5	EU474LCOF	0.060	0.003	0.003	0.003																
6	EU483LCOF	0.062	0.002	0.002	0.002	0.005															
7	EU475LCOF	0.062	0.002	0.002	0.002	0.005	0.003														
8	EU470LCOF	0.060	0.000	0.000	0.000	0.003	0.002	0.002													
9	EU473LCOF	0.058	0.002	0.002	0.002	0.005	0.003	0.003	0.002												
10	EU472LCOF	0.060	0.000	0.000	0.000	0.003	0.002	0.002	0.000	0.002											
11	EU431LCOF	0.066	0.030	0.030	0.030	0.034	0.032	0.032	0.030	0.032	0.030										
12	EU432LCOF	0.066	0.030	0.030	0.030	0.034	0.032	0.032	0.030	0.032	0.030	0.003									
13	EU434LCOF	0.066	0.030	0.030	0.030	0.034	0.032	0.032	0.030	0.032	0.030	0.003	0.000								
14	EU436LCOF	0.066	0.030	0.030	0.030	0.033	0.031	0.032	0.030	0.031	0.030	0.003	0.003	0.003							
15	EU441LCOF	0.066	0.030	0.030	0.030	0.034	0.032	0.032	0.030	0.032	0.030	0.003	0.000	0.000	0.003						
16	EU243LCOF	0.079	0.064	0.064	0.064	0.068	0.066	0.064	0.064	0.062	0.064	0.064	0.064	0.064	0.068	0.064					
17	EU23LCOF	0.088	0.069	0.069	0.069	0.073	0.071	0.071	0.069	0.071	0.069	0.080	0.080	0.080	0.084	0.080	0.088				
18	EU29LCOF	0.088	0.069	0.069	0.069	0.073	0.071	0.071	0.069	0.071	0.069	0.080	0.080	0.080	0.084	0.080	0.088	0.000			
19	EU45LCOF	0.088	0.069	0.069	0.069	0.073	0.071	0.071	0.069	0.071	0.069	0.080	0.080	0.080	0.084	0.080	0.088	0.000	0.000		
20	EU422LCOF	0.088	0.069	0.069	0.069	0.073	0.071	0.071	0.069	0.071	0.069	0.080	0.080	0.080	0.084	0.080	0.088	0.000	0.000	0.000	
21	EU381LCOF	0.088	0.069	0.069	0.069	0.073	0.071	0.071	0.069	0.071	0.069	0.080	0.080	0.080	0.084	0.080	0.088	0.000	0.000	0.000	0.000

22	EU279LCOF	0.088	0.069	0.069	0.069	0.073	0.071	0.071	0.069	0.071	0.069	0.080	0.080	0.080	0.084	0.080	0.088	0.000	0.000	0.000	0.000
23	EU73LCOF	0.084	0.068	0.068	0.068	0.072	0.070	0.070	0.068	0.070	0.068	0.068	0.068	0.068	0.068	0.068	0.068	0.042	0.042	0.042	0.042
24	EU425LCOF	0.093	0.072	0.072	0.072	0.077	0.074	0.074	0.072	0.074	0.072	0.071	0.071	0.071	0.075	0.071	0.068	0.057	0.057	0.057	0.057
25	EU426LCOF	0.090	0.072	0.072	0.072	0.077	0.074	0.074	0.072	0.074	0.072	0.068	0.068	0.068	0.073	0.068	0.066	0.054	0.054	0.054	0.054
26	EU427LCOF	0.090	0.072	0.072	0.072	0.077	0.074	0.074	0.072	0.074	0.072	0.068	0.068	0.068	0.073	0.068	0.066	0.054	0.054	0.054	0.054
27	EU428LCOF	0.093	0.072	0.072	0.072	0.077	0.074	0.074	0.072	0.074	0.072	0.071	0.071	0.071	0.075	0.071	0.068	0.057	0.057	0.057	0.057
28	EU130LCOF	0.087	0.077	0.077	0.077	0.077	0.079	0.079	0.077	0.079	0.077	0.068	0.068	0.068	0.068	0.068	0.072	0.064	0.064	0.064	0.064
29	EU131LCOF	0.087	0.077	0.077	0.077	0.077	0.079	0.079	0.077	0.079	0.077	0.068	0.068	0.068	0.068	0.068	0.072	0.064	0.064	0.064	0.064
30	EU132LCOF	0.089	0.079	0.079	0.079	0.079	0.081	0.081	0.079	0.081	0.079	0.070	0.070	0.070	0.070	0.070	0.074	0.066	0.066	0.066	0.066
31	EU401LCOF	0.089	0.079	0.079	0.079	0.079	0.081	0.081	0.079	0.081	0.079	0.070	0.070	0.070	0.070	0.070	0.074	0.066	0.066	0.066	0.066
32	EU320LCOF	0.095	0.074	0.074	0.074	0.079	0.076	0.076	0.074	0.076	0.074	0.073	0.073	0.073	0.073	0.073	0.068	0.050	0.050	0.050	0.050
33	EU321LCOF	0.095	0.074	0.074	0.074	0.079	0.076	0.076	0.074	0.076	0.074	0.073	0.073	0.073	0.073	0.073	0.068	0.050	0.050	0.050	0.050
34	EU503LCOF	0.102	0.076	0.076	0.076	0.081	0.078	0.078	0.076	0.078	0.076	0.070	0.070	0.070	0.074	0.070	0.066	0.051	0.051	0.051	0.051
35	GMGMJ702-14	0.097	0.078	0.078	0.078	0.078	0.080	0.080	0.078	0.080	0.078	0.079	0.079	0.079	0.079	0.079	0.081	0.050	0.050	0.050	0.050
36	EU297LCOF	0.092	0.080	0.080	0.080	0.085	0.082	0.082	0.080	0.078	0.080	0.073	0.073	0.073	0.077	0.073	0.078	0.099	0.099	0.099	0.099
37	EU274LCOF	0.101	0.086	0.086	0.086	0.091	0.088	0.088	0.086	0.088	0.086	0.081	0.081	0.081	0.081	0.081	0.080	0.062	0.062	0.062	0.062
38	EU276LCOF	0.098	0.088	0.088	0.088	0.088	0.090	0.090	0.088	0.090	0.088	0.086	0.086	0.086	0.086	0.086	0.082	0.064	0.064	0.064	0.064
39	EU169LCOF	0.086	0.074	0.074	0.074	0.079	0.076	0.076	0.074	0.072	0.074	0.077	0.077	0.077	0.077	0.077	0.079	0.076	0.076	0.076	0.076
40	EU395LCOF	0.108	0.095	0.095	0.095	0.095	0.098	0.095	0.095	0.098	0.095	0.107	0.103	0.103	0.102	0.103	0.101	0.125	0.125	0.125	0.125
41	EU17LCOF	0.072	0.054	0.054	0.054	0.058	0.056	0.056	0.054	0.052	0.054	0.060	0.060	0.060	0.060	0.060	0.058	0.083	0.083	0.083	0.083

		21	22	23	24	25	26	27	28	29	30	31	32	33	34	35	36	37	38	39	40	41
1	EU10LCOF																					
2	EU92LCOF																					
3	EU469LCOF																					
4	EU476LCOF																					
5	EU474LCOF																					
6	EU483LCOF																					
7	EU475LCOF																					
8	EU470LCOF																					
9	EU473LCOF																					

10	EU472LCOF																				
11	EU431LCOF																				
12	EU432LCOF																				
13	EU434LCOF																				
14	EU436LCOF																				
15	EU441LCOF																				
16	EU243LCOF																				
17	EU23LCOF																				
18	EU29LCOF																				
19	EU45LCOF																				
20	EU422LCOF																				
21	EU381LCOF																				
22	EU279LCOF	0.000																			
23	EU73LCOF	0.042	0.042																		
24	EU425LCOF	0.057	0.057	0.025																	
25	EU426LCOF	0.054	0.054	0.023	0.002																
26	EU427LCOF	0.054	0.054	0.023	0.002	0.000															
27	EU428LCOF	0.057	0.057	0.025	0.000	0.002	0.002														
28	EU130LCOF	0.064	0.064	0.025	0.023	0.021	0.021	0.023													
29	EU131LCOF	0.064	0.064	0.025	0.023	0.021	0.021	0.023	0.000												
30	EU132LCOF	0.066	0.066	0.027	0.025	0.023	0.023	0.025	0.002	0.002											
31	EU401LCOF	0.066	0.066	0.027	0.025	0.023	0.023	0.025	0.002	0.002	0.003										
32	EU320LCOF	0.050	0.050	0.028	0.038	0.036	0.036	0.038	0.041	0.041	0.042	0.042									
33	EU321LCOF	0.050	0.050	0.028	0.038	0.036	0.036	0.038	0.041	0.041	0.042	0.042	0.000								
34	EU503LCOF	0.051	0.051	0.030	0.036	0.034	0.034	0.036	0.042	0.042	0.044	0.044	0.005	0.005							
35	GMGMJ702-14	0.050	0.050	0.037	0.037	0.039	0.039	0.037	0.034	0.034	0.036	0.036	0.044	0.044	0.046						
36	EU297LCOF	0.099	0.099	0.083	0.086	0.083	0.083	0.086	0.085	0.085	0.087	0.087	0.083	0.083	0.082	0.099					
37	EU274LCOF	0.062	0.062	0.044	0.052	0.050	0.050	0.052	0.046	0.046	0.048	0.048	0.052	0.052	0.053	0.050	0.086				
38	EU276LCOF	0.064	0.064	0.047	0.055	0.052	0.052	0.055	0.044	0.044	0.045	0.045	0.056	0.056	0.058	0.048	0.093	0.005			
39	EU169LCOF	0.076	0.076	0.070	0.070	0.068	0.068	0.070	0.068	0.068	0.070	0.070	0.065	0.065	0.071	0.065	0.088	0.076	0.079		
40	EU395LCOF	0.125	0.125	0.109	0.115	0.112	0.112	0.115	0.117	0.117	0.119	0.119	0.124	0.124	0.129	0.124	0.117	0.114	0.117	0.107	
41	EU17LCOF	0.083	0.083	0.068	0.068	0.066	0.066	0.068	0.070	0.070	0.072	0.072	0.066	0.066	0.066	0.072	0.068	0.079	0.081	0.075	0.100

Table S3. The morphological matrix scored 24 characters of males related to size, head, thorax and genitalia.

Πίνακας S3. Πίνακας με τους 24 μορφολογικούς χαρακτήρες σχετικούς με το μέγεθος σώματος, κεφαλής, θώρακα και γεννητικού οπλισμού άρρενος.

		1	2	3	4	5	6	7	8	9	10	11	12	13	14	15	16	17	18	19	20	21	22	23	24
		Body length	Wing length	Eyes margins	Lower facial margin	Number of ommatidia	Length of pile on eyes	Vertical triangle just behind	Vertex behind posterior ocelli	Ocellar triangle anteriorly	Distance from pos. ocelli to	Facial pollinosity	Pollinosity along eye	Face pilosity	Antenna	Shape of basoflagellomer	Ventral pile on pedicel	Length of pile on scutum	Colour of pile on scutum and	Hypandrium	Posterior surstyle lobe	Pedicel extremely	Hind tibia very curved	Vein M1	Vein R4+5
		0=6mm; 1=7mm;	0=4-4.5; 1=5-5.5;	0=parallel;	0=not protrudin	0=1-3; 1=6-8;	0=2-2.5; 1=3-3.5;	0=parallel;	0=with shallow	0=raised; 1=not	0=<1; 1=2; 2=3;	0=silver-white;	0=patch of	0=white; 1=white	0=dark brown;	0=oval with	0=yellow; 1=yellow	0=as half of the	0=white to yellow;	0=without "notch";	0=oval, narrowed	0=yes; 1=no	0=yes; 1=no	0=not invaginate	0=not curved;
	Species																								
E. funeralis	sp.1	0	1	2	2	2	1	1	1	0	2	0	1	0	0	2	1	0	0	0	1	1	1	1	0
E. sogdianus	sp.2	1	1	2	2	1	0	0	1	0	2	0	0	0	2	2	0	1	0	1	0	1	1	1	0
E. strigatus	sp.3	1	0	1	2	2	1	2	1	0	2	1	0	1	2	0	0	0	0	0	1	1	1	1	0
E. amoenus	sp.4	1	2	0	0	1	1	2	0	1	3	2	0	0	1	0	0	1	2	2	0	1	1	1	0
E. montanum	sp.5	1	1	2	2	2	2	1	1	0	1	1	1	1	0	1	0	0	1	0	1	1	1	1	0
E. consimilis	sp.6	2	1	1	1	2	2	2	0	0	1	2	1	0	2	0	1	0	0	0	1	1	1	1	0
E. narcissi	sp.7	0		1		1	0	1				0	1	1	2	0			2	0	2	1	1	1	0
E. vanderbergei	sp.8	0	0	1	1	2						0	0	0	2	0	1		2	1	1	1	1	1	0
E. pannonicus	sp.9	2	1	2	1	2	2	2	0	0	0	0	0	1	0	2	1	1	1	1	2	1	1	0	0
Platynochaetus setosus	sp.10	3	3	2	3	0	4	2	1	1	1	0	2	1	3	1	0	2	0	3	2	0	0	0	2
Megatrigon tabanoides	sp.11	3	3	0	1	3	3	2	1	1	0	3	2	0	3	0	2	2	3	3	2	1	1	1	1
Merodon erivanicus	sp.12	3	3	2	1	4	3	2	1	1	0	2	2	0	0	0	0	2	1	3	2	1	1	0	2

SI CHAPTER 5

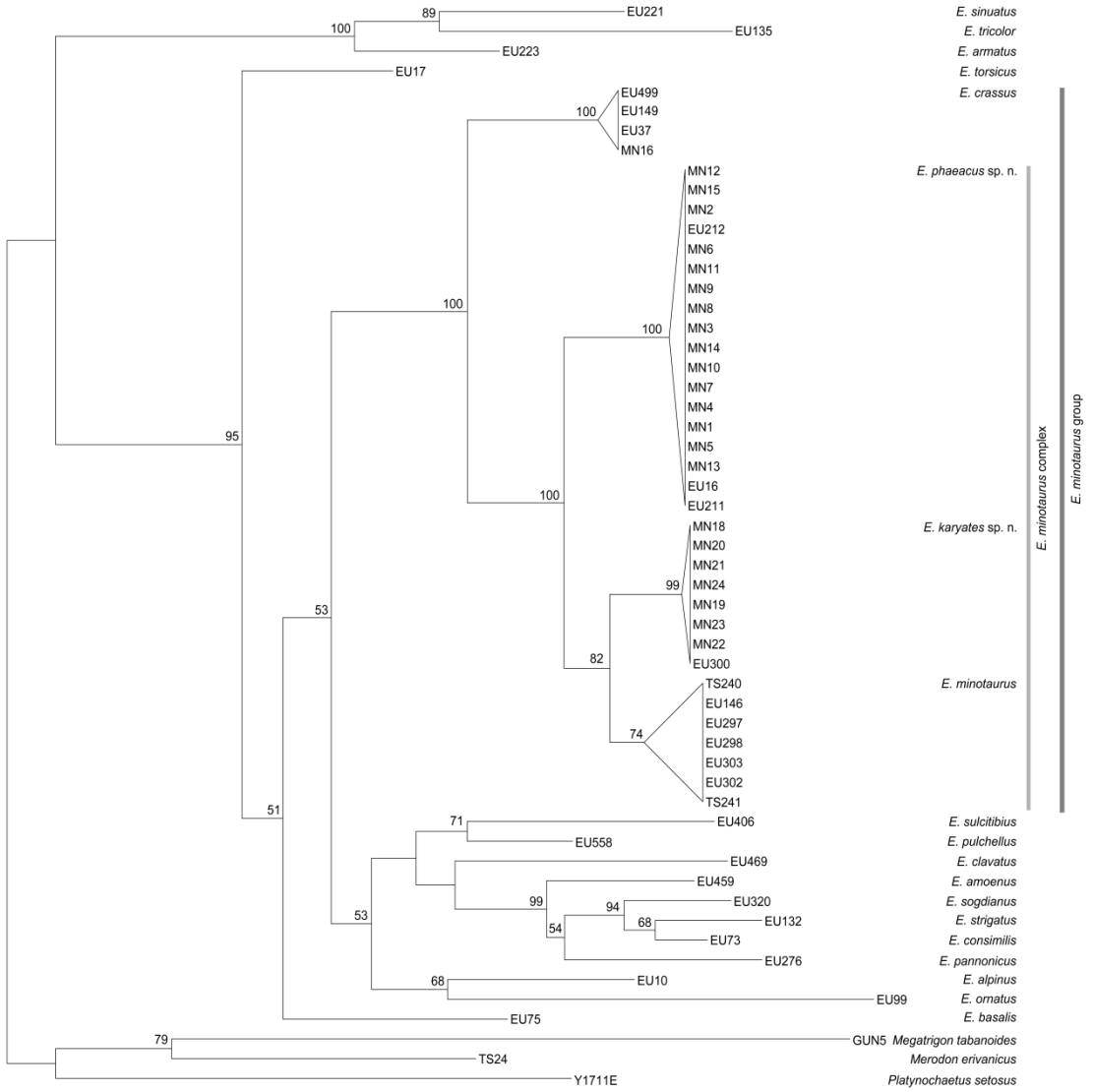

Fig. S1. Maximum likelihood analysis for the concatenated 3' and 5' fragment of COI gene fragment (COI dataset); values above branches indicate bootstrap replicates (only values >50 are illustrated).

Σχήμα S1. Αποτελέσματα ανάλυσης με την μέθοδο της Μέγιστης Πιθανοφάνειας (ML) για την ομάδα δεδομένων COI, η οποία συμπεριλάμβανε τα συζευγμένα θραύσματα του COI γονιδίου. Για να ελεγχθεί η στατιστική στήριξη των κλάδων, πραγματοποιήθηκαν 1000 επαναλήψεις bootstrap, των οποίων οι τιμές παρουσιάζονται πάνω από τους κλάδους του ML δέντρου (μόνον τιμές μεγαλύτερες του 50).

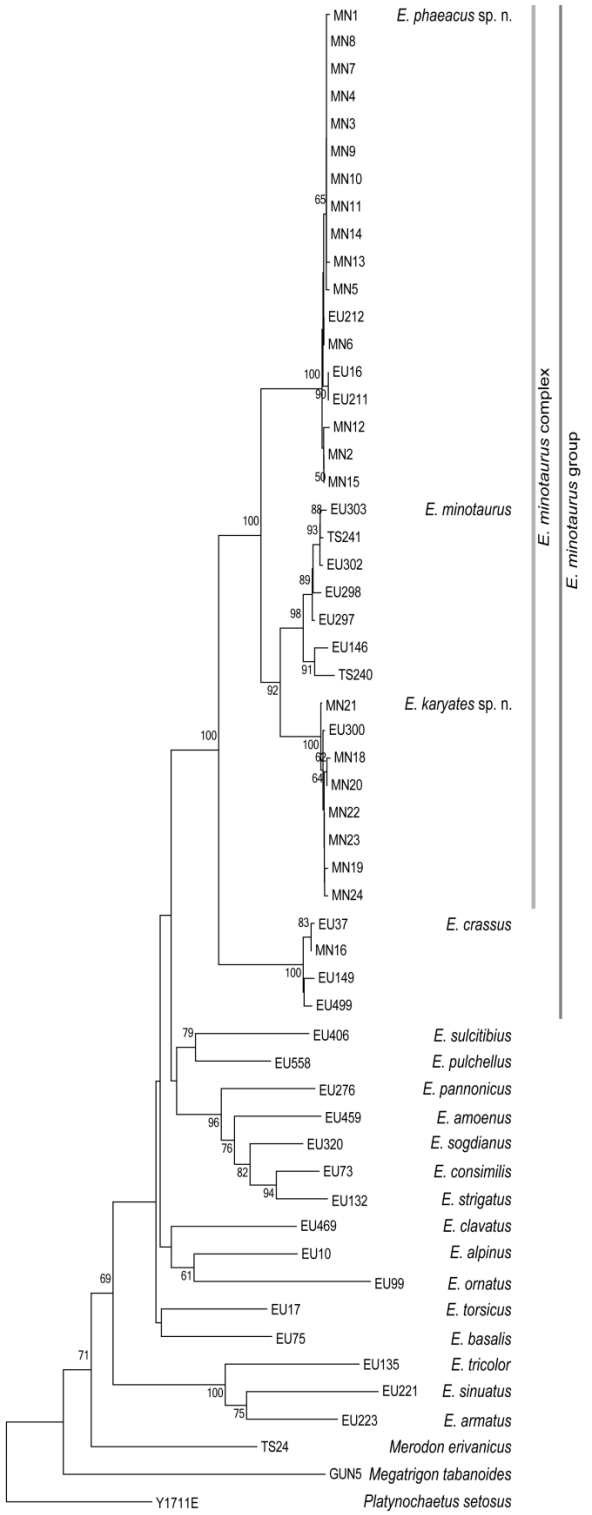

Fig. S2. Neighbor-Joining analysis for the concatenated 3' and 5' fragment of COI gene fragment (COI dataset); values in the branches indicate bootstrap replicates (only values >50 are illustrated).

Σχήμα S2. Αποτελέσματα ανάλυσης με την μέθοδο της Σύνδεσης Γειτόνων (NJ) για την ομάδα δεδομένων COI, η οποία συμπεριλάμβανε τα συζευγμένα θραύσματα του COI γονιδίου. Για να ελεγχθεί η στατιστική στήριξη των κλάδων, πραγματοποιήθηκαν 1000 επαναλήψεις bootstrap, των οποίων οι τιμές παρουσιάζονται πάνω από τους κλάδους του NJ δέντρου (μόνον τιμές μεγαλύτερες του 50).

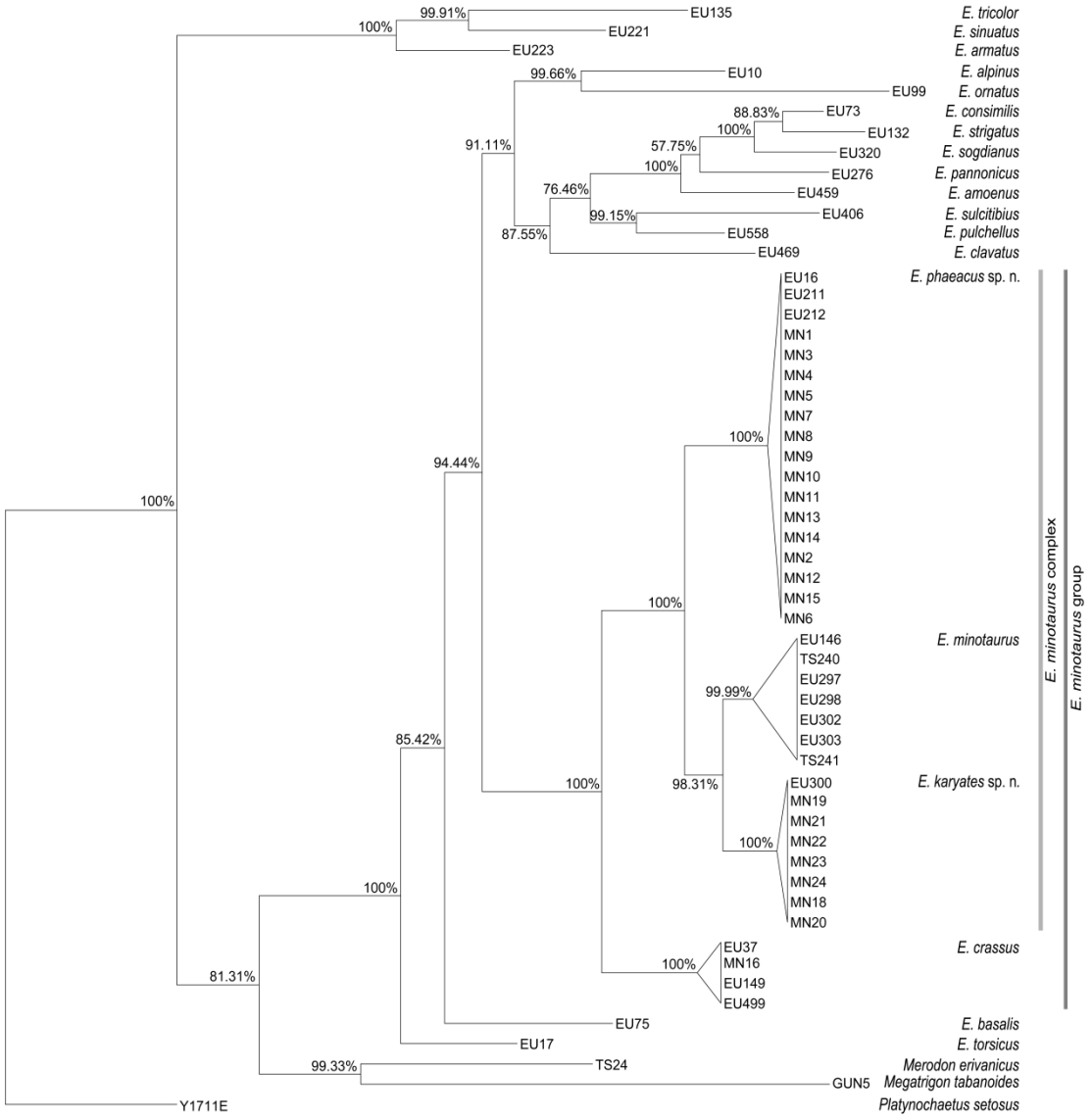

Fig. S3. Bayesian analysis for the concatenated 3' and 5' fragment of COI gene fragment (COI dataset); values indicate Bayesian probability.

Σχήμα S3. Αποτελέσματα ανάλυσης με την μέθοδο της Μπεϊεσιανής Συμπερασματολογίας (BI) για την ομάδα δεδομένων COI, η οποία συμπεριλάμβανε τα συζευγμένα θραύσματα του COI γονιδίου. Οι αριθμοί στους κλάδους δηλώνουν τις εκ των υστέρων πιθανότητες.

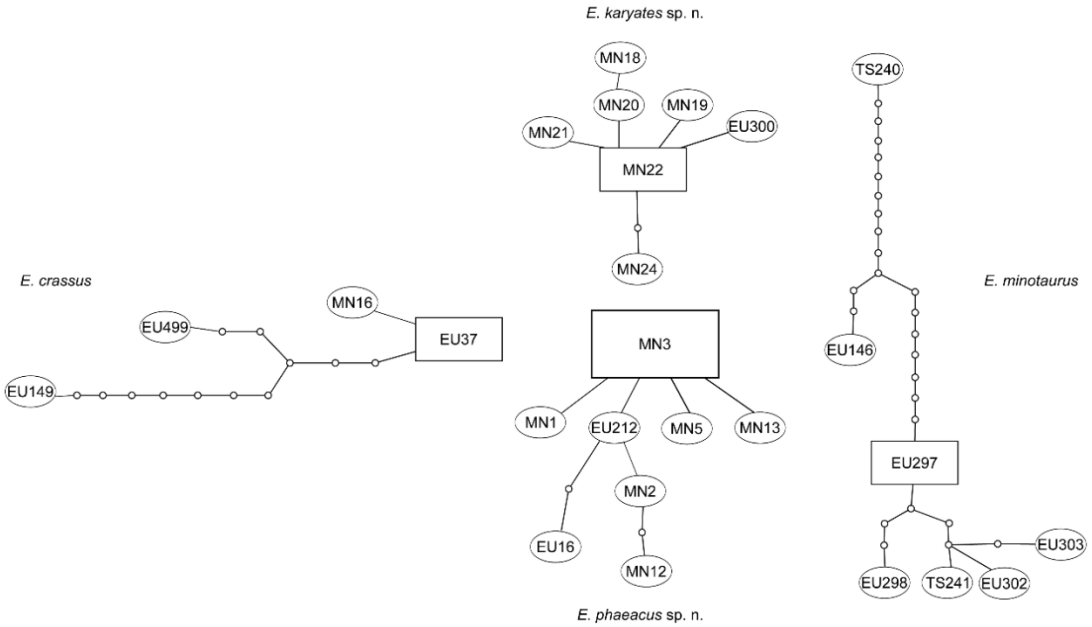

Fig. S4. Haplotype networks constructed using the statistical parsimony algorithm for the concatenated 3' and 5' fragment of COI gene fragment (COI subset) of the *E. minotaurus* group.

Σχήμα S4. Αποτελέσματα ανάλυσης των δικτύων στατιστικής φειδωλότητας τα οποία αφορούν στη διαφοροποίηση των μιτοχονδριακών απλοτύπων για την ομάδα ειδών *E. minotaurus* (υπο-ομάδα δεδομένων COI), η οποία συμπεριλάμβανε τα συζευγμένα θραύσματα του COI γονιδίου.

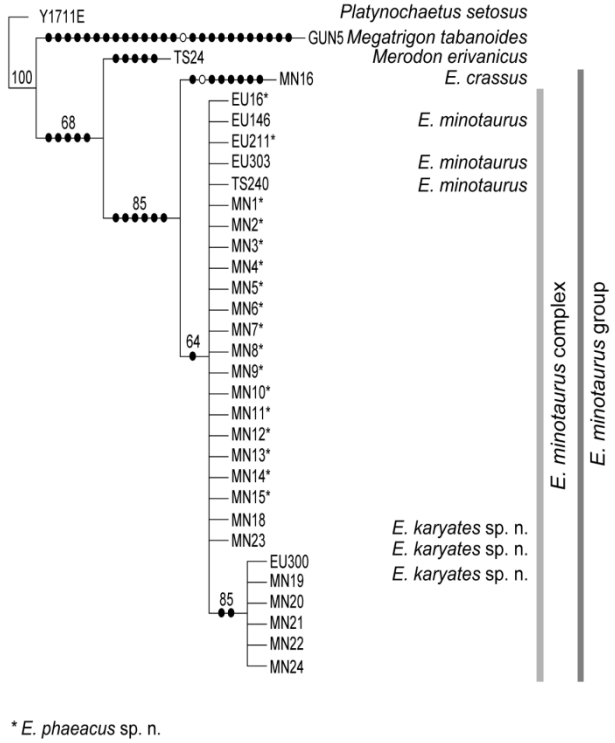

Fig. S5. Maximum parsimony analysis of the 28S gene fragment (28S dataset); only one tree was produced (Length 90 steps, CI=93, RI=81); filled circles denote unique changes and open circles non-unique. Bootstrap support values are illustrated above the branches.

Σχήμα S5. Αποτελέσματα ανάλυσης με την μέθοδο της φειδωλότητας (MP) για την ομάδα δεδομένων 28S, η οποία συμπεριλάμβανε το θραύσμα του 28S γονιδίου. Παρήχθη ένα δέντρο, το οποίο και παρουσιάζεται εδώ (Μήκος 90 εξελικτικά βήματα, CI=93, RI=81). Οι μοναδικές νουκλεοτιδικές υποκαταστάσεις σημειώνονται με μαύρο κύκλο, και οι μη-μοναδικές με απλή περιφέρεια κύκλου Για να ελεγχθεί η στατιστική στήριξη των κλάδων, πραγματοποιήθηκαν 1000 επαναλήψεις bootstrap, των οποίων οι τιμές παρουσιάζονται πάνω από τους κλάδους του MP δέντρου.

Table S1. List of specimens used for wing geometric morphometric analysis by geographical area and species.

Πίνακας S1. Κατάλογος των δειγμάτων των εντόμων, τα οποία χρησιμοποιήθηκαν για την γεωμετρική μορφομετρία πτερύγων ανά γεωγραφική περιοχή και είδος.

Species	**Country**	**Nearest place name**	**Locality**	♂	♀	∑
E. karyates sp. n.	Greece	Peloponnese	Karyes, 25km N from Sparti	4	5	9
E. minotaurus	Greece	Crete	Chania	2	1	3
			Heraclion	1	/	1
			Rethymnon	2	1	3
E. phaeacus sp. n.	Greece	Corfu	Ano Korakiana	10	/	10
			Liapades	3	1	4
		Mt Olympos	Ag. Paraskevi	1	1	2
	Montenegro	Rumija	near lake	1	/	1
Total				24	9	33

Table S2. Results of PCA and ANOVA conducted on wing shape variables.

Πίνακας S2. Αποτελέσματα των αναλύσεων PCA και ANOVA, οι οποίες διεξήχθησαν με μεταβλητή το σχήμα των πτερύγων.

	PCA			**ANOVA**	
	Eigenvalue	Total variance	Cumulative variance	F	p
		(%)	(%)		
PC1	4.07	20.35	20.35	15.59	**0.000001**
PC2	3.08	15.41	35.75	15.22	**0.000002**
PC3	2	10	45.75	11	**0.000047**
PC4	1.69	8.44	54.19	46.65	**0**
PC5	1.51	7.54	61.73	3.31	**0.040316**
PC6	1.31	6.57	68.3	1.6	0.206824
PC7	1.08	5.41	73.72	1.16	0.317677
PC8	1.04	5.18	78.9	4.38	**0.015009**

SI CHAPTER 6

Table S1. List of the specimens used for the molecular analyses, their locality information and GenBank accession numbers. GenBank accession numbers of newly-generated sequences (this study) are in boldface and of previously-generated are in normal.

Πίνακας S1. Κατάλογος των δειγμάτων εντόμων, τα οποία χρησιμοποιήθηκαν για τις μοριακές αναλύσεις. Δίνονται πληροφορίες σχετικές με την τοποθεσία συλλογής των εντόμων και οι κωδικοί καταχώρησης στη βάση δεδομένων GenBank. Οι κωδικοί GenBank των αλληλουχιών, οι οποίες παρήχθησαν στην παρούσα έρευνα, δίνονται με έντονη γραμματοσειρά, ενώ με κανονική, δίνονται οι κωδικοί GenBank παλαιότερων αλληλουχιών.

Sequence ID	Specimen voucher	Accession no of 5'-end fragment of COI	Species name	Haplotype ID	Cluster Membership	Disposition	Sex	Geographic cluster	Country	Nearest place name	Longitude	Latitude	Collection Date
EU101	G2250	**MG560030**	*Eumerus sulcitibius* Róndani, 1868	Es1	2	FSUNS	M	Greece-Aegean	Greece	Lesvos	26.199104	39.228701	10/04/2011
EU11	G3002	**MG560025**	*Eumerus sulcitibius* Róndani, 1868	Es1	2	FSUNS	M	Greece-Aegean	Greece	Andros	24.890773	37.893197	09/10/2012
EU136	G3027	**MG559812**	*Eumerus argyropus* Loew, 1848	Earg1	3	FSUNS	F	Serbia	Serbia	Fruska gora	19.85498	45.18593	08/08/2013
EU142	AG12	**MG559858**	*Eumerus amoenus* Loew, 1848	Eam15	1	FSUNS	M	Serbia	Serbia	Dubasnica	21.9492	44.02281	23/08/2013
EU143	AK68	**MG559859**	*Eumerus amoenus* Loew, 1848	Eam16	1	FSUNS	M	Turkey	Turkey	Baffa Lake II	28.487806	37.469806	20/09/2013
EU144	G3022	**MG559860**	*Eumerus amoenus* Loew, 1848	Eam17	1	FSUNS	M	Croatia	Croatia	Vucemilovici (Grgic)	15.255082	44.50428	26/06/2011
EU145	AJ41	**MG559948**	*Eumerus clavatus* Becker, 1923	Ec1	1	FSUNS	M	Turkey	Turkey	(Milac)	27.729654	37.342639	09/2013

EU159	G3028	**MG559813**	*Eumerus argyropus* Loew, 1848	Earg1	3	FSUNS	M	Greece-Aegean	Greece	Andros	24.915047	37.839642	25/05/2012
EU16	G0278	KY865446	*Eumerus phaeacus* Chroni, Grković & Vujić, in litt.	Eph1	1	FSUNS	M	Greece-Continental	Greece	Mt Olympus	22.5863	39.8785	17/05/2011
EU160	UOTA_MEL042237, G2870	**MG559814**	*Eumerus argyropus* Loew, 1848	Earg3	3	FSUNS	M	Greece-Aegean	Greece	Chios	25.9914	38.393	9-11/11/2012
EU161	UOTA_MEL042377, G2871	**MG559815**	*Eumerus argyropus* Loew, 1848	Earg1	3	FSUNS	M	Greece-Aegean	Greece	Chios	25.9915	38.394	9-11/11/2012
EU162	UOTA_MEL042519, G2872	**MG559816**	*Eumerus argyropus* Loew, 1848	Earg1	3	FSUNS	M	Greece-Aegean	Greece	Chios	25.9916	38.395	9-11/11/2013
EU167	G3032	**MG560031**	*Eumerus sulcitibius* Róndani, 1868	Es4	1	FSUNS	M	Greece-Crete	Greece	Lassithi	25.479969	35.20236	16/10/2012
EU169	G3034	KX083387	*Eumerus sulcitibius* Róndani, 1868	Es1	2	FSUNS	M	Greece-Aegean	Greece	Andros	24.904967	37.845616	25/05/2012
EU170	G3035	**MG560032**	*Eumerus sulcitibius* Róndani, 1868	Es1	2	FSUNS	M	Greece-Aegean	Greece	Lesvos	26.3725	39.070833	25/05/2009
EU173	Đ42	**MG560001**	*Eumerus pusillus* Loew, 1848	Epus3	2	FSUNS	F	Morocco	Morocco	Middle Atlas	-5.138577	33.501592	01/05/2013
EU174	AJ46	**MG560002**	*Eumerus pusillus* Loew, 1848	Epus2	1	FSUNS	M	Turkey	Turkey	Turkey1	27.419082	37.471953	18/09/2013
EU175	AJ37	**MG560003**	*Eumerus pusillus* Loew, 1848	Epus1	1	FSUNS	M	Turkey	Turkey	Turkey1	27.41908	37.471951	18/09/2013
EU176	AJ31	**MG560004**	*Eumerus pusillus* Loew, 1848	Epus1	1	FSUNS	F	Turkey	Turkey	Turkey1	27.419078	37.471949	18/09/2013

EU177	AJ64	**MG560005**	*Eumerus pusillus* Loew, 1848	Epus2	1	FSUNS	M	Turkey	Turkey	Cesme	26.285194	38.313972	09/2013
EU178	G3036	**MG560006**	*Eumerus pusillus* Loew, 1848	Epus2	1	FSUNS	M	Greece-Aegean	Greece	Andros	24.901763	37.842993	08/10/2012
EU179	G3037	**MG560007**	*Eumerus pusillus* Loew, 1848	Epus2	1	FSUNS	M	Greece-Aegean	Greece	Andros	24.901765	37.842995	08/10/2012
EU180	G3038	**MG560008**	*Eumerus pusillus* Loew, 1848	Epus2	1	FSUNS	M	Greece-Aegean	Greece	Andros	24.901767	37.842997	08/10/2012
EU181	G3039	**MG560009**	*Eumerus pusillus* Loew, 1848	Epus2	1	FSUNS	M	Greece-Aegean	Greece	Samos	26.651697	37.775094	19/10/2010
EU182	G3040	**MG560010**	*Eumerus pusillus* Loew, 1848	Epus4	1	FSUNS	M	Greece-Peloponnese	Greece	Mt Erymanthos	21.776045	37.95039	02/09/2012
EU183	UOTA_MEL091485	**MG560011**	*Eumerus pusillus* Loew, 1848	Epus1	1	FSUNS	M	Greece-Aegean	Greece	Lesvos	26.53359	39.074815	25/9/2013
EU184	UOTA_MEL091475	**MG560012**	*Eumerus pusillus* Loew, 1848	Epus5	1	FSUNS	M	Greece-Aegean	Greece	Lesvos	26.53361	39.074817	25/9/2013
EU185	G3041	**MG559914**	*Eumerus basalis* Loew, 1848	Eb3	1	FSUNS	M	Croatia	Croatia	Rijeka Dubrovacka	18.086173	42.667778	28/06/2011
EU186	AK77	**MG559915**	*Eumerus basalis* Loew, 1848	Eb4	1	FSUNS	M	Greece-Continental	Greece	Chalcidice	23.438159	40.023235	21/09/2013
EU187	AK90	**MG559916**	*Eumerus basalis* Loew, 1848	Eb1	1	FSUNS	M	Greece-Continental	Greece	Chalcidice	23.43816	40.023236	21/09/2013
EU188	AK88	**MG559917**	*Eumerus basalis* Loew, 1848	Eb1	1	FSUNS	M	Greece-Continental	Greece	Chalcidice	23.438161	40.023237	21/09/2013
EU189	AK78	**MG559918**	*Eumerus basalis* Loew, 1848	Eb4	1	FSUNS	M	Greece-Continental	Greece	Chalcidice	23.438162	40.023238	21/09/2013
EU190	AL2	**MG559919**	*Eumerus basalis* Loew, 1848	Eb1	1	FSUNS	M	Greece-Contine	Greece	Evros	26.073889	41.050278	10/09/2013

								ntal					
EU191	G3042	**MG559920**	*Eumerus basalis* Loew, 1848	Eb1	1	FSUNS	M	Greece-Aegean	Greece	Samos	26.651697	37.775094	19/10/2010
EU192	G3043	**MG559921**	*Eumerus basalis* Loew, 1848	Eb5	1	FSUNS	M	Greece-Aegean	Greece	Samos	26.7656	37.7102	17/05/2010
EU193	UOTA_MEL091457 iG	**MG559922**	*Eumerus basalis* Loew, 1848	Eb1	1	FSUNS	M	Greece-Aegean	Greece	Lesvos	26.53359	39.074815	25/9/2013
EU195	AJ58	**MG559959**	*Eumerus pulchellus* Loew, 1848	Epul8	1	FSUNS	M	Turkey	Turkey	Baffa Lake I	27.403972	37.481944	17/09/2013
EU197	G3048	**MG559960**	*Eumerus pulchellus* Loew, 1848	Epul9	2	FSUNS	M	Italy	Italy	Sardinia	8.5926832	39.558	26/05/2008
EU198	G3049	**MG559961**	*Eumerus pulchellus* Loew, 1848	Epul10	2	FSUNS	F	Italy	Italy	Sardinia	8.5926833	39.557	26/05/2008
EU20	0560	**MG559899**	*Eumerus armatus* Ricarte & Rotheray, 2012	Earm2	1	FSUNS	M	Greece-Aegean	Greece	Lesvos	26.197467	39.255628	2/5/2008
EU200	UOTA_MEL042544	**MG559962**	*Eumerus pulchellus* Loew, 1848	Epul11	1	FSUNS 2013	M	Greece-Aegean	Greece	Chios	25.9914	38.393	9-11/11/2012
EU201	UOTA_MEL042502, G2877	**MG559963**	*Eumerus pulchellus* Loew, 1848	Epul8	1	FSUNS 2013	M	Greece-Aegean	Greece	Chios	25.991	38.39	9-11/11/2012
EU202	UOTA_MEL085018	**MG559923**	*Eumerus basalis* Loew, 1848	Eb6	1	FSUNS 2013	M	Greece-Aegean	Greece	Lesvos	26.5933	39.0142	31/8/2013
EU203	UOTA_MEL085039	**MG559924**	*Eumerus basalis* Loew, 1848	Eb7	1	FSUNS	M	Greece-Aegean	Greece	Lesvos	26.5935	39.0144	31/8/2013

EU204	UOTA_MEL095166	**MG559964**	*Eumerus pulchellus* Loew, 1848	Epul12	1	FSUNS 2013	F	Greece-Aegean	Greece	Lesvos	26.53359	39.074815	26/10/2013
EU21	0731	**MG559845**	*Eumerus amoenus* Loew, 1848	Eam1	1	FSUNS	M	Greece-Aegean	Greece	Chios	25.9916	38.394	9-11/11/2013
EU211	G0277	KY865453	*Eumerus phaeacus* Chroni, Grković & Vujić, in litt.	Eph1	1	FSUNS	F	Greece-Continental	Greece	Mt Olympus	22.5868	39.8788	17/05/2011
EU212	G0269	KY865454	*Eumerus phaeacus* Chroni, Grković & Vujić, in litt.	Eph1	1	FSUNS	M	Montenegro	Montenegro	Rumija	19.21739	42.11201	02/05/2011
EU22	1017	**MG559846**	*Eumerus amoenus* Loew, 1848	Eam2	1	FSUNS	M	Greece-Continental	Greece	Dadia	26.238949	41.124601	10-12/8/2012
EU222	G1775	**MG559900**	*Eumerus armatus* Ricarte & Rotheray, 2012	Earm3	1	FSUNS	M	Greece-Aegean	Greece	Samos	26.664797	37.730927	06/6/2012
EU223	G1020	KY865456	*Eumerus armatus* Ricarte & Rotheray, 2012	Earm3	1	FSUNS	M	Greece-Aegean	Greece	Samos	26.742116	37.740527	9/6/2010
EU224	G1789	**MG559901**	*Eumerus armatus* Ricarte & Rotheray, 2012	Earm3	1	FSUNS	M	Greece-Aegean	Greece	Samos	26.800574	37.709742	08/6/2012
EU23	1002	KX083364	*Eumerus amoenus* Loew, 1848	Eam3	1	FSUNS	M	Greece-Continental	Greece	Dadia	26.238947	41.1245	10-12/8/2012
EU234	G3064	**MG559861**	*Eumerus amoenus* Loew, 1848	Eam18	1	FSUNS	M	Greece-Aegean	Greece	Samos	26.683611	37.786944	23/10/2010
EU238	G3066	**MG559862**	*Eumerus amoenus* Loew, 1848	Eam19	1	FSUNS	M	Bulgaria	Bulgaria	Melnik	23.3927	41.52303	09/09/2012
EU24	E0900	**MG559847**	*Eumerus amoenus* Loew, 1848	Eam4	1	FSUNS	M	Greece-Crete	Greece	Karpathos	27.1849	35.7689	8-10/6/2012
EU240	UOTA_MEL0	**MG559965**	*Eumerus pulchellus* Loew,	Epul13	1	FSUNS	M	Greece-Aegean	Greece	Samothrace	25.509109	40.463322	21-22/4/2012

	41757, E0887		1848										
EU241	UOTA_MEL041754, E0886	**MG559966**	*Eumerus pulchellus* Loew, 1848	Epul3	1	FSUNS	M	Greece-Aegean	Greece	Samothrace	25.509111	40.463323	21-22/4/2012
EU242	UOTA_MEL041761, E0885	**MG559967**	*Eumerus pulchellus* Loew, 1848	Epul3	1	FSUNS	M	Greece-Aegean	Greece	Samothrace	25.509114	40.463325	21-22/4/2012
EU243	G3054	KX083385	*Eumerus basalis* Loew, 1848	Eb1	1	FSUNS	M	Greece-Aegean	Greece	Rhodes	27.852756	36.230879	16/10/2012
EU244	G3055	**MG559925**	*Eumerus basalis* Loew, 1848	Eb8	1	FSUNS	M	Greece-Crete	Greece	Kampos, Crete	25.674112000000001	35.016129999999997	12/10/2012
EU25	G2220	**MG559848**	*Eumerus amoenus* Loew, 1848	Eam5	1	FSUNS	M	Montenegro	Montenegro	Boka Kotorska	18.648915	42.490395	08/10/2010
EU26	G2258	**MG559849**	*Eumerus amoenus* Loew, 1848	Eam6	1	FSUNS	M	Greece-Aegean	Greece	Lesvos	26.453	39.055	13/04/2011
EU279	06828	KY272854	*Eumerus amoenus* Loew, 1848	Eam3	1	FSUNS	F	Turkey	Turkey	(near Camurhamamı Koyu)	28.057068	38.452905	06/07/2014
EU281 EU700	06768	**MG559902**	*Eumerus armatus* Ricarte & Rotheray, 2012	Earm5	1	FSUNS	Unknown	Turkey	Turkey	(near Davutlar)	27.29633	37.7025	06/02/2014
EU291	06738	**MG559903**	*Eumerus armatus* Ricarte & Rotheray, 2012	Earm4	2	FSUNS	M	Greece-Aegean	Greece	Rhodes	28.058878	36.116748	29/05/2014
EU292	06740	**MG559904**	*Eumerus armatus* Ricarte & Rotheray, 2012	Earm4	2	FSUNS	M	Greece-Aegean	Greece	Rhodes	28.05888	36.11675	29/05/2014
EU293	06743	**MG559905**	*Eumerus armatus* Ricarte & Rotheray, 2012	Earm4	2	FSUNS	M	Greece-Aegean	Greece	Rhodes	28.058889	36.116751	29/05/2014
EU294	06747	**MG559906**	*Eumerus armatus* Ricarte & Rotheray, 2012	Earm4	2	FSUNS	M	Greece-Aegean	Greece	Rhodes	28.058892	36.116746	29/05/2014

EU30	0738	**MG560026**	*Eumerus sulcitibius* Róndani, 1868	Es2	2	FSUNS	M	Greece-Aegean	Greece	Chios	25.9914	38.393	9-11/11/2012
EU305	06454	**MG560033**	*Eumerus sulcitibius* Róndani, 1868	Es1	2	FSUNS	F	Greece-Crete	Greece	Rethymnon	24.633061	35.152495	25/04/2014
EU307	06436	**MG559817**	*Eumerus argyropus* Loew, 1848	Earg4	1*	FSUNS	M	Greece-Crete	Greece	Rethymnon	24.67051	35.138514000000001	25/04/2014
EU31	G2292	**MG560027**	*Eumerus sulcitibius* Róndani, 1868	Es1	2	FSUNS	F	Greece-Aegean	Greece	Lesvos	26.254769	39.357622	03-04/06/2012
EU313	06433	**MG560034**	*Eumerus sulcitibius* Róndani, 1868	Es1	2	FSUNS	F	Greece-Crete	Greece	Rethymnon	24.67051	35.138514000000001	25/04/2014
EU314	06447	**MG560035**	*Eumerus sulcitibius* Róndani, 1868	Es5	2	FSUNS	F	Greece-Crete	Greece	Chania	24.468983	35.285762	25/04/2014
EU315	06449	**MG560036**	*Eumerus sulcitibius* Róndani, 1868	Es1	2	FSUNS	F	Greece-Crete	Greece	Chania	24.468984	35.285763	25/04/2014
EU317	06699	**MG559968**	*Eumerus pulchellus* Loew, 1848	Epul14	1	FSUNS	F	Greece-Crete	Greece	Chania	24.018428	35.231311	27/05/2014
EU318	06744	**MG559863**	*Eumerus amoenus* Loew, 1848	Eam20	1	FSUNS	M	Greece-Aegean	Greece	Rhodes	28.058877	36.116747	29/05/2014
EU32	G2288	**MG560028**	*Eumerus sulcitibius* Róndani, 1868	Es1	2	FSUNS	M	Greece-Aegean	Greece	Lesvos	26.254768	39.35762	03-04/06/2012
EU323	06683	**MG559969**	*Eumerus pulchellus* Loew, 1848	Epul15	1	FSUNS	F	Greece-Crete	Greece	Lassithi	25.436796	35.172534	25/05/2014
EU327	07029	**MG559970**	*Eumerus pulchellus* Loew, 1848	Epul16	2	FSUNS	F	Morocco	Morocco	Middle Atlas	-4.180925	34.071142	23/06/2014
EU328	07028	**MG559971**	*Eumerus pulchellus* Loew, 1848	Epul16	2	FSUNS	F	Morocco	Morocco	Middle Atlas	-4.180927	34.071145	23/06/2014

EU333	06468	**MG559864**	*Eumerus amoenus* Loew, 1848	Eam5	1	FSUNS	F	Greece-Peloponnese	Greece	Achaia, near Erimanthos 1	21.772531	38.115177	20/04/2014
EU335	06753	**MG559926**	*Eumerus basalis* Loew, 1848	Eb1	1	FSUNS	F	Greece-Aegean	Greece	Rhodes	27.938431	36.284938	06/01/2014
EU336	06400	**MG559972**	*Eumerus pulchellus* Loew, 1848	Epul17	1	FSUNS	F	Greece-Crete	Greece	Chania	24.01843	35.231315	24/04/2014
EU337	06345	**MG560037**	*Eumerus sulcitibius* Róndani, 1868	Es6	1	FSUNS	F	Greece-Crete	Greece	Lassithi	25.433274	35.183053	22/04/2014
EU338	06352	**MG560038**	*Eumerus sulcitibius* Róndani, 1868	Es6	1	FSUNS	F	Greece-Crete	Greece	Lassithi	25.433275	35.183054	22/04/2014
EU340	06349	**MG560039**	*Eumerus sulcitibius* Róndani, 1868	Es6	1	FSUNS	F	Greece-Crete	Greece	Lassithi	25.433276	35.183055	22/04/2014
EU341	06439	**MG560040**	*Eumerus sulcitibius* Róndani, 1868	Es1	2	FSUNS	F	Greece-Crete	Greece	Chania	24.468985	35.285764	25/04/2014
EU343	E1277	**MG559927**	*Eumerus basalis* Loew, 1848	Eb1	1	FSUNS	F	Croatia	Croatia	Rijeka Dubrovacka	18.086175	42.66778	28/06/2011
EU346	E1299	**MG559973**	*Eumerus pulchellus* Loew, 1848	Epul3	1	FSUNS	F	Greece-Aegean	Greece	Andros	24.904967	37.845616	23/05/2012
EU347	E1337	**MG559865**	*Eumerus amoenus* Loew, 1848	Eam21	1	FSUNS	F	Greece-Aegean	Greece	Naxos	25.561416	37.11825	28/05/2012
EU353	AJ85	**MG559974**	*Eumerus pulchellus* Loew, 1848	Epul18	1	FSUNS	F	Turkey	Turkey	(Marmaris NP)	28.185722	36.828722	19/09/2013
EU358	AK7	**MG559975**	*Eumerus pulchellus* Loew, 1848	Epul19	1	FSUNS	Unknown	Turkey	Turkey	(Marmaris NP)	28.185719	36.828719	Unknown
EU366	E1266	**MG559818**	*Eumerus argyropus* Loew, 1848	Earg5	1	FSUNS	F	Greece-Peloponnese	Greece	Kalentzi	21.767333	37.949917	02/09/2012

EU373	E1339	**MG560041**	*Eumerus sulcitibius* Róndani, 1868	Es7	2	FSUNS	F	Greece-Aegean	Greece	Naxos	25.43333	37.11667	13/10/2012
EU374	E1340	**MG559819**	*Eumerus argyropus* Loew, 1848	Earg5	1	FSUNS	F	Montenegro	Montenegro	Mt Durmitor	19.06862	42.98897	30/08/2012
EU376	E1342	**MG559949**	*Eumerus clavatus* Becker, 1923	Ec2	1	FSUNS	F	Greece-Continental	Greece	Mt Olympus	22.406949	40.083744	04/09/2013
EU379	E0790	**MG559976**	*Eumerus pulchellus* Loew, 1848	Epul20	1	FSUNS	M	Greece-Aegean	Greece	Limnos	25.116	39.861	05-07/04/2012
EU380	E0791	**MG559820**	*Eumerus argyropus* Loew, 1848	Earg1	3	FSUNS	F	Greece-Continental	Greece	Evros	26.1726	41.023	21-23/09/2012
EU381	E0792	KY272853	*Eumerus amoenus* Loew, 1848	Eam3	1	M-Uaegean	F	Greece-Continental	Greece	Evros	26.09328	40.9942	20-22/09/2012
EU382	E0794	**MG559866**	*Eumerus amoenus* Loew, 1848	Eam22	1	FSUNS	F	Greece-Continental	Greece	Evros	26.0933	40.9943	20-22/09/2012
EU383	E0796	**MG559867**	*Eumerus amoenus* Loew, 1848	Eam23	1	FSUNS	M	Greece-Continental	Greece	Evros	26.1012	40.9887	20-22/09/2012
EU385	07431	**MG559977**	*Eumerus pulchellus* Loew, 1848	Epul21	2	FSUNS	M	Spain	Spain	Lugros Sierra Nevada	-3.257778	37.183056	18/06/2014
EU389	E1326	**MG559950**	*Eumerus clavatus* Becker, 1923	Ec3	1	FSUNS	F	Serbia	Serbia	Vojvodina	22.015413	44.543226	Unknown
EU39	0830	**MG559907**	*Eumerus basalis* Loew, 1848	Eb1	1	FSUNS	M	Greece-Crete	Greece	Karpathos	27.1849	35.7689	8/6/2012
EU390	E1327	**MG559951**	*Eumerus clavatus* Becker, 1923	Ec2	1	FSUNS	F	Serbia	Serbia	Vojvodina	22.015414	44.543227	Unknown
EU391	E1328	**MG559868**	*Eumerus amoenus* Loew, 1848	Eam19	1	FSUNS	F	Bulgaria	Bulgaria	Melnik	23.3926	41.52302	09/09/2012

EU393	E1330	**MG559869**	*Eumerus amoenus* Loew, 1848	Eam24	1	FSUNS	F	Greece-Crete	Greece	Lassithi	25.4666667	35.15	16/10/2012
EU394	E0799	**MG559821**	*Eumerus argyropus* Loew, 1848	Earg1	3	FSUNS	F	Greece-Continental	Greece	Evros	26.1513	41.0296	21-23/09/2012
EU396	E0786	**MG559978**	*Eumerus pulchellus* Loew, 1848	Epul3	1	FSUNS	F	Greece-Aegean	Greece	Thassos	24.6788	40.6538	20-21/05/2012
EU398	E1331	**MG559870**	*Eumerus amoenus* Loew, 1848	Eam25	1	FSUNS	F	Greece-Aegean	Greece	Andros	24.940205	37.825861	10/10/2012
EU399	G0285	**MG559871**	*Eumerus amoenus* Loew, 1848	Eam26	1	FSUNS	F	Greece-Aegean	Greece	Samos	26.769917	37.707966	16/04/2011
EU400	G0281	**MG559872**	*Eumerus amoenus* Loew, 1848	Eam3	1	FSUNS	F	Montenegro	Montenegro	Boka Kotorska	18.648914	42.490394	31/04/2011
EU402	G1158	**MG559873**	*Eumerus amoenus* Loew, 1848	Eam27	1	FSUNS	F	Italy	Italy	Toscana	10.016754	44.140409	14/5/2012
EU403	G0987	**MG559822**	*Eumerus argyropus* Loew, 1848	Earg6	3	FSUNS	F	Greece-Aegean	Greece	Samos	26.8286111	37.7844444	8/6/2010
EU404	G1797	**MG559979**	*Eumerus pulchellus* Loew, 1848	Epul22	1	FSUNS	F	Greece-Aegean	Greece	Rhodes	27.945683	36.274662	16/04/2012
EU405	E1332	**MG559874**	*Eumerus amoenus* Loew, 1848	Eam3	1	FSUNS	F	Greece-Aegean	Greece	Rhodes	28.058878	36.116748	15/10/2012
EU406	E1333	KY865461	*Eumerus sulcitibius* Róndani, 1868	Es1	1	FSUNS	F	Greece-Crete	Greece	Lassithi	25.4666667	35.15	13/10/2012
EU408	E1335	**MG559875**	*Eumerus amoenus* Loew, 1848	Eam3	1	FSUNS	F	Greece-Continental	Greece	Volos	22.974453	39.390946	06/10/2012
EU412	E0992	**MG559980**	*Eumerus pulchellus* Loew, 1848	Epul3	1	FSUNS	F	Greece-Continental	Greece	Evros	26.1699	41.0398	11-13/08/2012
EU413	E0945	**MG559876**	*Eumerus amoenus* Loew, 1848	Eam28	1	FSUNS	F	Greece-Contine	Greece	Evros	26.1795	40.9959	20-22/09/2012

								ntal					
EU42	G2247	**MG559952**	*Eumerus pulchellus* Loew, 1848	Epul1	1	FSUNS	M	Greece-Aegean	Greece	Lesvos	26.282572	39.363437	12/04/2011
EU420	E0834	**MG559981**	*Eumerus pulchellus* Loew, 1848	Epul3	1	FSUNS	F	Greece-Crete	Greece	Karpathos	27.187303	35.767996	08/06/2012
EU422	E0862	KY272855	*Eumerus amoenus* Loew, 1848	Eam3	1	FSUNS	F	Greece-Crete	Greece	Karpathos	27.17488	35.741306	8-10/06/2012
EU423	G1000	**MG559877**	*Eumerus amoenus* Loew, 1848	Eam3	1	FSUNS	F	Greece-Aegean	Greece	Samos	26.8286111	37.784444	6/6/2010
EU430	E1257	**MG559878**	*Eumerus amoenus* Loew, 1848	Eam3	1	FSUNS	F	Greece-Ionian	Greece	Corfu	19.837308	39.739863	8/8/2014
EU435	6	**MG559879**	*Eumerus amoenus* Loew, 1848	Eam29	1	FSUNS	F	Greece-Ionian	Greece	Corfu	19.916724	39.512151	8/8/2014
EU438	9	**MG559982**	*Eumerus pulchellus* Loew, 1848	Epul23	1*	FSUNS	F	Greece-Ionian	Greece	Corfu	19.837307	39.739862	10/8/2014
EU439	10	**MG559823**	*Eumerus argyropus* Loew, 1848	Earg7	1	FSUNS	F	Greece-Ionian	Greece	Corfu	19.837307	39.739862	10/8/2014
EU44	0749	**MG559850**	*Eumerus amoenus* Loew, 1848	Eam7	1	FSUNS	M	Greece-Aegean	Greece	Chios	25.9915	38.394	9-11/11/2012
EU440	11	**MG559880**	*Eumerus amoenus* Loew, 1848	Eam30	1	FSUNS	F	Greece-Ionian	Greece	Corfu	19.837309	39.739864	10/8/2014
EU442	13	**MG559881**	*Eumerus amoenus* Loew, 1848	Eam31	1	FSUNS	F	Greece-Ionian	Greece	Corfu	19.837307	39.739862	10/8/2014
EU444	15	**MG559824**	*Eumerus argyropus* Loew, 1848	Earg5	1	FSUNS	F	Greece-Peloponnese	Greece	Mt Chelmos, 1736m	22.198873	38.005689	07/8/2014
EU445	16	**MG559928**	*Eumerus basalis* Loew, 1848	Eb1	1	FSUNS	M	Greece-Peloponnese	Greece	Tripoli	22.121539	37.82588	4/8/2014

EU446	17	**MG559825**	*Eumerus argyropus* Loew, 1848	Earg5	1	FSUNS	M	Greece-Peloponnese	Greece	Mt Maenalo, 1664m	22.260191	37.659227	5/8/2014
EU447	18	**MG559826**	*Eumerus argyropus* Loew, 1848	Earg8	1	FSUNS	F	Greece-Peloponnese	Greece	Mt Maenalo, 1664m	22.260192	37.659228	5/8/2014
EU448	19	**MG559827**	*Eumerus argyropus* Loew, 1848	Earg5	1	FSUNS	F	Greece-Peloponnese	Greece	Mt Maenalo, 1664m	22.260193	37.659229	5/8/2014
EU449	20	**MG559828**	*Eumerus argyropus* Loew, 1848	Earg6	3	FSUNS	M	FYRO Macedonia	FYRO Macedonia	Kozuf-Konsko	22.33559	41.1866	3/8/2014
EU45	0752	KX083366	*Eumerus amoenus* Loew, 1848	Eam3	1	FSUNS	M	Greece-Aegean	Greece	Chios	25.9914	38.393	9-11/11/2013
EU450	21	**MG559829**	*Eumerus argyropus* Loew, 1848	Earg1	3	FSUNS	M	FYRO Macedonia	FYRO Macedonia	Kozuf-Konsko	22.33558	41.18658	3/8/2014
EU451	22	**MG559830**	*Eumerus argyropus* Loew, 1848	Earg6	3	FSUNS	F	FYRO Macedonia	FYRO Macedonia	Kozuf-Konsko	22.33557	41.18657	3/8/2014
EU452	23	**MG559831**	*Eumerus argyropus* Loew, 1848	Earg8	1	FSUNS	M	Greece-Peloponnese	Greece	Mt Maenalo, Kardaras	22.290722	37.626489	5/8/2014
EU453	24	**MG559832**	*Eumerus argyropus* Loew, 1848	Earg5	1	FSUNS	M	Greece-Peloponnese	Greece	Mt Maenalo, Kardaras	22.290723	37.62649	5/8/2014
EU454	25	**MG559833**	*Eumerus argyropus* Loew, 1848	Earg5	1	FSUNS	M	Greece-Peloponnese	Greece	Mt Maenalo, Kardaras	22.290724	37.626491	5/8/2014
EU455	26	**MG559834**	*Eumerus argyropus* Loew, 1848	Earg5	1	FSUNS	M	Greece-Peloponnese	Greece	Mt Maenalo, Kardaras	22.290725	37.626492	5/8/2014
EU456	27	**MG559835**	*Eumerus argyropus* Loew, 1848	Earg5	1	FSUNS	F	Greece-Peloponnese	Greece	Mt Maenalo, Kardaras	22.290726	37.626493	5/8/2014
EU457	28	**MG559882**	*Eumerus amoenus* Loew, 1848	Eam32	1	FSUNS	F	Greece-Peloponnese	Greece	Mt Taygetos, Kod Kafica	22.265414	37.066157	6/8/2014

EU458	29	**MG559836**	*Eumerus argyropus* Loew, 1848	Earg5	1	FSUNS	F	Greece-Peloponnese	Greece	Mt Taygetos, Kod Kafica	22.265413	37.066156	6/8/2014
EU459	30, E1260	KY865462	*Eumerus amoenus* Loew, 1848	Eam33	1	FSUNS	F	Greece-Peloponnese	Greece	Mt Taygetos, Kod Kafica	22.265413	37.066156	6/8/2014
EU460	31	**MG559837**	*Eumerus argyropus* Loew, 1848	Earg5	1	FSUNS	M	Greece-Peloponnese	Greece	Mt Maenalo ski center	22.266275	37.646359	5/8/2014
EU461	32	**MG559838**	*Eumerus argyropus* Loew, 1848	Earg9	1	FSUNS	M	Greece-Peloponnese	Greece	Mt Maenalo ski center	22.266276	37.64636	5/8/2014
EU462	33	**MG559839**	*Eumerus argyropus* Loew, 1848	Earg10	1	FSUNS	F	Greece-Peloponnese	Greece	Mt Maenalo ski center	22.266277	37.646361	5/8/2014
EU464	07979	**MG559840**	*Eumerus argyropus* Loew, 1848	Earg11	2	FSUNS	M	Turkey	Turkey	Mt Davraz	30.75871	37.781694	21/07/2014
EU466	07980	**MG559841**	*Eumerus argyropus* Loew, 1848	Earg12	2	FSUNS	M	Turkey	Turkey	Mt Davraz	30.75872	37.781695	21/07/2014
EU467	07653	**MG559842**	*Eumerus argyropus* Loew, 1848	Earg7	2	FSUNS	M	Turkey	Turkey	Mt Davraz	30.75925	37.782694	03/09/2014
EU469	07982	KX083351	*Eumerus clavatus* Becker, 1923	Ec1	1	FSUNS	F	Turkey	Turkey	Mt Davraz	30.75871	37.781694	21/07/2014
EU47	1092	**MG559851**	*Eumerus amoenus* Loew, 1848	Eam8	1	FSUNS	M	Greece-Continental	Greece	Dadia	26.238948	41.1246	10-12/8/2012
EU470	07984	KX083356	*Eumerus clavatus* Becker, 1923	Ec1	1	FSUNS	F	Turkey	Turkey	Yenisarbademli	31.2954	37.697777	26/07/2014
EU472	07985	KX083358	*Eumerus clavatus* Becker, 1923	Ec1	1	FSUNS	F	Turkey	Turkey	Mt Davraz	30.75873	37.781696	21/07/2014
EU473	07986	KX083357	*Eumerus clavatus* Becker, 1923	Ec4	1	FSUNS	F	Turkey	Turkey	Yenisarbademli	31.294071	37.697471	04/09/2014

EU474	07987	KX083353	*Eumerus clavatus* Becker, 1923	Ec5	1	FSUNS	F	Turkey	Turkey	Mt Davraz	30.75925	37.782694	03/09/2014
EU475	07988	KX083355	*Eumerus clavatus* Becker, 1923	Ec6	1	FSUNS	F	Turkey	Turkey	Yenisarbademli	31.294072	37.697472	04/09/2014
EU476	07989	KX083352	*Eumerus clavatus* Becker, 1923	Ec1	1	FSUNS	M	Turkey	Turkey	Yenisarbademli	31.294073	37.697473	04/09/2014
EU483	07993	KX083354	*Eumerus clavatus* Becker, 1923	Ec7	1	FSUNS	F	Turkey	Turkey	Yenisarbademli	31.2955	37.697778	26/07/2014
EU52	0933	**MG559809**	*Eumerus argyropus* Loew, 1848	Earg1	3	FSUNS	M	Greece-Continental	Greece	Dadia	26.201644	41.126203	11-13/8/2012
EU53	0966	**MG559810**	*Eumerus argyropus* Loew, 1848	Earg1	3	FSUNS	M	Greece-Continental	Greece	Dadia	26.18777	41.123651	20-22/9/2012
EU54	0986	**MG559811**	*Eumerus argyropus* Loew, 1848	Earg2	3	FSUNS	M	Greece-Continental	Greece	Dadia	26.201645	41.126204	11-13/8/2012
EU56	G3003	**MG559953**	*Eumerus pulchellus* Loew, 1848	Epul2	2	FSUNS	Unknown	Italy	Italy	Sardinia	8.5926834	39.551	26/05/2008
EU58	0797	**MG559954**	*Eumerus pulchellus* Loew, 1848	Epul3	1	FSUNS	M	Greece-Continental	Greece	Dadia	26.238948	41.1246	20-22/9/2012
EU59	G2248	**MG559955**	*Eumerus pulchellus* Loew, 1848	Epul4	1	FSUNS	M	Greece-Aegean	Greece	Lesvos	26.28257	39.363435	12/04/2011
EU61	0912	**MG559992**	*Eumerus pusillus* Loew, 1848	Epus1	1	FSUNS	M	Greece-Crete	Greece	Karpathos	27.1849	35.7689	8-10/6/2012
EU62	0835	**MG559993**	*Eumerus pusillus* Loew, 1848	Epus1	1	FSUNS	M	Greece-Crete	Greece	Karpathos	27.1845	35.7686	8/6/2012
EU63	0863	**MG559994**	*Eumerus pusillus* Loew, 1848	Epus1	1	FSUNS	M	Greece-Aegean	Greece	Chios	25.9914	38.393	19-22/5/2012
EU64	0739	**MG559995**	*Eumerus pusillus* Loew, 1848	Epus1	1	FSUNS	M	Greece-Aegean	Greece	Chios	25.9911	38.39	9-11/11/2012

EU65	0879	**MG559996**	*Eumerus pusillus* Loew, 1848	Epus1	1	FSUNS	M	Greece-Aegean	Greece	Naxos	25.5198	36.9958	15-17/5/2009
EU66	0861	**MG559997**	*Eumerus pusillus* Loew, 1848	Epus2	1	FSUNS	M	Greece-Aegean	Greece	Naxos	25.5195	36.9955	12-14/6/2012
EU67	G0999	**MG560029**	*Eumerus sulcitibius* Róndani, 1868	Es3	1*	FSUNS	M	Greece-Aegean	Greece	Samos	26.660015	37.760447	12/06/2010
EU68	G1003	**MG559852**	*Eumerus amoenus* Loew, 1848	Eam9	1	FSUNS	M	Greece-Aegean	Greece	Samos	26.825633	37.783533	8/6/2010
EU7	G1014	**MG559898**	*Eumerus armatus* Ricarte & Rotheray, 2012	Earm1	1	FSUNS	M	Greece-Aegean	Greece	Samos	26.845875	37.787948	7/6/2010
EU74	G0991	**MG559908**	*Eumerus basalis* Loew, 1848	Eb1	1	FSUNS	M	Greece-Aegean	Greece	Ikaria	26.084756	37.601523	11/6/2010
EU75	G0992	KY865448	*Eumerus basalis* Loew, 1848	Eb1	1	FSUNS	M	Greece-Aegean	Greece	Ikaria	26.084755	37.601522	11/6/2010
EU76	G1178	**MG559853**	*Eumerus amoenus* Loew, 1848	Eam10	1	FSUNS	M	Italy	Italy	Toscana	10.30408	43.73424	10-11/5/2012
EU77	G1202	**MG559854**	*Eumerus amoenus* Loew, 1848	Eam11	1	FSUNS	M	Italy	Italy	Toscana	10.30407	43.73425	10-11/5/2012
EU78	G1155	**MG559956**	*Eumerus pulchellus* Loew, 1848	Epul5	2	FSUNS	M	Italy	Italy	Toscana	10.1907	44.0579	12/5/2012
EU80	G1198	**MG559855**	*Eumerus amoenus* Loew, 1848	Eam12	1	FSUNS	M	Italy	Italy	Toscana	10.30406	43.73423	10-11/5/2012
EU81	G0986	**MG559957**	*Eumerus pulchellus* Loew, 1848	Epul6	1	FSUNS	M	Greece-Aegean	Greece	Ikaria	26.084756	37.601523	11/6/2010
EU82	G3005	**MG559958**	*Eumerus pulchellus* Loew, 1848	Epul7	1	FSUNS	M	Greece-Aegean	Greece	Rhodes	27.852752	36.230875	16/10/2012
EU85	G3008	**MG559856**	*Eumerus amoenus* Loew, 1848	Eam13	1	FSUNS	M	Greece-Continental	Greece	Magnissia	22.974454	39.390947	06/10/2012

EU87	G3010	**MG559998**	*Eumerus pusillus* Loew, 1848	Epus1	1	FSUNS	M	Greece-Crete	Greece	Lassithi	25.680493	35.189494	14/10/2012
EU88	G3011	**MG559999**	*Eumerus pusillus* Loew, 1848	Epus1	1	FSUNS	M	Greece-Continental	Greece	Attiki	23.641944	38.008056	07/10/2012
EU89	G3012	**MG560000**	*Eumerus pusillus* Loew, 1848	Epus1	1	FSUNS	M	Greece-Crete	Greece	Chania	23.892027	35.513917	11/10/2012
EU92	G3014	KX083350	*Eumerus clavatus* Becker, 1923	Ec1	1	FSUNS	M	Serbia	Serbia	Pcinja	21.924421	42.342952	06/09/2012
EU93	G0276	**MG559857**	*Eumerus amoenus* Loew, 1848	Eam14	1	FSUNS	M	Greece-Continental	Greece	Mt Olympus	22.5863	39.8785	17/05/2011
EU94	G2283	**MG559909**	*Eumerus basalis* Loew, 1848	Eb1	1	FSUNS	M	Greece-Aegean	Greece	Lesvos	26.254769	39.357622	03-04/06/2012
EU95	0551	**MG559910**	*Eumerus basalis* Loew, 1848	Eb2	1	FSUNS	M	Greece-Aegean	Greece	Lesvos	26.4197	39.1706	23/10/2008
EU96	0829	**MG559911**	*Eumerus basalis* Loew, 1848	Eb1	1	FSUNS	M	Greece-Crete	Greece	Karpathos	27.185	35.769	8/6/2012
EU97	0822	**MG559912**	*Eumerus basalis* Loew, 1848	Eb1	1	FSUNS	M	Greece-Crete	Greece	Karpathos	27.186	35.7691	8/6/2012
EU98	G2215	**MG559913**	*Eumerus basalis* Loew, 1848	Eb1	1	FSUNS	M	Croatia	Croatia	Umag	13.514941	45.458234	03/10/2010
EU510	UOTA_MEL094835	**MG559929**	*Eumerus basalis* Loew, 1848	Eb1	1	FSUNS 2015	M	Greece-Peloponnese	Greece	Aegina	23.543	37.7515	9-11/08/2013
EU511	UOTA_MEL062483	**MG559883**	*Eumerus amoenus* Loew, 1848	Eam3	1	FSUNS 2015	M	Greece-Peloponnese	Greece	Aegina	23.4871	37.7266	15-17/06/2013
EU516	UOTA_MEL094029	**MG559884**	*Eumerus amoenus* Loew, 1848	Eam5	1	FSUNS 2015	M	Greece-Aegean	Greece	Iraklia	25.468	36.8288	4-6/04/2013
EU517	UOTA_MEL094037	**MG559885**	*Eumerus amoenus* Loew, 1848	Eam34	1	FSUNS 2015	M	Greece-Aegean	Greece	Iraklia	25.469	36.8289	4-6/04/2013

EU518	UOTA_MEL120066	**MG559886**	*Eumerus amoenus* Loew, 1848	Eam35	1	FSUNS 2015	M	Greece-Aegean	Greece	Chios	25.9283	38.208	6-8/06/2014
EU519	UOTA_MEL117050	**MG559887**	*Eumerus amoenus* Loew, 1848	Eam3	1	FSUNS 2015	M	Greece-Aegean	Greece	Folegandros	24.853	36.6619	12-14/06/2014
EU520	FSUNS09297	**MG559888**	*Eumerus amoenus* Loew, 1848	Eam3	1	FSUNS	M	Malta	Malta	Malta	14.352046	35.944652	10/04/2015
EU521	FSUNS09298	**MG559889**	*Eumerus amoenus* Loew, 1848	Eam3	1	FSUNS	M	Malta	Malta	Malta	14.345659	35.929031	10/04/2015
EU522	UOTA_MEL129453	**MG559843**	*Eumerus argyropus* Loew, 1848	Earg7	3	FSUNS 2015	M	Greece-Continental	Greece	Pieria	22.4822	40.1052	01-10/08/2014
EU523	FSUNS10094	**MG559844**	*Eumerus argyropus* Loew, 1848	Earg1	3	FSUNS	Unknown	Greece-Aegean	Greece	Chios	25.9283	38.208	6-8/06/2014
EU524	UOTA_MEL083250	**MG559930**	*Eumerus basalis* Loew, 1848	Eb1	1	FSUNS 2015	M	Greece-Aegean	Greece	Anafi	25.7438	36.363	15-17/06/2013
EU525	UOTA_MEL083078	**MG559931**	*Eumerus basalis* Loew, 1848	Eb1	1	FSUNS 2015	M	Greece-Aegean	Greece	Anafi	25.744	36.365	15-17/06/2013
EU526	UOTA_MEL099003	**MG559932**	*Eumerus basalis* Loew, 1848	Eb1	1	FSUNS 2015	M	Greece-Continental	Greece	Pieria	22.4989	40.1105	9-16/08/2013
EU527	UOTA_MEL115046	**MG559933**	*Eumerus basalis* Loew, 1848	Eb1	1	FSUNS 2015	M	Greece-Aegean	Greece	Folegandros	24.9169	36.6244	18/05/2014
EU528	UOTA_MEL115065	**MG559934**	*Eumerus basalis* Loew, 1848	Eb9	1	FSUNS 2015	F	Greece-Aegean	Greece	Folegandros	24.9171	36.6246	18/05/2014
EU530	UOTA_MEL116327	**MG559935**	*Eumerus basalis* Loew, 1848	Eb1	1	FSUNS 2015	M	Greece-Aegean	Greece	Chios	26.0163	38.2762	10/06/2014
EU531	UOTA_MEL062537	**MG559936**	*Eumerus basalis* Loew, 1848	Eb1	1	FSUNS 2015	M	Greece-Peloponnese	Greece	Aegina	23.505	37.7218	15-17/2013

EU532	UOTA_MEL094855	**MG559937**	*Eumerus basalis* Loew, 1848	Eb1	1	FSUNS 2015	M	Greece-Peloponnese	Greece	Aegina	23.4737	37.7258	9-11/08/2013
EU534	UOTA_MEL085870	**MG559938**	*Eumerus basalis* Loew, 1848	Eb9	1	FSUNS 2015	F	Greece-Aegean	Greece	Ios	25.3252	36.7538	21/06/2013
EU558	UOTA_MEL082471, 10064	KY865464	*Eumerus pulchellus* Loew, 1848	Epul24	1	M-Uaegean	M	Greece-Aegean	Greece	Anafi	25.7736	36.3565	15-17/06/2013
EU559	UOTA_MEL087592	**MG559983**	*Eumerus pulchellus* Loew, 1848	Epul3	1	FSUNS 2015	F	Greece-Aegean	Greece	Anafi	25.7728	36.357	12/05/2013
EU560	UOTA_MEL062485	**MG559984**	*Eumerus pulchellus* Loew, 1848	Epul25	1	FSUNS 2015	F	Greece-Peloponnese	Greece	Aegina	23.4871	37.7266	15-17/06/2013
EU563	UOTA_MEL115070	**MG559985**	*Eumerus pulchellus* Loew, 1848	Epul3	1	FSUNS 2015	F	Greece-Aegean	Greece	Folegandros	24.9169	36.6244	18/05/2014
EU564	UOTA_MEL115059	**MG559890**	*Eumerus amoenus* Loew, 1848	Eam21	1	FSUNS 2015	F	Greece-Aegean	Greece	Folegandros	24.9169	36.6244	18/05/2014
EU565	UOTA_MEL085708	**MG559986**	*Eumerus pulchellus* Loew, 1848	Epul3	1	FSUNS 2015	M	Greece-Aegean	Greece	Ios	25.309	36.7011	20-21/06/2013
EU566	UOTA_MEL123627	**MG559987**	*Eumerus pulchellus* Loew, 1848	Epul3	1	FSUNS 2015	M	Greece-Aegean	Greece	Iraklia	25.47	36.8505	17-20/05/2014
EU567	UOTA_MEL123809	**MG559988**	*Eumerus pulchellus* Loew, 1848	Epul26	1	FSUNS 2015	M	Greece-Aegean	Greece	Iraklia	25.4702	36.8445	17-20/05/2014
EU569	UOTA_MEL082102	**MG559989**	*Eumerus pulchellus* Loew, 1848	Epul3	1	FSUNS 2015	M	Greece-Aegean	Greece	Kea	24.3246	37.643	26-28/06/2013
EU570	UOTA_MEL093059	**MG559990**	*Eumerus pulchellus* Loew, 1848	Epul3	1	FSUNS 2015	M	Greece-Aegean	Greece	Paros	25.2236	37.1475	11-15/05/2013

EU572	FSUNS 10078	**MG559991**	*Eumerus pulchellus* Loew, 1848	Epul27	1	FSUNS	Unknown	Greece-Aegean	Greece	Tinos	25.0309	37.6522	28/03-1/04/2014
EU537	UOTA_MEL123660	**MG560013**	*Eumerus pusillus* Loew, 1848	Epus2	1	FSUNS 2015	M	Greece-Aegean	Greece	Iraklia	25.47	36.8505	17-20/05/2014
EU538	UOTA_MEL123655	**MG560014**	*Eumerus pusillus* Loew, 1848	Epus1	1	FSUNS 2015	M	Greece-Aegean	Greece	Iraklia	25.49	36.851	17-20/05/2014
EU539	UOTA_MEL085799	**MG560015**	*Eumerus pusillus* Loew, 1848	Epus2	1	FSUNS 2015	M	Greece-Aegean	Greece	Ios	25.309	36.7011	20-21/06/2013
EU541	UOTA_MEL081971	**MG560016**	*Eumerus pusillus* Loew, 1848	Epus6	1	FSUNS 2015	M	Greece-Aegean	Greece	Kea	24.3822	37.6719	26-28/06/2013
EU542	UOTA_MEL081924	**MG560017**	*Eumerus pusillus* Loew, 1848	Epus6	1	FSUNS 2015	M	Greece-Aegean	Greece	Kea	24.3825	37.6723	26-28/06/2013
EU543	UOTA_MEL096069	**MG560018**	*Eumerus pusillus* Loew, 1848	Epus2	1	M-Uaegean	M	Greece-Continental	Greece	Pieria	22.468	40.1123	26/05-2/06/2013
EU546	UOTA_MEL081197	**MG560019**	*Eumerus pusillus* Loew, 1848	Epus1	1	FSUNS 2015	M	Greece-Crete	Greece	Heraklion Province	25.3937	35.2494	5/08/2013
EU547	UOTA_MEL081201	**MG560020**	*Eumerus pusillus* Loew, 1848	Epus1	1	FSUNS 2015	M	Greece-Crete	Greece	Heraklion Province	25.3939	35.2497	5/08/2013
EU549	UOTA_MEL109271	**MG560021**	*Eumerus pusillus* Loew, 1848	Epus1	1	FSUNS 2015	M	Greece-Peloponnese	Greece	Antikythera	23.3278	35.8283	9-11/04/2014
EU552	UOTA_MEL094905	**MG560022**	*Eumerus pusillus* Loew, 1848	Epus1	1	FSUNS 2015	F	Greece-Peloponnese	Greece	Aegina	23.4971	37.7108	9-11/08/2013
EU556	FSUNS 09301	**MG560023**	*Eumerus pusillus* Loew, 1848	Epus3	2	FSUNS	F	Malta	Malta	Malta	14.377013	35.85557	09/04/2015
EU573	UOTA_MEL134868	**MG559891**	*Eumerus amoenus* Loew, 1848	Eam36	1	FSUNS 2015	F	Greece-Aegean	Greece	Lesvos	26.568	39.084	22/05-02/06/2015

EU576	UOTA_MEL092482	**MG560042**	*Eumerus sulcitibius* Róndani, 1868	Es1	2	FSUNS 2015	M	Greece-Aegean	Greece	Paros	25.123	37.0604	30/03-01/04/2013
EU577	UOTA_MEL092480	**MG560043**	*Eumerus sulcitibius* Róndani, 1868	Es1	2	FSUNS 2015	F	Greece-Aegean	Greece	Paros	25.123	37.0604	30/03-01/04/2013
TS251	FSUNS06505	**MG559892**	*Eumerus amoenus* Loew, 1848	Eam19	1	FSUNS	M	Greece-Continental	Greece	Mt Olympus	22.470193999999999	40.112067000000003	21/05/2014
TS254	FSUNS06361	**MG559893**	*Eumerus amoenus* Loew, 1848	Eam37	1	FSUNS	M	Greece-Crete	Greece	Lassithi	25.454886999999999	35.162945000000001	22/04/2014
TS255	FSUNS06337	**MG559894**	*Eumerus amoenus* Loew, 1848	Eam38	1	FSUNS	M	Greece-Crete	Greece	Lassithi	25.433274000000001	35.183053000000001	22/04/2014
TS256	06325	**MG559895**	*Eumerus amoenus* Loew, 1848	Eam39	1	FSUNS	M	Greece-Crete	Greece	Lassithi	25.464773000000001	35.255029999999998	22/04/2014
TS257	06378	**MG559896**	*Eumerus amoenus* Loew, 1848	Eam38	1	FSUNS	M	Greece-Crete	Greece	Heraclion	25.510197	35.306020	23/04/2014
TS258	FSUNS06377	**MG559897**	*Eumerus amoenus* Loew, 1848	Eam37	1	FSUNS	M	Greece-Crete	Greece	Heraclion	25.510192	35.306016	23/04/2014
TS259	08593	**MG559939**	*Eumerus basalis* Loew, 1848	Eb1	1	FSUNS	M	Greece-Peloponnese	Greece	Laconia	22.427665000000001	36.693294000000002	6/10/2014
TS260	08602	**MG559940**	*Eumerus basalis* Loew, 1848	Eb1	1	FSUNS	M	Greece-Peloponnese	Greece	Laconia	22.4276655	36.6932945	6/10/2014
TS261	FSUNS08531	**MG559941**	*Eumerus basalis* Loew, 1848	Eb1	1	FSUNS	M	Greece-Continental	Greece	Mt Parnassos	22.402258	38.531551	04/10/2014
TS263	FSUNS08532	**MG559942**	*Eumerus basalis* Loew, 1848	Eb1	1	FSUNS	M	Greece-Continental	Greece	Mt Parnassos	22.402259	38.531552	04/10/2014
TS264	E1241	**MG559943**	*Eumerus basalis* Loew, 1848	Eb10	1	FSUNS	M	Greece-Crete	Greece	Kampos, Crete	25.674113	35.01614	12/10/2012
TS267	AK89	**MG559944**	*Eumerus basalis* Loew, 1848	Eb1	1	FSUNS	M	Greece-Contine	Greece	Chalcidice	23.438163	40.023239	21/09/2013

								ntal					
TS268	AK80	**MG559945**	*Eumerus basalis* Loew, 1848	Eb1	1	FSUNS	M	Greece-Continental	Greece	Chalcidice	23.438164	40.023239	21/09/2013
TS269	AK79	**MG559946**	*Eumerus basalis* Loew, 1848	Eb1	1	FSUNS	M	Greece-Continental	Greece	Chalcidice	23.438165	40.023241	21/09/2013
TS270	AK74	**MG559947**	*Eumerus basalis* Loew, 1848	Eb1	1	FSUNS	M	Greece-Continental	Greece	Chalcidice	23.438166	40.0232342	21/09/2013
TS247	E1397	**MG560024**	*Eumerus pusillus* Loew, 1848	Epus2	1	FSUNS	M	Greece-Crete	Greece	Lassithi	25.680495	35.189496	14/10/2012
MN1	FSUNS 11413	KY865468	*Eumerus phaeacus* Chroni, Grković & Vujić, in litt.	Eph2	1	FSUNS	M	Greece-Ionian	Greece	Corfu	19.786956	39.69882	24/5/2016
MN2	FSUNS 11415	KY865469	*Eumerus phaeacus* Chroni, Grković & Vujić, in litt.	Eph1	1	FSUNS	M	Greece-Ionian	Greece	Corfu	19.786958	39.69884	24/5/2016
MN3	FSUNS 11419	KY865470	*Eumerus phaeacus* Chroni, Grković & Vujić, in litt.	Eph1	1	FSUNS	M	Greece-Ionian	Greece	Corfu	19.78696	39.69887	24/5/2016
MN4	FSUNS 11458	KY865471	*Eumerus phaeacus* Chroni, Grković & Vujić, in litt.	Eph1	1	FSUNS	M	Greece-Ionian	Greece	Corfu	19.756369	39.673537	24/5/2016
MN5	FSUNS 11457	KY865472	*Eumerus phaeacus* Chroni, Grković & Vujić, in litt.	Eph3	1	FSUNS	M	Greece-Ionian	Greece	Corfu	19.756372	39.673539	24/5/2016
MN6	FSUNS 11546	KY865473	*Eumerus phaeacus* Chroni, Grković & Vujić, in litt.	Eph1	1	FSUNS	M	Greece-Ionian	Greece	Corfu	19.837306	39.739862	24/5/2016

MN7	FSUNS 11461	KY865474	*Eumerus phaeacus* Chroni, Grković & Vujić, in litt.	Eph1	1	FSUNS	F	Greece-Ionian	Greece	Corfu	19.756374	39.673541	24/5/2016
MN8	FSUNS 11460	KY865475	*Eumerus phaeacus* Chroni, Grković & Vujić, in litt.	Eph1	1	FSUNS	M	Greece-Ionian	Greece	Corfu	19.756377	39.673543	24/5/2016
MN9	FSUNS 11448	KY865476	*Eumerus phaeacus* Chroni, Grković & Vujić, in litt.	Eph1	1	FSUNS	M	Greece-Ionian	Greece	Corfu	19.786962	39.69889	24/5/2016
MN10	FSUNS 11430	KY865477	*Eumerus phaeacus* Chroni, Grković & Vujić, in litt.	Eph1	1	FSUNS	M	Greece-Ionian	Greece	Corfu	19.786955	39.69879	24/5/2016
MN11	FSUNS 11459	KY865478	*Eumerus phaeacus* Chroni, Grković & Vujić, in litt.	Eph1	1	FSUNS	M	Greece-Ionian	Greece	Corfu	19.75638	39.673545	24/5/2016
MN12	FSUNS 11432	KY865479	*Eumerus phaeacus* Chroni, Grković & Vujić, in litt.	Eph4	1	FSUNS	M	Greece-Ionian	Greece	Corfu	19.786953	39.69876	24/5/2016
MN13	FSUNS 11436	KY865480	*Eumerus phaeacus* Chroni, Grković & Vujić, in litt.	Eph1	1	FSUNS	M	Greece-Ionian	Greece	Corfu	19.786952	39.69874	24/5/2016
MN14	FSUNS 11426	KY865481	*Eumerus phaeacus* Chroni, Grković & Vujić, in litt.	Eph1	1	FSUNS	M	Greece-Ionian	Greece	Corfu	19.78695	39.69872	24/5/2016
MN15	FSUNS 11437	KY865482	*Eumerus phaeacus* Chroni, Grković & Vujić, in litt.	Eph1		FSUNS	M	Greece-Ionian	Greece	Corfu	19.786947	39.69869	24/5/2016

page intentionally left blank

CONCLUSION

CONCLUSION

The results of the current dissertation support that the mitochondrial gene fragment COI is adequate to (a) diagnose and delimit species in the hoverfly genus *Eumerus*; (b) reveal monophyletic lineages and 'molecular' taxon groups (two major lineages and seven taxon groups); (c) infer high number of mitochondrial haplotypes and show the high genetic diversity within the genus; and (d) detect star-like patterns, which may indicate expansion events. Notwithstanding, mtDNA phylogenetic analyses suggested phylogenetic affinities between *Eumerus* species, in some cases, they were not conclusive; the employment of additional molecular markers (even of microsatellites), more species and/ or more sequences per species should be sought to determine any unresolved tree topology or confirm the inferred ones.

Phylogenetic analyses based only to morphological characters succeeded to diagnose species within the genus, however they were not always sufficient to conclude for phylogenetic affinities among species, pointing out the necessity employing of DNA barcodes, or a combination of morphological and molecular data. Indeed, integrative approach methods supported identification and description of five new species within *Eumerus* (*E. aurofinis* Grković, Vujić & Radenković, 2015; *E. torsicus* Grković & Vujić, 2015; *E. crassus* Grković, Vujić & Radenković, 2015; *E. montanum* Grković, Radenković & Vujić, 2017; *E. rubrum* Grković & Vujić, 2017), resolved one synonymy (*E. alpinus* vs. *E. olivaceus*) and revised the geographical range of one species (*E. uncipes* Rondani, 1850 in Corfu Island, Greece). The aforementioned results point out to the necessity for a revision of the genus by employing integrative taxonomy approaches, which will seek to answer questions arisen from the current dissertation: why two major lineages were noticed within the genus? how many species and taxon groups exist within the genus?

Morphological (male genitalia, antenna segments, wing geometric morphometry), molecular (COI and 28S gene fragments) and mtDNA phylogeographic and biogeographic analyses were employed to study the species and their phylogenetic relationships within the *E. minotaurus* taxon group. All analyses (alone or in combination), apart of the ones of the nuclear marker, indicated one species (*E. anatolicus* sp. n.) and one cryptic species complex (*E. karyates* Chroni, Grković & Vujić sp. n.; *E. minotaurus* Claussen & Lucas, 1988; and *E. phaeacus* Chroni, Grković & Vujić sp. n.). MtDNA phylogeographic analysis of the species of *E.*

minotaurus group suggested that the formation of the mid-Aegean Trench and the Messinian Salinity Crisis were related with the speciation within *E. minotaurus* group. The acquirement of mtDNA sequences of all species encompassing the *E. minotaurus* group, and their inclusion to phylogenetic and phylogeographic inferences could clarify further the speciation processes acted on the species of *E. minotaurus* group, and enhance the consideration of the constructive role of the historical processes consolidated the Aegean on species distribution.

The spatial genetic structure analyses inferred the presence of (a) two genetic clusters ascribed to allopatric and peripatric processes, as well as to landscape discontinuities formed as a result of palaeogeological and palaeoclimatic events (in four species); (b) one genetic cluster, pointing to the hypothesis of relict taxa (in five species); and (c) high- and low-genetic divergent regions in the Mediterranean. A better representation of the species range with inclusion of (more) specimens from the Mediterranean peninsulas (where/ if the species occur) would succor to shed light on any observed obscurities in the spatial genetic patterns, and undertake the formation of the Mediterranean peninsulas in shaping the population structure of *Eumerus* species.

page intentionally left blank

ΠΕΡΙΛΗΨΗ

ΠΕΡΙΛΗΨΗ

Η μοναδικότητα των οργανισμών έχει αποτελέσει πολλαπλό αντικείμενο έρευνας. Από βιολογική άποψη, η μοναδικότητα αυτή εκφράζεται ως ποικιλότητα χαρακτήρων που αντανακλούν την παραλλακτικότητα του γονιδιώματος, η οποία τελικά συγκροτεί την βασική έκφανση της βιοποικιλότητας, το αποτέλεσμα εξέλιξης εκατομμυριών ετών. Η ανάγκη για διερεύνηση της βιοποικιλότητας υποστηρίζεται από την ταξινομική, δια της οποίας τα είδη αναγνωρίζονται, περιγράφονται και ονοματίζονται. Η μοριακή συστηματική αποτελεί ειδική ταξινομική μέθοδο κατά την οποία χρησιμοποιούνται εργαλεία της μοριακής γενετικής ώστε να ταξινομηθούν είδη, να εξαχθούν συμπεράσματα που αφορούν στις φυλογενετικές σχέσεις μεταξύ ατόμων ή/και ειδών, και να παραχθεί επαρκής πληροφορία που να περιγράφει την φυσική ιστορία και τις εξελικτικές σχέσεις του υπό μελέτη οργανισμού με άλλους συγγενικούς. Οι φυλογενετικές σχέσεις αποδίδονται μέσω των φυλογενετικών δέντρων, τα οποία βασίζονται σε ομοιότητες και αποκλίσεις των κοινών προγονικών χαρακτήρων. Αναλόγως του χειρισμού των δεδομένων και της προσέγγισης που ακολουθείται για την κατασκευή του φυλογενετικού δέντρου, διακρίνονται δυο κατηγορίες μεθόδων φυλογενετικής ανάλυσης: οι μέθοδοι ομαδοποίησης (π.χ. μέθοδος σύνδεσης γειτόνων, Neighbor Joining, NJ), και οι μέθοδοι διερεύνησης δέντρων (Μέγιστη Φειδωλότητα, Maximum Parsimony, MP· Μέγιστη Πιθανοφάνεια, Maximum Likelihood, ML· και Μπεϊεσιανή Συμπερασματολογία, Bayesian Inference, BI), με τις φυλογενετικές μεθόδους MP, ML και BI να πρωτοστατούν.

Ένα από τα πολυτιμότερα μοριακά εργαλεία για την διερεύνηση των φυλογενετικών σχέσεων είναι η χρήση των μοριακών δεικτών, δηλαδή συντηρημένες, κωδικές περιοχές του DNA, με δημοφιλέστερο τον γενετικό γραμμωτό κώδικα (DNA barcoding). Οι μοριακοί δείκτες έχουν, αναμφίβολα, συμβάλλει στην αναγνώριση ατόμων/ειδών, στη διάγνωση νέων ειδών, στην ανακάλυψη κρυπτικών γενεαλογικών γραμμών και στην διαλεύκανση βιολογικών και εξελικτικών διεργασιών. Οι περιοχές γονιδίων που χρησιμοποιούνται ευρέως, και χρησιμοποιήθηκαν στην παρούσα διδακτορική διατριβή, είναι δυο θραύσματα του γονιδίου της μιτοχονδριακής υπομονάδας της οξειδάσης I του κυτοχρώματος c (ένα από αυτά ήταν η κωδική περιοχή γνωστή και ως DNA barcode, COI) και της μεταβλητής περιοχής D2 του πυρηνικού ριβοσωμικού γονίδιου 28S (nuclear 28S D2 ribosomal DNA gene, 28S). Ειδικότερα, το μιτοχονδριακό DNA (mtDNA) έχει γνωρίσει μεγάλη αποδοχή λόγω

των πλεονεκτημάτων που διαθέτει: έλλειψη ανασυνδυασμού, μητρική κληρονομικότητα (απλοειδές), ευκολία στην απομόνωση και προσδιορισμό (μεγάλος αριθμός αντιγράφων που απαιτεί μικρό μέγεθος δείγματος), πολυμορφικότητα και υψηλό ρυθμό μεταλλαξιγένεσης (5-10 φορές περισσότερο συγκριτικά με το πυρηνικό DNA).

Τα μοριακά δεδομένα έχουν αποδειχθεί πιο αξιόπιστα και κατάλληλα για φυλογενετικές μελέτες σε σχέση με άλλα δεδομένα, π.χ. βασιζόμενα στην μορφολογία ή τη φυσιολογία, διότι αφορούν χαρακτηριστικά αυστηρώς κληρονομούμενα που δεν επηρεάζονται από περιβαλλοντικούς παράγοντες, η περιγραφή τους δεν είναι υποκειμενική, είναι άφθονα κ.λπ. Φυσικά, κατά την οριοθέτηση ενός είδους, την συναγωγή συμπερασμάτων για τις εξελικτικές σχέσεις ή τις αιτίες που οδήγησαν σε ειδογένεση, είναι σημαντικό να λαμβάνονται υπόψη περισσότεροι του ενός μοριακοί δείκτες, ή/ και να συνθεωρούνται άλλες συμπληρωματικές μέθοδοι. Πλέον, μιλάμε για την ενοποιητική ταξινομική (Integrative Taxonomy), στην οποία συνθεωρούνται δεδομένα μορφολογικά (π.χ. γεωμετρική μορφομετρία πτερύγων), μοριακά (DNA, RNA και πρωτεΐνες), βιοχημικά (π.χ. αλλοένζυμα), πολλές φορές, αντιπαραβάλλοντας περιβαλλοντικούς (π.χ. θερμοκρασία) ή/ και οικολογικούς (π.χ. χρήση ενδιαιτήματος) παράγοντες.

Οι πληθυσμοί αποτελούν δυναμικές οντότητες, καθώς έχουν την ικανότητα να μεταβάλλονται προσαρμοζόμενοι στις περιβαλλοντικές αλλαγές. Αποτέλεσμα τέτοιων προσαρμογών είναι η ειδογένεση, το αποτέλεσμα της εξελικτικής διαδικασίας, κατά την οποία από ένα είδος προκύπτει ένα ή περισσότερα. Γενικά, για να ορισθεί ένα (νέο) είδος, πρέπει τα άτομα που το απαρτίζουν να προέρχονται από έναν κοινό πρόγονο, να διαθέτουν από κοινού παρόμοια (μοριακά και μορφολογικά) χαρακτηριστικά, και να μπορούν να αναπαράγονται μεταξύ τους δίνοντας γόνιμους απογόνους. Υπάρχουν τέσσερις μηχανισμοί ειδογένεσης ως αποτέλεσμα απομόνωσης των πληθυσμών (συνεπώς, με περιορισμό ανταλλαγής γονιδίων), τόσο αναπαραγωγικής (συμπάτρια και παραπάτρια ειδογένεση) όσο και γεωγραφικής (αλλοπάτρια και περιπάτρια ειδογένεση).

Ένα φυλογενετικό δέντρο μπορεί να αναδείξει την παρουσία ειδογένεσης ή φαινόμενα όπως η γενετική στενωπός, διασπορά – βικαριανισμός ή μετανάστευση. Συχνά, χρησιμοποιούνται μιτοχονδριακά δεδομένα, όχι μόνο για τον προσδιορισμό των φυλογενετικών σχέσεων μεταξύ των ειδών, αλλά και για την γεωγραφική αποτύπωση, και ανάδειξη της εξελικτικής και βιογεωγραφικής ιστορίας τους. Ο

επιστημονικός αυτός κλάδος ονομάζεται φυλογεωγραφία, και γνωρίζει ραγδαία εξέλιξη τα τελευταία χρόνια. Η φυλογεωγραφία, συχνά, εμφανίζεται στενά συνδεδεμένη με την εφαρμογή της υπόθεσης του μοριακού ρολογιού (molecular clock hypothesis). Η υπόθεση αυτή υποστηρίζει την ύπαρξη ενός σταθερού ρυθμού εξέλιξης (ρυθμός νουκλεοτιδικών ή αμινοξικών υποκαταστάσεων), που μπορεί να είναι γρήγορος ή πιο αργός ανάλογα με τα υπό μελέτη γονίδια. Η εφαρμογή της υπόθεσης του μοριακού ρολογιού συμβάλλει στην εκτίμηση των χρόνων απόσχισης των ειδών.

Στην παρούσα διδακτορική διατριβή μελετάται το *Eumerus* Meigen, 1822, ένα πλούσιο σε είδη γένος της οικογένειας των Συρφίδων. Οι Συρφίδες (Diptera: Syrphidae) συγκροτούν μια μεγάλη ομάδα εντόμων, με περισσότερα από 6100 περιγραμμένα είδη, που προσφέρουν σημαντικές οικοσυστηματικές υπηρεσίες (π.χ. στην επικονίαση των φυτών). Ειδικότερα, το γένος *Eumerus* εμφανίζει ευρύτατη κατανομή, αριθμώντας περίπου 256 είδη παγκοσμίως, με 140 από αυτά να έχουν καταγραφεί στην Παλαιαρκτική Ζώνη, 75 από τα οποία στην Ευρώπη, κυρίως στις νότιες περιοχές της. Αξίζει να αναφέρουμε ότι πολλά από αυτά τα είδη περιγράφηκαν πρόσφατα, ή πρόκειται να περιγραφούν, με κάποια από αυτά στο πλαίσιο της διατριβής αυτής (βλ. Κεφάλαια 3 – 5).

Περιοχές μελέτης της διατριβής αποτελούν κυρίως η Βαλκανική Χερσόνησος, συμπεριλαμβανομένων των νησιών του Αιγαίου, καθώς και άλλες χώρες της Μεσογείου. Οι περιοχές αυτές χαρακτηρίζονται από μια πολύπλοκη γεωλογική και κλιματική ιστορία, η οποία επηρέασε την φυλογένεση και φυλογεωγραφία πολλών οργανισμών και συνέβαλε στα σύγχρονα βιογεωγραφικά πρότυπα βιοποικιλότητας και ενδημισμού. Η βιοποικιλότητα της Μεσογείου είναι άρρηκτα συνδεδεμένη με αλλαγές παλαιογεωγραφικές (έντονα φαινόμενα τεκτονισμού και ευστατισμού) και παλαιοκλιματικές (εναλλαγές κλίματος, παγετώνες) που υπέστη η περιοχή μετά το Τεταρτογενές (έως το Ολόκαινο, οπότε και ολοκληρώθηκαν). Σημαντική επίδραση στη βιοποικιλότητα είχαν, επίσης, το ανάγλυφο της περιοχής και η παρουσία του ανθρώπου. Χαρακτηριστικά παραδείγματα περιοχών μεγάλης βιοποικιλότητας και ενδημισμού της Μεσογείου λόγω των παραπάνω παραγόντων, συνιστούν η Βαλκανική Χερσόνησος και η Ανατολία. Οι περιοχές αυτές έχουν χαρακτηρισθεί ως θερμά σημεία βιοποικιλότητας, λόγω του ρόλου τους ως καταφύγια κατά την διάρκεια των παγετώνων, και πηγές διασποράς ειδών προς την Κεντρική και Βόρεια Ευρώπη κατά τις μεσοπαγετωνικές περιόδους. Τα νησιά του Αιγαίου αποτελούν

Μεσογειακή περιοχή με υψηλή βιοποικιλότητα και ενδημισμό, απόρροια γεωγραφικής θέσης και παλαιογεωγραφικής ιστορίας: έντονος κατακερματισμός της περιοχής, δημιουργία της μεσο-Αιγαιακής Τάφρου (mid-Aegean Trench, MAT), Κρίση Αλατότητας του Μεσσηνίου (Messinian Salinity Crisis, MSC) κ.λπ.

Η παρούσα διατριβή προσβλέπει να διερευνήσει έναν περιορισμένο αριθμό ειδών του γένους *Eumerus* και την γεωγραφική κατανομή τους στην Βαλκανική Χερσόνησο (και σε παρακείμενες περιοχές), εφαρμόζοντας την μέθοδο της ενοποιητικής ταξινομικής. Για πρώτη φορά στο γένος *Eumerus* επιχειρείται η χρήση μορφολογικών και μοριακών εργαλείων σε συνδυασμό με μεθόδους φυλογένεσης και φυλογεωγραφίας. Διερευνήθηκαν τα κάτωθι ερωτήματα: (1) Είναι οι μιτοχονδριακές αλληλουχίες επαρκείς για την διάγνωση και οριοθέτηση ειδών στο γένος *Eumerus*; Πώς μπορεί η συνθεώρηση των μορφολογικών χαρακτηριστικών να συμβάλλει στην αναγνώριση των ειδών; (2) Μπορούν οι μοριακοί δείκτες να ανιχνεύσουν συμπλέγματα κρυπτικών ειδών και να υποδείξουν τις εξελικτικές διεργασίες που έχουν οδηγήσει στα παρατηρούμενα πρότυπα ειδογένεσης και βιογεωγραφίας; και (3) Υπάρχουν χωρικά πρότυπα γενετικής ποικιλότητας στο γένος *Eumerus*; Ποιός ο ρόλος των ασυνεχειών του τοπίου (π.χ. ενός βουνού), της απομόνωσης λόγω απόστασης (isolation by distance) ή των παλαιογεωλογικών και πλαιοκλιματικών αλλαγών στα παρατηρούμενα χωρικά γενετικά πρότυπα;

Ένα από τα βασικά προβλήματα στην μελέτη του γένους *Eumerus* είναι η δυσκολία ταυτοποίησης και ταξινόμησης των ειδών του, τόσο διότι δεν υπάρχει μια ολοκληρωμένη και αξιόπιστη κλείδα, όσο και διότι η βιβλιογραφία βρίθει συνωνύμων ονομάτων των περιγραφέντων ειδών. Έτσι, στο Κεφάλαιο 2, δημιουργήθηκε ένα μοριακό σύστημα ταυτοποίησης βάσει του μιτοχονδριακού γονιδίου COI (θραύσμα COI-3′) ώστε να χρησιμοποιηθεί στην διάγνωση και οριοθέτηση (νέων) ειδών του γένους *Eumerus*, στην αναθεώρηση ειδών και στην επίλυση συνωνύμων. Χρησιμοποιήθηκαν 75 δείγματα από 28 είδη, προερχόμενα από την Παλαιαρκτική και Αφροτροπική Ζώνη. Επιπλέον, δημιουργήθηκαν δύο ομάδες δεδομένων (A, B), διαφορετικού μήκους νουκλεοτιδίων (A με 647 bp· B με 746 bp), με στόχο να διερευνηθεί η σημασία των περισσότερων πολυμορφικών τόπων στην ταυτοποίηση ειδών. Κατασκευάστηκαν φυλογενετικά δέντρα με την μέθοδο της διερεύνησης δέντρων (MP, ML και BI), εφαρμόστηκαν μοντέλα ‘Poisson tree processes’ (PTP models) και δίκτυα ανάλυσης Σύνδεσης Γειτόνων (NJ) για την πρόβλεψη,

αξιολόγηση και σύγκριση ορθής ομαδοποίησης ‘ταξινομικών’ ως προς των ‘μοριακών’ ειδών (taxa clusters).

Όλες οι προαναφερόμενες μέθοδοι κατέληξαν στην επιτυχή μοριακή ταυτοποίηση των εντομολογικών δειγμάτων. Τα αποτελέσματα από τις δύο ομάδες δεδομένων ήταν παρόμοια, με την ομάδα δεδομένων Α να παρέχει αρκετούς πολυμορφικούς χαρακτήρες για την αναγνώριση ειδών, αλλά με την ομάδα δεδομένων Β να λύνει κάποια προβλήματα στην τοπολογία των δέντρων και να ρίχνει περισσότερο φως στις φυλογενετικές σχέσεις μεταξύ των ειδών. Εντοπίστηκαν και συζητήθηκαν οι δυο μονοφυλετικοί κλάδοι, η τοπολογία των δέντρων και η παρουσία εφτά ομάδων ειδών (taxon groups) σύμφωνα με την φυλογενετική τους συγγένεια. Παρατηρήθηκε μεγάλος αριθμός μιτοχονδριακών απλοτύπων, και τα είδη εμφάνισαν μοναδικούς απλότυπους, οι οποίοι διαχωρίστηκαν με αρκετά εξελικτικά βήματα μεταξύ τους στα δίκτυα NJ. Το εύρημα αυτό είναι σχετικά ασύνηθες στις συρφίδες (π.χ. στο γένος *Melanostoma* Schiner, 1860), καθιστώντας το βασιζόμενο στο COI γονίδιο μοριακό σύστημα, κατάλληλο για την διάκριση μεταξύ των ειδών του *Eumerus*. Στο ίδιο κεφάλαιο, διερευνήθηκε και συζητήθηκε η ενδοειδική ποικιλότητα τριών ειδών (*E. amoenus* Loew, 1848, *E. pulchellus* Loew, 1848 και *E. pusillus* Loew, 1848).

Τα παραπάνω ευρήματα ανέδειξαν την σημασία εφαρμογής ενός μοριακού συστήματος ταυτοποίησης, και οδήγησαν στην περαιτέρω εφαρμογή του στην διάγνωση και οριοθέτηση (νέων) ειδών εντός του *Eumerus*, με απώτερο σκοπό μια ολιστική προσέγγιση της (ενοποιητικής) ταξινομικής (βλ. Κεφάλαια 3 – 4). Μελετώντας (μορφολογικά ή/και μοριακά/φυλογενετικά) δείγματα και είδη του γένους *Eumerus* προερχόμενα από τη νοτιοανατολική Ευρώπη (συμπεριλαμβανομένων των νησιών της Ανατολικής Μεσογείου), βρέθηκαν νέα είδη για την επιστήμη, αναθεωρήθηκε το όνομα ενός είδους με βάση την γεωγραφική του εξάπλωση, και έγινε πρώτη καταγραφή ενός είδους στην περιοχή.

Συγκεκριμένα, στο Κεφάλαιο 3, παρουσιάζονται τρία νέα είδη για την επιστήμη, που καταγράφηκαν σε περιοχές της Ανατολικής Μεσογείου: *Eumerus aurofinis* Grković, Vujić & Radenković 2015 (Λέσβος, Σάμος, Ρόδος και το Όρος Bozdağ της Τουρκίας), *E. torsicus* Grković & Vujić 2015 (Χίος, Κύπρος) και *E. crassus* Grković, Vujić & Radenković 2015 (Λέσβος). Η οριοθέτηση των δύο πρώτων ειδών βασίστηκε σε μορφολογικούς (δίνονται οι περιγραφές ειδών) και μοριακούς χαρακτήρες (θραύσμα Folmer COI-5′, υπολογισμός γενετικών αποτάσεων κ.λπ.), ενώ για το τρίτο

είδος μόνο σε μορφολογικούς (λόγω αδυναμίας διαθέσιμου γενετικού υλικού). Επιπλέον, αναθεωρήθηκε το είδος *E. alpinus* Rondani, 1857, και διαχωρίστηκε από το *E. olivaceus* Loew, 1848, με το πρώτο να καταγράφεται στις Άλπεις και στην Βαλκανική Χερσόνησο, και το δεύτερο, ως ενδημικό της Σικελίας (Ιταλία). Παρουσιάζεται κατάλογος με 25 καταγεγραμμένα είδη του γένους *Eumerus* στα νησιά της Ανατολικής Μεσογείου, συμπεριλαμβάνοντας τα ενδημικά είδη.

Στο Κεφάλαιο 4, παρουσιάζονται δύο ακόμη νέα είδη, *E. montanum* Grković, Radenković & Vujić sp. n. (Μαυροβούνιο, Ελλάδα) και *E. rubrum* Grković & Vujić sp. n. (Ελλάδα), και γίνεται πρώτη καταγραφή του *E. uncipes* Rondani, 1850 για τη νοτιοανατολική Ευρώπη. Τα είδη αυτά είναι μέλη τριών διαφορετικών ομάδων ειδών, των *E. strigatus* sensu Speight *et al.* (2013), *E. tricolor* sensu Chroni *et al.* (2017), και *E. clavatus*, όπως προσδιορίστηκε στην παρούσα ερευνητική εργασία, αντίστοιχα. Ορίζονται διαγνωστικοί χαρακτήρες για την κάθε ομάδα είδους και δίνονται περιγραφές των νέων ειδών. Η φυλογενετική θέση των *E. montanum* sp. n. και *E. uncipes* (μη διαθέσιμο γενετικό υλικό για το *E. rubrum* sp. n.) διαπιστώθηκε και επαληθεύτηκε μέσω φυλογενετικών δέντρων (MP, NJ και ML) και ενός δικτύου 'split network'. Χρησιμοποιήθηκαν 41 αλληλουχίες (και 3 αλληλουχίες ως εξωομάδα) από 15 είδη του γένους *Eumerus*. Σε όλες τις αναλύσεις, το *E. uncipes* ομαδοποιήθηκε με το *E. clavatus*, σχηματίζοντας την ομάδα είδους *E. clavatus*, και το *E. montanum* sp. n. με το *E. strigatus* σχηματίζοντας την ομάδα είδους *E. strigatus*.

Στο πλαίσιο της ενοποιητικής ταξινομικής διερευνήθηκε η ταξινομική και φυλογενετική θέση του *E. montanum* sp. n. σε σχέση με άλλα είδη της ομάδας *E. strigatus*. Χρησιμοποιήθηκαν μορφολογικά (24 χαρακτήρες: κεφάλι, θώρακας, κοιλιά, γεννητικός οπλισμός άρρενος) και μοριακά δεδομένα (612 bp, 21 αλληλουχίες *Eumerus* από 7 είδη, 3 αλληλουχίες ως εξωομάδα). Επίσης, υπολογίστηκαν οι γενετικές αποστάσεις (K2P genetic distance) μεταξύ αυτών των ειδών. Κατασκευάστηκαν τρία MP δέντρα, όπου στο ένα υπήρχαν μόνο μοριακά δεδομένα, στο δεύτερο μόνο μορφολογικά και στο τρίτο συνδυασμός και των δυο τύπων δεδομένων, ώστε να αξιολογηθεί η ποιότητα της πληροφορίας στην εξακρίβωση της φυλογενετικής θέσης του *E. montanum* sp. n. Οι αναλύσεις του πρώτου και τρίτου MP δέντρου επαλήθευσαν την φυλογενετική συγγένεια μεταξύ των *E. montanum* sp. n. και *E. strigatus*, ενώ η ανάλυση του δεύτερου MP δέντρου δεν ομαδοποίησε αυτά τα δυο είδη, πιθανότατα λόγω ανεπαρκούς αριθμού μορφολογικών χαρακτήρων.

Προσεκτική μορφολογική εξέταση έδειξε ομοιότητα στα σχήματα του τέταρτου κοιλιακού στερνίτη στα αρσενικά άτομα των *E. montanum* sp. n. και *E. strigatus*.

Τα Κεφάλαια 3 – 4 αύξησαν τον συνολικό αριθμό ειδών του *Eumerus* για τη νοτιοανατολική Ευρώπη από 31 σε 37, αναδεικνύοντας την βιοποικιλότητα και τον ενδημισμό της περιοχής. Η περιοχή αυτή, συγκεκριμένα η Βαλκανική Χερσόνησος και τα νησιά του Αιγαίου, έχουν αναγνωριστεί ως περιοχές με υψηλά επίπεδα βιοποικιλότητας συρφίδων, π.χ. του γένους *Merodon*, συμπεριλαμβάνοντας κρυπτικά και ενδημικά είδη. Κατά την μοριακή ταυτοποίηση δειγμάτων *Eumerus*, αποκαλύφθηκε ένας κρυπτικός εξελικτικός κλάδος στο είδος *E. minotaurus* Claussen & Lucas, 1988. Ως κρυπτικά ορίζονται τα είδη που μορφολογικά είναι παρόμοια, αλλά συνιστούν διακριτές γενεαλογικές γραμμές. Τα κρυπτικά είδη είναι αποτέλεσμα αργής φαινοτυπικής διαφοροποίησης ή εξελικτικής σύγκλισης, ως αποτέλεσμα μορφολογικής προσαρμογής σε ένα συγκεκριμένο περιβάλλον.

Λαμβάνοντας υπόψη τα παραπάνω, στο Κεφάλαιο 5 μελετήθηκε η ομάδα ειδών (taxon groups) *Eumerus minotaurus*, και διαγνώσθηκαν εντός της ομάδας ειδών ένα νέο είδος, *E. anatolicus* Grković, Vujić & Radenković sp. n. (Μοβολλά/Muğla, Τουρκία· δίνεται η περιγραφή είδους), και τρία κρυπτικά είδη εντός του *E. minotaurus*: *E. karyates* Chroni, Grković & Vujić sp. n. (Πελοπόννησος), *E. minotaurus* (Κρήτη και Κάρπαθος) και *E. phaeacus* Chroni, Grković & Vujić sp. n. (Κέρκυρα και Όρος Όλυμπος· Όρος Rumija, Μαυροβούνιο). Η ομάδα ειδών *E. minotaurus* χαρακτηρίζεται μορφολογικά από επιμηκυμένο μίσχο στην κεραία (elongated pedicel) και από το σχήμα του γεννητικού οπλισμού των αρρένων.

Για την διαπίστωση και επαλήθευση της φυλογενετικής θέσης των ειδών της ομάδας ειδών *E. minotaurus*, συμπεριλήφθηκαν τα είδη από τα οποία απαρτίζεται αυτή η ομάδα ειδών (*E. crassus*, *E. karyates* sp. n., *E. minotaurus* και *E. phaeacus* sp. n.· δεν συμπεριλήφθηκε το *E. anatolicus* sp. n. λόγω μη διαθεσιμότητας γενετικού υλικού), και 15 επιπλέον είδη *Eumerus*. Χρησιμοποιώντας τον μιτοχονδριακό μοριακό δείκτη του γονιδίου COI (θραύσματα COI-3′ και COI-5′· 1238 bp), εφαρμόστηκαν με επιτυχία δυο τύποι αναλύσεων που είτε προϋπέθεταν την κατασκευή φυλογενετικών δέντρων (tree-based species delimitation: MP, ML, NJ, BI, split network και PTP models), είτε όχι (non-tree-based species delimitation: γενετικές αποστάσεις, K2P pairwise distances και δίκτυο απλοτύπων με τον αλγόριθμο της στατιστικής φειδωλότητας, TCS network). Όλες οι παραπάνω αναλύσεις έδειξαν όμοια τοπολογία δέντρων στην ομάδα ειδών *E. minotaurus*, με το

E. crassus να ομαδοποιείται ξεχωριστά από το σύμπλεγμα *E. minotaurus*. Εντός του συμπλέγματος, τα είδη *E. karyates* sp. n. και *E. minotaurus* ομαδοποιήθηκαν μαζί, και ξεχωριστά από το *E. phaeacus* sp. n. Σχετικά με τον πυρηνικό δείκτη 28S (510 bp), κατασκευάστηκε MP δέντρο, το οποίο όμως λόγω της αδυναμίας του να διακρίνει όλες τις εξελικτικές γραμμές (αλλά και της δυσκολίας στην απομόνωση του γονιδίου), τελικά απορρίφθηκε.

Για την εξακρίβωση και οριοθέτηση των κρυπτικών ειδών συμπεριλήφθησαν μόνο τα είδη της ομάδας ειδών *E. minotaurus*, και, στο πλαίσιο της ενοποιητικής ταξινομικής, συνθεωρήθηκαν μορφολογικά (κεραίες, γεννητικός οπλισμός άρρενος) και μοριακά (COI) χαρακτηριστικά, καθώς και η γεωμετρική μορφομετρία πτερύγων. Η τελευταία μέθοδος έχει αποδειχθεί ιδιαίτερα δημοφιλής και αξιόπιστη στην οικογένεια των συρφίδων αναφορικά με διαειδικές διαφοροποιήσεις, και επιβεβαίωσε τα μοριακά ευρήματα. Βάσει της παλαιογεωγραφίας του Αιγαίου, μελετήθηκαν πιθανά βιογεωγραφικά πρότυπα και διεργασίες ειδογένεσης (μιτοχονδριακά φυλογεωγραφικά πρότυπα), και κατασκευάστηκε η βιογεωγραφική ιστορία της ομάδας ειδών *E. minotaurus* ώστε να προβλεφθούν οι προγονικές περιοχές γεωγραφικής κατανομής. Εξετάστηκαν τρεις διαφορετικές εφαρμογές βαθμονόμησης του μοριακού ρολογιού (molecular clock calibration) και εκτιμήθηκαν οι χρόνοι απόσχισης. Η βαθμονόμηση του μοριακού ρολογιού που συμπεριλαμβάνει πάνω από ένα γεωλογικά γεγονότα φαίνεται να είναι πιο αξιόπιστη συγκριτικά με το ένα σημείο βαθμονόμησης ή τον ρυθμό εξέλιξης του mtDNA των αρθροπόδων. Συγκεκριμένα, με βάση τους χρόνους απόσχισης, βρέθηκε ότι η διαφοροποίηση ειδών προέκυψε ως αποτέλεσμα (α) της μεσο-Αιγαιακής Τάφρου (12-9 εκατ. χρόνια), που διαχώρισε τους ανατολικούς από τους δυτικούς πληθυσμούς, και (β) της Κρίσης Αλατότητας του Μεσσηνίου (5.96-5.33 εκατ. χρόνια), όπου στο τέλος της περιόδου αυτής διαχωρίστηκε ο πληθυσμός Κρήτης και Καρπάθου, από αυτόν της Πελοποννήσου (γεωγραφική απομόνωση της Κρήτης από την Πελοπόννησο στα 5.5-5 εκατ. χρόνια). Φαίνεται ότι η ειδογένεση κάθε είδους της ομάδας ειδών *E. minotaurus* ευνοήθηκε σε μετέπειτα χρόνο (κατά το τέλος του Πλειόκαινου), και ολοκληρώθηκε κατά τον Πλειστόκαινο. Οι χρόνοι απόσχισης και ειδογένεσης συμπίπτουν με την απομόνωση της γεωγραφικής περιοχής από όπου προέρχεται το κάθε είδος.

Τέλος, το Κεφάλαιο 6, συνιστά μια συνολική και ευρεία μελέτη σε εννέα είδη του γένους *Eumerus*: *E. amoenus* Loew, 1848, *E. argyropus* Loew, 1848, *E. armatus* Ricarte & Rotheray, 2012, *E. basalis* Loew, 1848, *E. clavatus* Becker, 1923, *E.*

phaeacus Chroni, Grković & Vujić, in litt., *E. pulchellus* Loew, 1848, *E. pusillus* Loew, 1848 και *E. sulcitibius* Rondani, 1868. Τα είδη αυτά επιλέχθηκαν λόγω της ευρείας γεωγραφικής τους εξάπλωσης στην Μεσόγειο (Ανατόλια, Βαλκανική, Ιβηρική και Ιταλική Χερσόνησοι) καθώς και σε χώρες των Βαλκανίων (Βουλγαρία, FYRO Macedonia και Σερβία). Στο κεφάλαιο αυτό: (1) εκτιμήθηκε η ενδοειδική γενετική διαφοροποίηση στα παραπάνω εννέα είδη *Eumerus* με την χρήση των DNA barcodes μέσω υπολογισμού μοναδιαίων και πληροφοριακών για τη φειδωλότητα θέσεων (singleton και parsimony informative sites), αριθμού απλοτύπων καθώς και κατασκευής δικτύων ανάλυσης NJ)· (2) εξετάστηκαν πιθανά χωρικά πρότυπα ενδοειδικής ποικιλότητας (αριθμός γενετικών ομάδων· genetic clusters) μέσω της Μπεϊεσιανής μεθόδου για χωρική ομαδοποίηση (Spatially-explicit Bayesian clustering) ως συνάρτηση ασυνεχειών του τοπίου (βουνά, θάλασσες: Αιγαίο, Ιβηρική και Ιταλική Χερσόνησοι, Διναρικές Άλπεις και Οροσειρά Πίνδου· landscape discontinuities), απομόνωσης λόγω απόστασης (isolation by distance), ή/και παλαιογεωλογικών και παλαιοκλιματικών γεγονότων· (3) ταυτοποιήθηκαν περιοχές υψηλής και χαμηλής γενετικής απόκλισης (high- and low-divergent regions)· και (4) συζητήθηκαν οι πιθανοί γενεσιουργοί παράγοντες που οδήγησαν στα παρατηρούμενα χωρικά γενετικά πρότυπα.

Η ύπαρξη χωρικών γενετικών προτύπων (δύο γενετικές ομάδες) επιβεβαιώθηκε σε τέσσερα είδη (*E. armatus*, *E. pulchellus*, *E. pusillus* και *E. sulcitibius*), και φαίνεται να είναι αποτέλεσμα αλλοπατρικών (*E. armatus*) και περιπατρικών διεργασιών (*E. sulcitibius*) ή παλαιογεωλογικών και παλαιοκλιματικών γεγονότων (*E. pulchellus* και *E. pusillus*), και όχι απομόνωσης λόγω απόστασης. Στα υπόλοιπα πέντε είδη (*E. amoenus*, *E. argyropus*, *E. basalis*, *E. clavatus* και *E. phaeacus* sp. n.) σχηματίστηκε μια γενετική ομάδα, η οποία δεν συσχετίζεται με απομόνωση λόγω απόστασης, υποδηλώνοντας ότι τα είδη αυτά είναι πιθανόν υπολειμματικά είδη (relict taxa).

Εξετάζοντας τα χωρικά γενετικά πρότυπα, ταυτοποιήθηκαν περιοχές υψηλής γενετικής απόκλισης (νησιά του (Ανατολικού) Αιγαίου, Ανατόλια (εκτός από το είδος *E. clavatus*), Κροατία (εκτός από το είδος *E. basalis*), Μάλτα, Μαυροβούνιο και Σερβία), και χαμηλής (Βαλκανική Χερσόνησος, νότια Ιταλία, Μαρόκο και Ισπανία). Οι περιοχές με υψηλή γενετική απόκλιση είναι νησιωτικές και ορεινές περιοχές με μεγάλο κατακερματισμό και απομόνωση, που ευθύνονται για τον περιορισμό ανταλλαγής γονιδιακής ροής κ.λπ. Από την άλλη, οι περιοχές με χαμηλή γενετική

απόκλιση, όπως οι Βαλκανική και Ιταλική Χερσόνησοι, είναι ηπειρωτικές περιοχές όπου οι μετακινήσεις ειδών/ πληθυσμών ήταν πιο εύκολες, και διευκόλυναν την ανταλλαγή γονιδιακής ροής μεταξύ των πληθυσμών.

Τα μιτοχονδριακά δίκτυα απλοτύπων επαλήθευσαν τα παρατηρούμενα χωρικά πρότυπα, ενώ παρατηρήθηκαν υψηλή μιτοχονδριακή ποικιλότητα (με μοναδικούς, αλλά και κοινούς απλότυπους) και περιπτώσεις αστροειδών δομών (star-like structures), που υπέδειξαν πρόσφατα ή εν εξελίξει επεισόδια επέκτασης της προγονικής γεωγραφικής κατανομής (expansion events).

page intentionally left blank

Curriculum vitae

Antonia Chroni was born in Lesvos Island, Greece. She is Biochemist and Biotechnologist (University of Thessaly, 2010). Her curious nature has led her to conduct her BSc thesis at the Laboratory of Insect Evolutionary Molecular Biology of the University of Pavia (Faculty of Sciences MMFFNN, Department of Animal Biology) in Italy, where she employed a molecular sexing system in the olive fruit fly, *Bactrocera oleae*.

She continued her studies with the Franco-Hellenic MSc in Conservation Biodiversity (University of Montpellier II, France and University of the Aegean, Greece, 2012). During her MSc internship, she was introduced to the world of pollinators. While in her MSc, she started to work on the research project Thales "The POLlinators of the AEGean archipelago: dIversity and threatS (POL-AEGIS)" (2012 – 2015) implemented at the Laboratory of Biogeography & Ecology, University of the Aegean. In 2013 she was involved into the Project ExpeER (under grant agreement no. 262060), "Ecosystem Research", with project title: "GeNetic status Of *EumeruS*: conservatIon implications (GNOSIS)", and her first visit in the University of Novi Sad took place (June – July 2013). Her visits in Novi Sad continued as (a) part of the project Thales (November 2013 – January 2014), (b) PhD Fellowship Research holder, IKY – State Scholarships Foundation (Greece; WP2-SHORT TERMS-19348, June – November 2014), and (c) Erasmus+ Programme scholarship holder (code G ATHINE 41, February – May 2017). She has attended the PhD course – Current trends in Phylogenetics (Biosystematics Group, Wageningen University, The Nerthelands, 14-18 October 2013).

In the frame of her PhD, she focused on the hoverfly genus *Eumerus*, consisting a relatively important pollinators group, keen to answer questions regarding the genus molecular taxonomy, phylogenesis, phylogeography, and spatial population genetics in the Balkans and in the Mediterranean Basin.